Triphenylamine and Carbazole Based Donor-Acceptor Systems for Dye-Sensitized Solar Cell, Bio-Imaging, and Sensor Applications

A Thesis Submitted for the Degree of

DOCTOR OF PHILOSOPHY

In Chemistry

By

TAMILARASAN D.

Reg. No. 11CHPH27

Under the Supervision of

Prof. R. BALAMURUGAN



SCHOOL OF CHEMISTRY UNIVERSITY OF HYDERABAD HYDERABAD- 500 046 TELANGANA

INDIA

JULY 2020

70
My Beloved
Grandmother...

DECLARATION

I hereby declare that the matter embodied in the thesis entitled "Triphenylamine and Carbazole Based Donor-Acceptor Systems for Dye-Sensitized Solar Cell, Bio-Imaging, and Sensor Applications" is the result of investigation carried out by me in the School of Chemistry, University of Hyderabad, Hyderabad, India, under the supervision of **Prof. Rengarajan Balamurugan**.

In keeping with the general practice of reporting scientific observations, due acknowledgements have been made on the basis of the findings of other investigators. Any omission, which might have occurred by oversight or error, is regretted. This research work is free from Plagiarism. I hereby agree that my thesis can be deposited in Shodhganga/INFLIBNET. A report on plagiarism statistics from the University Librarian is enclosed.

University of Hyderabad

July 2020

Tamilarasan D.

(11CHPH27)

Prof. R. Balamurugan

(Supervisor)

Dr. R. Balamurugan
Professor
School of Chemistry
University of Hyderabad
Hyderabad-46, India.



This is to certify that the thesis entitled "Triphenylamine and Carbazole Based Donor-Acceptor Systems for Dye-Sensitized Solar Cell, Bio-Imaging, and Sensor Applications" submitted by Mr. Tamilarasan D. holding registration number 11CHPH27 in partial fulfilment of the requirements for award of Doctor of Philosophy in the School of Chemistry is a bonafide work carried out by him under my supervision and guidance.

This thesis is free from plagiarism and has not been submitted previously in part or in full to this or any other University or Institution for award of any degree or diploma.

Parts of the thesis have been:

A. Published in following publication

- **1. Duraiyarasu Tamilarasan**, Ramalingam Suhasini, Viruthachalam Thiagarajan, Rengarajan Balamurugan, *Eur. J. Org. Chem.* **2020**, 993–1000 (**Chapter 2**)
- **2. Duraiyarasu Tamilarasan**, Loka Reddy Velatooru, Ramalingam Suhasini, Viruthachalam Thiagarajan, Bramanandam Manavathi, Rengarajan Balamurugan, *ACS Appl. Bio Mater.* **2020** (*Under Revision*) (**Chapter 2**)
- **3. Duraiyarasu Tamilarasan**, Loka Reddy Velatooru, Bramanandam Manavathi, Rengarajan Balamurugan (*Manuscript to be submitted*) (**Chapter 3**)

Patent: Rengarajan Balamurugan, Duraiyarasu Tamilarasan, Bramanandam Manavathi, Loka Reddy, WIPO Application No. PCT/IB2019/057180; *Indian Patent* 201841031942, **2018** (*Under Evaluation*) (Chapter 2).

B. Presented in the following conferences

1. ICOS 21-2016; 2. ChemFest-2015; 3. ChemFest-2018.

Further the student has passed the following courses towards fulfilment of course work requirement for Ph.D.

Course code	Name	Credits	Pass/Fail
CY-801	Research Proposal	3	Pass
CY-805	Instrumental Methods A	3	Pass
CY-810	Basic Concepts and Coordination Chemistry	3	Pass
CY-850	Chemistry of Materials	3	Pass

Dean

(School of Chemistry)

Dehaol of Chemistry
University of Hyderabed
P.O. Central University
Sachibowii, Hyderabad 640 045.

Prof. R. Balamurugan

(Thesis Supervisor)

Dr. R. Balamurugan Professor School of Chemistry University of Hyderabad Hyderabad-46, India.

ACKNOWLEDGMENT

I feel that the acknowledgment is the most valuable part apart from work because, without other's support and encouragement, it would have been impossible to travel this journey.

I would like to express my deep sense of gratitude and profound thanks to my research supervisor **Prof. Rengarajan Balamurugan** for his excellent guidance, encouragement. For freedom, he gave me in carrying out various research projects. His optimistic approach and patience towards every aspect were admirable and inspiring. Throughout my Ph.D. tenure, he is always approachable, helpful, friendly, and extremely tolerant in every situation. I am fortunate enough to join his research group.

I take this opportunity to thank Prof. Anunay Samanta, Dean, School of Chemistry, for providing the facilities needed for our research. I sincerely thank my doctoral committee members Prof. R. Nagarajan and Prof. V. Baskar, for their guidance and encouragement. I extend my sincere thanks to former Deans and all the faculty members, School of Chemistry, for their cooperation on various aspects.

I would like to thank my research collaborators Prof. Bramanandam Manavathi, Dr. Loka Reddy Velatooru (School of Life Sciences, UoH) for applications of Bio-Imaging, Dr. Viruthachalam Thiagarajan, Ramalingam Suhasini (School of Chemistry, Bharathidasan University, Trichy, Tamilnadu) for Sensor Applications, Dr. V. Ganapathy, Reshma, and Dr. R. Easwaramoorthi, Suresh (CSEM, ARCI, Hyderabad) for the application of Dye-Sensitized solar cell.

It is my responsibility to thank all my lab members Dr. Srinivasa Rao Koppolu, Dr. Ganesh Kumar Thota, Dr. Raveedrababu Kothapalli, Dr. Naganaboina Naveen, Dr. Vanajakshi Gudla, Dr. S. Manojveer, Dr. Ramana Niddana, Dr. S. Sakthivel, T. Chandrahas, Mou Mandal, G. Ramesh, K. Sayyad Basha, Arun, Rina, Tausif, Anjali and Dr. Manoj (Post-Doc), Venkat Ramulu (Post-Doc) for their help, support throughout the tenure and creating cheerful work atmosphere.

I heartfully thank Dr. Rathitharan (Jaffna University, Srilanka), Dr. T. M. Rangarajan, Dr. B. Shankar, D. Maheshwaran (MKU), N. Palaniappan (CUG), N. Senthilnathan, R. Arumugam and my family members for their big help and support during my Ph.D. tenure.

I sincerely thank all the non-teaching staff of the School of Chemistry for their assistance on various occasions. I would like to acknowledge DST-SERB for providing the basic requirements and UGC for financial support.

I would like to thank my seniors and friends Dr. Viji, Dr. Ramesh, Dr. Prakash, Dr. Ramkumar, Dr. Suman, Dr. Naveen, Sathish (RN lab), Dr. Vignesh, Dr. Ganesh, Dr. Srinivas, (KM lab), Dr. Madhava charry, Dr. Murali Krishna, Dr. Bharani, Dr. Shiva Prasad (DBR lab), Dr. Suresh, Dr. Shanmugaraja, Dr. Ramusagar, Dr. Uday, Dr. Harish, Dr. Anand, Dr. Sathyanarayana, Dr. Ramesh, Dr. Mohan (MP lab), Dr. Tamizharasi (DB lab), Dr. Bhanuchandra, Dr. Prabagar, Dr. Ramesh (AKS lab), Dr. Rahul Soman, Dr. Sathish, Dr. Nandakishore, Obaiya (PKP lab), Dr. Sudalai, Dr. Anil (AN lab), Dr. Krishna, Dr. Srinivasan (Post-doc) (MVR lab), Dr. Santhanaraj Prabhu, Dr. Kishore (VB lab), Dr. Sathish, Dr. Narendra Babu (SP Lab) for their support, pleasant company, and cooperation during my Ph.D. tenure.

I also extended heartfelt thanks to Jayaprakash Sir (Jaguruthi coaching Centre, Hyderabad), friends Marimuthu, Yuvaraj, Aravinth, for their help and support during my CSIR coaching studies. Dr. Prakash, Dr. Rajkumar, Dr. Rajakumar, Dr. Vellaisamy, Dr. Dickins, Dr. Jeeva, Nelson, Anthony, Dr. Dinesh, Dr. Vikranth, Dr. Ashok, Dr. Chandrasekar (UoH), Dr. Kamalesh, Dr. Mohan, Dr.Rajkumar, Dr.Muthuraja, Dr. Balachandar, Dr. Siva, Dilip (NRC visiting project students) for their pleasant company with me for playing cricket during my Ph.D. tenure.

I would like to thanks my teachers and friends from my 1st std to Post-graduation. Teachers: Jayarackini, Mercy Sister, Vasanthi Sister, and Friends: Gowthaman, Rajesh, Thiagarajan, Raja, Radha, Anandharaj, Ramarajan (1-5 std). Thomas sir, David sir, Arockiaraj, Ramkumar, Kannan, Anand, Jagathese (6-12th std). Dr. Jaswant, Muthukumar, Thanasekaran, Arasan, Devaraj, Muniyandi anna, Kalaiselvan anna, Selvaraj anna, Karthi anna (UG, Karur). Dr. Rajendra Prasad, Dr. Yamuna, Seenivasan, Manimegalai, Vanithamani, Muthusamy, Ganesh (PG, Coimbatore), and also special thanks to Dr. Anand, Anand Babu, Dr. Muthu Mareeshwaran (MKU) for their special support during my studies.

Tamilarasan D.

University of Hyderabad

TABLE OF CONTENTS

List of Abbreviations Used	Page No i
Synopsis	vii
Chapter 1: Organic Donor-Acceptor Systems	1
1.1 Introduction	1
1.2 Donors	2
1.3 Acceptors	4
1.4 Bridges	5
1.5 Applications of Donor-Acceptor Systems	6
1.5.1 Application in Organic Photovoltaics (OPVs)	6
1.5.2 Donor-Acceptor Systems in Dye-Sensitized Solar Cells (DSSCs)	8
1.5.3 Organic Donor-Acceptor in Organic Light-Emitting Diodes (OLEDs)	11
1.5.4 Organic Donor-Acceptors in Organic Field-Effect Transistors (OFETs) and Organic Thin-Film Transistors (OTFTs)	13
1.5.5 Applications of Organic Donor-Acceptors in Fluorescence Resonance Energy Transfer (FRET)	14
1.5.6 Applications of Donor-Acceptors in Optoelectronics	15
1.5.7 Donor-Acceptors as Sensors	16
1.5.8 Applications of Donor-Acceptors in Bio-Imaging	18
1.6 Our Present work	20
1.7 References	21
$Chapter \ 2: \ 1, 3-Dicarbonyl-Bridged \ Donor-Acceptor \ Compounds \ and \ Their \ BF_2$ $Complexes: \ Synthesis \ and \ Their \ Applications \ in \ Dye-Sensitized \ Solar \ Cells,$ $Bio\text{-imaging, and } \ Cyanide \ Sensing$	27
2.1 Introduction	27
2.2 Synthesis of 1,3-Dicarbonyl Bridged Donor-Acceptor Systems	28
2.3 Photophysical Properties of the Donor-Acceptor Compounds	34
2.3.1 Absorption Studies	34
2.3.2 Emission Studies	35
2.3.3 Electrochemistry	36
2.4 Density Functional Theory (DFT) Studies	38

2.5 Applications of the 1,3-Dicarbonyl Bridged Donor-Acceptor Systems	39
2.5.1 Dye-Sensitized Solar Cells (DSSCs)	39
2.5.1.1 Working Principle of Dye-Sensitized Solar Cells	41
2.5.1.2 Metal-Free Organic Donor-Acceptors for Dye-Sensitized Solar Cells (DSSCs)	42
2.5.2 Bio-Imaging	46
2.5.3 Cyanide Sensing	55
2.5.3.1 Absorption and Emission Properties of 2.3-BF ₂ in the Presence and Absence of CN	58
2.5.3.2 Absorption and Emission Spectral Studies in the Presence and Absence of Anions	60
2.5.3.3 Selectivity and Effect of Anion Interference	62
2.5.3.4 Detection Mechanism	65
2.5.3.5 Computational Studies	68
2.5.3.6 Test Strip Detection of Cyanide Ion	70
2.6 Conclusion	70
2.7 Experimental Section	71
2.7.1 General Information	71
2.7.2 Device Fabrication	71
2.7.2.1 Characterization	72
2.7.3 Cell Lines and Cell Culture	72
2.7.3.1 Test Concentrations	72
2.7.3.2 Cytotoxicity	72
2.7.3.3 Fluorescence Microscopy	73
2.7.3.4 Wound Healing Assay	73
2.7.3.5 In Vivo Tubulin Interaction Assay	74
2.7.4 Experimental Procedure and Analytical Data	74
2.8 References	91
2.9 Representative ¹ H, ¹³ C, ¹¹ B, ¹⁹ F NMR	98
Chapter 3: Bis-Donor Incorporated Donor-Acceptor Systems and Their Applications in Bio-Imaging and DSSC	117
3.1 Introduction	117
3.2 Synthesis of the Bis-Donor Containing Donor-Acceptor Systems	120

3.3 Optical Properties	122
3.4 Cyclic Voltammetric Studies	123
3.5 DFT Studies	124
3.6 Application in Bio-Imaging	125
3.6.1 Effect of Donor-Acceptor Compounds on Cell Viability and Cell Migration	126
3.6.2 Colocalization of Donor-Acceptor Compounds in HeLa Cells	129
3.7 Application of the Dyes 3.11 and 3.12 in DSSC	130
3.8 Conclusion	131
3.9 Experimental Section	132
3.9.1 General Information	132
3.9.2 Cell Lines and Cell Culture	132
3.9.3 Experimental Procedure and Analytical data	132
3.10 References	138
3.11 Representative ¹ H, ¹³ C NMR	140
Chapter 4: Bis-Acceptor Based Donor-Acceptor Systems and Their Application in DSSC	147
4.1 Introduction	147
4.1.1 Effect of Acceptor Geometry in DSSC	150
4.2 Synthesis of the Acceptor Enriched Donor-Acceptor Systems	151
4.3 Optical Properties	153
4.4 Cyclic Voltammetry	155
4.5 DFT studies	156
4.6 Application in Dye-Sensitized Solar Cell	157
4.7 Conclusion	159
4.8 Experimental section	159
4.8.1 General Information	159
4.8.2 Experimental Procedure and Analytical Data	159
4.9 References	168
4.10 Representative ¹ H, ¹³ C NMR	170
Appendix	
Table 1 Crystal Data and Structure Refinement for Compound 2.1	179

Table 2 Crystal Data and Structure Refinement for Compound 2.2	180
Table 3 Crystal Data and Structure Refinement for Compound 2.3	181
Table 4 Crystal Data and Structure Refinement for Compound 3.11	182
List of Publications and Patent	183
Poster and Oral Presentation	184

LIST OF ABBREVIATIONS USED

A-D-A Acceptor-Donor-Acceptor

AIE Aggregation Induced Emission

AIEE Aggregation-Induced Emission Enhancement

Ag Silver

AcOH Acetic acid

AlCl₃ Aluminum trichloride

BODIPY Boron Dipyrromethene

BHJ Bulk Hetero Junction (Bu)₃SnCl Tributyltin chloride

n-BuLi n-Butyllithium

¹¹B NMR Boron Nuclear Magnetic Resonance

BF₃.OEt₂ Boron trifluoro diethyl etherate

Bu₄NClO₄ Tetrabutylammonium perchlorate

BF₂ Boron difluoride

BSA Bovine Serum Albumin

B3LYP Becke, 3-parameter, Lee–Yang–Par

CuPc Copper phthalocyanine

¹³C NMR Carbon Nuclear Magnetic Resonance

CH₃OH (MeOH) Methanol

CH₂Cl₂ (DCM) Dichloromethane

HCl Hydrochloric Acid

DFT Density Functional Theory

C_Z Carbazole

CN⁻ Cyanide ion

CDCl₃ Deuterated chloroform

CH₃COCl Acetyl chloride

CD₃CN Acetonitrile-D₃

CuI Copper iodide

CH₃CN Acetonitrile

DMSO-d₆ Deuterated dimethyl sulfoxide- d₆

DSSCs Dye-Sensitized Solar Cells

DPP Diketopyrrolopyrroles

DTTCNQ 4,8-bis(dicyanomethylene)-4,8-dihydrobenzo[1,2-b:4,5-b0]-dithiophene

DMTCNQ 2,5-dimethyl-7,7,8,8-tetracyanoquinodimethane

DMDCNQI 2,5-dimethy-dicyanoquinonediimine

D-A-D Donor-Acceptor-Donor

D-A Donor-Acceptor

D-A-π-A Donor-Acceptor- π-Acceptor

D(D)- π -A Donor (Donor) - π -Acceptor

DI Deionized

DMEM Dulbecco's Modified Eagle's Medium

DMSO Dimethyl sulfoxide

DMF Dimethylformamide

DAPI 4',6-diamidino-2-phenylindole

EtOAc Ethyl acetate

Et₃N Triethylamine

Energy oxidation

Eg Energy gap

ESI Electrospray ionization

FTO Fluorine-doped tin oxide

F₂TCNQ 2,5-difluoro-7,7,8,8-tetracyanoquinodimethane

F₄TCNQ 2,3,5,6-difluoro-7,7,8,8-tetracyanoquinodimethane

FF Fill factor

FBS Foetal Bovine Serum

¹⁹F NMR Fluorine Nuclear Magnetic Resonance

HOMO Highest Occupied Molecular Orbital

HeLa Henrietta Lacks

HepG2 Hepatoma G2

HEK293T Human embryonic kidney 293T

HRMS High Resolution Mass Spectrometry

H₂O₂ Hydrogen peroxide

¹H NMR Proton Nuclear Magnetic Resonance

H₂O Water

IBX 2-Iodoxybenzoic acid

ID Isoindigo

ITO Indium-doped tin oxide

ICT Intramolecular Charge Transfer

 $IC_{50}\pm SD$ 50% Inhibitory Concentration \pm Standard Deviation

IPA Isopropyl alcohol

IR Infrared

 $J_{\rm sc}$ short-circuit current density (mA cm⁻²)

KMnO₄ Potassium permanganate

KF Potassium fluoride

K₂CO₃ Potassium carbonate

LiI Lithium iodide

LiOH Lithium hydroxide

LUMO Lowest Unoccupied Molecular Orbital

 $\tau_f(ns)$ Lifetime (nano seconds)

MCF-7 Michigan Cancer Foundation-7

MC Merocyanine

MTT 3-(4,5-dimethylthiazol-2-yl)-2,5-diphenyl tetrazolium bromide

MHz Megahertz

MnO₂ Manganese dioxide

MP Melting point

NDIs Naphthalene Diimides

NaH Sodium hydride

NA Not Active

NaHCO₃ Sodium bicarbonate

NaSO₄ Sodium sulfate

NaOH Sodium hydroxide

NPh₂ Diphenylamine

ORTEP Oak Ridge Thermal Ellipsoid Plot

OLED Organic Light Emitting Diode

OFETs Organic Field-Effect Transistors

OPVs Organic Photovoltaics

OE Oligoethylene

OV Oligovinylenes

OP Oligo-p-Phenylene

OF Oligo-2,7-fluorenes

OTP Oligothiophene

OPV Oligo-p-phenylenevinylenes

OPE Oligo-*p*-phenylene ethynylene

POCl₃ Phosphorous oxy trichloride

PTSA.H₂O *p*-Toluenesulfonic acid monohydride

PPh₃ Triphenylphosphine

Pd(PPh₃)₄ Tetrakis(triphenylphosphine)palladium(0)

Pt Platinum

 $P_{\rm in}$ Input the incident light power

PBS Phosphate-buffered saline

2PA 2 Photon Absorption

PCE Power Conversion Efficiency

Pc Phthalocyanine

PDI Perylene Diimides

PCBM Phenyl C₆₁ Butyric Acid Methyl Ester

PT3B1 Poly [4,7-bis-(3- dodecylthiophene-2-yl) benzothiadiazole-co-thiophene

PC₇₀BM [6,6] phenyl-C71-butyric acid methyl ester

QD Quinacridone

φ_f Quantum fluorescene

Ru Ruthenium

Retardation factor

SubNc Subnaphthalocyanine

SQ Squaraine

SNTCNQ 1,2,5-thiadiazolotetracyanoquinodimethane

TCNQ 7,7,8,8-tetracyanoquinodimethane

TiO₂ Titanium dioxide

THF Tetrahydrofuran

TDDFT Time-Dependent Density Functional Theory

TLC Thin Layer Chromatography

TPA Triphenylamine

TBA cyanide Tetrabutylammonium cyanide

TMS Tetramethyl silane

TCSPC Time-Correlated Single-Photon Counting

TiCl₄ Titanium tetrachloride

TiO₂ Titanium dioxide

UV-Vis Ultraviolet-visible

 V_{oc} Open-circuit voltage (V)

 $V_{\text{max}}J_{\text{max}}$ Maximum voltage and current

 λ_{max} $\lambda_{maximum}$

 λ em λ emission

SYNOPSIS

This thesis, entitled "Triphenylamine and Carbazole Based Donor-Acceptor Systems for Dye-Sensitized Solar Cell, Bio-Imaging, and Sensor Applications," contains four chapters. Introduction about the donor-acceptor systems and their applications in different fields have been reviewed in chapter 1. The actual work has been presented in chapters 2-4. Each of these three work chapters contains related literature background, synthesis, characterization, applications, experimental section and references. A brief write-up on each chapter is given below.

Chapter 1: Organic Donor-Acceptor Systems

Chapter 1 discusses the basic construct of different donor-acceptor systems. It gives an account of various donors, acceptors, and bridges used for the development of donor-acceptor systems. Applications of donor-acceptor systems in the field of Organic Photovoltaics (OPVs) devices, Dye-Sensitized Solar Cells (DSSCs), Organic Light-Emitting Diodes (OLEDs), Organic Field-Effect Transistors (OFETs), Organic Thin-Film Transistors (OTFTs), Fluorescence Resonance Energy Transfer (FRET), Optoelectronics, Sensors and Bio-imaging of live cells have been reviewed. Finally, a brief description on the design of the donor-acceptor systems used in the present study has provided.

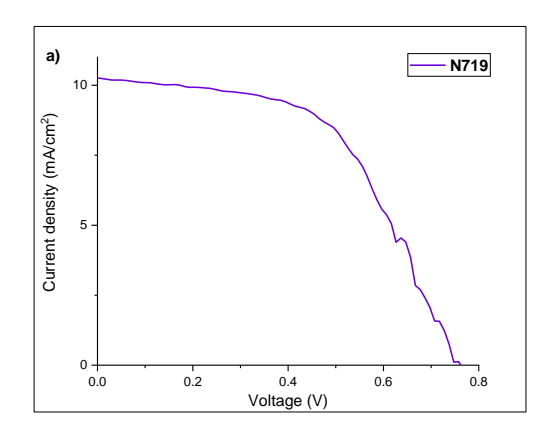
Chapter 2: 1,3-Dicarbonyl-Bridged Donor-Acceptor Compounds and Their BF₂ Complexes: Synthesis and Their Applications in Dye-Sensitized Solar Cells, Bio-imaging, and Cyanide Sensing

Chapter 2 presents the synthesis and characterization of a set of new organic dyes based on triphenylamine and carbazole donors and dicyanovinylene acceptors connected through a 1,3-dicarbonyl bridge and their corresponding BF₂ complexes (Figure 1). The synthesis is straightforward and utilizes Claisen ester condensation to make the 1,3-dicarbonyl bridge, Knoevenagel condensation, for introducing the dicyanovinylene moiety and Stille coupling for incorporating thiophene ring as the key reactions. Some of the synthesized compounds have been tested for their applications in dye-sensitized solar cells (DSSCs), live-cell imaging, and sensing. The compounds 2.2 and 2.4 were tested for dye-sensitized solar cell applications and found to generate a power conversion efficiency (PCE) of 0.12% and 0.25%, respectively. In comparison, the reference N719 dye produced a PCE of 4.16%.

Figure 1: Structures of the synthesized 1,3-diketone bridged donor-acceptor systems and their corresponding difluoro boron complexes.

Table 1. DSSC performances of Donor-Acceptors (2.2, 2.4) and reference N719.

Dye	J _{sc} (mA/cm ²)	$V_{ m oc}$ (V)	FF	η (%)
2.2	0.468	0.486	52.30	0.12
2.4	0.585	0.649	65.06	0.25
N719	10.26	0.760	53.38	4.16



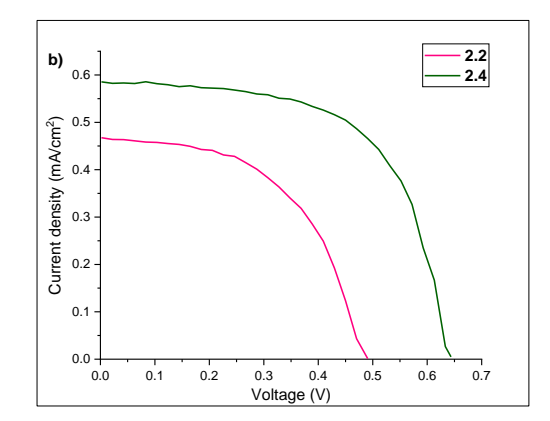


Figure 2. Photocurrent density- voltage (*J-V*) curves for the donor-acceptor based dye-sensitized solar cells with TiO₂ electrodes. a) Reference dye N719; b) Dye 2.2 and 2.4.

The compounds **2.1-2.3** and **2.1-BF₂-2.3-BF₂** have been tested for their application in bioimaging with the HeLa cancer cell line. The results showed that the compounds selectively bind to the β -tubulin in Hela cancer cells to provide a bright green image of the microtubule network. The selectivity towards β -tubulin has been established by co-localization experiments using Alexa Fluor 546 (Figure 3). From the cytotoxicity measurements, it was established that except compound **2.1**, all the other compounds are non-toxic (Table 2).

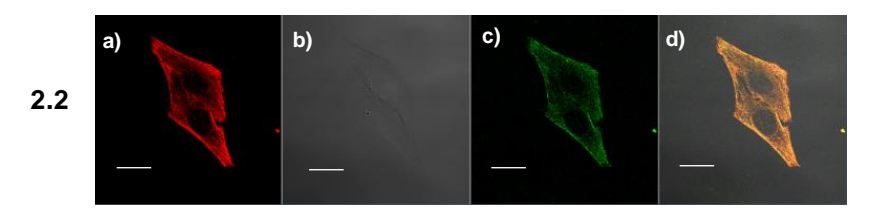


Figure 3. Representative confocal images of HeLa cancer cells co-stained with Alexa Fluor 546 and dyes. a) Alexa Fluor 546 (red channel: excited at 543-550 nm and emission at 700 nm); b) Bright field; c) **2.2** (Green channel: excited at 488-500 nm and emission at 550 nm); d) Merging all the images. Scale bar is 10 μm.

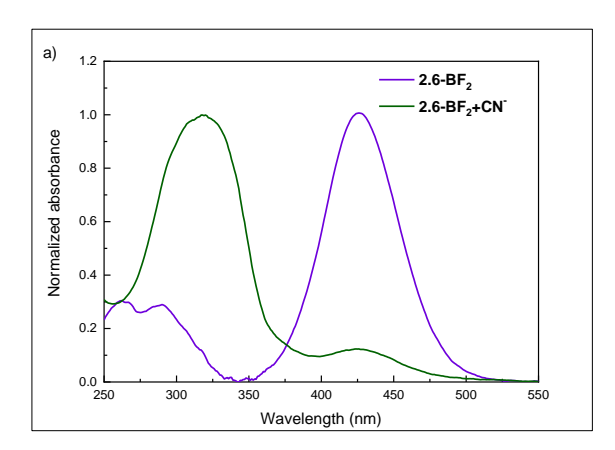
Table 2. In vitro cytotoxic evaluation of donor-acceptor compounds against HeLa cell line

S. No	Dye	IC50±SD (μg/ml) on HeLa
1	2.1	10.34±1.56
2	2.2	NA
3	2.3	NA
4	2.1 -BF $_2$	NA
5	2.2 -BF $_2$	NA
6 7	2.3-BF ₂ ^a Doxorubicin	NA 1.82±0.45

[[]a] Doxorubicin was employed as a positive control. NA indicates that the derivatives are not active at $100 \ \mu g/mL$ concentration. The values represent the mean \pm SE of three individual observations.

Furthermore, the donor-acceptor complex **2.3-BF**₂ has been tested for its sensing ability for cyanide ions. Unfortunately, the compound **2.3-BF**₂ showed poor performance for the detection of cyanide ions. Based on the results, compound **2.6-BF**₂ was designed, synthesized and tested for cyanide ion sensing using tetrabutylammonium cyanide. Interestingly, the compound **2.6-BF**₂ responded remarkably well for the detection of cyanide ion in tetrabutylammonium cyanide. Also, it did not recognize the other anions such as Cl⁻, Br⁻, I⁻, acetate ion, phosphate ion, PF₆⁻, bicarbonate ion, F⁻, perchlorate ion, etc. The detection of cyanide ion was followed using UV-Vis and fluorescence spectroscopy, and ¹H NMR techniques. It is proposed that the sensing is due to the addition of cyanide ion to the carbonyl of the BF₂-complex. Interestingly, the addition is reversible upon addition of excess water. Based on the NMR experiments, a mechanism has been proposed for the reversible sensing.

Figure 4. Molecular structure of the cyanide ion sensor.



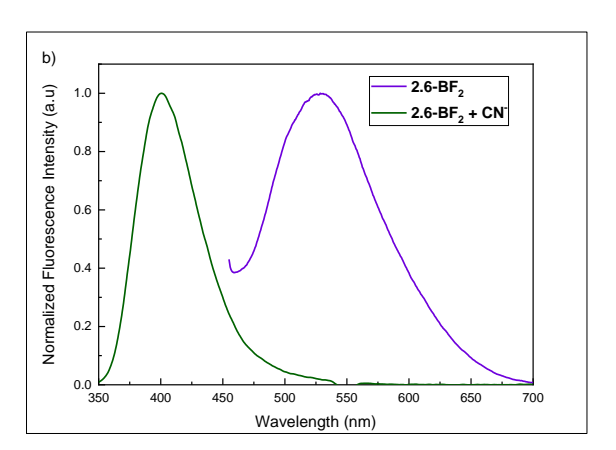


Figure 5. a) Absorption spectrum of **2.6-BF**₂ in the presence and absence of CN⁻ (10 equivalent) in acetonitrile; b) Emission spectrum of **2.6-BF**₂ in the presence and absence of CN⁻ (10 equivalent) in acetonitrile.

Chapter 3: Bis-Donor Incorporated Donor-Acceptor Systems and Their Applications in Bio-Imaging and DSSC

In chapter 3, work related to bis-donor containing donor-acceptor (D(D)- π -A) dyes (Figure 6) has been presented. In these dyes, triphenylamine and N-phenyl carbazole (donors) are independently connected to cyano acrylic acid acceptor through extended double bonds. The synthesis of these probes starts with the addition of corresponding lithiated donor to donor carbaldehyde. The secondary benzyl alcohols, thus obtained, were separately oxidized and converted into their α , β -unsaturated aldehyde derivatives. Knoevenagel reaction with cyanoacetic acid on each of them resulted in the final probes **3.1** and **3.2**.

Figure 6. Molecular structures of the dual donor-based donor-acceptor systems (D(D)- π -A).

The compounds **3.1** and **3.2** selectively stained the β -tubulin in HeLa cancer cell. Also, these dyes have tested for cytotoxicity in three different cell lines, *viz.* human cervical cancer cell line (HeLa), human breast cancer (MCF7) and normal embryonic kidney cells (HEK293T). Interestingly, dye **3.1** has shown significant cytotoxic/antiproliferative activity on HeLa and MCF7 cancer cell lines, and less on normal cell HEK293T. The dye **3.2** displayed less cytotoxic/antiproliferative activity on all the three different cell lines. Hence there is a possibility for developing potential antiproliferative agents based on these structures.

Table 3. *In vitro* cytotoxic evaluation of bis-donor based donor-acceptor derivatives against HeLa, MCF7, HEK293T cell lines

S.No	Dye	IC50±SD (μg/ml)	IC50±SD (μg/ml)	IC50±SD (μg/ml)
		on HeLa	on MCF7	on HEK293T
1	3.1	13.51±1.22	67.01±5.76	NA
2	3.2	NA	NA	NA

NA indicates that the derivatives are not active at $100 \,\mu\text{g/mL}$ concentration. The values represent the mean \pm SE of three individual observations.

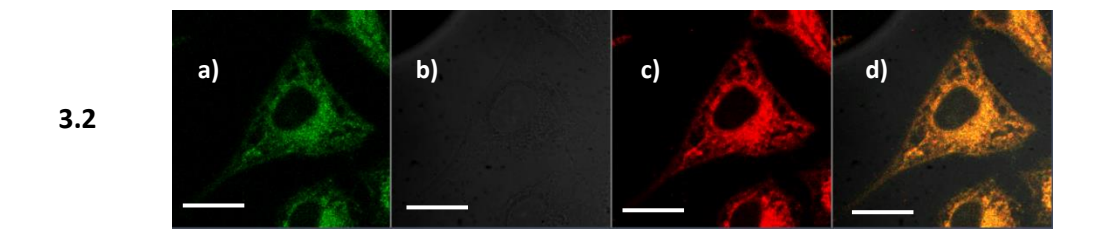
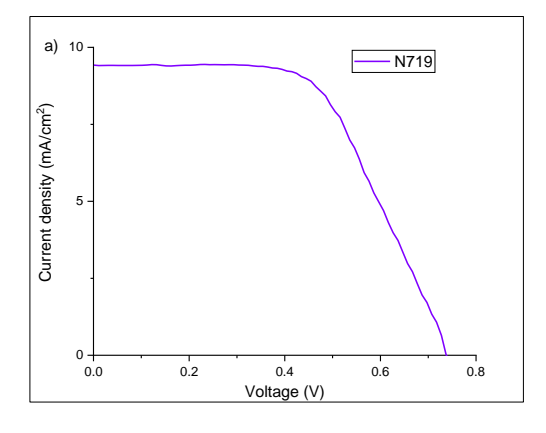


Figure 7. Representative confocal images of HeLa cancer cells co-stained with Alexa Fluor 546 and dye **3.2**. a) Organic dye **3.2** (Green channel: excited at 488-500 nm and emission at 550 nm); b) Bright field; c) β -tubulin (red channel: excited at 543-550 nm and emission at 700 nm); d) Merging all the images. Scale bar is 10 μ m.

Moreover, both the dyes have been tested for dye-sensitized solar cell applications. The dyes **3.1** and **3.2** have generated power conversion efficiency (PCE) of 0.64%, 0.68%, respectively, while the reference dye **N719** generated a PCE of 4.01%.

Table 4. Performance of dye-sensitized solar cell based on compounds 3.1, 3.2, and reference N719.

Dye	$J_{\rm sc}$ (mA/cm ²)	Voc (V)	FF	η (%)
3.1	1.6	0.55	70	0.64
3.2	1.74	0.57	69	0.68
N719	9.40	0.740	58.5	4.01



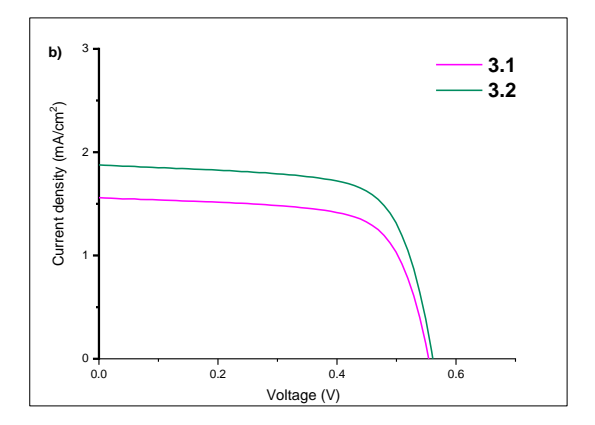


Figure 8. Photocurrent density-voltage (J-V) curves for the donor-acceptor $(D(D)-\pi-A)$ based dyesensitized solar TiO_2 electrodes. a) Reference **N719** dye; b) Dye **3.1** and **3.2**.

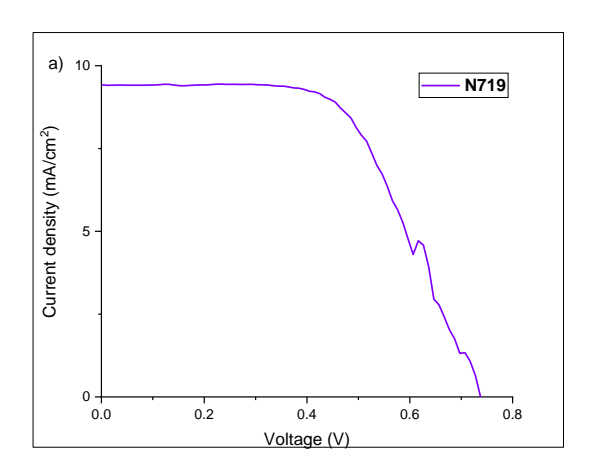
Chapter 4: Bis-Acceptor Based Donor-Acceptor Systems and Their Application in DSSC

Chapter 4 discusses our work on the E- and Z- isomers of acceptor-enriched donor-acceptor based organic dyes and the evaluation of dye-sensitized solar cells based on them. The new organic dyes have triphenylamine and N-phenyl carbazole donors and cyanoacrylic acid and dicyanovinylene acceptors connected through π -conjugation. The synthesis of these dyes involves a couple of Knoevenagel reactions to incorporate the cyanoacrylic acid and dicyanovinylene units selectively at the desired positions.

Figure 9. Structures of the synthesized acceptor enriched organic dyes.

Table 5. DSSC parameters of dye-sensitized solar cell performance of **4.1a** and **4.1b** and the reference **N719**.

Dye	J _{sc} (mA/cm ²)	Voc (V)	FF	η (%)
4.1a	0.24	0.554	61.8	0.1
4.1b	0.47	0.623	77.5	0.22
N719	9.40	0.740	58.5	4.01



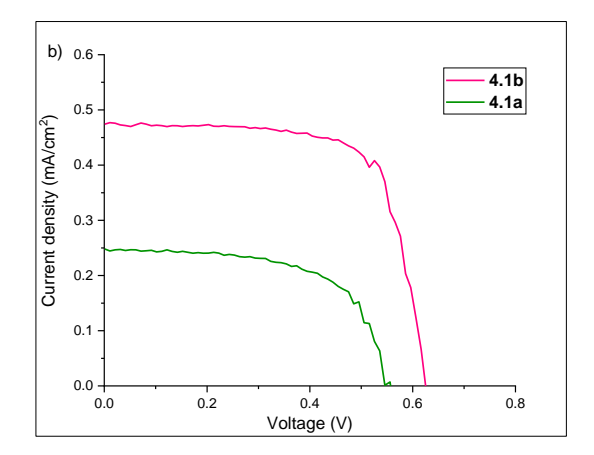


Figure 10. Photocurrent density-voltage (J-V) curves for the donor-acceptor based dye-sensitized solar TiO₂ electrodes. a) Reference **N719** dye; b) Dye **4.1a** and **4.1b**.

The triphenylamine based *E*- and *Z*- isomers (**4.1a** and **4.1b**) and the reference dye **N719** were tested in dye-sensitized solar cells. The device made using the *E*-isomer **4.15b** exhibited a power conversion efficiency of 0.22%. On the other hand, the device made with the *Z*-isomer **4.15a** has performed with a power conversion efficiency of 0.1%. The **N719** reference device exhibited a power conversion efficiency of 4.01%. The devices with **4.15a** and **4.15b** exhibited a better fill factor compared to that of the reference device **N719**.

Note: Scheme, Compound, Figure and Table numbers given in this abstract are different from those given in Chapter 2, 3 and 4.

Organic Donor-Acceptor Systems

1.1 Introduction

Organic donor-acceptor systems find widespread application in different fields. In general, donors are the groups capable of donating electrons, and the acceptors are the groups capable of accepting electrons. In organic donor-acceptor systems the donor and the acceptor are linked through a conjugated π -system which is usually called as a π -spacer and is essential for the electron transfer processes. The nature and construct of donor-bridge-acceptor plays a crucial role in energy and electron transport processes. ^{1a} The spacer may be termed as a bridge or a wire depending on its function. If the charge is localized on the spacer during the electron transfer process from the donor to acceptor, it is called as a "wire." On the other hand, when the charge does not localize on the spacer group during the charge transfer process, the spacer is called as a "bridge." The electron and energy transfer processes strongly depend on the donor-acceptor distance and the electronic structure of the bridge. Therefore, these parameters help to design and develop different types of donor-bridge-acceptor systems, which would have specific applications in organic solar cells,² organic light-emitting diodes (OLED),³ organic field-effect transistors (OFETs),4 sensors5 and optoelectronic devices,6, etc. A variety of donors, acceptors, and π -bridges have developed over the years with an intense activity in the field of optoelectronic devices. The next section will provide a brief account on each.



Figure 1.1. General structure of a donor-acceptor system.

1.2 Donors

Several small-molecule donors have been reported to date. A literature survey reveals that some of the donor moieties show widespread applications in organic photovoltaic devices (OPVs). Structures of representative donor molecules are shown in Figure 1.2. Generally, electron-rich nitrogen-containing compounds act as donors. This includes macrocycles such as phthalocyanine derivatives (18-π electron macrocycle, Pc, 1.1),^{7a} subnaphthalocyanine having a centre boron surrounded by three units of interlinked benzoisoindoles SubNc, 1.2.^{7b} Other commonly encountered donors are merocyanine MC, 1.3,^{7c} squaraine SQ, 1.4,^{7d} diketopyrrolopyrroles DPP, 1.5,^{7e} boron-dipyrromethene BODIPY, 1.6,^{8a, 8b} oligothiophene 1.7,^{8c} quinacridone QD, 1.8,^{8d} fused acenes 1.9,^{8e} triphenylamine 1.10,⁹ carbazole 1.11,¹⁰ triarylamine 1.12, dialkylamine 1.13, indoline 1.14, tetrahydroquinoline 1.15 and phenothiazine PTZ, 1.16a/phenoxazine POZ, 1.16b.¹¹ Researchers have constructed donor dyes with several functional groups to enhance their applicability and efficiency and specificity.

$$M = Cu, Zn, AICI, TIO$$

$$1.2$$

$$C_2H_5$$

$$1.1$$

$$C_4H_9$$

$$C_2H_5$$

$$1.4$$

$$1.5$$

Figure 1.2. Chemical structures of representative dye-based donors (dotted circle indicates the donor moiety present in the molecule).

1.3 Acceptors

Acceptors are the electron-withdrawing natured molecules that can be incorporated with donor molecules for application in OPV and other organic electronic devices. The acceptors also receive the same level of importance as that of the donor molecules with regard to the performance of organic electronic devices. Big molecules such as, fullerenes 1.17, 1.18, 12 isoindigo ID, 1.19, perylene diimides PDIs, 1.20, naphthalene diimides NDIs, 1.21,13 were extensively used. Small acceptor molecules having multiple electron withdrawing fluoro, cyano groups such as 7,7,8,8-tetracyanoquinodimethane TCNO, 1.22, 2,5-difluoro-7,7,8,8tetracyanoquinodimethane F₂TCNQ, 1.23, 2,3,5,6-difluoro-7,7,8,8-tetracyanoquinodimethane 1,2,5-thiadiazolotetracyanoquinodimethane SNTCNO, bis(dicyanomethylene)-4,8-dihydrobenzo[1,2-b:4,5-b']-dithiophene **DTTCNQ**, **1.26**, 2,5dimethyl-7,7,8,8-tetracyanoquinodimethane DMTCNQ, 1.27, 2,5-dimethydicyanoquinonediimine DMDCNQI, 1.28, malononitrile, and cyanoacetic acid have also been commonly employed in OFETs and organic photovoltaic applications. ¹⁴ Representative small molecule acceptors are provided in Figure.1.3.

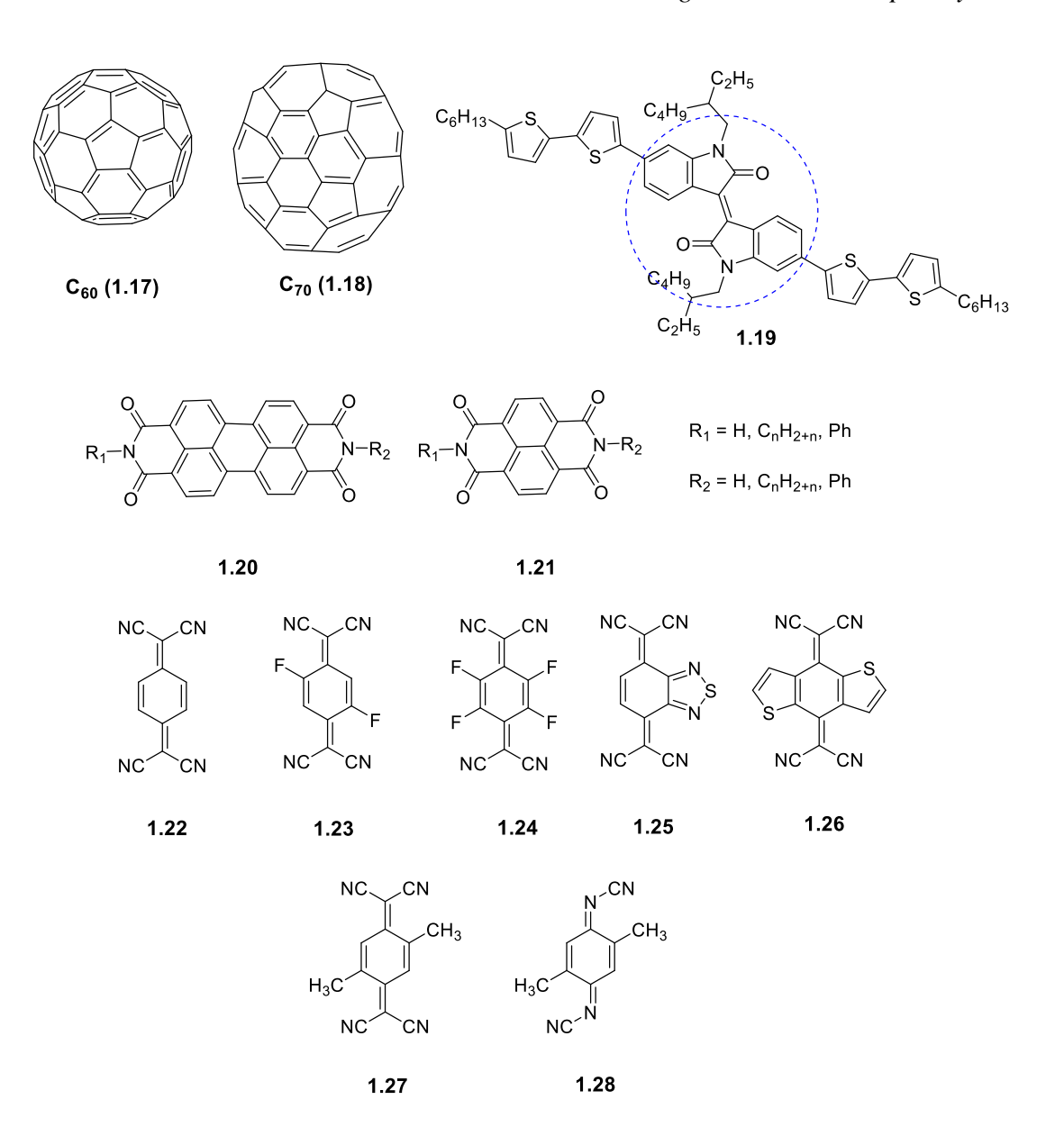


Figure 1.3. Chemical structures of representative dye-based acceptors molecules (dotted circle indicates the acceptor moiety).

1.4 Bridges

Bridges are usually conjugated π -systems capable of transporting the charge. Considerable amount of work has been carried out to evaluate the electron transfer properties of bridge molecules in D-B-A systems such as, oligo ethylene **OE**, **1.29**, oligo vinylenes **OV**, **1.30**, oligo-p-phenylene **OP**, **1.31**, oligo-2,7-fluorenes **OF**, **1.32**, oligothiophenes **OTP**, **1.33**, oligo-p-phenylenevinylenes **OPV**, **1.34** and oligo-p-phenylene ethynylene **OPE**, **1.35** in donor-bridge-acceptor (**D-B-A**) systems. ¹⁵ The structures of these bridges are given in Figure 1.4.

Figure 1.4. Structures of representative bridge moieties for electron transfer processes.

1.5 Applications of Donor-Acceptor Systems

Donor-acceptors systems have vastly been applied in developing different optoelectronic devices and in the field of biology due to their tunable optical properties, economic synthesis, easy isolation, flexibility, lightweight properties, and metal-free nature. As a result, researchers have paid much attention to develop different types of donor-acceptor systems using different kinds of bridge molecules for numerous applications such as dye-sensitized solar cells (DSSCs), organic light-emitting diodes (OLEDs), organic field-effect transistors (OFETs), organic photovoltaic devices (OPVs), optoelectronics, bio-imaging and sensors etc. The following sections give a brief information on the applications of the donor-acceptor systems in the prominent field.

1.5.1 Application in Organic Photovoltaics (OPVs)

The organic photovoltaics can convert light energy into electrical energy by using a semiconducting material. The photovoltaic research has started since 1950, using various organic and inorganic semiconductors. In 1986, the first donor-acceptor based OPV device was made by Tang. The device was constructed based on a bilayer hetero-junction type solar cell, and it was found to produce 1% solar power efficiency. Copper phthalocyanine (CuPc) and perylene tetracarboxylic acid derivatives (PV) were used as donor and acceptor respectively in this study.

Pc (1.36) PV (1.37)
$$\eta = 1\%$$
, Tang

Figure 1.5. Donor acceptor molecules used by Tang for OPV applications.

In 1991, Hiramoto *et al.*^{16b} had developed a three-layered OPV device in which the interlayer is made up of donor-acceptor interfaces using mixed pigments. The pigments at the interlayer acted as a highly efficient carriers of photogeneration. In 1995, Yu *et al.*^{16c} and Halls *et al.*,^{16d} independently, developed bulk heterojunction concept, and the donors and acceptors were used in bulk volume. The efficiencies of OPVs made based on this concept increased significantly. In the year of 2011, Dodabalapur and co-workers^{17a} reported an efficiency of 2.54% PCE using poly[4,7-bis-(3-dodecylthiophene-2-yl) benzothiadiazole-co-thiophene **PT3B1/PC**₇₀**BM** [6,6] phenyl-C71-butyric acid methyl ester **1.38** and **1.39** in the ratio of 1:4.

$$\begin{array}{c} \text{S-N} \\ \text{T3B1 polymer (1.38)} \\ \text{Dodabalapur and co-workers} \\ \\ \text{PC}_{70}\text{BM (1.39)} \\ \text{Dodz}_{12}\text{H}_{25} \\ \text{pC}_{12}\text{H}_{25} \\ \text{pCzs, X= S (η = 3.28 %, 1.40)} \\ \text{pCzse, X= Se (η = 3.52 %, 1.41)} \\ \text{pBDTS, X= Se (η = 3.05 %, 1.43)} \\ \text{Chen et $al.} \\ \text{Che$$

NC
$$\int_{N_{2}}^{N_{2}}$$
 $\int_{N_{2}}^{N_{2}}$ $\int_{N_{2}}^{N_{2}}$

Sharma and co-workers

Figure 1.6. Representative donor-acceptor systems for bulk heterojunction (BHJ) OPV applications.

Chen *et al.*^{17b} have developed new systems wherein the donor and acceptor are part of the polymer chain. They developed polymer containing thiophene- and selenophene-bridged donor-acceptor system of carbazole and benzo[1,2-b:4,5-b']dithiophene donor and benzo[c][1,2,5]benzothiadiazole acceptor. These systems resulted in a PCE of 3.05%-3.52%. In 2013, Sharma and co-workers^{17c} designed an A-D-A system using dithienylcarabazole donor and nitrophenylacrylonitrile acceptor **1.45**. This system along with PC₇₀BM showed and improved solar power conversion efficiency of 4.96%.

Nguyen and co-workers^{17d} reported an OPV device based on phenyl substituted diketopyrrolopyrroles and PC₇₁BM donor-acceptor system in 60:40 ratio to produce a PCE of 3.45%. Furthermore, Narayan and co-workers^{17e} have reported 3.2% PCE from a thiophene donor polymer and perylene acceptor based bulk heterojunction solar cell. In 2016, Vaidya and co-workers^{18a} produced a PCE of 6.53% from a bulk heterojunction solar cell based on dithieno pyrrole and butyl rhodamine with fullerene derivatives (A-D-D-A). Naphthothiadiazole and benzodithiophene-containing donor-acceptors connected via graphenic nanosheets produced 4.44- 4.78% efficiency as reported by Agbolaghi.^{18b}

1.5.2 Donor-Acceptor Systems in Dye-Sensitized Solar Cells (DSSCs)

Dye-sensitized solar cells (DSSCs) are the devices that can convert solar energy into electricity by using organic/inorganic dyes. In 1991, based on a breakthrough research, Gratzel and co-workers reported an inorganic solar cell based on the ruthenium complex (Black dye, **1.46**), accomplishing a power conversion efficiency of 7.1-7.9%. Later, 10% efficiency of

ruthenium-based black was reported by the same group. The ruthenium-based dyes entirely act as p-n junction inorganic solar cells.¹⁹

TBA⁺—OOC

N-Ru-N=C=S

TBA⁺—OOC

$$\eta = 7.1-7.9\%$$
 (1.46)

Black Dye

Figure. 1.7 Ruthenium based black dye.

The donor-acceptor based organic dye-sensitized solar cells have received much attention in the recent years, thanks to low-cost, high flexibility, metal-free nature and facile synthesis of organic dyes. Although these are several reports in the DSSC using different donor-acceptor systems, a few of the significant systems that are relevant to the present work are presented here. In 2003, Arakawa and co-workers^{20a} reported coumarin based organic dyes for application in DSSC. In this system, coumarin moiety acts as donor and cyanoacetic acid acts as acceptor connected through thiophene. The new designed donor-acceptor molecule has produced 7.7 % PCE 1.47. Yanagida and co-workers^{20b} have reported a PCE of 6.6% using a donor-acceptor system 1.48 having bisdiethylphenylamine donor and cyanoacetic acid acceptor linked through a conjugated triene moiety. Also, Hara and co-workers^{20c} have reported donor-acceptor based hexylthiophene functionalized carbazole dyes 1.49 performed in the DSSC for the power conversion efficiency 8.3%.

Furthermore, Misra *et al.*^{21a} have achieved a power conversion efficiency of 4.96% from a DSSC using ferrocene substituted triphenylamine based donor-acceptor (D-A) system **1.50**. In 2015, Gratzel and co-workers^{21b} produced 7.20% of PCE by using a D-A system based on triphenylamine π -conjugated with cyanoacetic acid through a phenothiazine bridge **1.51**. Following this, Hua and co-workers ^{21c} reported a 7.23% of PCE from indeno-thiophene based green (D-A- π -A) sensitizer **1.52**.

Electron donor (DTPC) Electron acceptor (BTEBA)
$$C_{6}H_{13} \qquad C_{6}H_{13} \qquad C_{6}H_$$

Figure 1.8. Structures of representative donor-acceptor systems for DSSC applications.

Shao and co-workers^{22a} have synthesized and studied the properties of dithienopicenocarbazole-based organic dyes **1.53** for DSSC applications. The dyes performed well to produce 13.0% of power conversion efficiency. Zheng and co-workers^{22b} have reported triazatruxene-based organic dye sensitizer for the application of DSSC. The organic dyes were generating 7.51% of maximum power conversion efficiency **1.54**.

1.5.3 Organic Donor-Acceptor in Organic Light-Emitting Diodes (OLEDs)

The emissive electroluminescent properties of certain organic compounds, when they are made as thin film emit light in response to an electric current. These compounds are classified as an organic light-emitting diodes (OLEDs) and also known as an organic EL (Electroluminescent) diode. Organic dyes with donor-acceptor systems have widely been investigated for their organic light-emitting diode (OLEDs) applications due to their high fluorescence, electroluminescent and high semiconducting properties. With organic molecules, a possibility towards the selection of emission colors, particularly in blue, green, yellow, and red regions were reported.²³ Adachi and co-workers^{24a} have reported the synthesis and OLED application of multi-layered triphenylamine and 1,3,4-oxadiazole based organic donor-acceptor system 1.55. Later, Lee and co-workers^{24b} reported red dopants constructed with chromene-containing donor-acceptor systems for OLED application. In this work, the 4-

dicyanomethylene-chromene moiety acts as an acceptor and julolidine, and triphenylamine acts as donor unit **1.56**.

Vaidyanathan and co-workers

Figure 1.9. Representative donor-bridge-acceptor systems for OLED applications.

D'Aleo *et al.*^{25a} have developed chalcone and curcuminoid based fluorescent dyes for application as OLED **1.57**. Also, García-Frutos and coworkers^{25b} have designed and synthesized azaindole connected triphenylamine based donor-acceptor system for organic light-emitting diode application **1.58**. Huang and coworkers^{25c} have reviewed concisely various

donor-acceptor systems for OLED applications. This report is devoted to -CN containing molecules such as mono or multi -CN groups attached aromatic rings, heterocycles, and acrylonitrile derivatives for the application as OLED materials **1.59** and **1.60**. Thomas and coworkers^{26a} have synthesized and studied the photophysical properties of carbazole-based emitters. The carbazole chromophore in responsible for the OLED properties in these systems. Patra and co-workers^{26b} have synthesized and studied the photophysical properties of donor-acceptors based on benzothiadiazole and benzotriazole acceptors with fluorene donors for the organic light-emitting diode application. Yellowish-orange light-emitting electron-deficient phenone incorporated electron-rich triphenylamine derivatives were designed and developed by Vaidyanathan and co-workers **1.61** and **1.62**.²⁷

1.5.4 Organic Donor-Acceptors in Organic Field-Effect Transistors (OFETs) and Organic Thin-Film Transistors (OTFTs)

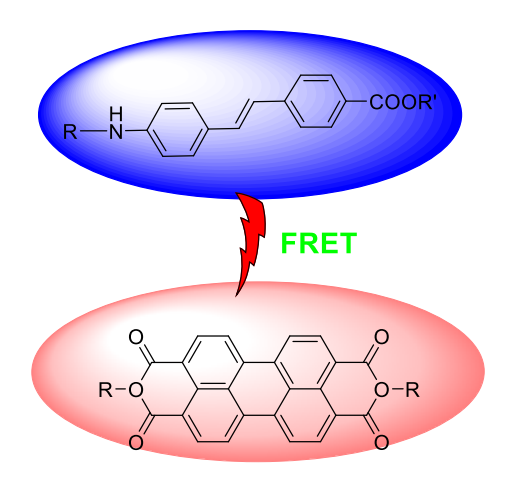
The field-effect transistors (OFETs) are a kind of transistor, which, by using electric field, control the flow of current. Organic field-effect transistors (OFETs) are generally organic semiconductors. The transistors are used in signal amplifiers or off/on switches. A concise review of small molecule donor-acceptors based organic field emitting transistors has been published by Brooks.^{28a} This review covers the application of small molecules such as pentacene, perylene, Buckminsterfullerene, tetrathiafulvalene (TTF), tetracyanoquinodimethane (TCNQ) and rubrene (tetraphenylnaphthacene) as OFET materials.

Figure 1.10. D- π -A- π -D systems for OFET applications.

Rao and co-workers.^{28b} have developed an unsymmetrical diketopyrrolopyrroles based D- π -A- π -D system for application in OFETs **1.63** and **1.64**. Recently, co-crystal-based donor-acceptor system as OFET material has been reported by Zhang *et al.*,^{28c} in which they studied different types of donor-acceptors such as porphyrin, perylene, TCNQ, coronene, etc.

1.5.5 Applications of Organic Donor-Acceptors in Fluorescence Resonance Energy Transfer (FRET)

The fluorescence resonance energy transfer (FRET) is a nonradioactive energy transfer from a donor moiety to an acceptor moiety. The FRET is also known as a Forster resonance energy transfer. FRET molecules can be used in biomedical research and drug discovery. The donor-acceptor based organic molecules have extensively been used as fluorescence resonance energy transfer materials. In 2006, Medintz and co-workers^{29a} have reviewed small-molecule fluorophores having FRET applications. Few of the significant donor-acceptor based systems for FRET applications have discussed briefly in the following section. Ajayaghosh *et al.*^{29b, 29c} have developed donor-acceptor based supramolecular structure of donor self-assembly with tuneable emission shift. Further, they have studied the light-harvesting applications by using organogels as a scaffold for the excitation energy transfer. Banerjee and coworkers^{29d} have investigated the resonance energy transfer from stilbene-perylene based donor-acceptor materials **1.65**.



Banerjee and co-workers (1.65)

Figure 1.11. A representative donor-acceptor system for the FRET application.

Bhattacharya and co-workers^{29e} have reported a pyrazoline–doxorubicin-based donor-acceptor molecule as a FRET-based biosensor having application in live-cell imaging. Bhattacharyya and co-workers^{30a} developed FRET-based donor-acceptor systems for application in biological field. The designed molecules have been found to bind to the human serum with native and non-native states. Bag *et al.*^{30b} have developed a triazolyl based donor-acceptor system for FRET application. In 2016, Huang and co-workers^{30c} have published a review on single-molecule fluorescence resonance energy transfer (smFRET) molecules for application in the field of molecular biology. It is a powerful technique for learning the

conformation dynamics and interactions of individual biomolecules. Also, Singh and co-workers^{30d} have reported redox-sensitive of xanthene-coumarin-chlorambucil based molecules for the FRET applications. In 2018, Banerjee *et al.*^{30e} designed donor-acceptor based conducting polymers {polymer light-emitting diode (PLED)} for FRET applications.

1.5.6 Applications of Donor-Acceptors in Optoelectronics

In addition to applications as OPVs, DSSCs, OLEDs, OTFTs materials, organic donor-acceptors find applications in optoelectronic device also. Optoelectronics is a subfield of photonics. It is the study and application of electronic device and system that involves light in any form like sources, control, and detector. Yang and co-workers^{31a} have reported a donor-acceptor based tetrathiafulvalene and fullerene derivatives for application in memory devices with electrical bistability. Pal and co-workers^{31b} have developed D/A and A/D assemblies for the field of optoelectronics and investigated the substituent effects. In 2008, Jenekhe and co-workers^{31c} synthesized didecyloxyphenylene (donor) based copolymers for optoelectronic applications and the donor didecyloxyphenylene has been studied with different acceptors such as, thieno-pyrazine, benzothiadiazole, quinoxaline, pyridine, etc.

PI(AMTPA) (x:y=0:100) PI(AMTPA95-APAP5) (x:y=5:95) PI(AMTPA90-APAP10) (x:y=10:90) PI(APAP) (x:y=100:0)

PI- Polyimide AMTPA-4,4'-diamino-4"-methyltriphenylamine APAP-N,N-bis(4-aminophenyl)aminopyrene

Chen and co-workers

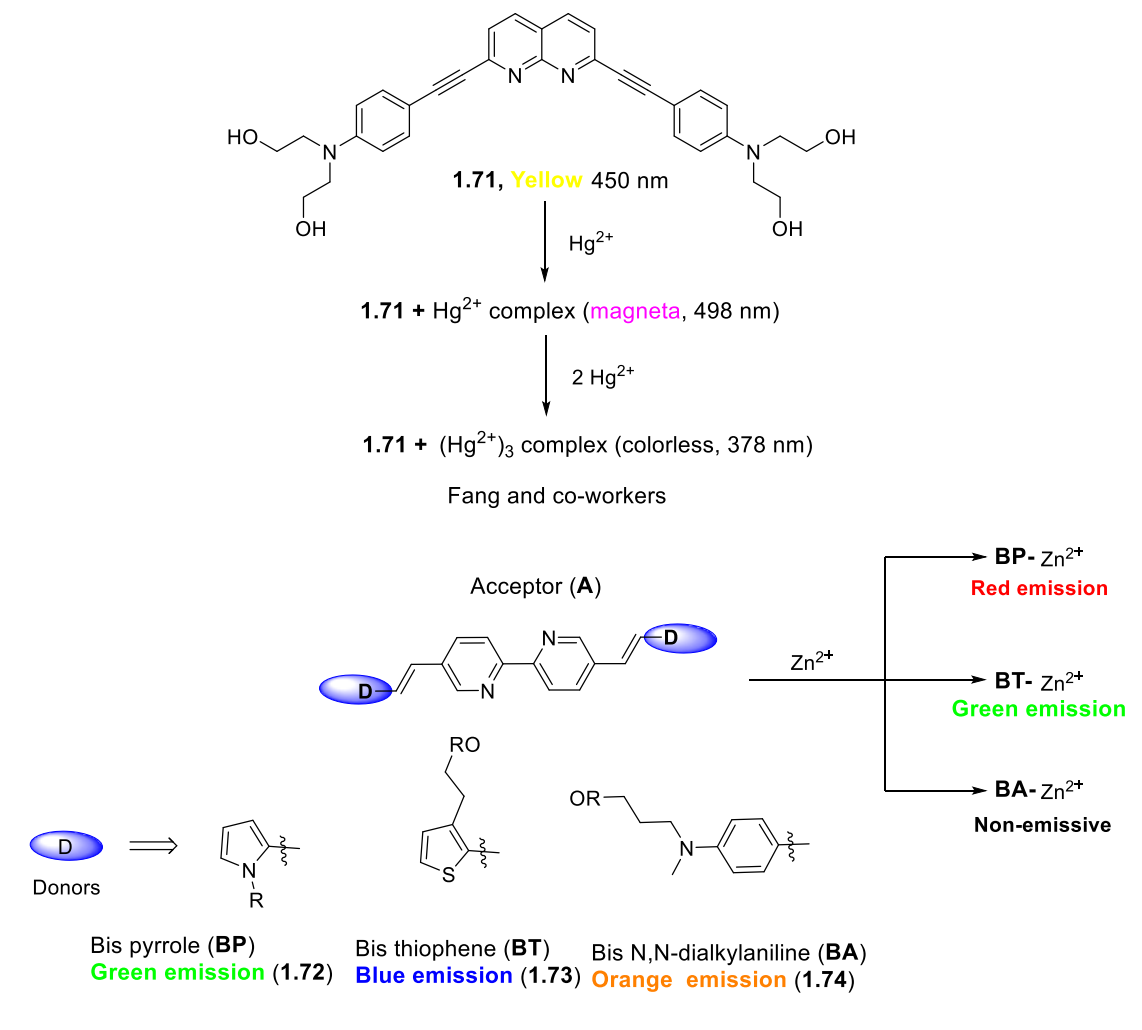
Figure 1.12. Structures of representative donor-acceptor molecules for optoelectronic applications.

Triphenylamine-pyrene incorporated donor-acceptor systems were reported by Chen and co-workers^{31d} for the application in an organic polymer-based electrical memory device **1.66** and **1.67**. Zhu and co-workers^{31e} developed β -functionalized imidazole attached porphyrin complexes **1.68-1.70**. It has shown prominent photovoltaic and optoelectronic properties.

1.5.7 Donor-Acceptors as Sensors

Donor-acceptor compounds, due to their tunable photophysical properties, find widespread application as sensor. The sensor is a device that can recognize the physical phenomena of light, moisture, heat, pressure, and other environmental factors, etc. Its output is a human-readable display or transmitted electronically over network signals. To date, a large number of organic donor-acceptor based sensors are known. A few of them have been discussed below. In 2005, Fang and co-workers^{32a} designed a D-A-D system comprising of ethynyl unit bridged to central naphthyridine with two di(hydroxyethyl)aniline moieties at terminal of the molecule **1.71** (Figure.1.13) and used it for the detection of mercury ions. Bharadwaj and co-workers^{32b} have reported the dimethyaminophenyl and diazine based donor-acceptors for the detection of Ag⁺ ions. Ajayaghosh and co-workers^{32c} have reported donor-acceptor-donor based fluorophores for sensor application to detect zinc ions **1.72-1.74**. In addition, these compounds were found to have cell-imaging applications. In 2014, Thilagar and co-workers^{32d} developed

a system in which a triphenylamine (donor) is incorporated with two acceptor groups, a diaryl boron and a BODIPY. This system (1.75 and 1.76) is chromogenic and fluorogenic and could be employed for fluoride ion recognition. Mukherjee and co-workers^{32e} have reported small molecule-based turn-off fluorescent sensors for the detection of nitroaromatic explosive materials. Yin and co-workers have reported an aqueous fluorescent probe for cyanide detection by using triphenylamine derivatives 1.77 and 1.78.^{32f}



Ajayaghosh and co-workers

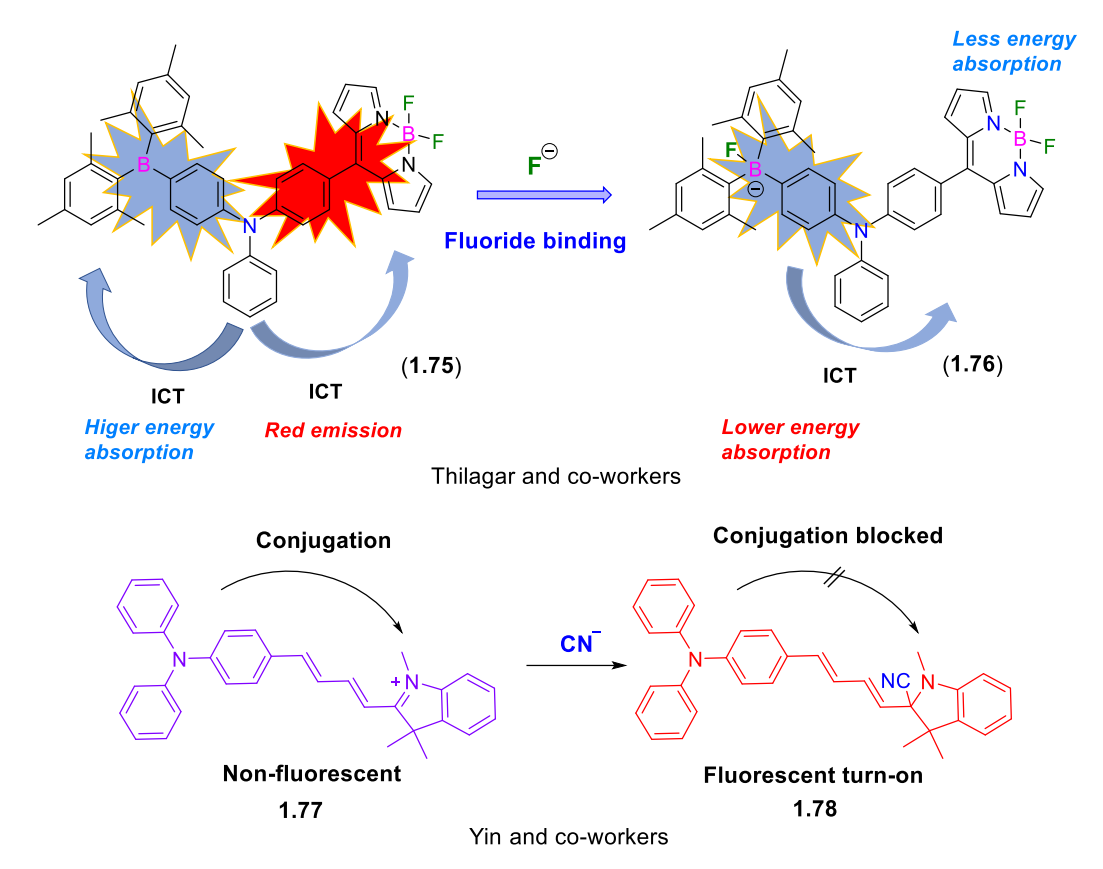


Figure 1.13. Representative donor-acceptor based sensors.

Zang and co-workers^{33a} have reported the detection of alkane vapours by using a nanofibril donor-acceptor composite of carbazole-perylene derivatives. In 2018, perylene diimides derivatives were used for the detection of hydrazine by Jin and co-workers, in which perylene acts as an acceptor and piperidyl, pyrrolidinyl, and n-hexylamino are attached in perylene core..^{33b} Further, Su and co-workers^{33c} have developed polymer film based isoindigo donor-acceptor system for the detection of ammonia. Dhamodharan and co-workers^{33d} have reported efficient recognition of Cu(II) ion by using with triphenylamine and phenothiazine-based donor-acceptor systems.

1.5.8 Applications of Donor-Acceptors in Bio-Imaging

Bio-imaging is another important field where donor-acceptor compounds find a significant application. In many cases, these probes are useful for decisive prediction of the biochemical process. Bio-imaging is a noninvasive technique for visualizing biological processes in real-time. It is a powerful tool for detecting the internal functions of the body and diseases. In 2013, Tan and co-workers^{34a} synthesized two-photon fluorescent donor- π -acceptor probes based on naphthalene core for the detection of H₂S in HeLa liver cells **1.79-1.80**. Chow^{34b} has reported two-photon emissive thiophene based donor-acceptor molecules for *in vitro* live-cell imaging. Moreover, Zhou and co-workers^{34c} have developed dipyridyl acceptor unit with six different

types of donor units such as, carbazole, anthracene, triazole, (4,4-diethoxyphenyl)amino, imidazole, and diphenylamine connected through π -spacer for the application in live-cell imaging. The compounds having diphenylamine and (4,4-diethoxyphenyl) amino donor units have strong fluorescence in the live cells **1.81-1.85**.

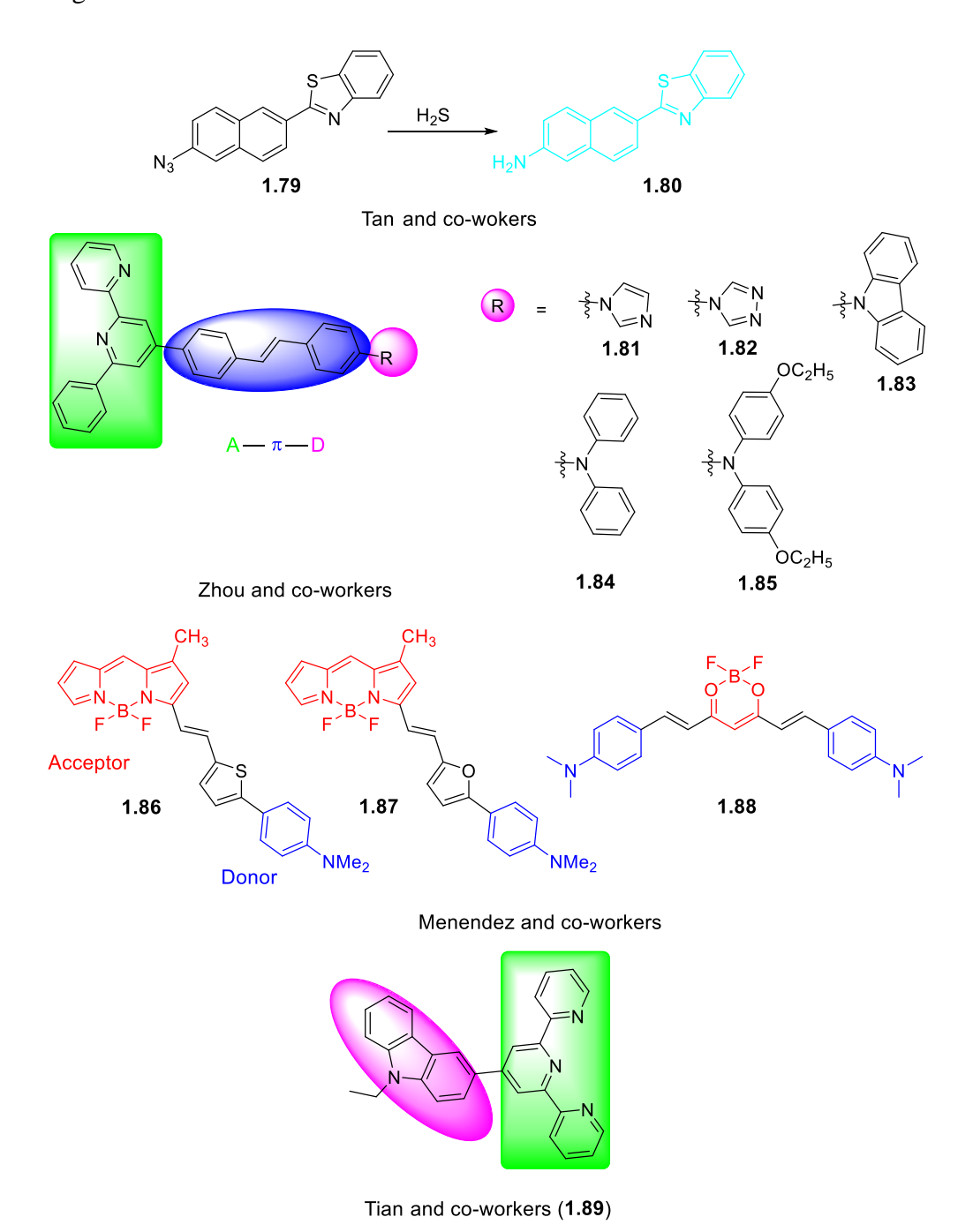


Figure 1.14. Representative donor-acceptor systems for bio-imaging applications.

In 2015, Menendez and co-workers^{34d} reported a review on near-infrared fluorescent molecules for *in vivo* bio-imaging applications. Particularly, the bio-imaging of β -amyloid plaques in Alzheimer's disease **1.86-1.88**. Tian and co-workers^{34e} have developed donor-

acceptor system based on Zn(II) complex of terpyridine attached carbazole for the application of HepG2 live-cell imaging.

1.6. Our Present Work

Over the years, so many donor-acceptor systems have been developed using different donors, acceptors, and bridges having different electronic properties and have been tested for various applications. We planned to make donor-acceptor systems in which the donor and the acceptor are linked through a 1,3-dicarbonyl bridge. The reason for choosing a 1,3-diketone bridge is as follows.

- 1. The 1,3-dicarbonyl can exit in the enolic form, which will ensure the conjugation between the donor and the acceptor. So, depending in the state it may act as an on/off for intramolecular charge transfer.
- 2. The 1,3-dicarbonyl can coordinate to metal ions. Hence, there is a possibility that it can bind to TiO₂ to test them in dye-sensitized solar cells (DSSC). The acceptor group will facilitate efficient electron transfer from the donor.
- 3. The electronic properties of these systems could be varied by making BF₂ complexes using the 1,3-dicarbonyl moiety.

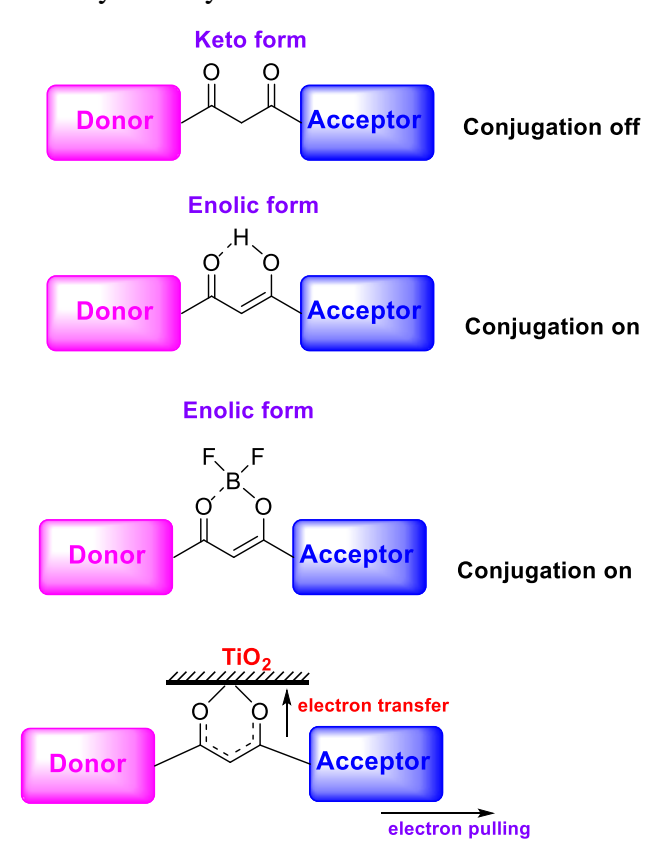


Figure 1.15. Structures of the planned 1,3-dicarbonyl bridged donor-acceptor systems.

Also, we wished to make bis-donor and multi acceptor-based donor- acceptor systems as having more donor and acceptor groups strongly influence the photophysical properties. With this idea, we planned to make the donor-acceptor systems using triphenylamine, carbazole donor, and dicyano, cyano acetic acid acceptors. Also, it was planned to incorporate thiophene units for better electron transportation.

Figure 1.16. Structures of the donors and acceptors used in this study.

1.7 References

- 1. (a) Albinsson, B.; Eng, M. P.; Pettersson, K.; Winters, M. U. *Phys. Chem. Chem. Phys.* **2007**, *9*, 5847. (b) Ratner, M. A.; Jortner, J. *Molecular Electronics A 'Chemistry for the 21st Century' Monograph*, Blackwell Science Ltd, Oxford, 1st edn, **1997**, p. 43.
- (a) O'Regan, B.; Gratzel, M. *Nature*, **1991**, *353*, 737. (b) Bach, U.; Lupo, D.; Comte, P.; Moser, J. E.; Weissortel, F.; Salbeck, J.; Spreitzer, H.; Gratzel, M. *Nature*, **1998**, *395*, 583.
 (c) Lin, Y.; Li, Y.; Zhan, X. *Chem. Soc. Rev.* **2012**, *41*, 4245.
- 3) (a) Tang, C. W.; Vanslyke, S. A.; Appl. Phys. Lett. 1987, 51, 913. (b) Burroughs, H.; Bradley, D. D. C.; Brown, A. R.; Marks, R. N.; Mackay, K.; Friend, R. H.; Burns, P. L.; Holmes, A. B. Nature 1990, 347, 539. (c) Kraft, A.; Grimsdale, A. C.; Holmes, A. B. Angew. Chem. 1998, 110, 416; Kraft, A.; Grimsdale, A. C.; Holmes, A. B. Angew. Chem. Int. Ed. 1998, 37, 402.
- 4) (a) Bao, Z.; Rogers, J. A.; Katz, E. J. Mater. Chem. 1999, 9, 1895. (b) Song, Y.; Di, C.; Yang, X.; Li, S.; Xu, W.; Liu, Y.; Yang, L.; Shuai, Z.; Zhang, D.; Zhu, D. J. Am. Chem. Soc. 2006, 128, 15940.

- 5) (a) Cui, Y.; Chen, Q.; Zhang, D.-D.; Cao, J.; Han, B.-H. *J. Polym. Sci. Part A: Polym. Chem*, **2010**, 48, 1310. (b) Wenfeng, L.; Hengchang, M.; Con, L.; Yuan, M.; Chunxuan, Q.; Zhonwei, Z.; Zengming, Y.; Haiying, C.; Ziqiang, L. *RSC Adv.* **2015**, 5, 6869. (c) Yang, X.; Chen, X.; Lu, X.; Yan, C.; Xu, Y.; Hang, X.; Qu, J.; Liu, R. *J. Mater. Chem. C*, **2016**, 4, 383.
- 6) (a) Shirota, Y. J. Mater. Chem. 2000, 10, 1. (b) Cravino, A.; Roquet, S.; Aleveque, O.; Leriche, P.; Frere, P.; Roncali, J. Chem. Mater. 2006, 18, 2584. (c) Hindson, J. C.; Ulgut, B.; Friend, R. H.; Greenham, N. C.; Norder, B.; Kotlewskic, A.; Dingemans, T. J. J. Mater. Chem. 2010, 20, 937.
- (a) Senge, M. O.; Fazekas, M.; Notaras, E. G. A.; Blau, W. J.; Zawadzka, M.; Locos, O. B.; Mhuircheartaigh, E. M. N. Adv. Mater. 2007, 19, 2737. (b) Ma, B.; Woo, C. H.; Miyamoto, Y.; Frechet, J. M. J. Chem. Mater. 2009, 21, 1413. (c) Kronenberg, N. M.; Deppisch, M.; Wurthner, F.; Lademann, H. W. A.; Deing, K.; Meerholz, K. Chem. Commun. 2008, 6489. (d) Silvestri, F.; Irwin, M. D.; Beverina, L.; Facchetti, A.; Pagani, G. A.; Marks, T. J. J. Am. Chem. Soc. 2008, 130, 17640. (e) Walker, B.; Tamayo, A. B.; Dang, X.-D.; Zalar, P.; Jung, P.; Seo, H.; Garcia, A.; Tantiwiwat, M.; Nguyen, T.-Q. Adv. Funct. Mater. 2009, 19, 3063.
- 8) (a) Rousseau, T.; Cravino, A.; Bura, T.; Ulrich, G.; Ziessel, R.; Roncali, J. *Chem. Commun.*2009, 1673. (b) Rousseau, T.; Cravino, A.; Bura, T.; Ulrich, G.; Ziessel, R.; Roncali, J. *J. Mater. Chem.* 2009, 19, 2298. (c) Mishra, A.; Uhrich, C.; Reinold, E.; Pfeiffer, M.; Bäuerle, P. *Adv. Energy Mater.* 2011, 1, 265. (d) Chen, J. J.-A.; Chen, T. L.; Kim, B. S.; Poulsen, D. A.; Mynar, J. L.; Frechet, J. M. J.; Ma, B. *ACS Appl. Mater. Interfaces* 2010, 2, 2679. (e) Wu, W.; Liu, Y.; Zhu, D. *Chem. Soc. Rev.* 2010, 39, 1489.
- 9) He, C.; He, Q.; He, Y.; Lia, Y.; Bai, F.; Yanga, C.; Ding, Y.; Wang, L.; Ye, J. Sol. Energy Mater. Sol. Cells **2006**, *90*, 1815.
- 10) Zhou, E.; Yamakawa, S.; Zhang, Y.; Tajima, K.; Yang, C.; Hashimoto, K. *J. Mater. Chem.* **2009**, *19*, 7730.
- 11) Liang, M.; Chen, J. Chem. Soc. Rev. 2013, 42, 3453.
- 12) He, Y.; Li. Y. Phys. Chem. Chem. Phys. 2011, 13, 1970.
- (a) Mei, J.; Graham, K. R.; Stalder, R.; Reynolds, J. R. Org. Lett. 2010, 12, 660.
 (b) Anthony, J. E.; Facchetti, A.; Heeney, M.; Marder, S. R.; Zhan, X. Adv. Mater. 2010, 22, 3876.
 (c) Choi, H.; Paek, S.; Song, J.; Kim, C.; Cho, N.; Ko, J. Chem. Commun. 2011, 47, 5509.
- 14) Zhang, J.; Xu, W.; Sheng, P.; Zhao, G.; Zhu, D. Acc. Chem. Res. 2017, 50, 1654.

- 15) (a) Albinsson, B.; Eng, M. P.; Pettersson, K.; Winters, M. U. *Phys. Chem. Chem. Phys.*2007, 9, 5847. (b) Gilbert, M.; Albinsson, B. *Chem. Soc. Rev.* 2015, 44, 845.
- 16) (a) Tang, C. W. Appl. Phys. Lett. 1986, 48, 183. (b) Hiramoto, M.; Fujiwara, H.; Yokoyama, M. Appl. Phys. Lett. 1991, 58, 1062. (c) Yu, G.; Gao, J.; Hummelen, J. C.; Wudi, F.; Heeger, A. J. Science 1995, 270, 1789. (d) Halls, J. J. M.; Walsh, C. A.; Greenham, N. C.; Marseglia, E. A.; Friend, R. H.; Morattlt, S. C.; Holmest, A. B. Nature, 1995, 376, 498.
- (a) Sonar, P.; Williams, E. L.; Singh, S. P.; Dodabalapur, A. *J. Mater. Chem.* 2011, 21, 10532. (b) Chen, H.-Y.; Yeh, S.-C.; Chen, C.-T.; Chen, C.-T. *J. Mater. Chem.* 2012, 22, 21549. (c) Singh, M.; Kurchania, R.; Mikroyannidis, J. A.; Sharma, S. S.; Sharma, G. D. *J. Mater. Chem. A* 2013, 1, 2297. (d) Lin, J. D. A.; Liu, J.; Kim, C.; Tamayo, A. B.; Proctor, C. M.; Nguyen, T.-Q. *RSC Adv.* 2014, 4, 14101. (e) Shivanna, R.; Shoaee, S.; Dimitrov, S.; Kandappa, S. K.; Rajaram, S.; Durrant, J. R.; Narayan, K. S. *Energy Environ. Sci.* 2014, 7, 435.
- (a) Busireddy, M. R.; Mantena, V. N. R.; Chereddy, N. R.; Shanigaram, B.; Kotamarthi, B.; Biswas, S.; Sharma, G. D.; Vaidya, J. R. *Phys. Chem. Chem. Phys.* **2016**, *18*, 32096.
 (b) Agbolaghi, S. *New J. Chem.* **2018**, *42*, 20041.
- 19) O'Regan, B.; Gratzel, M. *Nature*, **1991**, *353*, 737.
- 20) (a) Hara, K.; Kurashige, M.; Dan-oh, Y.; Kasada, C.; Shinpo, A.; Suga, S.; Sayamaa, K.; Arakawa, H. New J. Chem. 2003, 27, 783. (b) Kitamura, T.; Ikeda, M.; Shigaki, K.; Inoue, T.; Anderson, N. A.; Ai, X.; Lian, T.; Yanagida, S. Chem. Mater. 2004, 16, 1806. (c) Wang, Z.-S.; Koumura, N.; Cui, Y.; Takahashi, M.; Sekiguchi, H.; Mori, A.; Kubo, T.; Furube, A.; Hara, K. Chem. Mater. 2008, 20, 3993.
- 21) (a) Misra, R.; Maragani, R.; Patel, K. R.; Sharma, G. D. *RSC Adv.* **2014**, *4*, 34904. (b) Antony, M. P.; Moehl, T.; Wielopolski, M.; Moser, J.-E.; Nair, S.; Yu, Y.-J.; Kim, J.-H.; Kay, K.-Y.; Jung, Y.-S.; Yoon, K. B.; Gratzel, C.; Zakeeruddin, S. M.; Gratzel, M. *ChemSusChem* **2015**, *8*, 3859. (c) Shen, Z.; Chen, J.; Li, X.; Li, X.; Zhou, Y.; Yu, Y.; Ding, H.; Li, J.; Zhu, L.; Hua, J. *ACS Sustainable Chem. Eng.* **2016**, *4*, 3518.
- (a) Yang, Z.; Liu, C.; Li, K.; Cole, J. M.; Shao, C.; Cao, D. ACS Appl. Energy Mater.
 2018, 4, 1435. (b) Pan, B.; Zhu, Y.-Z.; Ye, D.; Li, F.; Guo, Y.-F.; Zheng, J.-Y. New J. Chem. 2018, 42, 4133.
- 23) (a) Tang, C. W.; VanSlyke, S. A. *Appl. Phys. Lett.* **1987**, *51*, 913. (b) Adachi, C.; Tsutsui, T.; Saito, S. *Appl. Phys. Lett.* **1990**, *56*, 799.

- 24) (a) Tamoto, N.; Adachi, C.; Nagai, K. Chem. Mater. 1997, 9, 1077. (b) Zhang, X. H.; Chen, B. J.; Lin, X. Q.; Wong, O. Y.; Lee, C. S.; Kwong, H. L.; Lee, S. T.; Wu, S. K. Chem. Mater. 2001, 13, 1565.
- (a) D'Aléo, A.; Felouat, A.; Fages, F. Adv. Nat. Sci: Nanosci. Nanotechnol. 2015, 6, 015009.
 (b) Martin, C.; Borreguero, C.; Kennes, K.; Auweraer, M. V.; Hofkens, J.; Miguel, G.; García-Frutos, E. M. ACS Energy Lett. 2017, 2, 2653.
 (c) Cao, X.; Zhang, D.; Zhang, S.; Tao, Y.; Huang, W. J. Mater. Chem. C 2017, 5, 7699.
- 26) (a) Joseph, V.; Thomas, K. R. J.; Singh, M.; Sahoo, S.; Jou, J.-H. Eur. J. Org. Chem.
 2017, 6660. (b) Islam, S. N.; Sil, A.; Patra, S. K. Dalton Trans. 2017, 46, 5918.
- 27) Kajjam, A. B.; Kumar, P. S. V.; Subramanian, V.; Vaidyanathan, S. *Phys. Chem. Chem. Phys.* **2018**, *20*, 4490.
- 28) (a) Brooks, J. S. *Chem. Soc. Rev.* **2010**, *39*, 2667. (b) Bharath, D.; Chithiravel, S.; Sasikumar, M.; Chereddy, N. R.; Shanigaram, B.; Bhanuprakash, K.; Krishnamoorthy, K.; Rao, V. J. *RSC Adv.* **2015**, *5*, 94859. (c) Zhang, J.; Jin, J.; Xu, H.; Zhang, Q.; Huang, W. *J. Mater. Chem. C*, **2018**, *6*, 3485.
- (a) Sapsford, K. E.; Berti, L.; Medintz, I. L. Angew. Chem. Int. Ed. 2006, 45, 4562. (b) Ajayaghosh, A.; Vijayakumar, C.; Praveen, V. K.; Babu, S. S.; Varghese, R. J. Am. Chem. Soc. 2006, 128, 7174. (c) Ajayaghosh, A.; Praveen, V. K.; Vijayakumar, C. Chem. Soc. Rev. 2008, 37, 109. (d) Maiti, D. K.; Bhattacharjee, R.; Datta, A.; Banerjee, A. J. Phys. Chem. C 2013, 117, 23178. (e) Rana, D. K.; Dhara, S.; Bhattacharya, S. C. Phys. Chem. Chem. Phys. 2014, 16, 5933.
- 30) (a) Chowdhury, R.; Chattoraj, S.; Mojumdar, S. S.; Bhattacharyya, K. *Phys. Chem. Chem. Phys.* 2013, *15*, 16286. (b) Bag, S. S.; Jana, S.; Yashmeen, A.; Senthilkumar, K.; Bag, R. *Chem. Commun.* 2014, *50*, 433. (c) Sasmal, D. K.; Pulido, L. E.; Kasal, S.; Huang, J. *Nanoscale*, 2016, *8*, 19928. (d) Gangopadhyay, M.; Mengji, R.; Paul, A.; Venkatesh, Y.; Vangala, V.; Jana, A.; Singh, N. D. P. *Chem. Commun.* 2017, *53*, 9109. (e) Banerjee, D.; Kar, A. K. *Phys. Chem. Chem. Phys.* 2018, *20*, 23055.
- 31) (a) Chu, C. W.; Ouyong, J.; Tseng, J.-H.; Yang, Y. *Adv. Mater.* **2005**, *17*, 1440. (b) Mukherjee, B.; Mohanta, K.; Pal, A. J. *Chem. Mater.* **2006**, *18*, 3302. (c) Liu, C.-L.; Tsai, J.-H.; Lee, W.-Y.; Chen, W.-C.; Jenekhe, S. A. *Macromolecules* **2008**, *41*, 6952. (d) Yu, A.-D.; Kurosawa, T.; Lai, Y.-C.; Higashihara, T.; Ueda, M.; Liu, C.-L.; Chen, W.-C. *J. Mater. Chem.* **2012**, *22*, 20754. (e) Bodedla, G. B.; Wang, H.; Chang, S.; Chen, S.; Chen, T.; Zhao, J.; Wong, W.-K.; Zhu, X. *ChemistrySelect* **2018**, *3*, 2558.

- 32) (a) Huang, J.-H.; Wen, W.-H.; Sun, Y.-Y.; Chou, P.-T.; Fang, J.-M. *J. Org. Chem.* 2005, 70, 5827. (b) Ray, D.; Iyer, E. S. S.; Sadhua, K. K.; Bharadwaj, P. K. *Dalton Trans.* 2009, 5683. (c) Sreejith, S.; Divya, K. P.; Jayamurthy, P.; Mathew, J.; Anupama, V. N.; Philips, D. S.; Aneesa, P.; Ajayaghosh, A. *Photochem. Photobiol. Sci.* 2012, 11, 1715. (d) Swamy, P. C. A.; Thilagar, P. *Inorg. Chem.* 2014, 53, 2776. (e) Shanmugaraju, S.; Mukherjee, P. S. *Chem. Commun.* 2015, 51, 16014. (f) Huo, F.; Kang, J.; Yin, C.; Chao, J.; Zhang, Y. *Sens. Actuators B* 2015, 215, 93–98.
- (a) Wang, C.; Bunes, B. R.; Xu, M.; Wu, N.; Yang, X.; Gross, D. E.; Zang, L. ACS Sens.
 2016, 1, 552. (b) Huang, Y.; Zhang, S.; Zhong, G.; Li, C.; Liu, Z.; Jina, D. Phys. Chem. Chem. Phys. 2018, 20, 19037. (c) Lu, C.-F.; Shih, C.-W.; Chen, C.-A.; Chin, A.; Su, W.-F. Adv. Funct. Mater. 2018, 1803145. (d) Anand, V.; Sadhasivam, B.; Dhamodharan, R. New J. Chem. 2018, 42, 18979.
- 34) (a) Mao, G.-J.; Wei, T.-T.; Wang, X.-X.; Huan, S.-y.; Lu, D.-Q.; Zhang, J.; Zhang, X.-B.; Tan, W.; Shen, G.-L.; Yu, R.-Q. *Anal. Chem.* **2013**, *85*, 7875. (b) Chow, C.-F. *RSC Adv.* **2013**, *3*, 18835. (c) Jina, F.; Xua, D.-L.; Zhua, H.-Z.; Yana, Y.; Zheng, J.; Zhang, J.; Zhou, H.-P.; Wu, J.-Y.; Tiana, Y.-P. *Dyes Pigm.* **2014**, *109*, 42. (d) Staderini, M.; Martin, M. A.; Bolognesi, M. L.; Menendez, J. C. *Chem. Soc. Rev.* **2015**, *44*, 1807. (e) Kong, C.; Peng, M.; Shen, H.; Wang, Y.; Zhang, Q.; Wang, H.; Zhang, J.; Zhou, H.; Yang, J.; Wu, J.; Tian, Y. *Dyes Pigm.* **2015**, *120*, 328.

1,3-Dicarbonyl-Bridged Donor-Acceptor Compounds and Their BF₂ Complexes: Synthesis and Their Applications in Dye-Sensitized Solar Cells, Bio-imaging, and Cyanide Sensing

2

Abstract

This chapter gives an account of our efforts in synthesizing 1,3-dicarbonyl-bridged donor-acceptor systems and their corresponding BF₂ complexes and studying their applications in DSSC, live-cell imaging, and sensing. The donors employed in the systems are substituted triphenylamine and carbazole, and the main acceptor is dicyanovinylene moiety. Their photophysical and electrochemical properties have been evaluated. Though these compounds have been found be less efficient for DSSC applications have shown tremendous potential for selective and direct imaging of microtubulin network in live cells and cyanide sensing.

2.1 Introduction

The 1,3-dicarbonyl group is an interesting scaffold that has regularly been used in organic synthesis due to the active methylene group and in inorganic chemistry for making metal complexes due to its excellent chelating ability. Generally, 1,3-dicarbonyl compounds exist in keto-enol tautomerism. The position of the equilibrium depends on the nature of the solvent, temperature, etc. When a donor and an acceptor is bridged through a 1,3-dicarbonyl, it can act as an on/off switch for the intramolecular charge transfer. In the enolic form, smooth intramolecular charge transfer is expected. When the 1,3-dicarbonyl moiety is made to complex with BF₂, the corresponding complexed moiety can act as an acceptor as well, maintaining the intramolecular charge transfer. BF₂ complexes of β -ketonate, β -ketoiminate, diiminate, boronils, and boron dipyrromethene (BODIPY) have been prepared and studied for their optical properties and applications.

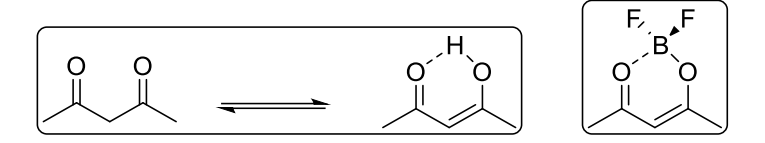


Figure 2.1. Structures of 1,3-dicarbonyl in keto-enol form and difluoro boron complex.

It is anticipated that if a donor and an acceptor are attached on either side of the 1,3-dicarbonyl, there will be effective intramolecular electron transfer to the 1,3-dicarbonyl moiety due to the pulling of electrons by the electron-withdrawing group. In this situation, if the 1,3-dicarbonyl is made coordinated to TiO₂ it can transfer the electron to the TiO₂ layer effciently.



Figure 2.2 Design of new donor-acceptor system.

With this plan, a series of donor-acceptor systems were synthesized. Donors such as triarylamine and carbazole were employed as they have promising election donating property and have widely been used to make donor-acceptor systems for various applications.^{1, 2} In a couple of compounds, long-chain alkoxy groups were introduced in order to minimize aggregation issues encountered generally with aromatic rings. The synthesized compounds have been characterized by various analytical techniques. Based on their photophysical properties, they were tested for their application in DSSC, live-cell imaging, and sensing.

Figure 2.3. Structures of synthesized donor-acceptor systems.

2.2 Synthesis of 1,3-Dicarbonyl Bridged Donor-Acceptor Systems

The synthesis of the 1,3-dicarbonyl bridged donor-acceptor systems involve Claisen ester condensation and palladium-catalyzed coupling reactions as the key reactions. The ester was kept on the donor moiety (triarylamine and carbazole), and the methyl ketone was kept on the aryl, which was eventually attached to the acceptor.

The synthesis of compounds **2.1** and **2.2** was started from commercially available triphenylamine. It was converted into methyl (4-diphenylamino)benzoate, **2.9** in three steps involving formylation, oxidation, and esterification, as shown in Scheme 2.1.^{3a, 3b} Compound **2.9** was treated with aryl methyl ketones **2.10** and **2.12** to make corresponding 1,3-dicarbonyl

compounds **2.11** and **2.13**. These compounds were then coupled with **2.17** under Stille coupling conditions to make the donor-acceptor compounds **2.1** and **2.2**. The aryltin reagent **2.17** used in the coupling reaction was synthesized from thiophene-2-carbaldehyde in four steps involving the protection of aldehyde, stannylation, deprotection and Knoevenagel reaction with dicyanomethylene. During the Stille coupling, removal of stannyl, impurities were difficult in the presence of compounds **2.1** and **2.2**. In the literature, KF was used for removing tin impurities, but in this case, it did not work. So, we removed the stannyl impurities using cold MeOH filtration. The yield of compounds **2.1** and **2.2** were slightly lower in this filtration method.

Scheme 2.1. Synthesis of donor-acceptors 2.1 and 2.2.

The synthesis of compounds **2.3-2.5** is depicted in Scheme 2.2. Methyl ketones of triphenylamine, dihexyloxytriphenyl amine, n-hexylcarbazole were treated separately with the methyl ester derivative **2.19** under Claisen condensation conditions to make the corresponding 1,3-dicarbonyl derivatives **2.20a-2.20c**. Deprotection followed by PPh₃-promoted reaction with malononitrile resulted in the desired products **2.3-2.5** in moderate yields.

Scheme 2.2. Synthesis of donor-acceptors 2.3 - 2.5.

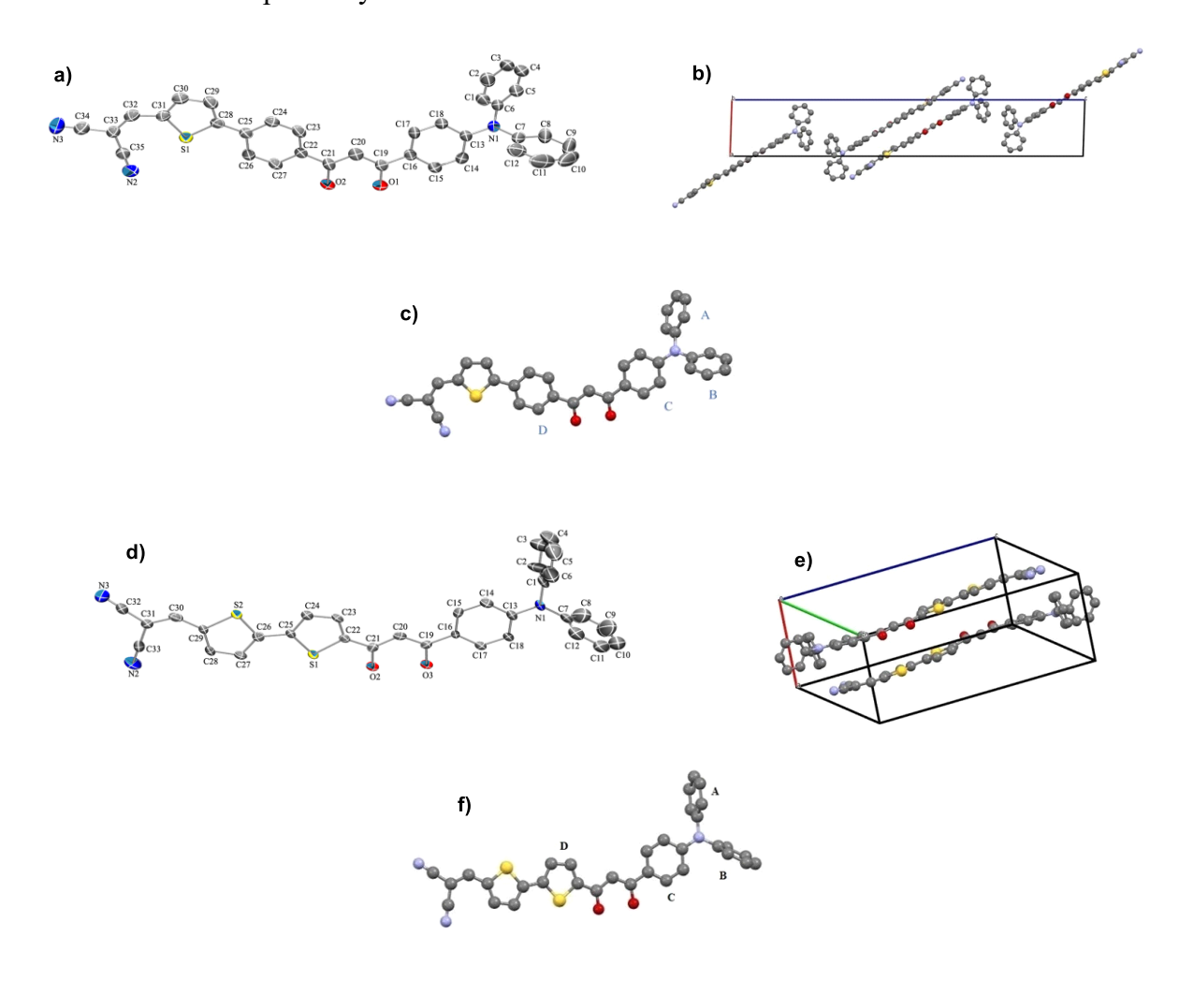
Finally, the corresponding BF₂-complexes of the 1,3-dicarbonyl bridged donor-acceptor compounds **2.1-2.5** were synthesized by treating them separately with BF₃·OEt₂ at room temperature (Scheme 2.3).⁵ The BF₂-complexes **2.1-BF₂-2.5-BF₂** were obtained as intense colored material in moderate yields. During the addition of BF₃·OEt₂ to the 1,3-dicarbonyl

compounds, the reaction mixture turned from yellow to red color. In general, boron complexes exhibit strong absorbance, sharp fluorescence, and high quantum yields.

Scheme 2.3. Synthesis of BF₂-complexes of the 1,3-dicarbonyl bridged donor-acceptor compounds.

The synthesized compounds were characterized thoroughly by different spectroscopic methods. In CDCl₃, the final 1,3-dicarbonyl compounds existed in their enolic form exclusively as inferred from the signal around 16 δ ppm. In addition to this, olefinic hydrogen of the dicyanovinylene group appeared between 6.7-7.0 δ ppm. The structures of the compounds **2.1**-**2.3** were further confirmed by single-crystal X-ray structure analysis. In the solid-state, compounds **2.1-2.3** existed in their keto form. The structures are depicted in Figure 2.4.

All the three red-colored compounds were subjected to grow single crystal in toluene at room temperature. The X-ray crystal structures reveal that the triphenylamine aryl rings are non-planer nature in all three structures. The compound **2.1** crystallized in the monoclinic crystal system with the P21/n space group. The dihedral angles between the benzene rings are 62.76° [A/B], 67.49° [A/C], 71.57° [A/D], 65.92° [B/C], 74.37° [B/D] and 8.51° [C/D] (Figure 2.4c). In the crystal packing, adjacent molecules are packed as 'head-to-tail' arrangement. These chains (excluding the two-terminal benzene rings) modeled a sheet-like arrangement of molecules and were separated by an interlayer distance of 3.49 Å. The compounds **2.2** and **2.3** were crystallized in triclinic crystal system with P-1 space group. The dihedral angles between the benzene rings are 66.10° [A/B], 83.35° [A/C], 88.82° [A/D], 76.36° [B/C], 74.41° [B/D], 7.99° [C/D] and 74.76° [A/B], 72.12° [A/C], 75.77° [A/D], 74.31° [B/C], 72.35° [B/D], 3.71° [C/D] respectively (Figure 2.4f and 2.4i). Both the structures packed in sheet-like structures with 'head-to-tail' arrangement and the molecules were separated by an interlayer distance of 3.52 and 3.37 Å respectively.



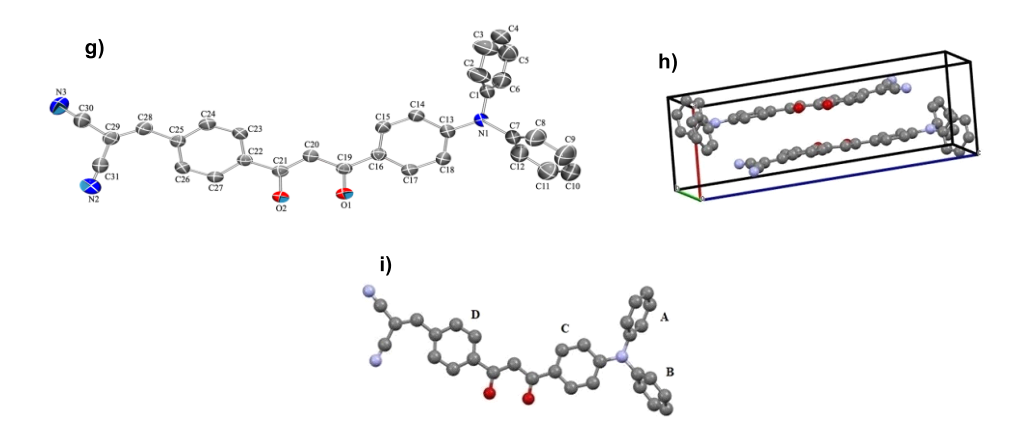


Figure 2.4. ORTEP and crystal packing structures of compounds 2.1 (a, b, c), 2.2 (d, e, f), and 2.3 (g, h, i).

2.3 Photophysical Properties of the Donor-Acceptor Compounds

2.3.1 Absorption Studies

The absorption spectra of the synthesized donor-acceptor compounds 2.1-2.5 and 2.1-BF₂-2.5-BF₂ in dichloromethane solutions were recorded and are shown in Figure 2.5. Their corresponding photophysical data are summarized in Table 2.1. Compounds 2.1, 2.2, 2.1-BF₂, and 2.2-BF₂ have an extra π -spacer in the form of thiophene/(s). Compounds 2.1-2.5 showed broad absorption maxima at 402 nm, 479 nm, 437 nm, 444 nm, and 420 nm, respectively, along with a shoulder peak appearing in the range of 256-400 nm. The presence of the electronwithdrawing dicyanovinylene group contributes to the shift of the absorption maximum to the higher wavelength side. The shorter wavelength shoulder peak corresponds to weak ICT transition from the triphenylamine/carbazole moiety to the electron-withdrawing β-diketone, and the longer wavelength absorption maximum corresponds to a strong ICT transition from the triphenylamine/carbazole moiety to the strong electron-accepting dicyanovinylene group. The absorption spectra of all the BF₂-complexes **2.1-BF₂-2.5-BF₂** showed a very strong absorption band around 470-540 nm and is assigned to the intramolecular charge transfer from the donor to dicyanovinylene group. A shoulder in the shorter wavelength region is observed in each case around 310-445 nm, and is assigned to the intramolecular charge transfer transition from the donor to BF₂ moiety. Increasing the electron-withdrawing capability and the length of π -spacer led to redshift in absorption maximum along with broadening of the absorption spectra. In all the BF₂-complexes **2.1-BF₂-2.5-BF₂**, the strong electron-withdrawing nature of dicyanovinylene moiety suppressed the ICT transition between the donor and BF2 moiety,

which appeared as a shoulder around 310-445 nm. All the compounds had high molar extinction coefficients, and, particularly, the BF₂-complex having O-hexyl groups on the triphenylamine displayed a high molar extinction coefficient.

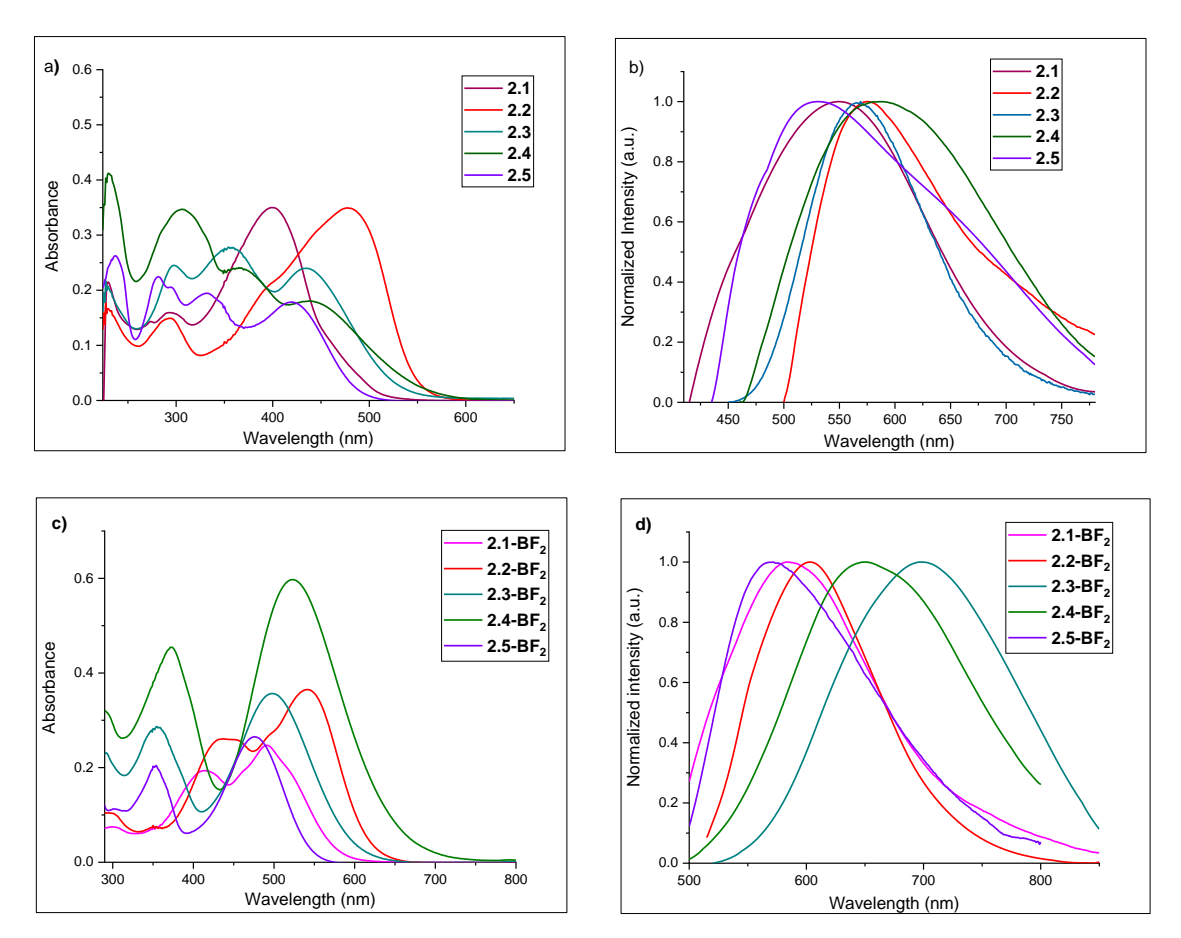


Figure 2.5. a) Absorption spectra of compounds **2.1-2.5**. b) Normalized emission spectra of compounds **2.1-2.5**. c) Absorption spectra of compounds **2.1-BF₂-2.5-BF₂**. d) Normalized emission spectra of compounds **2.1-BF₂-2.5-BF₂**. The UV-Vis and emission were recorded by using 1×10^{-5} M concentration in dichloromethane solvent.

2.3.2 Emission Studies

The emission spectra were recorded by exciting individual compounds at their absorption maxima. Upon excitation, all the compounds showed a broad emission peak with maxima centered in the range 530 to 590 nm [2.1 (550 nm), 2.2 (576 nm), 2.3 (568 nm), 2.4 (588 nm) and 2.5 (530 nm)]. Notably, increasing the π-spacer led to the stabilization of the CT, which resulted in redshift of the emission peak. The BF₂ complexes 2.1-BF₂-2.5-BF₂ exhibited emission maxima between 570 to 698 nm [2.1-BF₂ (586 nm), 2.2-BF₂ (604 nm), 2.3-BF₂ (698 nm), 2.4-BF₂ (649 nm) and 2.5-BF₂ (570 nm)]. The quantum yield of the compounds was around 0.2 in toluene. The Stokes shift for all the compounds was high. It is generally above 90 nm with a maximum of 200 nm for 2.3-BF₂ (Table 2.1).

Table 2.1. Photophysical properties of compound 2.1-2.5 and 2.1-BF₂-2.5-BF₂

Dye	λ _{max} (nm)	λ em (nm)	Stokes Shift (nm)	ε (M ⁻¹ cm ⁻¹)	$\mathbf{\phi}_{\mathbf{f}^{(a)}}$	$\tau_{\rm f}({ m ns})$
2.1	402	550	148	35,000	0.179±0.03	2.09 ns
2.2	479	576	97	35,000	0.145±0.05	1.32 ns
2.3	437	568	131	23,800	0.250±0.05	2.39 ns
2.4	444	588	144	18,000	0.19±0.02	1.94 ns
2.5	420	530	110	18,000	0.11±0.03	2.24 ns
2.1-BF ₂	492	586	94	27,000	0.18±0.01	2.88 ns
2.2-BF ₂	542	604	62	37,000	0.15±0.09	2.78 ns
2.3-BF ₂	498	698	200	36,000	0.25±0.04	4.55 ns
2.4-BF ₂	523	649	126	60,000	0.18±0.05	2.08 ns
2.5-BF ₂	476	570	94	26,000	0.16±0.04	2.71 ns

⁽a) Quinine sulfate in 0.1N sulphuric acid was used as the reference $[\Phi f = 0.546]$

The fluorescence lifetime of all the donor-acceptor derivatives in toluene has also been investigated using time-resolved fluorescence technique by exciting the sample at 440 nm. All compounds exhibited a single-exponential decay in toluene. Within the compounds containing triphenylamine, longer lifetime was observed for compound **2.3** (2.39 ns). The fluorescence decay profiles were recorded using time-correlated single-photon counting (TSCPC) technique by exciting the sample at 440 nm, and the results are presented in Table 2.1. Compound **2.3-BF2** exhibited a single-exponential decay in toluene with a lifetime of 4.55 ns. This confirms that the presence of single conformation in the excited state.

2.3.3 Electrochemistry

The electrochemical (redox) behavior of the compounds **2.1-2.5** and **2.1-BF₂-2.5-BF₂** was studied by cyclic voltammetry using their solutions in DCM at room temperature in 100mV s⁻¹ scan rate with Bu₄NClO₄ (tetrabutylammonium perchlorate) as a supporting electrolyte. While Ag/Ag⁺ was taken as a reference electrode, Pt electrode was kept as a working electrode as well

as a counter electrode. All the compounds exhibited electrochemical behavior in the cyclic voltammetry experiment, and the electrochemical parameters are displayed in Table 2.2. The redox behavior of the compounds 2.1-2.5 and $2.1-BF_2-2.5-BF_2$ are shown in Figure 2.6a and 2.6b, respectively. In all the compounds, oxidation potential occurred due to the strong electron-donating group triphenylamine/carbazole moiety, and the reduction potential appeared due to the dicyanovinylene unit. Compounds 2.4 and $2.4-BF_2$ exhibited two oxidation potential peaks. On the other hand, carbazole containing compounds 2.5 and $2.5-BF_2$ showed a quite different pattern from the triphenylamine derivatives. The HOMO energy levels of dyes were calculated from E_{onset} of the oxidation potential of the dyes by using the following equation.

$$HOMO(eV) = -(E_{onset.ox} + 4.8) eV$$
 (1)

The LUMO energy levels were obtained from the UV-Visible spectra in the Tauc plot, and the equation is

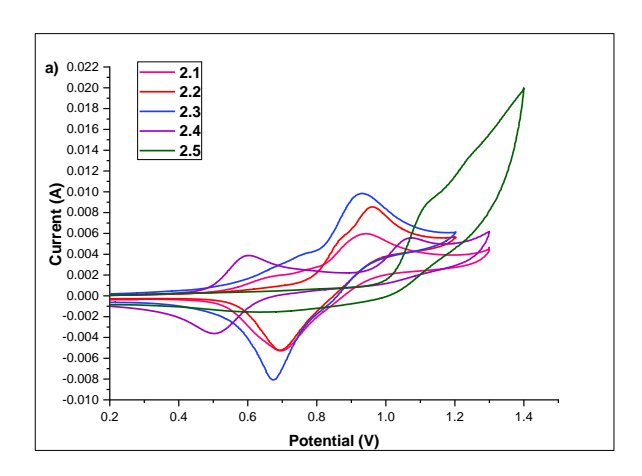
$$LUMO (eV) = E_g - HOMO$$
 (2)

Table 2.2. Cyclic voltammetry studies

Dye	E° onset	НОМО	LUMO	НОМО	LUMO
	$(\mathbf{V})^{a}$	$(eV)^b$	$(eV)^c$	$(eV)^d$	$(eV)^d$
2.1	0.82	-5.62	-3.07	-5.56	-3.52
2.2	0.78	-5.58	-3.28	-5.47	-3.42
2.3	0.80	-5.60	-3.1	-5.84	-3.37
2.4	0.93	-5.73	-3.33	-5.52	-3.3
2.5	1.0	-5.8	-3.15	-6.15	-3.37
2.1-BF ₂	0.84	-5.64	-3.31	-5.98	-3.64
2.2-BF2	0.87	-5.67	-3.59	-5.97	-3.77
2.3-BF ₂	0.86	-5.66	-3.46	-6.09	-3.76
2.4-BF2	0.96	-5.76	-3.71	-5.78	-3.65
2.5-BF ₂	1.12	-5.92	-3.57	-6.36	-3.79

^a Obtained from cyclic voltammetry, ${}^{b}HOMO(eV) = -(Eox-E(Ag/Ag+) + 4.8) eV$, ${}^{c}E_{LUMO} = Eg-HOMO$,

^d based on DFT calculation by Gaussian 09 software.



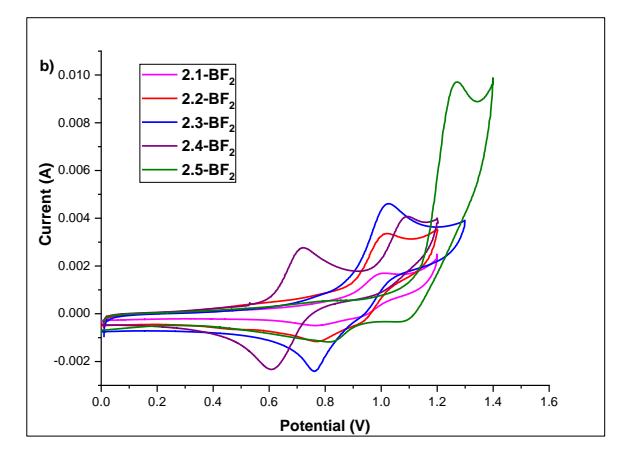
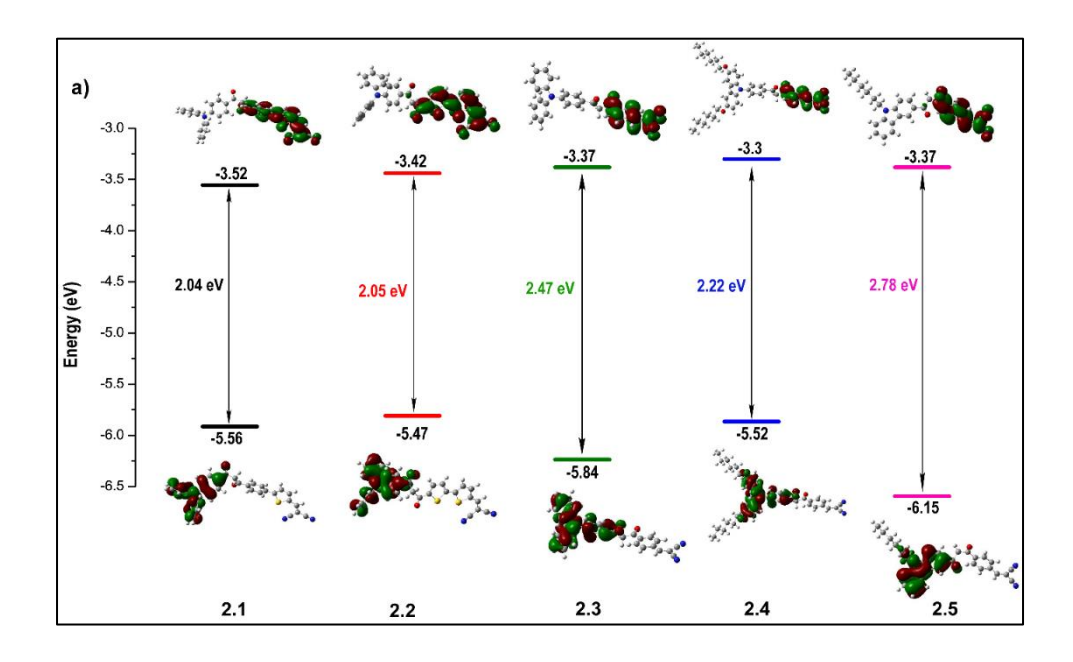


Figure 2.6. a) Cyclic Voltammogram of donor-acceptor system **2.1-2.5**. b) Cyclic Voltammogram of donor-acceptor with BF_2 **2.1-BF_2-2.5-BF_2**.

2.4 Density Functional Theory (DFT) Studies

Density Functional Theory (DFT) calculations were performed on these molecules to study the electronic distribution in the HOMO and LUMO levels of these compounds **2.1-2.5** and **2.1-BF₂-2.5-BF₂** by Gaussian 09 package using B3LYP/6-31G basic sets.⁷ All the compounds have shown small HOMO-LUMO band gaps, which means facile excitation from HOMO to LUMO.



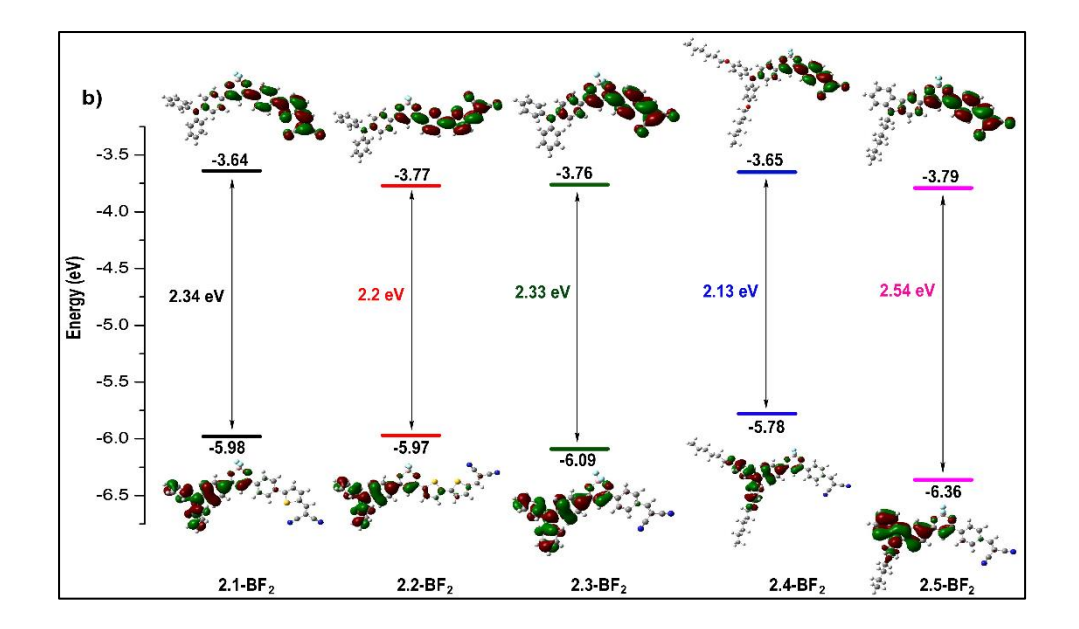


Figure 2.7. Electron density distribution in the frontier molecular orbitals of the compounds a) HOMO-LUMO of 1,3-diketone bridged donor-acceptor compounds **2.1-2.5**; b) HOMO-LUMO of 1,3-diketone bridged donor-acceptor complexed with BF₂ **2.1-BF**₂**-2.5-BF**₂.

In the ground state geometry of all the compounds **2.1-2.5** and **2.1-BF₂-2.5-BF₂** showed non-planer shape. The HOMO orbitals are localized on triphenylamine in **2.1-2.4** and on carbazole in the compound **2.5** and extending slightly to the 1,3-diketone moiety and not to the aryl groups connected to the dicyanovinylene group (Figure 2.7). The LUMO orbitals are localized on dicyanovinylene (acceptor moiety) and the aryl group connecting it to the 1,3-dicarbonyl moiety. However, in the difluoro boron complexes **2.1-BF₂-2.5-BF₂**, the HOMO extended from the donor moiety up to the BF₂ moiety, whereas the LUMO is localized from dicyanovinylene unit to the phenyl and thiophene moieties. The TD-DFT studies revealed that HOMO-LUMO calculated energy gap of compounds **2.1-2.5** were found to be, respectively, 2.04 eV, 2.05 eV, 2.47 eV, 2.22 eV and 2.78 eV, and the same for their corresponding boron complexes **2.1-BF₂-2.5-BF₂** were, respectively, 2.34 eV, 2.2 eV, 2.33 eV, 2.13 eV and 2.54 eV. In both the case, the energy gap of carbazole derivatives is slightly higher than that of the triphenylamine derivatives.

2.5 Applications of the 1,3-Dicarbonyl Bridged Donor-Acceptor Systems

2.5.1 Dye-Sensitized Solar Cells (DSSCs)

Due to the high demand for energy and depletion of fossil fuel energy sources, the development of renewable energy sources has been given greater importance in the last few decades.⁸ In this context, solar energy is the most promising source of energy, and quite a lot of efforts have been invested in developing solar cells. The high cost with conventional silicon-

based solar cells that are presently available in the market builds the necessity to develop cheaper alternatives. In this regard, organic solar cells have been developed, which enjoys advantages such as high flexibility, lightweight, and low-cost for making them. Among them, the dye-sensitized solar cells have been considered as the best alternative. In 1991, Gratzel and co-workers developed the dye-sensitized solar cells. In this system, ruthenium-based organic dyes were used to produce electric energy from solar energy and have attained a power conversion efficiency of 7.1%. At present, the researchers have improved the efficiency of ruthenium (II)- polypyridyl as an active material approaching the power conversion efficiency up to 9.5-11.18% (Figure 2.8). The research on metal-based organic dyes is still in focus on increasing the efficiency. However, the metal-based organic dyes have several drawbacks, especially the Ru based organic dyes. Ru metal is expensive, less abundant, having difficulty in purification during synthesis. For the very reason, metal-free organic dyes have been synthesized and applied in the field of dye-sensitized solar cells.

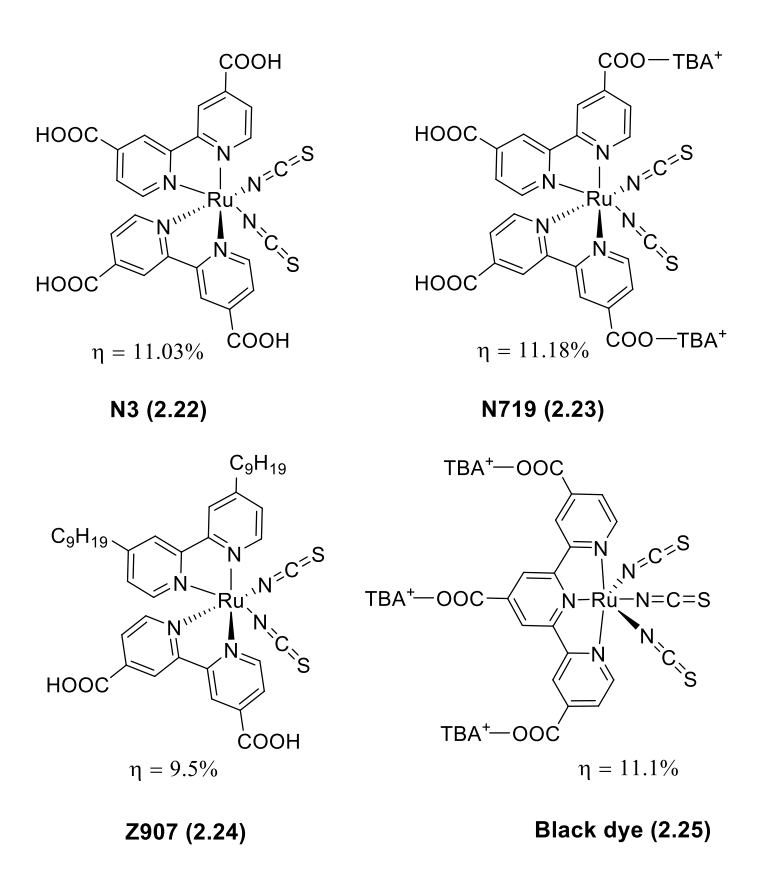


Figure 2.8. Ruthenium based organic dyes for the application in DSSCs.

2.5.1.1 Working Principle of Dye-Sensitized Solar Cells

The dye-sensitized solar cell directly converts the solar energy into electrical energy, and the device has been called as a photovoltaic semiconductor. The schematic diagram of the working principle of a solar cell is shown in Figure 2.9. The construction of the dye-sensitized solar cell device consists of five stages.¹²

- 1) A transparent conductive oxide layer is coated on a transparent glass plate (Indiumdoped tin oxide (ITO), Fluorine-doped tin oxide (FTO). It acts as an anode.
- 2) A nanocrystalline oxide layer (**TiO**₂) coated on the anode layer. The oxide layer will be activated to the electronic conduction.
- 3) A monolayer of the synthesized organic dye has been coated on the oxide layer. The dye molecules enhance light absorption.
- 4) It is drilled and holes are made at both edges of the platinum-coated transparent glass plate. It acts as the cathode layer for facilitating electron collection.
- 5) Finally, the anode and cathode plates are connected like the sandwich model, then the redox mediator electrolyte (I^-/I_3^-), is used for the dye regeneration.

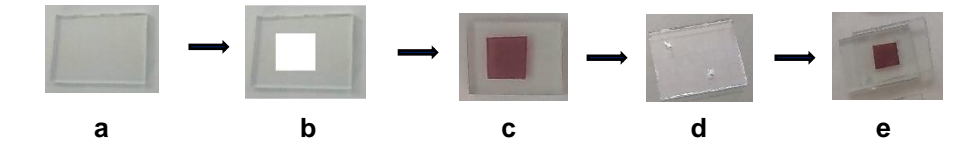


Figure 2.9. Construction of a dye-sensitized solar cell device. a) FTO glass plate, b) nanocrystalline TiO_2 layer, c) organic dye coated on the TiO_2 layer, d) drilled hole in platinum-coated FTO, e) stacked electrodes.

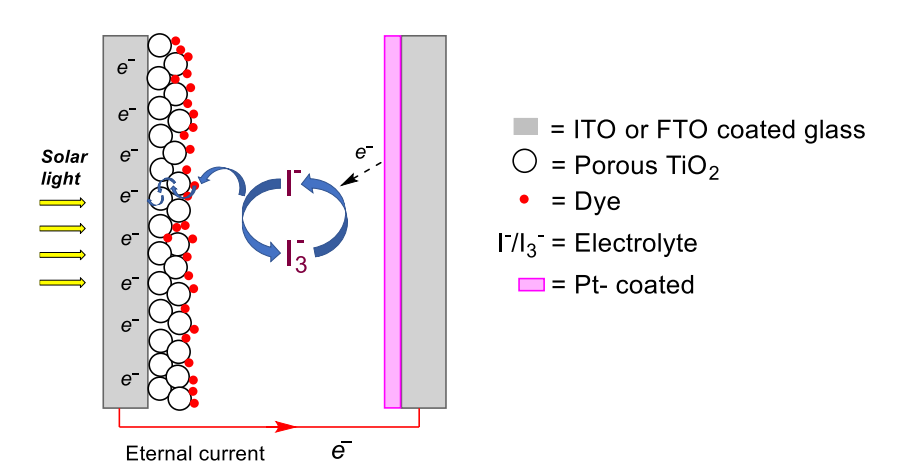


Figure 2.10. Schematic diagram of the working mechanism of the dye-sensitized solar cells.

After constructing the device, it is connected to the positive and negative end of the solar instrument. The incident photon is converted into electrical current and is transported through the device. In this, device ITO or FTO coated glass plates acts as an anode, platinum acts as a cathode, an oxide layer of TiO₂ has been an n-type semiconductor, electrolytes act as a redox mediator, and the dye has performed as a hole-transporting unit with the p-type semiconductor.

The overall performance can be expressed as power conversion efficiency (η) , and the fill factor (FF) and are given as follows.

$$FF = \frac{V_{\text{max}}J_{\text{max}}}{V_{\text{oc}}J_{\text{sc}}}$$
 (3)

$$\eta = \frac{P_{\text{max}}}{P_{\text{in}}} = \frac{V_{\text{oc}}J_{\text{sc}}FF}{P_{\text{in}}} \times 100\%$$
 (4)

FF - Fill factor

 $J_{\rm sc}$ - short-circuit current density (mA cm⁻²)

 V_{oc} - open-circuit voltage (V)

P_{in}- input the incident light power

 $V_{\text{max}}J_{\text{max}}$ - maximum voltage and current

Where the maximum power output received from J-V curve spectra.

2.5.1.2 Metal-Free Organic Donor-Acceptors for Dye-Sensitized Solar Cells (DSSCs)

The general structure of an organic dye, which is used in DSSC applications is shown in Figure 2.11. It has a strong electron-donating group, such as an amine. It is connected to an electron-withdrawing acceptor group through a π -bridge. The acceptor group generally has a carboxylic acid group so that it can be hooked to TiO₂ while constructing the cell.

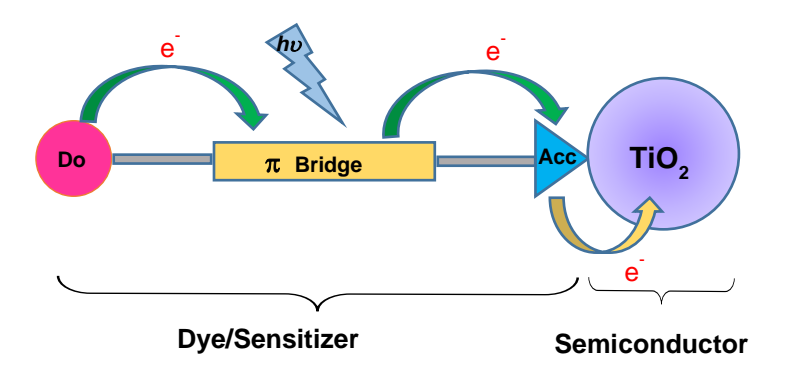


Figure 2.11. The general structure of metal-free organic dyes.

The metal-free dye-based donor-acceptor compounds are easy to synthesize and are comparatively low-cost materials. The absorption range of donor-acceptor units covers the visible region and some of the areas of the near-infrared region. Also, they generally have a high molar extinction coefficient. Some of the metal-free organic dyes shown in Figure 2.12.¹¹

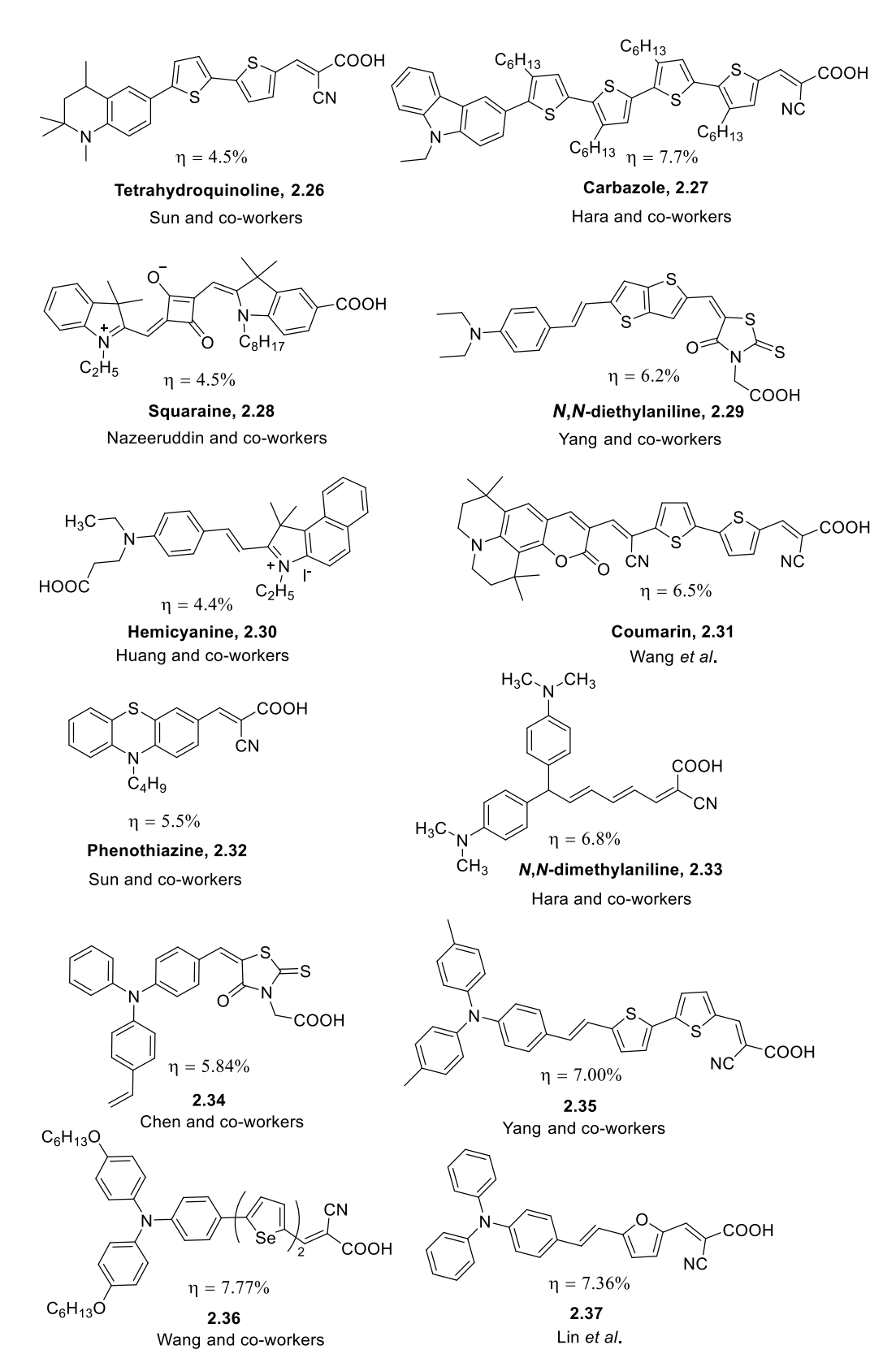


Figure 2.12. Selected donor-acceptor compounds for metal-free dye-sensitized solar cells.

Over the years, several donor-acceptor systems have been developed and studied for their application in DSSC. Among them, triphenylamine containing donor-acceptor compounds

have received significant attention in developing dye-sensitized solar cells due to their high charge carrier properties, flexibility and photostability. Modification in the triphenylamine moiety has also proved to improve the efficiency of DSSC. In addition, significant attention has been paid to check the effect of π -bridge on the efficiency of the DSSC. Chen and coworkers^{13a} have reported the triphenylamine based organic dyes for solar cell applications. They used the methine bridge as a π -conjugation with rhodamine-3-acetic acid as an acceptor unit **2.34**, and the dye has produced a PCE of 5.84%. Yang and co-workers ^{13b} reported 7.00% power conversion efficiency using a triphenylamine based donor-acceptor system in which triphenylamine is connected to cyano acetic acid unit through a bithiophene spacer 2.35. Wang and co-workers^{13c} synthesized triphenylamine based donor-acceptor system using different types of conjugated linkers such as furan, bifuran, thiophene, bithiophene, selenophene, and biselenophene. Among them, triphenylamine with biselenophene 2.36 had resulted in a PCE of 7.77%. Likewise, Lin et al. 13d reported 7.36% solar power conversion efficiency using a dye containing triphenylamine an cyano acrylic acid linked through a furan π -spacer 2.37. Zhu and co-workers^{13e} have reported a concise review on photovoltaic performances of metal-free organic dyes based on D- π -A to D-A- π -A motifs in solar cells.

Generally, the reported DSSC materials have designed with a carboxylate unit for anchoring to the oxide surface.

We hypothesized that there could be a better electron transfer when TiO_2 is made bound to the D-A molecule before the acceptor moiety, and the electron-withdrawing nature of the acceptor will facilitate the same. Due to the limited accessibility to the DSSC experiments in the collaborating institution, only compounds **2.2** and **2.4** were selected for the study based on their better photophysical properties. Ruthenium based **N719** dye was taken as the reference.

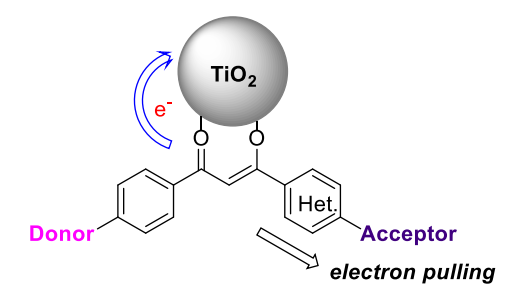
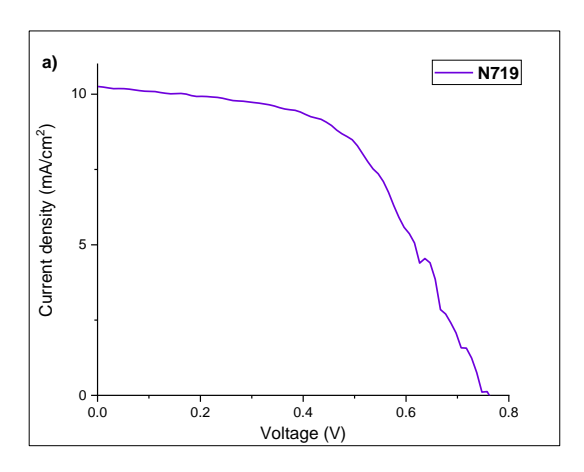


Figure 2.13. Structures of the compounds tested for the DSSC application and the standard N719 dye.

The photovoltaic current parameters of the dye-sensitized solar cells were determined using a simulated AM 1.5G irradiation (100 mWcm⁻²) in the presence of iodide/iodine electrolyte (0.6 M 1,2-dimethyl-3-n-propylimidazolium iodide, 0.1 M LiI, 0.05 M I₂, and 0.5 M 4-tert-butylpyridine in acetonitrile). The thickness of mesoporous TiO₂ was optimized to 10 μ m and the nanocrystalline layer to 2 μ m. The thickness of the layers was maintained identical in all the devices. The photovoltaic data are summarized in Table 2.3, and the photo-current density (J-V) curves measurements are shown in Figure 2.14.

Table 2.3. DSSC performance of donor-acceptors and reference N719.

Dye	$J_{\rm sc}$ (mA/cm ²)	$V_{oc}\left(\mathbf{V}\right)$	FF	η (%)
2.2	0.468	0.486	52.30	0.12
2.4	0.585	0.649	65.06	0.25
N719	10.26	0.760	53.38	4.16



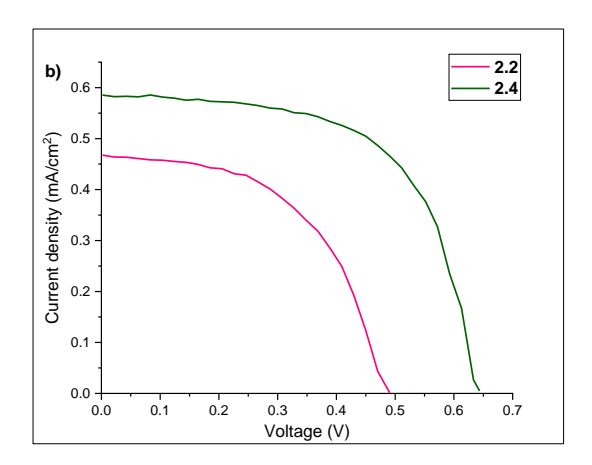


Figure 2.14. Photocurrent density-voltage (J-V) curves for the donor-acceptor based dye-sensitized solar cell with the TiO_2 electrode. a) Reference dye N719; b) Dye 2.2 and 2.4.

The **N719** reference device exhibited a power conversion efficiency of 4.16% with an open-circuit voltage of 0.760 V and a short circuit current density of 10.26 mA/cm². The devices sensitized with dye **2.4** exhibited a better performance when compared that with the dye **2.2**. The dye-containing *O*-hexyl incorporated triphenylamine **2.4** exhibited a power conversion efficiency of 0.25%. On the other hand, the dye **2.2** having triphenylamine moiety and extra π -spacer dithiophene units showed a lowe power conversion efficiency of 0.12.

2.5.2 Bio-Imaging

The large Stokes shift with high photostability of certain organic fluorescent dyes finds unique applications in the field of bio-imaging. Large Stoke shift of a dye can minimize the fluorescent self-quenching and avoid the fluorescent detection error due to the excitation of backscattering light. Additionally, the organic dyes with high photostability is highly advantageous for long-term illumination required generally for the investigation of biological processes. The selectivity and sensitivity of these fluorescent probes is a great deal in live-cell imaging as the cell has numerous organelles. Some of the fluorescent organic dyes which are routinely used in the field of bio-imaging are rhodamine (Rho, 2.38), fluorescein 2.39, flob boron-dipyrromethene (BODIPY, 2.40), floc perylene 2.41, flod cyanine 2.42, floe coumarin 2.43, flor naphthylamide 2.44, flog and carbazole 2.45 floh and are shown in Figure 2.15. These compounds are generally conjugated with the binding compound to effect site-specific binding.

Figure 2.15. Representative molecular structures of organic fluorescent dyes for bioimaging.

Apart from the above traditional dyes, several new organic dyes have been developed for imaging applications. Among them, triphenylamine based derivatives have exhibited low cytotoxicity, high photostability, significant Stokes shifts, and high molar extinction coefficient. These properties facilitate these dyes for their application in the field of bioimaging of live-cells. Teulade-Fichou and co-workers^{17a, 17b} have reported vinyl-triphenylamine based fluorescent probes **2.46** and **2.47** for the DNA to protein labeling studies using on-off fluorescence method. Tian and co-workers^{17c, 17d} synthesized D- π -A system based on triphenylamine, and the molecules **2.48** and **2.49** were tested with the HepG2 cancer cells and obtained images with AIE (aggregation-induced emission).

Figure 2.16. Representative molecular structures of triphenylamine derivatives for bio-imaging.

Qian and co-workers^{17e} have reported a donor-acceptor system based on triphenylamine linked to the BODIPY unit for bioimaging of MCF-7 cell line. Teulade-Fichou and co-workers^{17f} reported triphenylamine derivatives for selective imaging of mitochondria in MCF-7 and HeLa cell lines.

To date, only a very few reports are available for the live-cell imaging of microtubules specifically. Microtubules are tube-shaped protein polymers made of α - and β -tubulin dimers, which are present in the cytoskeleton of eukaryotic cells. It has essential for the live cells because they maintain the shape of the cell and involve in cell division, transport of vesicles, and other components throughout the cell. Since microtubules participate in cell division, they are a prominent target for the development of anticancer agents, herbicides, fungicides, and anthelminthic. 18,19

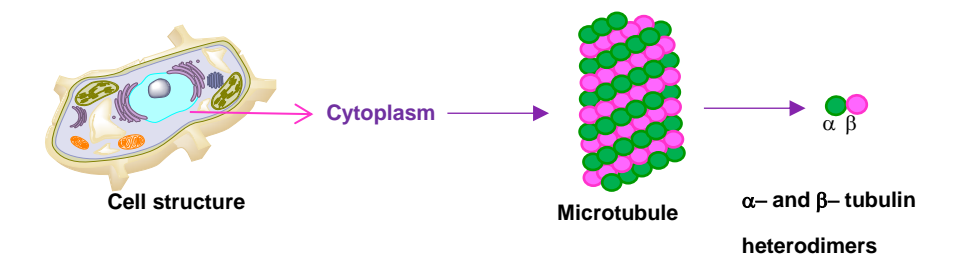


Figure 2.17. Arrangement of α - and β -tubulin heterodimers in the microtubule.

Zhang *et al.*²⁰ have reported a newly designed molecule for the imaging of β -tubulin using spiropyran (**SP**) conjugated with colchicine alkaloid (**Tu**) system **2.50**. The spiropyran derivative act as a fluorophore and the colchicine acts as a recognizing unit for binding to β -tubulin. Recently, fluorescent anticancer agents, 2-aminoquinazolines have been tested for imaging of microtubules without attaching them to tubulin-binding agents **2.51**.²¹ Also, Johnsson and co-workers²² have designed silicon-rhodamine (SiR) derivatives for live-cell imaging of the cytoskeleton **2.52**.

Figure 2.18. Molecular structure of the β -tubulin tracker.

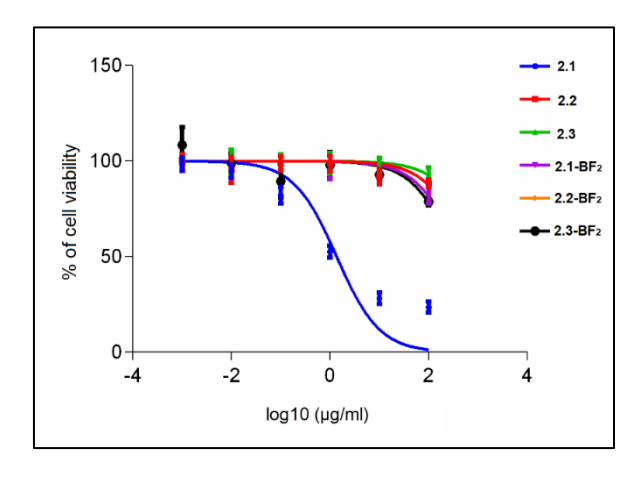
Chapter 2

The begin with the biological evaluation of the donor-acceptor derivatives their antiproliferative/cytotoxic activities in a human cervical cancer cell line (HeLa) using MTT assay were carried out first (Figure 2.19).²³ IC₅₀ values of the dyes for 24 hours on the HeLa cell line were calculated and are presented in Table 2.4. Except the compound **2.1** all other compounds are non-toxic. It is noteworthy that the cytotoxicity of compound **2.1** was also detected during wound healing experiments (Figure 2.20) the live-cell imaging experiments (Figure 2.21) as well. While the reference doxorubicin had an IC₅₀ value of 1.82 ± 0.45 µg/ml, compound **2.1** was found to have an IC₅₀ value of 10.34 ± 1.56 µg/ml.

Table 2.4. In vitro cytotoxic evaluation of donor-acceptor compounds against HeLa cell line

S. No	Dye	Ic50±SD (μg/ml) on HeLa
1	2.1	10.34±1.56
2	2.2	NA
3	2.3	NA
4	2.1 -BF $_2$	NA
5	2.2 -BF $_2$	NA
6	2.3-BF2	NA
7	^a Doxorubicin	1.82±0.45

[a] Doxorubicin was employed as a positive control. NA indicates that the derivatives are not active at $100 \mu g/mL$ concentration. The values represent the mean \pm SE of three individual observations.



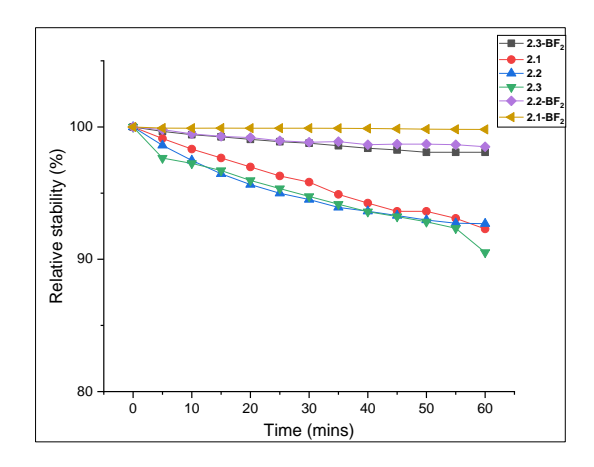
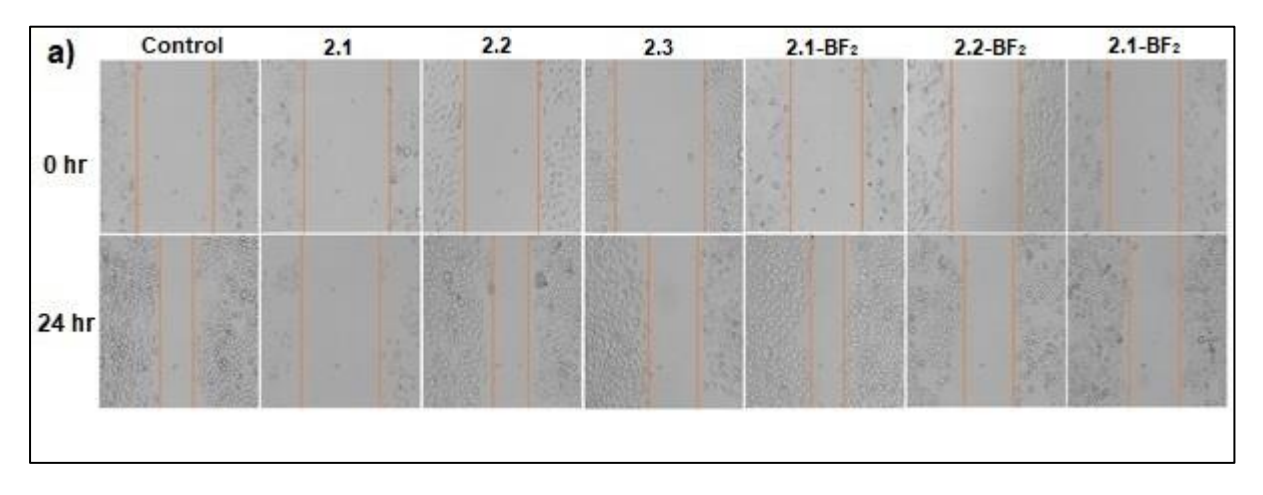


Figure 2.19. (a) Effect of Donor-Acceptor compounds 2.1-2.3 and $2.1-BF_2-2.3-BF_2$ on the viability of HeLa cells. (b) Photostability of 2.1-2.3 and $2.1-BF_2-2.3-BF_2$.

Next the photostability of compounds **2.1-2.3** and **2.1-BF₂-2.3-BF₂** was tested by continuous irradiation of light to the individual compounds in toluene solutions for 60 minutes and checking their FI at every 5 min interval. All the dyes are photostable. The difluoro boron complexes **2.1-BF₂-2.3-BF₂** were found to be more stable compared to their corresponding parent 1,3-dicarbonyl compounds **2.1-2.3** (Figure 2.19b).

In another set of experiments, the wound-healing abilities of the donor-acceptor compounds treated wounded HeLa cells were evaluated. In this experiment, mechanical scratching of the cell monolayer generates a cell-free environment and eventually creates an opportunity to study the ability of the cells to migrate to fill the gap. Confluent HeLa cells after mechanical wounding were treated with the donor-acceptor compounds **2.1-2.3**, **2.1-BF₂-2.3-BF₂**, and DMSO control separately. Photomicrographs of the cells at the time of treating and 24 h after treatment with compounds are shown in Figure 2.20. Clearly, the compound **2.1** did not promote wound healing, and thus the gaps were not filled by the cells even after 24 h as seen positively with other compounds and DMSO.



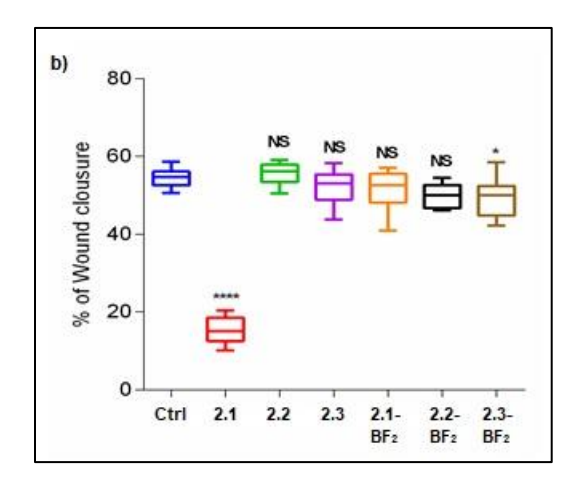


Figure 2.20. Effect of **2.1-2.3** and **2.1-BF₂-2.3-BF₂** on the migration of HeLa cells: (a) After mechanical wounding, confluent HeLa cells were treated with **2.1-2.3** and **2.1-BF₂-2.3-BF₂** and DMSO control. Representative photomicrographs of the wounded cell monolayer at 0 hr and 24 hr are shown; the scale bar is $100 \mu m$. (b) Graph showing the percent of wound closure of three independent experiments.

The high Stokes shifts of the synthesized fluorescent donor-acceptor compounds prompted us to study their application in live-cell imaging. The preliminary fluorescence microscopy observations indicated that these dyes entered into the HeLa cells, accumulated in the cytoplasm uniformly and remarkably emitted a green fluorescence leaving the nucleus. This uniform and spread fluorescence hinted at the possibility of the compounds binding to the cytoskeleton. In this regard, specific recognition of the donor-acceptor compounds for tubulins in microtubules of living cancer cells was evaluated by co-localization studies in the presence of anti-tubulin antibodies using Alexa Fluor 546 red under high magnification of an immunofluorescence microscope. Figure 2.21a corresponds to the image β-tubulin due to red fluorescence of the Alexa Fluor 546 red. The images of the same cells based on the emission at 550 nm (due to compounds **2.1-2.3** and **2.1-BF₂-2.3-BF₂**) by exciting at 488-500 nm were very much similar to that obtained with Alexa Fluor 546 red, but in bright green color (Figure 2.21c). Merging of the images a and c in each case generated yellow images (Figure 2.21d) of the tubulin by clear overlapping of the images due to Alexa Fluor 546 red and the donor-acceptor compounds. These observations clearly suggest the binding of the donor-acceptor compounds to β-tubulin in living cancer cells. Except for compound **2.1**, all other compounds gave welldefined images of microtubules in living cells. Among them, images due to compounds 2.2 and 2.2-BF₂ overlapped very well with those due to Alexa Fluor 546 red. Compound 2.1, being cytotoxic, gave a deformed cell structure.

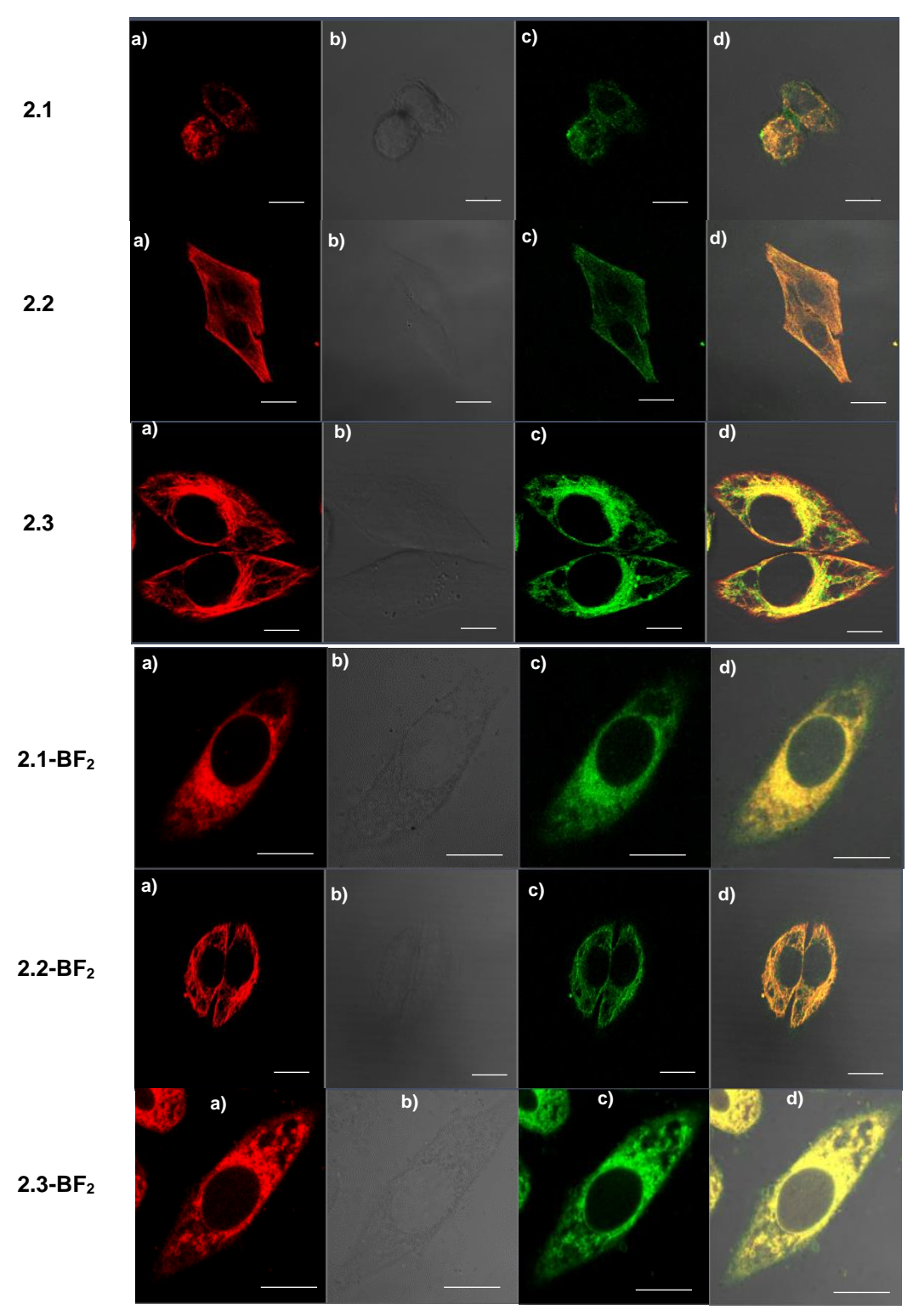


Figure 2.21. Confocal images of HeLa cancer cells co-stained with Alexa Fluor 546 and dyes. a) Alexa Fluor 546 (red channel: excited at 543-550 nm and emission at 700 nm); b) Bright field; c) **2.1-2.3** and **2.1-BF₂-2.3-BF₂** (Green channel: excited at 488-500 nm and emission at 550 nm); d) Merging all the images. Scale bar is 10 μm.

To evaluate whether the anti-tubulin antibody had played any role in binding of the donor-acceptor compounds to β -tubulin, an imaging experiment was carried out by treating

compound **2.2** with HeLa cancer cells without any antibodies. It gave a green fluorescent image of microtubule (Figure 2.22). DAPI was used in this experiment to stain the nucleus. This result is significant in the sense that the known tubulin markers either require tubulin specific antibodies or tubulin-binding ligands to tag with the fluorescent probes to image tubulins. Therefore, the title compounds are potential and cheaper alternates for the imaging of microtubules.

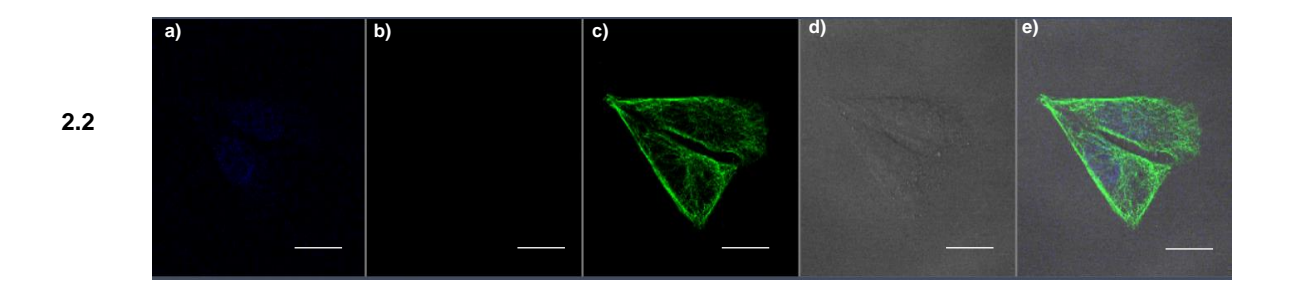


Figure 2.22. Confocal images of HeLa cancer cells without antibodies of β -tubulin. a) DAPI channel (exited at 400-418 nm); b) Without antibodies of β -tubulin; c) **2.2** (Green channel: excited at 488-500 nm and emission at 550 nm); d) Bright field; e) Overlapping all the above images. Scale bar is 10 μm.

Finally, an *in vivo* experiment was carried out to further confirm the binding of the compounds with tubulin. In this experiment, HeLa cancer cells were treated separately with the donor-acceptor compounds **2.1-2.3** and **2.1-BF₂- 2.3-BF₂** for 12 h hours. Then the cells were lysed, and the lysates were analyzed by gel electrophoresis. The fluorescence image of the gel using Bradford protein assay revealed that all the compounds bound to a 100 kDa protein which corresponds to the heterodimer of α - and β -tubulins (Figure 2.23).

It is believed that these compounds may act like combretastatin A-4, which has a cisstilbenoid structure. Combretastatin A-4 is a potent tubulin polymerization inhibitor, and it's corresponding trans isomer is not an active one.²⁴ Therefore, the aryl rings, rigidly oriented in the same direction of the title 1,3-dicarbonyl compounds (refer X-ray crystal structures of 1,3-dicarbonyl compounds) and their corresponding and BF₂ complexes, might be the reason for their tubulin-binding abilities.

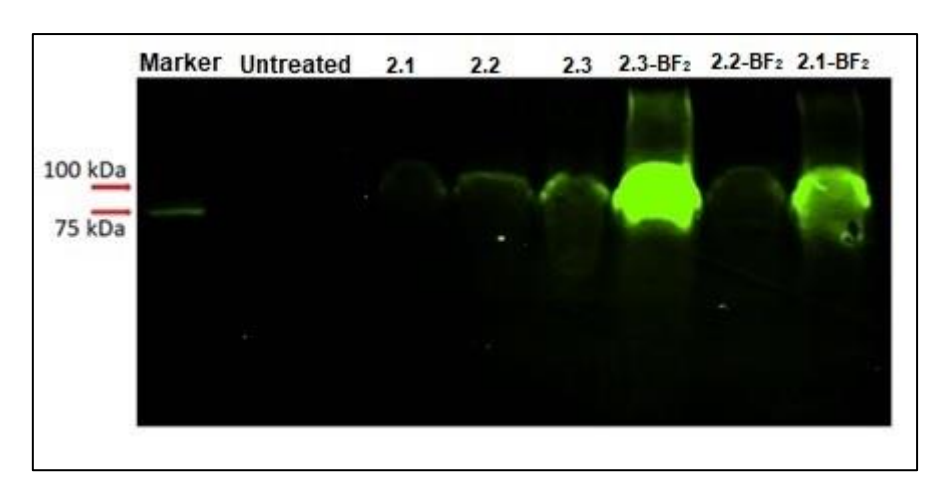


Figure 2.23. Interaction of compounds **2.1-2.3** and **2.1-BF₂-2.3-BF₂** with tubulin dimers through an *in vivo* experiment.

2.5.3 Cyanide Sensing

Among the several anions, cyanide ion (CN⁻) is a highly toxic anion, which has been extensively used in different industrial processes such as metallurgy, gold mining, tanning, plastic manufacturing, electroplating and production of synthetic fibers and resins.²⁵ Cyanide ions are produced by the hydrolysis of phosphate-based chemical warfare agents.²⁶ Cyanide ion has a strong affinity towards cytochrome c oxidase and forms a complex in the human bloodstream, which results in respiratory arrest and ultimately leads to death when the consumption exceeds 0.05 mg kg⁻¹ of body weight. ²⁷ The maximum allowed limit of cyanide ion in drinking water is generalized as 1.9 µM (70 ppb) by the WHO (World Health Organization).²⁸ Thus, efficient and selective detection of cyanide ion is a highly necessary task. Conventional methods like titrimetric,²⁹ electrochemical, ³⁰ spectrophotometric,³¹, and chromatographic analyses³² have been developed for quantitative detection of cyanide ion. However, limitations such as large time consumption, high cost, and requirement of highly skilled operators are associated with these methods. Development of optical sensors for selective and sensitive detection of cyanide ion has been explored in recent times.³³ These sensor systems have their own advantages like fast detection, operational simplicity and feasibility for naked-eye detection, thereby providing an opportunity for on-site analysis.³⁴ So far, different sensors based on hydrogen bonding interaction, supramolecular self-assembly, coordination of cyanide ion with a metal ion, boronic acid derivatives, nucleophilic addition reaction, deprotonation, etc. have been reported.³⁵ Amongt these, particular interest has been devoted to design fluorescent probes based on pyrylium, indolium, pyridinium, oxazine, acridinium, imidazole, carbazole, dicyano-vinyl group, quinoline, salicylaldehyde, trifluoroacetamide derivatives and other highly electron-deficient carbonyl compounds for selective detection of cyanide ion.³⁶

Earlier, fluorescent molecules with binding sites such as metal ions, H^+ , and boronic acid derivatives were developed for the detection of CN^- ion.³⁷ These systems have a good binding affinity towards cyanide anions. In comparison to the binding-based probes, reaction-based probes have received great attention nowadays due to their high selectivity with sensitivity in detecting cyanide ions. The cyanide ions involve in the nucleophilic addition reactions readily with electrophiles such as C=O, C=C, C=N, or C=N⁺ units. In the addition product, the π -conjugation is interrupted and thus shows an optical response. Michael addition of CN^- to the acceptor center of the dicyanovinylene unit in a donor-acceptor system is a trivial way of sensing cyanide ion as the intramolecular charge transfer is lost upon addition. BODIPY based molecules have also been used for the detection of cyanide ions. Fluorescent BODIPY molecules bind directly to CN^- ion and results in a change of its optical properties. Some of the representative CN^- ion sensors are shown in Figure 2.24 and Figure 2.25. ^{38, 39}

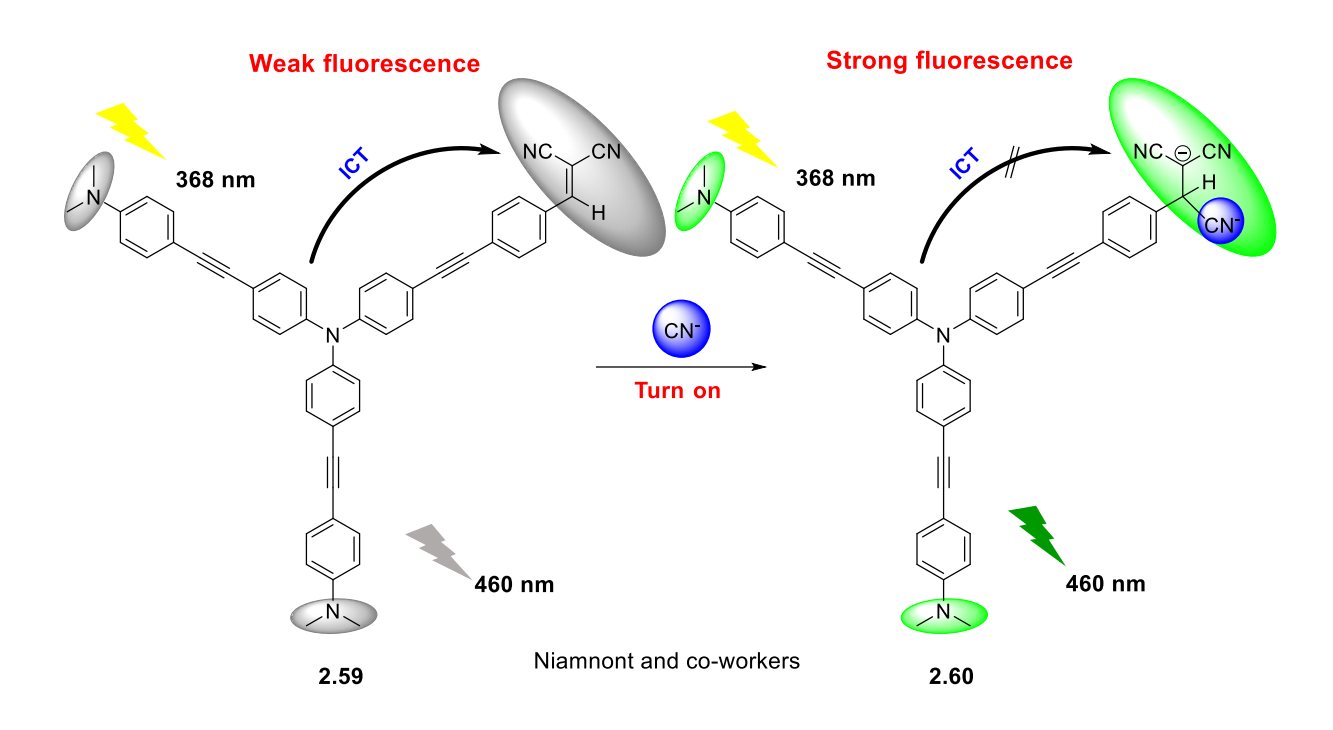


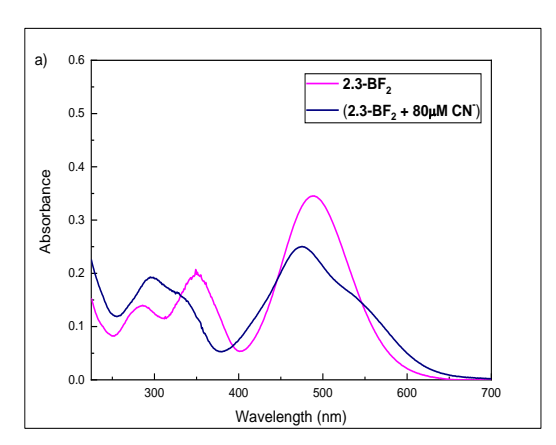
Figure 2.24. Representative CN⁻ ions sensors based on reaction with CN⁻ ions.

Figure 2.25. Representative molecular structure of BODIPY based molecules for the detection of CN ion.

From the existing literature on cyanide ion sensing, it is clear that CN⁻ can react with dicyanovinylene and BF₂ of BODIPY. In this regard, we were curious to know the outcome of the reaction and the photophysical properties of our compounds, which have both BF₂ and dicyanovinylene in the same molecule. Therefore, we started to test the compound **2.3-BF₂** with tetrabutylammonium cyanide for cyanide ion detection. The results indicated that the detection of CN⁻ was very poor from the dual acceptor units of compound **2.3-BF₂** (Figure 2.26).

2.5.3.1 Absorption and Emission Properties of 2.3-BF₂ in the Presence and Absence of CN⁻

The absorption and emission spectra of compound **2.3-BF**₂ in the presence and absence of tetrabutylammonium cyanide were recorded in acetonitrile and the spectra are given in Figure. 2.26. The compound **2.3-BF**₂ showed absorptions at 488 nm and 350 nm. The absorption bands at 488 nm 350 nm were observed due to the intramolecular charge transfer between triphenylamine to vinylene dicyano unit and triphenylamine to BF₂ complex respectively. Slight changes were observed in the absorption spectra of compound **2.3-BF**₂ when it was treated with tetrabutylammonium cyanide (7 μ M) in 1:11 equivalent and the absorption bands were shifted to 477 nm and 298 nm respectively. However, the emission band of compound **2.3-BF**₂ observed at 549 nm saw a 2.5-fold enhancement when excited at λ_{ex} = 393 nm in the presence of tetrabutylammonium cyanide (7 μ M solution in acetonitrile) in 1:11 equivalent.



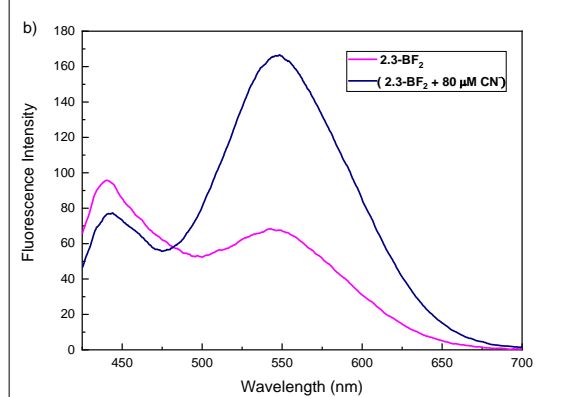


Figure. 2.26. a) The absorption spectrum of **2.3-BF**₂ in the presence and absence of TBA cyanide in acetonitrile (1:11 equivalent); b) Emission spectrum of **2.3-BF**₂ in the presence and absence of TBA cyanide in acetonitrile.

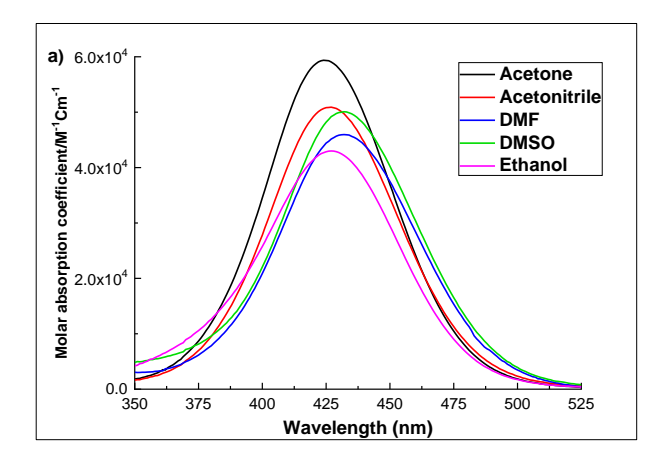
Based on this result, in order to simplify the system, we synthesized a simple system in which triphenylamine is connected with 1,3-diketone difluoro boron complex **2.67-BF**₂ for cyanide sensing application. The synthetic route for the synthesis of compound **2.67-BF**₂ is given in Scheme 2.4.

Figure 2.27. Molecular structures of compound 2.67-BF₂.

Scheme 2.4. Synthetic route to access compound 2.67-BF₂.

The compound **2.67-BF₂** was synthesized using a reported procedure.⁴⁰ The key intermediate **2.67** was obtained by the Claisen condensation of acetyl triphenylamine with ethyl acetate in the presence of strong base NaH. Addition of BF₂.OEt₂ to **2.67** in dichloromethane solvent afforded the target product.

The compound **2.67-BF**₂ responded remarkably well for the detection of cyanide ion in tetrabutylammonium cyanide. The detection of cyanide ion was optimized using UV-Vis and fluorescence spectroscopy.



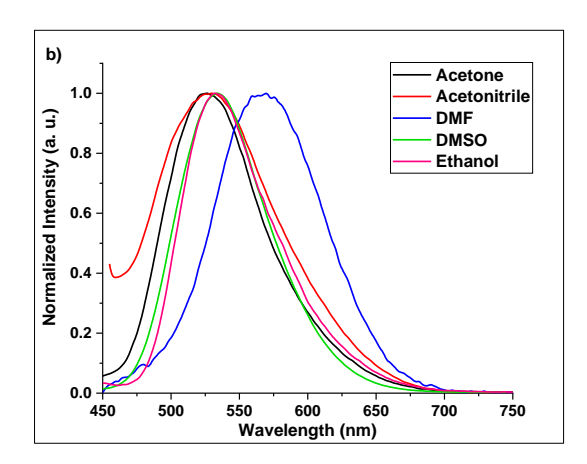
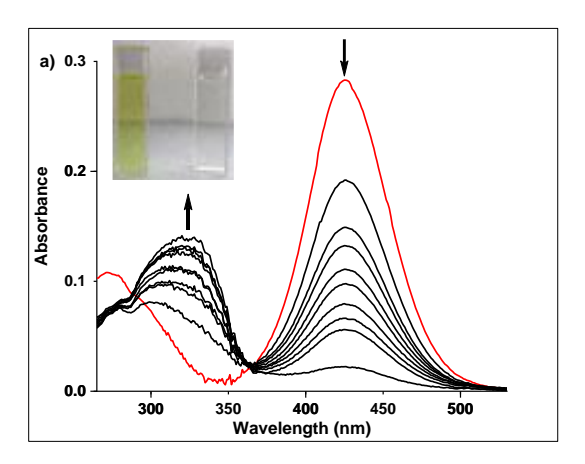


Figure 2.28. Absorption and emission spectra of 2.67-BF₂ in various solvents.



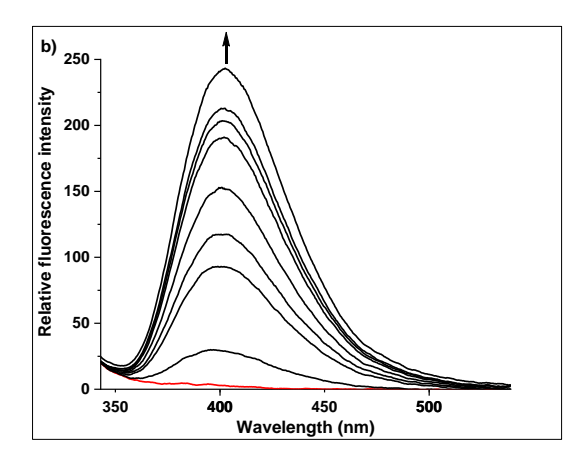


Figure 2.29. Absorption and emission spectra of **2.67-BF₂** (7 μ M) in the presence and absence of CN⁻ (0-400 μ M) in acetonitrile/water (98:2) solution.

2.5.3.2 Absorption and Emission Spectral Studies in the Presence and Absence of Anions

The absorption and emission spectra of **2.67-BF**₂ in the presence and absence of cyanide ions (tetrabutylammonium cyanide) in acetonitrile:H₂O (98:2) are shown in Figure 2.29. The acetonitrile:H₂O (98:2) system was chosen for cyanide ion sensing based on the photophysical results obtained from a series of experiments with different fractions of water in acetonitrile. Notable change in absorption and emission characteristics was noted in solvents systems containing less than 10% of the water in acetonitrile. On increasing the concentration of cyanide ion, the intensity of the ICT absorption band centered at 425 nm decreased along with the formation of a new absorption peak at 320 nm. The formation of an isosbestic point at 364

nm indicates the 1:1 interaction between the 2.67-BF2 and CN. The stoichiometry between 2.67-BF2 and CN was again confirmed from the Job's plot. As seen in the Job's plot curve (Figure 2.30), the measured absorbance variation at 320 nm reached a maximum value when the molar ratio of $[2.67-BF_2]/([2.67-BF_2] + [CN^-])$ was 0.50, which indicated a 1:1 interaction between 2.67-BF₂ and CN⁻. At a higher concentration of CN⁻, the absorption band at 425 nm disappeared completely, and the new band at 320 nm was only visible. This is due to the fact that electron density at acceptor moiety increases after the nucleophilic addition of CN⁻ which results in the formation of a new ICT state leading to the complete disappearance of the old ICT band at 425 nm. This change in the ICT behavior resulted in a color change from yellow to colorless, indicating that compound 2.67-BF2 could be employed as a colorimetric probe to detect CN⁻ with the naked eye (Figure 2.29a). Fluorescence spectra of **2.67-BF**₂ in acetonitrile: H₂O (98:2) were recorded by exciting at the isosbestic point (272 nm) after every addition of aliquots of tetrabutylammonium cyanide solution of known concentration to it. As shown in Figure 2.29b, **2.67-BF**₂ is non-fluorescent at this excitation wavelength in the absence of CN⁻. In contrast, presence of CN⁻ led to the formation of a new emission peak centered at 402 nm. The gradual addition of cyanide ion led to fluorescence enhancement at 402 nm due to the formation of a new ICT state.

The stock solution of 125 mM of **2.67-BF**₂ and CN⁻ were prepared in 98:2 acetonitrile-water mixtures. The absorption spectra in each case with different **2.67-BF**₂ -CN⁻ ratio in equal volume were recorded. Job's plot was drawn by plotting absorbance at 320 nm vs. [**2.67-BF**₂]/([CN⁻]+[**2.67-BF**₂]).

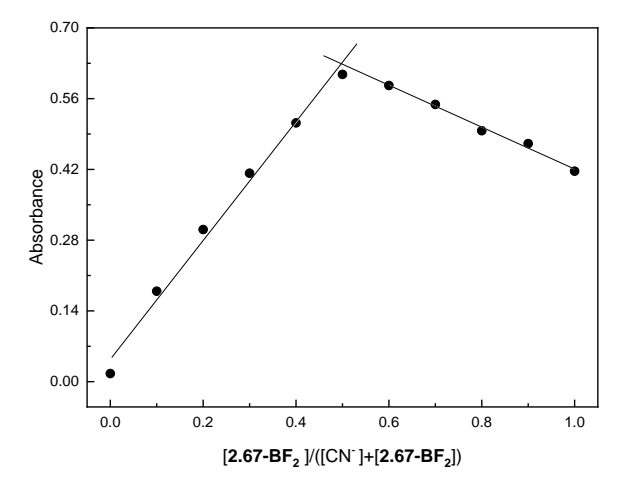


Figure 2.30: Job's plot for **2.67-BF**₂-CN⁻ in acetonitrile-water (98:2, v/v) exhibiting 1:1 binding stoichiometry.

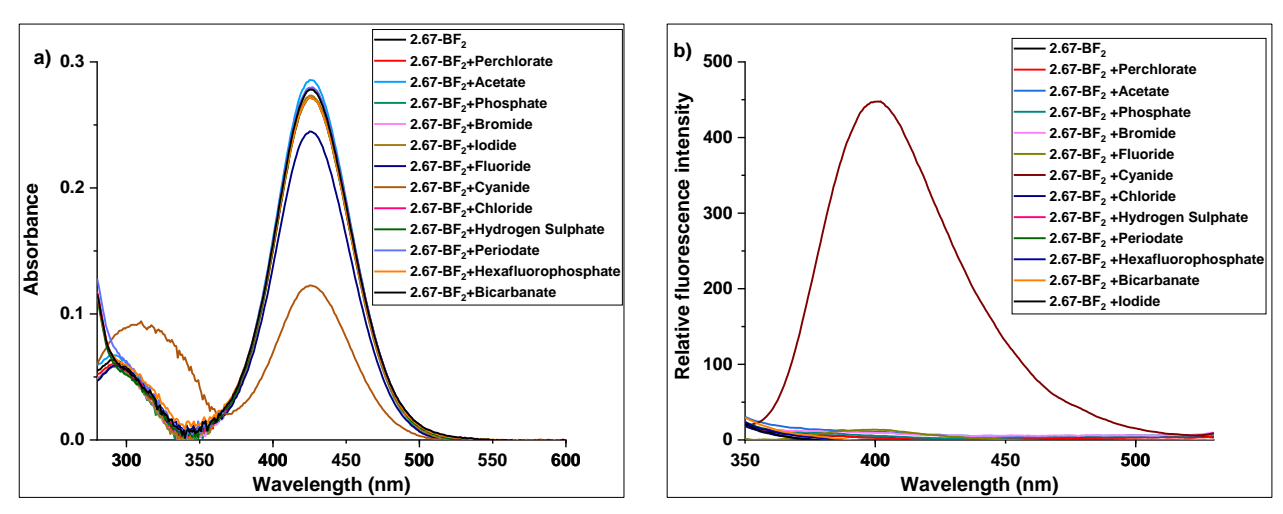
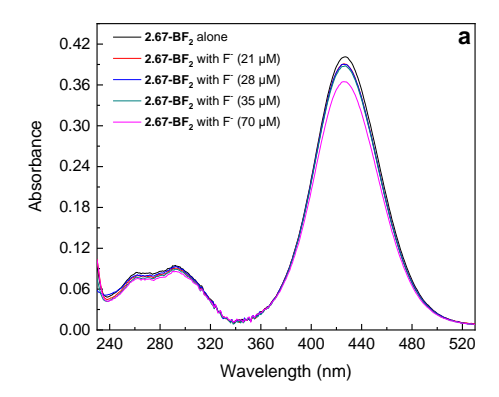


Figure 2.31. Absorption and emission spectra of **2.67-BF₂** (7 μ M) with various anions (60 μ M) in acetonitrile/water (98:2) solution.

2.5.3.3 Selectivity and Effect of Anion Interference

To evaluate the selectivity of cyanide ion over other anions, the optical response of **2.67-BF₂** in 98% acetonitrile with various anions in excess were evaluated using absorption and emission spectral studies (Figure 2.31). Among the tested anions (CN⁻, F⁻, Cl⁻, Br⁻, I⁻, AcO⁻, ClO₄⁻, PO₄³⁻, HSO₄⁻, IO₄⁻, PF₆⁻, HCO₃⁻) as their tetrabutylammonium salts at 10 equivalents excess concentration ($60 \mu mol$), the probe responded only to the cyanide ion with a remarkable color change from yellow to colorless. The addition of fluoride ion in excess also caused a slight influence on the absorption spectrum of **2.67-BF₂**, but with a much lower sensitivity than that of CN⁻. The absorption and emission spectra of **2.67-BF₂** in the presence and absence of F⁻ are depicted in Figure 2.32. In contrast to the absorption spectrum, there is no change in the fluorescence spectrum in the presence of F⁻. It was the case with the other anions as well. F⁻ is highly solvated in water and loses its basicity due to hydration in acetonitrile-water mixture. The slight change observed in the absorption spectrum may be due to the change in the solvation around the **2.67-BF₂** molecule. The comparatively lower hydration energy for the cyanide ion ($\Delta H_{hyd} = -64 \text{ kJ/mol}$) than that of the fluoride ion ($\Delta H_{hyd} = -505 \text{ kJ/mol}$) may be the reason for the higher selectivity and sensitivity of **2.67-BF₂** towards cyanide ion.⁴¹



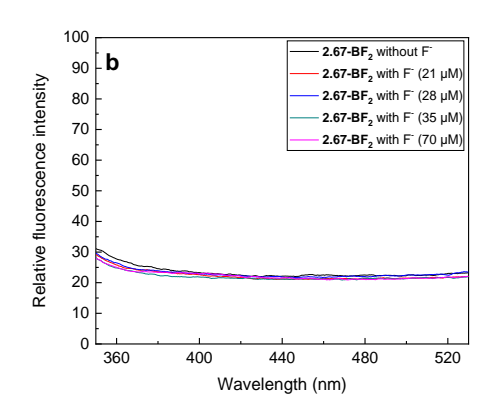


Figure 2.32. Absorption and emission spectra of **2.67-BF₂** (7μ M) in the presence and absence of fluoride ion in 98% acetonitrile.

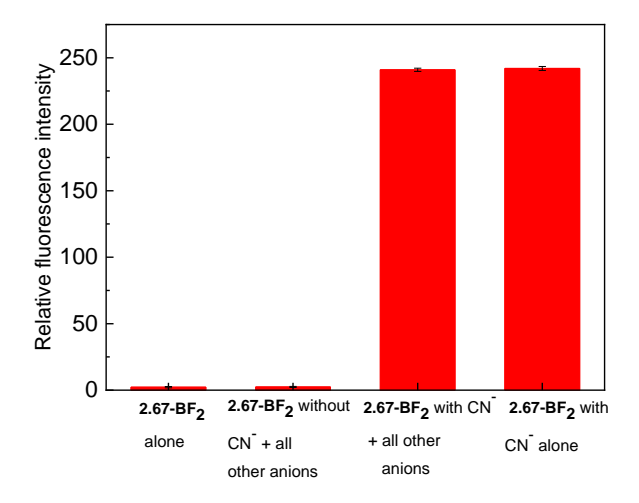


Figure 2.33. Competitive experiments in the **2.67-BF**₂-CN⁻ system with interfering anions ($\lambda_{ex} = 272$ nm). Selectivity profiles of **2.67-BF**₂ (7 μ M) in the presence of 60 μ M of various anions (F⁻, Cl⁻, Br⁻, I⁻, AcO⁻, ClO₄⁻, PO₄³⁻, HSO₄⁻, IO₄⁻, PF₆⁻, HCO₃⁻) in acetonitrile/water (98:2) with or without CN⁻.

To further explore the utility of **2.67-BF₂** as an ion-selective fluorescent sensor for CN⁻, the effect of other anion interference on the detection of CN⁻ was carried out upon the addition of 10 equivalents of other anions individually and all other anions combined in 98% acetonitrile solution (Figure 2.33). These results indicate that other anions did not induce any significant changes in the presence of CN⁻. Therefore, **2.67-BF₂** could be used as a fluorescent and colorimetric sensor for CN⁻ detection with excellent selectivity and specificity. From the fluorescence titration, the detection limit of cyanide ion using **2.67-BF₂** was found to be 0.36 μM.

Figure 2.34. Chemical structures of control compounds used to understand the CN⁻ sensing mechanism of **2.67-BF₂**.

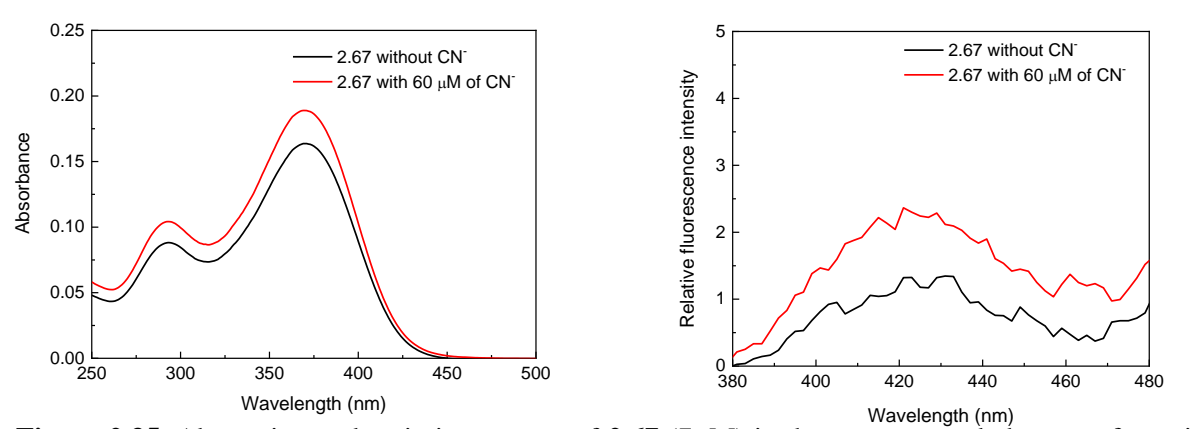


Figure 2.35. Absorption and emission spectra of **2.67** $(7\mu M)$ in the presence and absence of cyanide ion in 98% acetonitrile.

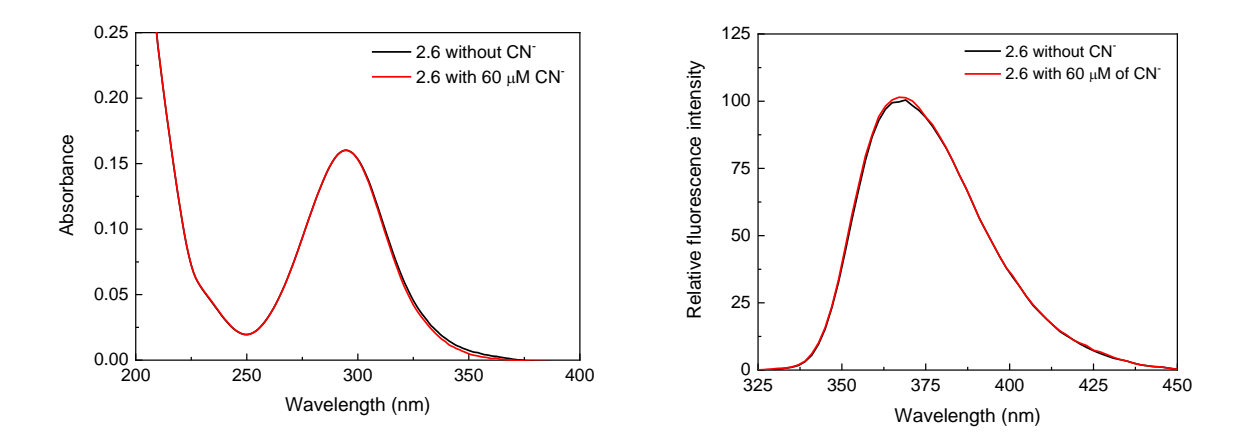


Figure 2.36. Absorption and emission spectra of **2.6** ($7\mu M$) in the presence and absence of cyanide ion in 98% acetonitrile.

In order to understand the binding mechanism and high selectivity of **2.67-BF**₂ towards CN⁻, similar kinds of photophysical studies were carried out with two control compounds, **2.67** and **2.6** (Figure 2.35 and 2.36). There is no significant change in the absorption and emission spectra of control compounds with all the anions studied, including CN⁻. It clearly indicates that difluoroboron moiety plays a crucial role in the sensing of CN⁻.

2.5.3.4 Detection Mechanism

The detection mechanism (Scheme 2.5) was elucidated by both experimental (¹H, ¹¹B and ¹⁹F NMR titrations, HRMS spectra) and theoretical studies. In the ¹H-NMR of **2.67-BF₂**, the olefinic proton (-H_a) and methyl protons (-CH_{3a}) appeared at 6.58 ppm and 2.22 ppm respectively in the acetonitrile-d₃ solvent. Upon the addition of two equivalents of tetrabutylammonium cyanide, both the protons -H_b and -CH_{3b} experienced a considerable upfield shift to 5.03 and 1.55 ppm, respectively. The methyl protons were merged with -CH₂-protons of tetrabutylammonium cyanide (Figure 2.37). Besides, some changes of peak positions in the aromatic region were observed.

Scheme 2.5. A plausible mechanism of addition of CN⁻ to **2.67-BF₂** and reversibility upon addition of excess water.

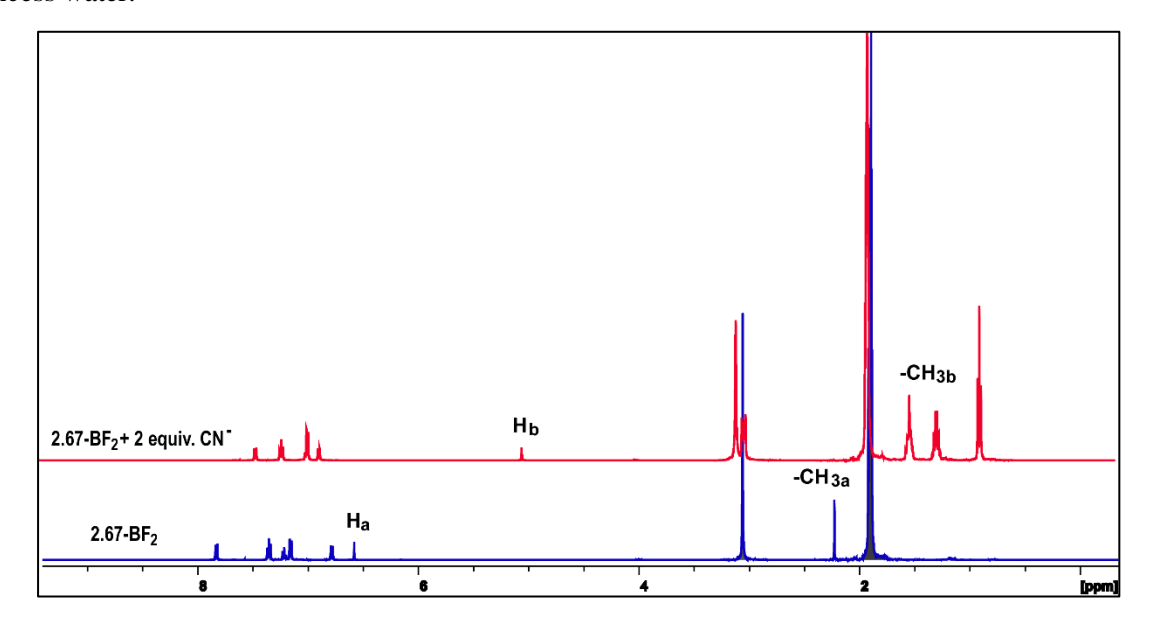


Figure 2.37. ¹H NMR spectra of compound **2.67-BF₂** in acetonitrile-d₃ and after the addition of 2 equiv. CN⁻ in acetonitrile-d₃.

Chapter 2

In order to elucidate the actual interaction between the cyanide ion and **2.67-BF₂**, NMR titrations have been carried out with different aliquots of tetrabutylammonium cyanide from 0.1 to 2.0 equivalents by ¹H, ¹¹B, ¹⁹F NMR spectroscopy in CDCl₃. Solvent CDCl₃ was chosen for this experiment because the peaks due to acetonitrile and water in CD₃CN appeared prominently in the aliphatic region of **2.67-BF₂**. Upon increasing the concentration of CN⁻ from 0 to 2.0 equivalents a gradual decrease in intensity of the olefinic -CH and CH₃ protons of **2.67-BF₂** and increase in intensity of the new peaks at 5.03 and 1.55 ppm were noted. The olefinic proton signal at 6.4 ppm and the methyl peak at 2.3 ppm completely disappeared in the presence of excess CN⁻ (Figure 2.38). The same spectral pattern was observed in ¹⁹F spectra as well (Figure 2.39). However, ¹¹B NMR was not informative (Figure 2.40).

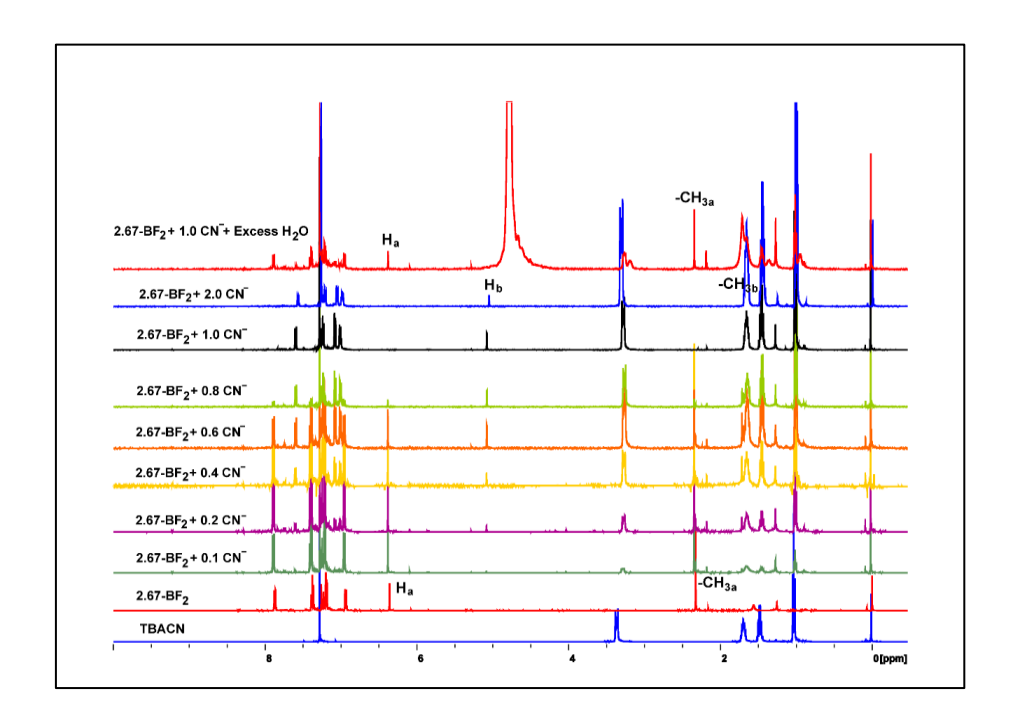


Figure 2.38. ¹H NMR spectra of titration experiment with tetrabutylammonium cyanide on **2.67-BF₂** in CDCl₃.

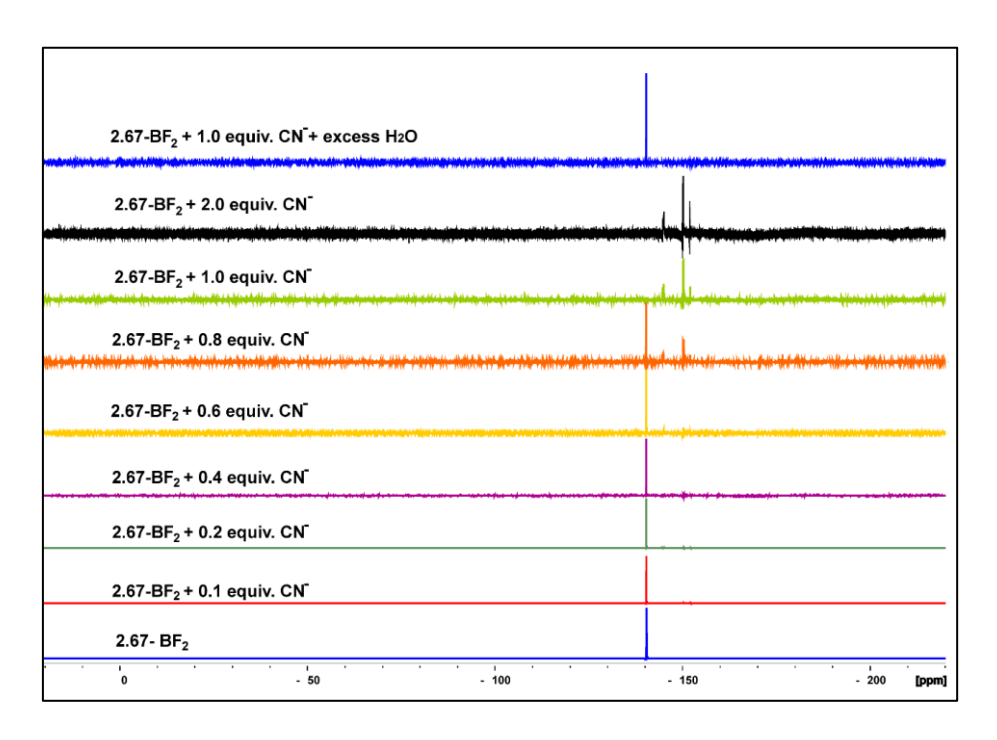


Figure 2.39. 19 F NMR spectra of titration of 2.67-BF2 with tetrabutylammonium cyanide in CDCl3.

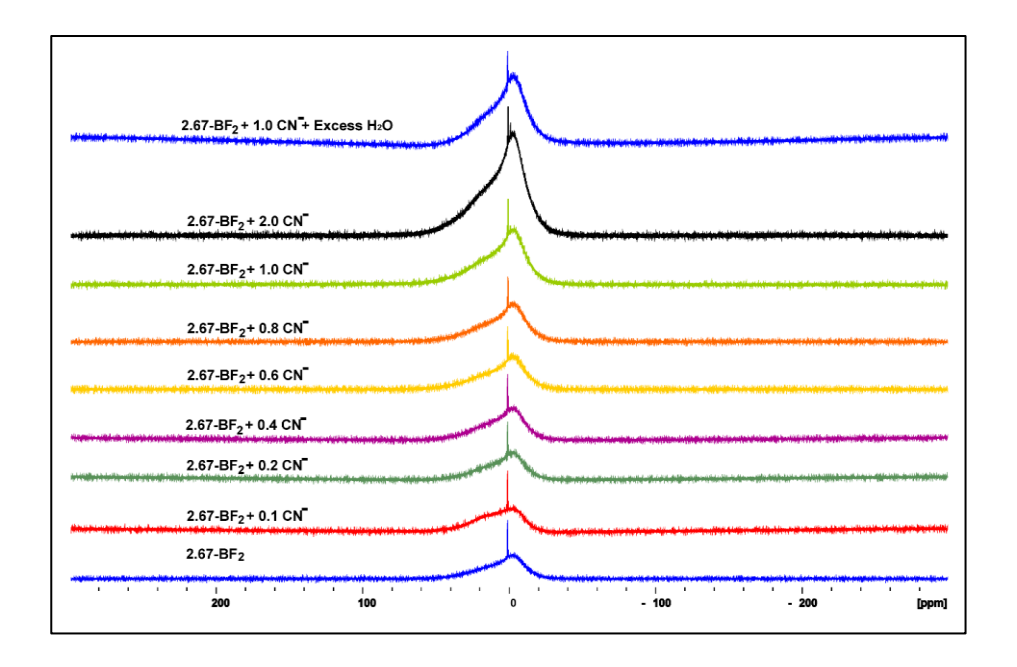


Figure 2.40. ¹¹B NMR titration of 2.67-BF₂ with tetrabutylammonium cyanide in CDCl₃.

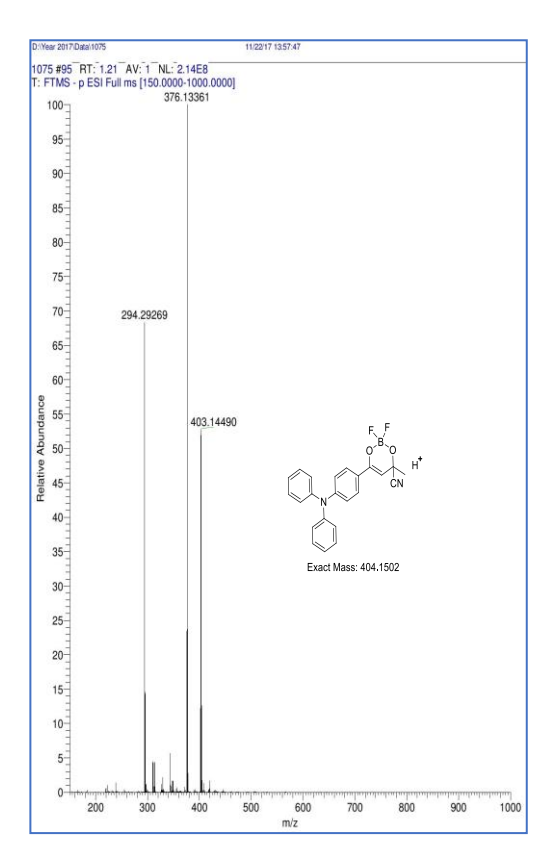


Figure 2.41: HRMS spectra of 2.67-BF₂+CN⁻.

These results indicate that the transformation of 2.67-BF₂ to 2.67-BF₂ -CN⁻, which was further confirmed by HRMS analysis. The molecular ion peak 2.67-BF₂appeared at 400.1291 corresponding to C₂₂H₁₈BF₂NO₂Na [M+Na]⁺. In the presence of 10 equivalents of CN-, 2.67-BF2 in acetonitrile:water (98:2) solution showed signal assignable to the formation of the 2.67-BF₂ + CN⁻ adduct at m/z, 403.1449 (Figure. 2.41). Based on the NMR titrations, a plausible structure for the adduct, as shown in Scheme 2.5, has been proposed. In an organic solvent, strong nucleophile CN can attack the carbonyl carbon to give the intermediate (I) in which the olefinic and methyl protons are expected

to experience upfield shifts. To our surprise, the actual NMR spectral characteristics of **2.67-BF₂** were restored by the addition of excess water to **2.67-BF₂** -CN⁻. This could be due to the leaving of cyanide ion from the **2.67-BF₂** +CN⁻ adduct, which in turn generates the starting compound (Scheme 2.5). The solvation of CN⁻ in water, perhaps, is the reason for the above reverse reaction. The ¹H and ¹⁹F NMR titrations reveal that there is no fluoride displacement in the presence of CN⁻. There are a few reports on cyanide ion sensors based on BODIPY and related compounds. The sensing mechanism proposed in the present study is different from those that are reported in these reports. ⁴²

2.5.3.5 Computational Studies

To further investigate the CN⁻ detection mechanism using **2.67-BF**₂, density functional theory (DFT) calculations were performed at the B3LYP/6-31G* level of the Gaussian 09 program to understand their electronic structures.⁵ Optimization of **2.67-BF**₂ and **2.67-BF**₂ +CN⁻ was performed in the gas phase. The calculated molecular orbitals and their energies are shown in Figure 2.42.

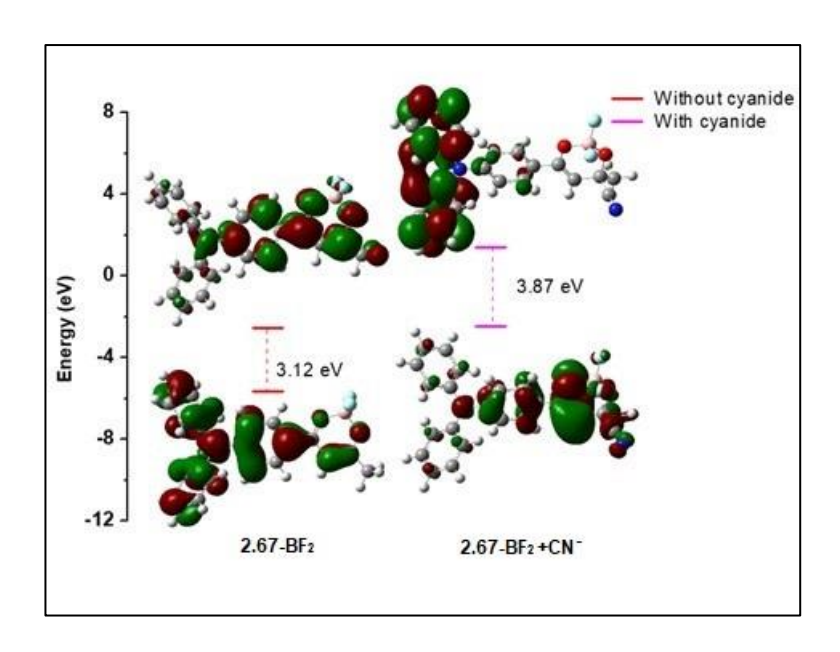


Figure 2.42. HOMO and LUMO of 2.67-BF₂ and 2.67-BF₂ +CN⁻.

In **2.67-BF**₂, the highest occupied molecular orbital (HOMO) is localized mainly onto the triphenylamine (TPA) unit, and the lowest unoccupied molecular orbital (LUMO) is localized mostly on the dioxaborine ring and one of the phenyl rings from TPA moiety connected to it. Interestingly, the nucleophilic addition of CN⁻ with **2.67-BF**₂ leads to a complete reversal of HOMO to LUMO and LUMO to HOMO. HOMO is localized mainly on the dioxaborine ring, and LUMO is localized on the two phenyl rings perpendicular to the plane of the molecule. It confirms that the nucleophilic addition of CN⁻ with **2.67-BF**₂ leads to the formation of a new ICT state, which in turn responsible for the enhancement in new ICT emission peak upon increasing the CN⁻ concentration. The increase in the energy gap between HOMO and LUMO is accountable for the blue-shifted emission in the presence of CN⁻.

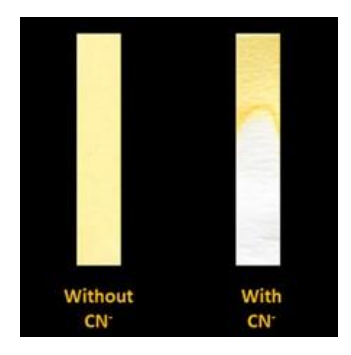


Figure 2.43. Test strip detection of CN⁻ in water.

2.5.3.6 Test Strip Detection of Cyanide Ion

A test-strip-based assay was developed to achieve the detection of CN⁻ in neat aqueous solution, and thereby using it in situ/on-site detection is viable. We chose the Whatman filter paper because this matrix ensures the probe is physisorbed well so that there is no leaching of the hydrophobic probe molecules in water. Whatman test strips were dipped into the acetonitrile solution of 2.67-BF₂ and left to dry in air. It was then immersed in 10 μM aqueous solution of tetrabutylammonium cyanide. As seen in Figure 2.43, significant color change from yellow to colorless was observed immediately. It proved that the test strips could be applied to detect CN⁻ qualitatively in water for rapid detection. The test strip experiments conducted at various concentrations were not useful as the color change was not prominent at lower concentrations.

2.6 Conclusion

In summary, the donor-acceptor systems incorporated with 1,3-dicarbonyl and their corresponding difluoroboron complexes **2.1-2.5** and **2.1-BF₂-2.5-BF₂** were synthesized successfully in good to moderate yields. Photophysical, electrochemical, and DFT studies were carried out on these compounds. The dyes **2.2** and **2.4** were tested for the application in dyesensitized solar cells, and found to show 0.12% and 0.25% power conversion efficiency, respectively. More optimization in making the device may be required in order to improve the PCE of these systems.

These high Stokes shift compounds showed promising applications in live-cell imaging of microtubules. The fluorescent donor-acceptor compounds 2.1-2.3 and $2.1-BF_2-2.3-BF_2$ can bind selectively to α - and β -tubulin dimer. These compounds exhibited good selectivity towards binding to β -tubulin, as revealed by the co-localization studies. These dyes can be used as a marker for the imaging of microtubules in live-cells without attaching them to tubulin specific antibody or tubulin-binding compound. Except one compound (2.1), all the compounds are non-cytotoxic. The core structure of these compounds, in principle, could be used for developing therapeutic agents for cancer treatment as tubulin is one of the drug targets for cancer therapy.

A simple compound **2.67-BF₂** was developed for the application in cyanide ion sensing. Nucleophilic addition of cyanide ion on difluoroboron β -diketonate completely changes the photophysical properties of **2.67-BF₂** and thereby offers selective detection of CN⁻ both

colorimetrically and fluorimetrically. **2.67-BF**₂ senses the CN⁻ with a detection limit of 0.36 µM without any interference from other anions. Test strip detection in water and immediate response make **2.67-BF**₂ a promising system for sensing of CN⁻.

2.7 Experimental Section

2.7.1 General Information.

All the Chemicals and solvents have purchased from various commercial sources. THF, toluene was dried over sodium metal before use. Fresh dichloromethane was used for a reaction after distilled over CaH₂. MeOH dried overusing Mg/I₂. ¹H and ¹³C spectra were recorded on a Bruker Avance 400 MHz and 500 MHz instruments in CDCl₃ and CD₃CN as a solvent with tetramethylsilane (TMS) as an internal standard. IR spectra were recorded on JASCO FT/IR-5300 and ATR-IR spectrometer. UV-Vis spectra were recorded on Shimadzu UV-3600, Cary 300 Bio and Fluorescence spectra were recorded on the Fluoromax-4 and Jasco FP-6300 spectrometer at room temperature. Cyclic voltammetry was obtained on Zahner electrochemical workstation under the N2 atmosphere at a scan rate of 100 mV/s. HOMO-LUMO calculations were carried out in Gaussian 09 package using B3LYP/6-31G basic sets. High-resolution mass spectra (HRMS) were recorded on micro mass ESI-TOF MS. XRD were collected from Bruker D8 Quest. XRD was collected from Bruker D8 Quest. Fluorescence lifetimes were measured with a Horiba DeltaFlex TCSPC system equipped with a NanoLED laser (435 nm, pulse width <200 ps) excitation source, and a PPD-850 photon detection module and time-correlated single-photon counting spectrometer (HORIBA Jobin Yvon IBH). The progress of the reaction was monitored by TLC and visualized under UV and Iodine chamber. Column chromatography was performed on silica gel (100-200 mesh size), using ethyl acetate and hexanes mixture as eluent.

2.7.2 Device Fabrication:

Fluorine doped tin oxide coated substrates (11Ω/sq) were cleaned using solvents such as soap solution, DI water, acetone, and IPA by sonicating for 20min each, the substrates were blown dry using compressed air. Mesoporous TiO₂ was deposited on the substrates by doctor blading technique followed by annealing at 500°C for 30 minutes. Nanocrystalline layer of P25 was deposited on top of the mesoporous layer and was subjected to annealing at 500°C for 30 min. The annealed substrates were subjected to 40mM TiCl₄ treatment at 100°C for 1h and then rinsed in DI water. The TiCl₄ treated substrates were sintered at 500°C for 30min. The substrates were dipped in dye (N719, 2.2, 2.4) for 24 h to ensure complete dye adsorption onto

the TiO₂ surface, followed by rinsing in ethanol to remove the excess dye. Counter electrodes were also prepared by coating platinum by doctor blading technique followed by annealing at 500°C for 30min. The photoanode and counter electrode were sandwiched with the help of a surlyn polymer. Electrolyte (0.6 M 1,2-dimethyl-3-n-propylimidazolium iodide, 0.1 M LiI, 0.05 M I₂, and 0.5 M 4-tert-butylpyridine in acetonitrile) was introduced through the hole in the counter electrode and sealed using cover glass and surlyn polymer to prevent electrolyte leakage.

2.7.2.1 Characterization: The thickness of each layer was measured using a profilometer (Bruker instruments). The current-voltage data were recorded using a solar simulator (oriel instruments) under AM 1.5 standards. The instrument was calibrated for 1 sunlight intensity using an NREL calibrated Si solar cell.

The device fabrication and characterization were carried out by Dr. V. Ganapathy, Reshma (CSEM, ARCI, Hyderabad, Telangana).

2.7.3 Cell Lines and Cell Culture

The cell lines HeLa (<u>human cervical cancer</u>) cell line was obtained from the National Centre for Cellular Sciences (NCCS), Pune, India. Cells were cultured in DMEM media, supplemented with 10% heat-inactivated fetal bovine serum (FBS), 1 mM NaHCO₃, 2 mM - glutamine, 100 units/ml penicillin and 100 μg/ml streptomycin. All cell lines were maintained in culture at 37° C in an atmosphere of 5% CO₂.

2.7.3.1 Test Concentrations:

Initially, stock solutions of each test substances were prepared in 100% Dimethyl Sulfoxide (DMSO, Sigma Chemical Co., St. Louis, MO) with a final concentration of 10 mg/ml. Exactly 20µl of stock was diluted to 1 ml in culture medium to obtain experimental stock concentration of 200µg/ml. This solution was further serially diluted with media to generate a dilution series of 0.001µg to 100 µg/ml. Exactly 100µl of each diluent was added to 100µl of cell suspension (total assay volume of 200µl) and incubated for 24 h at 37 °C in 5% CO₂. Respected volume of DMSO used as a control.

2.7.3.2 Cytotoxicity:

Cytotoxicity was measured using the MTT [3-(4, 5-dimethylthiazol-2-yl)-2, 5-diphenyl tetrazolium bromide] assay, according to the method of Mossman (1983). Briefly, the cells (3

x 10^3) were seeded in each well containing 0.1 ml of medium in 96 well plates. After overnight incubation at 37 °C in 5% CO₂, the cells were treated with 100 µl of different test concentrations of test compounds at identical conditions with five replicates each. The final test concentrations were equivalent to 0.001 to $100\mu g/ml$ or 0.001 to 100 ppm. The cell viability was assessed after 24 h, by adding 10 µl of MTT (5 mg/ml) per well. The plates were incubated at 37 °C for additional three hours. The medium was discarded and the formazan blue, which formed in the cells, was dissolved with 100 µl of DMSO. The rate of colour formation was measured at 570 nm in a spectrophotometer (Bio-Rad). The percent inhibition of cell viability was determined with reference to the control values (without test compound). The data were subjected to linear regression analysis and the regression lines were plotted for the best straight-line fit. The IC₅₀ (inhibition of cell viability) concentrations were calculated using the respective regression equation.

2.7.3.3 Fluorescence Microscopy:

For microscopic evaluation, HeLa cells were cultured on cover slips in the 6-well plates to 70% confluence and treated with 10 µg of compounds (2.1-2.3 and 2.1-BF2-2.3-BF2) in complete cell culture media for up to 12 h. In all experiments, a corresponding DMSO control was run in parallel for 12h. After incubating for 12 h, HeLa cells were washed with PBS for three times and fixed with 4% paraformaldehyde for 20min, mounted using with DAPI for visualization of nuclei, and incubated for 1 h in the dark. After incubation cells were visualized and captured by fluorescence microscopy (Olympus, USA) using excitation wavelengths between 400-418 for DAPI and 478-495 for compounds.

For reference, parallelly HeLa cells were cultured on cover slips in the 6-well plates to 70% confluence washed with PBS for three times and fixed with 4% paraformaldehyde for 20min, permeabilized with cold methanol for another 10min. After that, the cells were blocked with 5% BSA for 1 h. Subsequently, the cells were washed with PBS, and incubated with antitubulin antibody in 3% BSA (1:200, Sigma.) overnight at 4 °C. After being washed with PBS for three times, each cover slip was added 200μL of Alexa Fluor 546 anti-mouse secondary antibody in 3% BSA (1:500, Molecular probes) and incubated for 1h at room temperature. At last, HeLa cells was stained with 20μL of DAPI for 1 h and observed under confocal microscope (Olympus, USA).

2.7.3.4 Wound Healing Assay:

A wound healing assay was performed to observe the effect of the dyes **2.1-2.3** and **2.1-BF2-2.3-BF2** on the migration ability of the HeLa cells. The HeLa cells were seeded at 1×10^6 cells/well into six-well plates. After the cells were allowed to attach and reach 80% confluency, the monolayer cells were manually scratched with a sterile pipette tip and then change fresh medium to remove the cell debris. After removing cell debris, the cells were treated with 20 μ g of each compound in DMEM or only with DMEM (control). Each evaluated sample was plated in triplicate. Photographs of the scratch area were taken in treated and untreated cells using a Nikon Eclipse TE2000-S microscope (Nikon GmbH, Düsseldorf, Germany) at 0 hr and after 24 hr incubation. The closure was measured by wound area in each period and expressed as a percentage of the initial wound area at 0 h.

2.7.3.5 *In Vivo* Tubulin Interaction Assay:

To confirm the interaction of dyes **2.1-2.3** and **2.1-BF₂-2.3-BF₂** with tubulins and fluorescence activity, we performed *in vivo* tubulin interaction assay. Briefly, HeLa cells (1x10⁶ cells/well) were treated with or without dyes **2.1-2.3** and **2.1-BF₂-2.3-BF₂** for 12 h, and cell pellets were suspended in native page lysis buffer. The concentration of total proteins was determined using a Bradford protein assay (Bio-Rad Laboratories, Hercules, CA). An equal amount of protein from each sample was resolved on 10% native gel followed by electro transferred onto nitrocellulose transfer membrane (Millipore). The membrane was visualized under FITC filter by Bio-Rad's gel documentation system.

2.7.4 Experimental Procedure and Analytical Data

2.7.4.1 Synthesis of 4-(diphenyl amino) Benzaldehyde (2.7):^{3a}

POCl₃ (1.3 mL, 8.15 mmol) was added dropwise to a solution of triphenylamine **2.6** (1 g, 4.0 mmol) in dry DMF (10 mL) at 0 °C and allowed to stir at 50-55 °C for 16 h. The progress of the reaction was monitored by TLC using 20% EtOAc/hexanes mixture as a mobile phase.

After completion of the reaction, the reaction mixture was poured into ice-cold water and extracted with EtOAc (2×50 mL). The organic layer was washed with H₂O (50 mL) and brine solution (10 mL). The organic layer was dried over NaSO₄ and evaporated using a rotary evaporator under vacuum. The crude product was purified by column chromatography using 1:5 EtOAc/hexane to get the desired product as a pale-yellow solid (0.8 g, yield = 72%). R_f = 0.80. MP: 149-151 °C; ¹H NMR (400 MHz, CDCl₃): δ 9.80 (s, 1H), 7.67 (d, J = 8.8 Hz, 2H),

7.34 (t, J = 7.6 Hz, 4H), 7.17 (d, J = 6.8 Hz, 6H), 7.01 (d, J = 8.8 Hz, 2H); ¹³C NMR (100 MHz, CDCl₃): δ 190.5, 153.4, 146.2, 131.4, 129.8, 129.2, 126.4, 126.2, 119.4.

2.7.4.2 Synthesis of 4-(diphenyl amino) Benzoic acid (2.8):3b

To a stirred solution of 4-(diphenyl amino) benzaldehyde $\bf 2.7$ (2 g, 7.34 mmol) in 100 mL of acetone- $\bf H_2O$ (4:1 v/v) was added KMnO₄ portion wise. The reaction mixture was allowed

to stir at 60 °C for 4 h. The reaction mixture was concentrated under vacuum, filtered under suction and washed with water. The filtrate was acidified with dil. HCl (50 mL) to give a white precipitate which was filtered using a suction pump. It was washed with water and dried under

vacuum to get the titled compound as a white solid (1.84 g, yield = 71%). MP: 210-212 °C; R_f = 0.22 in 1:5 EtOAc/hexanes; ¹H NMR (400 MHz, CDCl₃): δ 7.90 (d, J = 8.8 Hz, 2H), 7.32 (t, J = 8.4 Hz, 4H), 7.17-7.12 (m, 6H), 6.99 (d, J = 8.8 Hz, 2H); ¹³C NMR (100 MHz, CDCl₃): δ 164.0, 152.8, 146.5, 131.7, 129.7, 126.2, 124.8, 120.9, 119.6.

2.7.4.3 Synthesis of Methyl 4-(diphenyl amino) Benzoate (2.9):

To a stirred solution of triphenylamine mono acid **2.8** (1 g, 2.56 mmol) in MeOH (40 mL) the acetyl chloride (0.9 mL, 12.84 mmol) was added in drops at 0 °C. The reaction mixture was

allowed to stir at room temperature for 16 h. The reaction was monitored by TLC using 20% EtOAc/Hexanes mixture. After completion of reaction, the reaction mixture was poured into water and neutralized with 1N NaOH solution followed by extraction with EtOAc. The organic layer was dried over sodium sulphate and concentrated

using rotavap. The compound was passed through a plug of short column to get a target product using 1:5 EtOAc/hexane; White solid (0.74 g, yield = 95%);MP: 100.2- 101.3°C; R_f = 0.80 in 1:5 EtOAc/hexanes; ¹H NMR (400 MHz, CDCl₃): δ 7.85 (d, J = 8.8 Hz, 2H), 7.30 (d, J = 7.6 Hz, 4H), 7.15-7.10 (m, 6H), 6.99 (d, J = 8.8 Hz, 2H), 3.87 (s, 3H); ¹³C NMR (100 MHz, CDCl₃): δ 167.0, 152.1, 146.8, 130.9, 129.6, 125.9, 124.5, 122.2, 120.1, 51.9; HRMS (ESI): calcd for $C_{20}H_{17}NO_2$ [M+H]⁺ 304.1332, Found 304.1331.

2.7.4.4 Synthesis of 1-(4-(diphenyl amino) phenyl)-3-(4-iodophenyl) Propane-1,3-dione (2.11):

A solution of methyl 4-(diphenyl amino) benzoate **2.9** (0.6 g, 1.98 mmol) was added to a stirred solution of NaH (0.4 g, 9.88 mmol) in dry toluene (20 mL) at room temperature under nitrogen atmosphere. The solution was allowed to stir at room temperature for 0.5 h. Then, 4-

iodo acetophenone **2.10** (0.48 g, 1.98 mmol) was added to the reaction mixture and stirred at refluxed condition for 21 h. The reaction mixture was allowed to cool to room temperature then neutralized with dil. HCl and extracted with EtOAc (2×20 mL).

The organic phase was combined and dried over anhydrous sodium sulphate to get residue. The residue was purified by column chromatography using 10% of EtOAc/Hexanes mixture to yield the titled compound as a yellow solid (0.72 g, yield = 70%). MP: 124-128 °C; R_f = 0.51 in 1:10 EtOAc/hexanes; ¹H NMR (400 MHz, CDCl₃): δ 17.07 (s, 1H), 7.82 (dd, J = 19.2, 8.4 Hz, 4H), 7.66 (d, J = 8.0 Hz, 2H), 7.34 (t, J = 6.8 Hz, 4H), 7.20-7.16 (m, 6H), 7.05 (d, J = 8.4 Hz, 2H), 6.73 (s, 1H); ¹³C NMR (100 MHz, CDCl₃): δ 185.8, 182.6, 152.0, 146.4, 137.8, 135.1, 129.6, 128.8, 128.4, 127.3, 125.9, 124.7, 120.0, 99.3, 92.1; IR (neat): υ 3409, 1584, 1487, 1230, 1179, 1003, 786, 750, 698 cm⁻¹; HRMS (ESI): calcd for C₂₇H₂₀INO₂ [M+H]⁺ 518.0611, found 518.0613.

2.7.4.5 Synthesis of 1-(5-bromothiophen-2-yl)-3-(4-(diphenyl amino) phenyl) Propane-1,3-dione (2.13):

Methyl 4-(diphenyl amino) benzoate 2.9 (0.8 g, 2.63 mmol) was added to a stirred solution

of NaH (0.5 g, 13.18 mmol) in dry toluene (20 mL) at room temperature for 0.5 h. 1-(5-bromothiophen-2-yl) ethan-1-one **2.12** (0.54 g, 2.63 mmol) was added to the reaction mixture and was stirred at reflux condition under atmosphere of nitrogen for

21 h. The reaction mixture was allowed to cool to room temperature then neutralized with dil. HCl and extracted with EtOAc (2 × 20 mL). The organic phase was combined and dried with anhydrous sodium sulphate. The product was purified by column chromatography using 10% of EtOAc/hexanes mixture. Yellow solid (0.72 g, yield = 58%); MP: 137-139 °C; R_f = 0.61 in 1:5 EtOAc/hexane; ¹H NMR (400 MHz, CDCl₃): δ 16.43 (s, 1H), 7.77 (d, J = 8.8 Hz, 2H), 7.48 (d, J = 3.6 Hz, 1H), 7.33 (t, J = 8.4 Hz, 4H), 7.28-7.15 (m, 7H), 7.03 (d, J = 8.4 Hz, 2H), 6.48 (s, 1H); ¹³C NMR (100 MHz, CDCl₃): δ 181.3, 180.1, 151.9, 148.3, 146.5, 138.2, 130.9, 130.6,

129.7, 129.6, 128.4, 126.0, 125.9, 124.7, 124.5, 120.2, 120.1, 91.6, 82.6; IR (neat): υ 2998, 1587, 1484, 1272, 1226, 1004, 787, 756, 694 cm⁻¹; HRMS (ESI): calcd for C₂₅H₁₈BrNO₂S [M+Na]⁺ 498.0134, found 498.0132.

2.7.4.6 Synthesis of 2-(thiophen-2-yl)-1,3-dioxolane (2.15): 4a

Compound **2.15** was synthesized using a literature procedure. Thiophene-2-carbaldehyde **2.14** (3 g, 26.75 mmol), ethylene glycol (3 ml, 53.50 mmol) and PTSA.H₂O (0.5 g, 2.67 mmol) were taken in benzene (50 mL) and allowed to stir vigorously for 16 h under reflux condition using a Dean-Stark setup. The reaction mixture was then poured into 10% aqueous NaOH (200 mL) solution and extracted with EtOAc (2 × 50

mL) and washed with water. The organic layer was combined and dried over anhydrous sodium sulphate. The organic phase was concentrated under vacuum. The crude was directly used for next step without further purification. Brown liquid (3.8 g, yield = 90%), R_f = 0.51 in 1:10 EtOAc/hexanes; ¹H NMR (400 MHz, CDCl₃): δ 7.35 (d, J = 12.4 Hz, 1H), 7.18 (s, 1H), 7.01 (s, 1H), 6.12 (s, 1H), 4.12 (t, J = 1.6 Hz, 2H), 4.01 (t, J = 3.2 Hz, 2H); ¹³C NMR (100 MHz, CDCl₃): δ 141.8, 128.3, 126.7,126.3, 126.2, 100.3, 65.2.

2.7.4.7 Synthesis of 5-(tributylstannyl) Thiophene-2-carbaldehyde (2.16):

To a stirred solution compound **2.15** (2 g, 12.80 mmol) in dry THF (50 mL) was added 1.6 M n-BuLi in hexane (12 mL, 19.20 mmol) under nitrogen atmosphere at -78°C for 1 h. Then

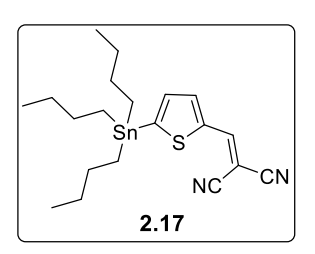
the reaction mixture was brought to -40 °C and stirred for 4 h. Then Bu₃SnCl (3.8 mL, 14.08 mmol) was added slowly to the reaction mixture at -78 °C and the reaction mixture was brought to room temperature and stirred for 24 h. After the reaction was complete, the reaction mixture was neutralized with 1M HCl (50 mL) and extracted with diethyl ether

 $(2 \times 30 \text{ mL})$. The organic phase was dried with anhydrous sodium sulphate and concentrated under vacuum. The crude was purified with column chromatography using 33 % of EtOAc/hexane mixture. Brownish yellow viscous liquid (3.4 g, yield = 66%); $R_f = 0.74$ in 1:5 EtOAc/hexanes; ¹H NMR (400 MHz, CDCl₃): δ 9.95 (s, 1H), 7.86 (s, 1H), 7.29 (s, 1H), 1.60-1.57 (m, 6H), 1.38-1.33 (m, 6H), 1.20-1.16 (m, 6H), 0.94-0.90 (m, 9H); ¹³C NMR (100 MHz, CDCl₃): δ 182.0, 151.6, 149.2, 136.8, 136.3, 28.9, 27.3, 13.7, 11.1; IR (neat): υ 3352, 2957, 2871, 2726, 1670, 1461, 1377, 1217, 1074, 873, 757, 662 cm⁻¹; HRMS (ESI): calcd for $C_{17}H_{30}OSSn$ [M+Na]⁺ 425.0932, found 425.0933.

2.7.4.8 Synthesis of 2-((5-(tributylstannyl) thiophen-2-yl) methylene) Malononitrile (2.17):

Malononitrile (0.010 g, 0.15 mmol), 5-(tributylstannyl) thiophene-2-carbaldehyde 2.16 (50

mg, 0.125 mmol), and PPh₃ (7 mg, 0.025 mmol) were stirred without solvent at 80 °C for 2.5 h. The reaction was monitor by TLC and the reaction was completed, the reaction mixture was diluted with water and extracted with EtOAc (2×5 mL). The organic layer was dried over anhydrous sodium sulphate and concentrated under vacuum. The crude



product was purified by column chromatography using 1:10 EtOAc/Hexanes mixture to yield brownish yellow viscus liquid (0.037 g, yield = 65%); R_f = 0.55 in 1:20 EtOAc/hexanes; 1 H NMR (400 MHz, CDCl₃): δ 7.85 (s, 2H), 7.30 (d, J = 4.0 Hz, 1H), 1.60-1.52 (m, 6H), 1.38-1.29 (m, 7H), 1.20-1.16 (m, 5H), 0.89 (t, J = 7.2 Hz, 9H); 13 C NMR (100 MHz, CDCl₃): δ 156.3, 149.9, 140.8, 138.3, 136.9, 114.4, 113.5, 76.7, 28.9, 27.2, 13.7, 11.3; IR (neat): υ 2951, 2915, 2217, 1571, 1406, 1313, 1272, 1065, 874, 750 cm⁻¹; HRMS (ESI): calcd for $C_{20}H_{30}N_2SSn$ [M+H] $^+$ 451.1224, found 451.1224.

2.7.4.9 Synthesis of 1-(5-bromothiophen-2-yl) ethan-1-one (2.12):

To a stirred solution of 2-bromothiophene (2 g, 12.27 mmol) in dry dichloromethane (30 mL) was added acetyl chloride (1.05 mL, 14.72 mmol) drop wise at 0 °C for 0.5 h. Anhydrous AlCl₃ (2 g, 14.72 mmol) was added portions wise. Then, the reaction was warmed to room temperature and stirred for 12 h. The reaction

dichloromethane (2 × 30 mL). The organic layer was combined and dried over with anhydrous Na₂SO₄. The solvent was concentrated using a rotavap. The crude was purified by column chromatography using 20% EtOAc/hexanes to yield brown- solid (1.65 g, yield = 65%); MP: 111-113 °C; R_f = 0.43 in 1:5 EtOAc/hexanes; ¹H NMR (500 MHz, CDCl₃): δ 7.41 (d, J = 4.0 Hz, 1H), 7.08 (d, J = 2.5 Hz, 1H), 2.49 (s, 3H); ¹³C NMR (125 MHz, CDCl₃): δ 189.7, 16.0, 132.6, 131.3, 122.9, 26.3.

2.7.4.10 Synthesis of 1-(4-(diphenyl amino) phenyl) ethan-1-one (2.18a):^{3a}

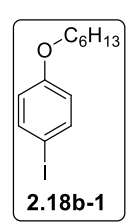
To a stirred solution of triphenylamine 2.6 (1 g, 4.0 mmol) in dry dichloromethane (20

mL) Anhydrous AlCl₃ (0.65 g, 4.9 mmol) was added portion wise into the solution at 0 °C for 0.5 h. Acetyl chloride (0.35 mL,4.9 mmol) was added dropwise to the reaction mixture. Then, the reaction was changed the temperature 25 °C for 12 h. The reaction mixture was poured into the ice cooled water and basified 1M NaHCO₃ solution followed by

extracted with dichloromethane (2 × 50ml). The organic layer was combined and dried over with anhydrous Na₂SO₄. The solvent was concentrated with rotavapor. The crude was purified 20% EtOAc/Hexane combination with column chromatography. Pale yellow solid; (0.9 g, yield = 77%), R_f = 0.76 in 1:5 EtOAc/hexanes; ¹H NMR (400 MHz, CDCl₃): δ 7.79 (d, J = 8.8 Hz, 2H), 7.31 (t, J = 8.4 Hz, 4H), 7.16-7.10 (m, 6H), 6.98 (d, J = 8.8 Hz, 2H), 2.52 (s, 3H); ¹³C NMR (100 MHz, CDCl₃): δ 196.6, 152.2, 146.5, 130.7, 129.7, 126.0, 124.7, 119.7, 26.4.

2.7.4.11 Synthesis of 1-(hexyloxy)-4-iodobenzene (2.18b-1):4c

Compound **2.18b-1** and **2.18b-2** was synthesized from literature procedure. 36a To a stirred solution of 4-iodo phenol (5 g, 22.72 mmol), K_2CO_3 (9.3 g, 68.17 mmol) in DMF (50 mL), n-bromo hexane (3.8 mL, 27.27 mmol) was added to it and allow to stir room temperature for 3 h. The reaction progress was monitored



by TLC. The reaction mixture was poured into 10% NaOH (200 mL) and extract with hexane (2 × 150 mL). The crude was directly use for next step. Brown liquid (6.5 g, yield = 94%), R_f = 0.68 in 1:10 EtOAc/hexane; ¹H NMR (400 MHz, CDCl₃): δ 7.53 (d, J = 8.8 Hz, 2H), 6.67 (d, J = 8.8 Hz, 2H), 3.90 (t, J = 6.4 Hz, 2H), 1.80-1.72 (m, 2H), 1.46-1.42 (m, 2H), 1.35-1.33 (m, 4H), 0.91 (t, J = 6.8 Hz, 3H); ¹³C NMR (100 MHz, CDCl₃): δ 159.1, 138.2, 117.0, 82.5, 68.2, 31.6, 29.2, 25.7, 22.7, 14.1.

2.7.4.12 Synthesis of 4-(hexyloxy)-N-(4-(hexyloxy) phenyl)-N-phenylaniline (2.18b-2):^{4d}

Aniline (0.3 g, 3.22 mmol), 1-(hexyloxy)-4-iodobenzene **2.18b-1** (2.5 g, 8.0 mmol), 1,10 phenanthroline (0.12 g, 0.64 mmol), CuI (0.12 g, 0.64 mmol) was added together in dry toluene

(30 mL) stirred room temperature for 0.5 h. Potassium tert-butoxide (1.8 g, 16.10 mmol) was added to the reaction mixture and heated reflux condition for 22 h. The reaction mixture was filtered and removed the solvent by rotavapor. The crude was purified with column chromatography using 10%

EtOAc/Hexanes mixture. Yellow viscos (1.36 g, yield = 94%); $R_f = 0.76$ in 1:5 EtOAc/hexanes; ¹H NMR (500 MHz, CDCl₃): δ 7.54 (d, J = 7.2 Hz, 1H), 7.19-7.15 (m, 2H), 7.04 (d, J = 7.2Hz, 3H), 6.95-6.90 (m, 2H), 6.85 (t, J = 6.0 Hz, 1H), 6.81 (d, J = 7.2 Hz, 3H), 6.68 (d, J = 7.2Hz, 1H), 3.92 (q, J = 5.6 Hz, 4H), 1.81-1.74 (m, 4H), 1.48-1.44 (m, 4H), 1.36-1.33 (m, 8H), 0.93-0.91 (m, 6H); ¹³C NMR (125 MHz, CDCl₃): δ 159.1, 155.4, 148.9, 141.1, 138.2, 129.0, 126.5, 120.9, 120.5, 117.0, 115.3, 68.3, 31.7, 29.4, 25.9, 22.7, 14.1; IR (neat): v 2925, 1587, 1499, 1385, 1163, 1112, 1034, 936, 822, 750, 698 cm⁻¹; HRMS (ESI): calcd for C₃₀H₃₉N O₂ [M+H]⁺ 446.3054, Found 446.3054.

2.7.4.13 Synthesis of 1-(4-(bis(4-(hexyloxy) phenyl) amino) phenyl) ethan-1-one (2.18b):

To a stirred solution of compound 2.18b-2 (1.3 g, 2.92 mmol) in dry dichloromethane (20

mL) Anhydrous AlCl₃ (0.78 g, 5.83 mmol) was added portion wise into the solution at 0 °C for 0.5 h. Acetic anhydride (0.28 mL, 2.92 mmol) was added dropwise to the reaction mixture. Then, the reaction was changed the temperature 25°C for 12 h. The reaction mixture was poured into the ice cooled water and acidified with dil. HCl and basified with 1M NaHCO₃ (50 mL)

solution followed by extracted with dichloromethane. The organic layer was combined and dried over with anhydrous Na₂SO₄. The solvent was concentrated with rotavapor. The crude was purified 20% EtOAc/Hexanes combination with column chromatography. Yellow viscos (0.7 g, yield = 50%), $R_f = 0.50 \text{ in } 1.5 \text{ EtOAc/hexanes; }^1\text{H NMR } (500 \text{ MHz, CDCl}_3): \delta 7.74 \text{ (d, }^3\text{ mHz, }^3\text{ mHz,$ J = 9.0 Hz, 2H, 7.08 (d, J = 8.5 Hz, 4H), 6.86 (d, J = 9.0 Hz, 4H), 6.81 (d, J = 9.0 Hz, 2H),3.93 (t, J = 6.5 Hz, 4H), 2.48 (s, 3H), 1.83-1.72 (m, 4H), 1.49-1.42 (m, 4H), 1.35-1.33 (m, 8H), 0.91 (t, J = 7.0 Hz, 6H); ¹³C NMR (125 MHz, CDCl₃): δ 196.3, 156.7, 153.0, 139.0, 127.8, 116.8, 115.5, 68.3, 31.6, 29.3, 25.8, 22.6, 14.1; IR (neat): υ 2930, 2858, 1680, 1509, 1468, 1422, 1241, 1106, 1019, 962, 827, 724 cm⁻¹; HRMS (ESI): calcd for C₃₂H₄₁NO₃ [M+Na]⁺ 510.2979, Found 510.2976.

2.7.4.14 Synthesis of 9-hexyl-9H-carbazole (2.18c-1):^{4e}

Compound **2.18c-1** was synthesized from literature procedure. NaH (1.4 g, 59.80 mmol), n-bromo hexane (5 mL, 35.88 mmol), were added to a stirred solution of carbazole (5 g, 29.43 mmol) in dry DMF (60 mL). The reaction mixture allows to stir room temperature for 0.5 h. the reaction progress was monitored by TLC. After consuming of carbazole, the reaction mixture was poured into the water



(500 mL) and precipitate was collected by filtration technique. White solid; (7 g, yield = 93%), $R_f = 0.60$ in 1:5 EtOAc/hexanes; ¹H NMR (400 MHz, CDCl₃): δ 8.24 (d, J = 7.2 Hz, 2H), 7.59-750 (m, 4H), 7.38 (d, J = 6.8 Hz, 2H), 4.36 (s, 2H), 1.96 (s, 1H), 1.42 (s, 6H), 1.01 (s, 3H); ¹³C NMR (100 MHz, CDCl₃): δ 140.5, 125.6, 122.9, 120.4, 118.7, 108.7, 43.0, 31.6, 29.0, 27.0, 22.6, 14.1.

2.7.4.15 Synthesis of 1-(9-hexyl-9H-carbazol-3-yl) ethan-1-one (2.18c):^{4f}

To a stirred solution of compound **2.18c-1** (2.0 g, 7.95 mmol) in dry dichloromethane (40 mL) Anhydrous AlCl₃ (2.1 g, 15.92 mmol) was added portion wise into the solution at 0 °C for

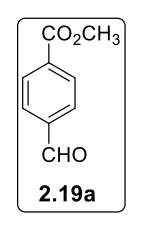
0.5 h. Acetic anhydride (0.75 mL, 7.96 mmol) was added dropwise to the reaction mixture. Then, the reaction was changed the temperature 25°C for 12 h. The reaction mixture was poured into the ice cooled water and acidified with HCl and basified with 1M NaHCO₃ solution followed by extracted with dichloromethane. The organic layer was combined and dried

over with anhydrous Na₂SO₄. The solvent was concentrated with rotavapor. The crude was purified 20% EtOAc/Hexanes combination with column chromatography. Yellow viscos (1.8 g, yield = 78%); R_f = 0.50 in 1:5 EtOAc/hexanes; ¹H NMR (400 MHz, CDCl₃): δ 8.65 (d, J = 1.2 Hz, 1H), 8.08-8.02 (m, 2H), 7.45 (t, J = 8.0 Hz, 1H), 7.32 (d, J = 8.0 Hz, 1H), 7.23-7.20 (m, 2H), 4.09-4.05 (m, 2H), 2.65 (s, 3H), 1.72 (d, J = 5.6 Hz, 2H), 1.239-1.233 (m, 6H), 0.85 (s, 3H); ¹³C NMR (100 MHz, CDCl₃): δ 197.0, 142.8, 140.8, 128.4, 126.1, 126.0, 122.9, 122.2, 121.4, 120.2, 119.6, 109.0, 107.9, 42.8, 31.2, 28.5, 26.6, 22.3, 13.7.

2.7.4.16 Synthesis of Methyl 4-formyl Benzoate (2.19a):

To a stirred solution of 4-formyl benzoic acid (2 g, 13.32 mmol) in MeOH (30 mL) was added acetyl chloride (4.8 mL, 66.61 mmol) dropwise at 0 °C. The reaction mixture was

allowed to stir at room temperature for 16 h. The reaction was monitored by TLC and the solvent was removed under reduced vacuum. The reaction mixture was diluted with EtOAc and neutralized with 1N NaOH solution followed by extraction with ethyl acetate (2×20 mL). The organic layer was dried over sodium sulphate and the filtrate was concentrated using rotavap. The crude was purified using 20%



EtOAc/hexane in a silica gel column. White solid (1.8 g, yield = 85%); MP: 83-84 °C; R_f = 0.46 in 1:5 EtOAc/hexane; ¹H NMR (400 MHz, CDCl₃): δ 10.08 (s, 1H), 8.18 (d, J = 6.8 Hz, 2H), 7.93 (d, J = 8.4 Hz, 2H), 3.94 (s, 3H); ¹³C NMR (100 MHz, CDCl₃): δ 191.8, 166.1, 139.2,

135.1, 130.3, 129.6, 52.7; IR (neat): υ 1722, 1680, 1500, 1386, 1112, 1014, 813, 761 cm⁻¹; HRMS (ESI): calcd for $C_9H_8O_3$ [M+H]⁺ 165.0546, found 165.0542.

2.7.4.17 Synthesis of methyl 4-(1,3-dioxolan-2-yl) Benzoate (2.19):

Methyl 4-formylbenzoate **2.19a** (2 g, 12.19 mmol), ethylene glycol (1.4 ml, 24.38 mmol) and PTSA.H₂O (0.47 g, 2.44 mmol) in toluene (50 mL) all mixed together and allowed for vigorous stirring for 16 h under reflux condition in a Dean-Stark setup. The reaction mixture was poured into 10% NaOH (200

mL) solution and extracted with EtOAc (2×50 mL) and washed with water. The organic layer was combined and dried over anhydrous sodium sulphate. The organic phase was concentrated under vacuum. The crude was directly used for further reactions. Pale yellow liquid (2.3 g, yield = 90%); $R_f = 0.43$ in 1:10 EtOAc/hexanes; ¹H NMR (400 MHz, CDCl₃): δ 8.04 (t, J = 6.8 Hz, 2H), 7.54 (t, J = 6.8 Hz, 2H), 5.82 (s, 1H), 4.10-4.07 (m, 2H), 4.02-4.01 (m, 2H), 3.88 (s, 3H); ¹³C NMR (100 MHz, CDCl₃): δ 166.7, 142.8, 130.8, 129.6, 126.4, 103.0, 65.3, 52.1; IR (neat): υ 3436, 2954, 2879, 1717, 1577, 1436, 1277, 1117, 849, 763, 732 cm⁻¹; HRMS (ESI): calcd for $C_{11}H_{12}O_4$ [M+H]⁺ 209.0808, found 209.0800

I. General Procedure for propane-1,3-dione:

Substituted ketone (1 equiv.) was added to the stirred solution of NaH (5 equiv.) in dry toluene (20 mL). The solution was allowed to stir room temperature for 0.5 h. Methyl 4-(1,3-dioxolan-2-yl) benzoate (1.2 equiv.) was added to the reaction mixture stirred refluxed condition under atmosphere of nitrogen for 21 h. The reaction mixture was allowed to cool room temperature then neutralized with dil. HCl and extracted with EtOAc (2×20 mL). The organic phase was combined and dried over with anhydrous sodium sulphate. The product was purified in column chromatography using 10% of EtOAc/Hexanes mixture.

2.7.4.18 Synthesis of 1-(4-(1,3-dioxolan-2-yl) phenyl)-3-(4-(diphenylamino) phenyl) propane-1,3-dione (2.20a):

Compound 1-(4-(diphenylamino) phenyl) ethan-1-one **2.18a** (1 g, 3.48 mmol) was added to a stirred suspension of NaH (0.696 g, 17.42 mmol) in dry toluene (20 mL). The solution was allowed to stir at room temperature for 0.5 h. Methyl 4-(1,3-dioxolan-2-yl) benzoate **2.19** (0.725 g, 3.48 mmol) was added to the reaction mixture

and refluxed under an atmosphere of nitrogen for 21 h. The reaction mixture was allowed to

cool at room temperature, neutralized with dil. HCl and extracted with EtOAc (2×20 mL). The organic phase was combined and dried over with anhydrous sodium sulphate. The product was purified by column chromatography using 10% of EtOAc/hexanes mixture. Yellow solid; MP: $122-124^{\circ}$ C;(1 g, yield = 62%); R_f = 0.35 in 1:3 EtOAc/hexanes; ¹H NMR (500 MHz, CDCl₃): δ 17.01 (s, 1H), 7.97 (d, J = 8.5 Hz, 2H), 7.84 (d, J = 9.0 Hz, 2H), 7.58 (d, J = 8.5 Hz, 2H), 7.34-7.31 (m, 4H), 7.17-7.14 (m, 6H), 7.03 (d, J = 9.0 Hz, 2H), 6.76 (s, 1H), 5.87 (s, 1H), 4.13-4.12 (m, 2H), 4.07-4.06 (m, 2H); ¹³C NMR (125 MHz, CDCl₃): δ 186.1, 183.3, 152.1, 146.6, 146.5, 142.0, 136.5, 129.7, 128.8, 127.1, 126.8, 126.1, 126.0, 124.7, 120.3, 103.2, 92.6, 65.5; IR (neat): υ 3000, 2920, 1722, 1670, 1484, 1272, 1169, 1107, 1024, 813, 699 cm⁻¹; HRMS (ESI): calcd for C₃₀H₂₅NO₄ [M+H]⁺ 464.1856, found 464.1858.

2.7.4.19 Synthesis of 1-(4-(1,3-dioxolan-2-yl) phenyl)-3-(4-(bis(4-(hexyloxy) phenyl) amino) phenyl) propane-1,3-dione (2.20b):

Compound **2.20b** was prepared from GP I. Yellow viscos (0.52 g, yield = 50%); R_f = 0.48 in 1:5 EtOAc/hexanes; ¹H NMR (500 MHz, CDCl₃): δ 17.12 (s, 1H), 7.96 (d, J = 8.5 Hz, 2H), 7.80 (d, J = 9.0 Hz, 2H), 7.57 (d, J = 8.0 Hz, 2H), 7.11 (d, J = 8.5 Hz, 4H), 6.87 (d, J = 9.0 Hz, 6H), 6.74 (s, 1H), 5.86

(s, 1H), 4.13-4.10 (m, 2H), 4.05-4.02 (m, 2H), 3.95 (t, J = 7.0 Hz, 4H), 1.82-1.76 (m, 4H), 1.49-1.46 (m, 4H), 1.37-1.35 (m, 8H), 0.92 (t, J = 7.0 Hz, 6H); ¹³C NMR (125 MHz, CDCl₃): δ 186.3, 182.5, 156.7, 152.8, 141.7, 139.0, 136.5, 128.8, 127.8, 126.9, 126.7, 125.7, 117.2, 115.5, 103.1, 92.2, 68.3, 65.4, 31.6, 29.3, 25.8, 22.6, 14.1; IR (neat): υ 2920, 2850, 1717, 1587, 1500, 1272, 1107, 1014 828, 766, 699 cm⁻¹; HRMS (ESI): calcd for C₄₂H₄₉NO₆ [M+H]⁺ 664.3633, Found 664.3636.

2.7.4.20 Synthesis of 1-(4-(1,3-dioxolan-2-yl) phenyl)-3-(9-hexyl-9H-carbazol-3-yl) propane-1,3-dione (2.20c):

Compound **2.20c** was prepared from GP I. Brown solid (0.52 g, yield = 40%), MP: 135-

136°C; $R_f = 0.36$ in 1:5 EtOAc/hexanes. H NMR (500 MHz, CDCl₃): δ 17.30 (s, 1H), 8.70 (s, 1H), 8.17 (d, J = 7.5 Hz, 1H), 8.11 (d, J = 9.0 Hz, 1H), 8.04 (d, J = 8.0 Hz, 2H), 7.62 (d, J = 8.0 Hz, 2H), 7.50 (t, J = 8.0 Hz, 1H), 7.39 (t, J = 8.5

Hz, 2H), 7.30 (t, J = 7.5 Hz, 1H), 6.97 (s, 1H), 5.89 (s, 1H), 4.25-4.24 (m, 2H), 4.16-4.13 (m,

2H), 4.07-4.06 (m, 2H), 1.85 (t, J = 8.0 Hz, 2H), 1.29 (d, J = 3.5 Hz, 6H), 0.87 (t, J = 7.0 Hz, 3H); 13 C NMR (125 MHz, CDCl₃): δ 187.9, 182.5, 143.1, 141.8, 141.1, 136.4, 127.0, 126.7, 126.4, 126.3, 125.3, 123.0, 122.9, 120.7, 120.5, 119.9, 109.3, 108.6, 103.1, 92.8, 65.4, 43.3, 31.5, 28.9, 26.9, 22.5, 14.0; IR (neat): υ 2956, 2847, 1716, 1587, 1437, 1323, 1236, 1184, 1019, 853, 776, 704 cm⁻¹; HRMS (ESI): calcd for C₃₀H₃₁NO₄ [M+H]⁺ 470.2326, Found 470.2327.

II. General Procedure for Benzaldehyde

To a stirred solution of substituted propane-1,3-dione (0.2 mmol, 1 equiv.) in acetone (5 mL), PTSA.H₂O (0.2 equiv.) was added to it and stirred room temperature for 3-4 h under nitrogen atmosphere condition. The reaction progress was monitored by TLC using 20% EtOAc/Hexane mixture. The reaction mixture was neutralized with NaHCO₃ (20 mL) and extracted with EtOAc (20 mL). The solvent was reduced under vacuum, the crude product was used for next reaction without further purifications.

2.7.4.21 Synthesis of 4-(3-(4-(diphenylamino) phenyl)-3-oxopropanoyl) benzaldehyde (2.21a):

To a stirred solution of compound 2.20a~(0.750~g,~1.617~mmol) in acetone (15 mL), was added PTSA.H₂O (0.062 g, 0.33 mmol) and stirred at room temperature for 3 h under nitrogen

atmosphere condition. The reaction progress was monitored by TLC using 20% EtOAc/hexane mixture. The reaction mixture was neutralized with NaHCO $_3$ (20 mL) and extracted with EtOAc (2 \times 15 mL). The crude was purified 20% EtOAc/Hexanes combination with column chromatography.

Yellow solid; MP: 130-132 °C; (0.58 g, yield = 86%), $R_f = 0.56$ in 1:3 EtOAc/hexanes; ¹H NMR (500 MHz, CDCl₃): δ 16.93 (s, 1H), 10.08 (s, 1H), 8.09 (d, J = 8.5 Hz, 2H), 7.97 (d, J = 8.5 Hz, 2H), 7.85 (d, J = 9.0 Hz, 2H), 7.35-7.32 (m, 4H), 7.18-7.14 (m, 6H), 7.03 (d, J = 10.5 Hz, 2H), 6.80 (s, 1H); ¹³C NMR (125 MHz, CDCl₃): δ 191.6, 187.2, 180.9, 152.4, 146.4, 140.9, 138.4, 129.9, 129.7, 129.0, 127.5, 126.1, 124.9, 119.9, 93.5; IR (neat): υ 3000, 2925, 1701, 1587, 1484, 1288, 1231, 1190, 782, 761, 699 cm⁻¹; HRMS (ESI): calcd for C₂₈H₂₁NO₃ [M+H]⁺ 420.1594, found 420.1595.

2.7.4.22 Synthesis of 4-(3-(4-(bis(4-(hexyloxy) phenyl) amino) phenyl)-3-oxopropanoyl) benzaldehyde (2.21b):

Compound 2.21b was prepared from GP II. Yellow viscos (0.45 g, yield = 90%), $R_f = 0.66$

in 1:5 EtOAc/hexanes; ¹H NMR (400 MHz, CDCl₃): δ 17.00 (s, 1H), 10.09 (d, J = 7.6 Hz, 1H), 8.08 (d, J= 8.4 Hz, 2H, 7.97-7.94 (m, 2H), 7.80 (d, J = 8.0 Hz,2H), 7.11 (d, J = 8.8 Hz, 4H), 6.88-6.85 (m, 6H), 6.78 (s, 1H), 3.94 (t, J = 6.8 Hz, 4H), 1.82-1.75 (m, 4H), 1.48-1.44 (m, 4H), 1.36-1.34 (m, 8H), 0.91 (t, J = 7.2

Hz, 6H); ¹³C NMR (100 MHz, CDCl₃): δ 191.7, 187.4, 180.2, 156.8, 153.2, 141.1, 138.9, 138.3, 130.2, 129.9, 129.6, 129.1, 127.9, 127.4, 125.5, 117.1, 115.6, 93.3, 68.4, 31.7, 29.4, 25.8, 22.7, 14.1; IR (neat): v 2920, 2858, 1701, 1592, 1463, 1287, 1179, 827, 781, 724 cm⁻¹; HRMS (ESI): calcd for C₄₀H₄₅NO₅ [M+H]⁺ 620.3371, Found 620.3371.

2.7.4.23 Synthesis of 4-(3-(9-hexyl-9H-carbazol-3-yl)-3-oxopropanoyl) benzaldehyde (2.21c):

Compound 2.21c was prepared from GP II. Yellow solid (0.2 g, yield = 79%), MP: 130-131°C; $R_f = 0.54$ in 1:5 EtOAc/hexanes; ¹H NMR (500 MHz, CDCl₃): δ 17.13 (s, 1H), 10.06 (s, 1H), 8.75 (s, 1H), 8.16 (d,

J = 8.0 Hz, 1H), 8.11 (d, J = 8.0 Hz, 3H), 7.95 (d, J = 7.5 Hz,

2H), 7.51 (t, J = 7.5 Hz, 1H), 7.42-7.39 (m, 2H), 7.31 (t, J = 7.5 Hz, 1H), 6.99 (s, 1H), 4.27 (t, $J = 7.0 \text{ Hz}, 2\text{H}, 1.89-1.83 \text{ (m, 2H)}, 1.36-1.26 \text{ (m, 6H)}, 0.87 \text{ (t, } J = 7.0 \text{ Hz}, 3\text{H}); ^{13}\text{C NMR} (125)$ MHz, CDCl₃): δ 191.7, 189.0, 180.3, 143.4, 141.1, 140.8, 138.3, 129.8, 127.4, 126.6, 126.3, 125.5, 123.1, 120.9, 120.8, 120.1, 109.4, 108.7, 43.4, 31.6, 29.0, 27.0, 22.6, 14.0; IR (neat): υ 2951, 2853, 1701, 1386, 1324, 1205, 1148, 823, 787, 751 cm⁻¹; HRMS (ESI): calcd for C₂₈H₂₇NO₃ [M+H]⁺ 426.2064, Found 426.2062.

2.7.4.24 Synthesis of 2-((5-(4-(3-(4-(diphenylamino) phenyl)-3-oxopropanoyl) phenyl) thiophen-2-yl) methylene) malononitrile (2.1):^{3c}

A mixture of compound **2.11** (0.7 g, 1.35 mmol), compound **2.17** (1.2 g, 2.70 mmol) and Pd (PPh₃)₄ (0.32 g, 0.27 mmol) were heated in toluene (12 mL) at 80 $^{\circ}$ C for 22 h under nitrogen

condition. The reaction was monitored by TLC using 33% of EtOAc/hexane mixture. The solvent was removed under reduced pressure with a rotavapor. The crude was purified with column chromatography

using ethyl acetate and hexane mixture. After separated product spot, that was mixed with cooled MeOH (20 mL) and filtered to give target product. Red solid (0.26 g, yield = 35%); MP: 211-214 °C; $R_f = 0.13$ in 1:3 EtOAc/hexanes; ¹H NMR (500 MHz, CDCl₃): δ 17.03 (s, 1H), 8.00 (d, J = 8.0 Hz, 1H), 7.85 (d, J = 9.0 Hz, 2H), 7.81 (s, 1H), 7.76 (d, J = 8.0 Hz, 2H), 7.74 (d, J = 4.0 Hz, 1H), 7.52 (d, J = 4.0 Hz, 1H), 7.33 (t, J = 8.0 Hz, 5H), 7.17 (t, J = 7.5 Hz, 6H), 7.04 (d, J = 9.0 Hz, 2H), 6.77 (s, 1H); ¹³C NMR (125 MHz, CDCl₃): δ 186.5, 181.7, 154.8, 152.3, 150.5, 146.5, 139.9, 137.1,135.3, 135.2, 129.7, 128.9, 128.0, 126.8, 126.1, 125.6, 124.9, 120.0, 114.0, 113.3, 92.7; IR (neat): υ 2920, 2849, 2224, 1660, 1572, 1424, 1276, 1189, 1013, 789 cm⁻¹; HRMS (ESI): calcd for C₃₅H₂₃N₃O₂S [M+H]⁺ 550.1584, found 550.1582.

2.7.4.25 Synthesis of 2-((5'-(3-(4-(diphenylamino) phenyl)-3-oxopropanoyl)-[2,2'-bithiophen]-5-yl) methylene) malononitrile (2.2):

Compound **2.13** (0.25 g, 0.52 mmol), compound **2.17** (0.47 g, 1.05 mmol) and Pd (PPh₃)₄ (0.13 g, 0.10 mmol) were mixed together in toluene (5 mL) and heated at 80 $^{\circ}$ C for 24 h under

nitrogen atmosphere. The reaction was monitored by TLC. After completion of the reaction solvent was removed under reduced pressure in a rotavap. The crude was purified with column chromatography using ethyl acetate with hexanes mixture. After separated

product spot, that was mixed with cooled MeOH (20 mL) and filtered to give target product. Red solid (0.092 g, yield = 32%); MP: 236-238 °C; R_f = 0.43 in 1:3 EtOAc/hexanes; ¹H NMR (500 MHz, CDCl₃): δ 16.48 (s, 1H), 7.79 (d, J = 8.0 Hz, 2H), 7.68 (d, J = 3.5 Hz, 2H), 7.42 (d, J = 3.0 Hz, 1H), 7.38 (d, J = 2.0 Hz, 1H), 7.33 (t, J = 7.5 Hz, 5H), 7.18-7.15 (m, 6H), 7.02 (d, J = 8.5 Hz, 2H), 6.58 (s, 1H); ¹³C NMR (125 MHz, CDCl₃): δ 182.0, 179.8, 152.2, 150.2, 147.8, 146.4, 144.4, 140.4, 140.0, 134.8, 130.4, 129.7, 128.6, 127.7, 126.1, 124.9, 120.0, 113.2, 92.1;

IR (neat): υ 2920, 2850, 2220, 1574, 1488, 1333, 1189, 1060, 783 cm⁻¹; HRMS (ESI): calcd for $C_{33}H_{21}N_3O_2S_2$ [M+H]⁺ 556.1148, found 556.1149.

III. General Procedure for Malononitrile Condensation:^{4b}

Malononitrile (1.2 equiv.), substituted corresponding aldehyde (1 equiv.), and PPh₃ (0.2 equiv.) were stirred at 80°C for 3-4 h. The reaction was monitor by TLC using 20% EtOAc/Hexane mobile phase. The reaction was diluted with water and extracted with EtOAc. The organic layer was dried over anhydrous sodium sulphate and concentrated using vacuum. The crude was purified with column chromatography using 1:5 EtOAc/Hexanes mixture.

2.7.4.26. 2-(4-(3-(4-(diphenyl amino) phenyl)-3-oxopropanoyl) benzylidene) malononitrile (2.3):

Compound 2.21a (0.350 g, 0.83 mmol), malononitrile (0.067 mL, 1.00 mmol), and PPh₃

(0.053 g, 0.200 mmol) were stirred without solvent at 80 °C for 3 h. The reaction was monitored by TLC. The reaction was diluted with water and extracted with EtOAc (2×20 mL). The organic layer was dried over anhydrous sodium sulphate and concentrated using vacuum. The

crude was purified with column chromatography using 1:5 EtOAc/hexanes mixture. Red solid (0.22 g, yield = 57%); MP: 179-181°C; $R_f = 0.51$ in 1:3 EtOAc/hexane; ¹H NMR (400 MHz, CDCl₃): δ 16.90 (s, 1H), 8.07 (d, J = 8.4 Hz, 2H), 7.98 (d, J = 8.4 Hz, 2H), 7.83 (t, J = 8.8 Hz, 3H), 7.34 (t, J = 8.0 Hz, 4H), 7.18 (d, J = 8.8 Hz, 6H), 7.03 (d, J = 8.8 Hz, 2H), 6.80 (s, 1H); ¹³C NMR (100 MHz, CDCl₃): δ 187.5, 179.5, 158.6, 152.5, 146.3, 140.8, 133.4, 130.9, 129.8, 129.1, 127.8, 127.1, 126.2, 125.0, 119.7, 113.5, 112.4, 93.6, 84.4; IR (neat): υ 3063, 2920, 2224, 1589, 1331, 1232, 1189, 1030, 931, 794, 761 cm⁻¹; HRMS (ESI): calcd for C₃₁H₂₁N₃O₂ [M+H]⁺ 468.1707, found 468.1707.

2.7.4.27 Synthesis of 2-(4-(3-(4-(bis(4-(hexyloxy) phenyl) amino) phenyl)-3-oxopropanoyl) benzylidene) malononitrile (2.4):

Compound **2.4** was prepared from GP III. Red viscos (0.19 g, yield = 45%), $R_f = 0.46$ in

1:5 EtOAc/hexanes; ¹H NMR (400 MHz, CDCl₃): δ 17.02 (s, 1H), 8.04-8.01 (m, 2H), 7.957-7.952 (m, 3H), 7.80-7.76 (m, 3H), 7.12 (d, J=8.8 Hz, 4H), 6.89-6.84 (m, 5H), 6.74 (s, 1H), 3.95 (t, J=5.6 Hz, 4H), 1.81-1.77 (m, 4H), 1.49-1.45 (m, 4H), 1.36-1.35 (m, 8H), 0.92 (t, J=6.8 Hz, 6H); ¹³C NMR (100 MHz,

CDCl₃): δ 187.5, 178.8, 158.5, 156.9, 153.3, 140.8, 138.7, 133.2, 130.8, 129.2, 127.9, 127.6, 125.2, 116.9, 115.6, 114.6, 113.5, 112.4, 93.3, 84.0, 68.3, 31.6, 29.3, 25.7, 22.6, 14.0; IR (neat): υ 2925, 2853, 2230, 1587, 1510, 1283, 1185, 1107, 1061, 854, 797 cm⁻¹; HRMS (ESI): calcd for C₄₃H₄₅N₃O₄ [M+H]⁺ 668.3483, Found 668.3483.

2.7.4.28 2-(4-(3-(9-hexyl-9H-carbazol-3-yl)-3-oxopropanoyl) benzylidene) malononitrile (2.5):

Compound **2.5** was prepared from GP III. Yellow solid (0.27 g, yield = 60%), MP: 225-227°C; $R_f = 0.46$ in 1:5 EtOAc/hexane; ¹H NMR (400 MHz, CDCl₃): δ 17.06 (s, 1H), 8.79 (s, 1H), 8.20-8.13 (m, 4H), 8.40 (d, J = 8.4 Hz, 2H), 7.79 (s, 1H),

7.53 (t, J = 7.2 Hz, 1H), 7.46 (d, J = 8.0 Hz, 2H), 7.32 (t, J = 7.2 Hz, 1H), 7.03 (s, 1H), 4.33 (t, J = 6.8 Hz, 2H), 1.88 (t, J = 6

= 10.8 Hz, 2H), 1.40 (br s, 2H), 1.31 (br s, 3H), 1.25 (br s,

1H), 0.86 (t, J = 6.8 Hz, 3H); ¹³C NMR (100 MHz, CDCl₃): δ 189.4, 179.1, 158.6, 143.6, 133.4, 130.9, 127.9, 126.8, 126.3, 125.6, 123.2, 123.1, 121.0, 120.8, 120.3, 113.5, 112.5, 109.5, 108.9, 94.0, 84.4, 43.5, 31.6, 29.0, 27.0, 22.6, 14.1; IR (neat): υ 2925, 2848, 2228, 1587, 1474, 1303, 1128, 1014, 844, 777 cm⁻¹; HRMS (ESI): calcd for C₃₁H₂₇N₃O₂ [M+H]⁺ 474.2176, Found 474.2176.

IV. General Procedure for Formation of 1,3-diketone with BF₂ Complexes:⁵

To a stirred solution of Corresponding 1,3-diketone substrate (1 equiv.) in dry dichloromethane (0.1 mmol, 5 mL), BF₃.OEt₂ (1.2 equiv.) was added dropwise to the reaction mixture at room temperature and maintained for another 0.5 h. The reaction colour was changed instantly, while added boron tri fluoro diethyl etherate. The reaction was quenched

0.2N NaOH with water and extracted dichloromethane solution. The crude product was further purified with column chromatography technique.

2.7.4.29 Synthesis of 2-((5-(4-(6-(4-(diphenylamino) phenyl)-2,2-difluoro-2H-1,3,2-dioxaborinin-4-yl) phenyl) thiophen-2-yl) methylene) malononitrile (2.1-BF₂):

Red solid (0.02 g, yield = 36%), MP: 268-270°C; $R_f = 0.13$ in 1:3 EtOAc/hexanes; ¹H

NMR (400 MHz, CDCl₃): δ 8.14 (d, J = 7.6 Hz, 1H), 8.00-7.98 (m, 2H), 7.83-7.75 (m, 5H), 7.39 (t, J = 7.6 Hz, 6H), 7.22 (d, J = 7.6 Hz, 5H), 7.02 (s, 1H), 6.98 (d, J = 8.8 Hz, 2H); ¹¹B NMR (128 MHz, CDCl₃): δ 1.28; ¹⁹F NMR (370 MHz, CDCl₃): δ -

140.0; IR (neat): υ 2922, 2853, 2220, 1732, 1573, 1486, 1340, 1189, 1032, 796, 692 cm⁻¹; HRMS (ESI): calcd for $C_{35}H_{22}BF_2N_3O_2S$ [M+H]⁺ 598.1567, found 598.1577.

2.7.4.30 2-((5'-(6-(4-(diphenylamino) phenyl)-2,2-difluoro-2H-1,3,2-dioxaborinin-4-yl)-[2,2'-bithiophen]-5-yl) methylene) malononitrile (2.2-BF₂):

Dark violet solid (0.02 g, yield = 35%), MP: 240-243°C; $R_f = 0.13$ in 1:3 EtOAc/hexanes; ¹H NMR (500 MHz, CDCl₃): δ 7.94 (d, J = 9.0 Hz, 2H), 7.89 (d, J = 9.5 Hz, 1H), 7.81 (d, J = 7.0 Hz, 2H), 7.69 (d, J = 3.5 Hz, 1H), 7.47 (d, J = 4.0 Hz, 1H), 7.43 (d, J = 4.0 Hz, 1H), 7.43 (d, J = 4.0 Hz, 1H), 7.45 (d, J = 4.0 Hz, 1H), 7.45 (d, J = 4.0 Hz, 1H), 7.47 (d, J = 4.0 Hz, 1H), 7.48 (d, J = 4.0 Hz, 1H), 7.49 (d, J = 4.0 Hz, 1H)

4.0 Hz, 1H), 7.39 (t, J = 8.0 Hz, 5H), 7.21 (d, J = 7.5 Hz, 4H), 6.96 (d, J = 9.0 Hz, 2H), 6.81 (s, 1H); ¹¹B NMR (160 MHz, CDCl₃): δ 0.95; ¹⁹F NMR (470 MHz, CDCl₃): δ -141.5; IR (neat): υ 2946, 2925, 2223, 1577, 1531, 1427, 1278, 1200, 1138, 1009, 901, 870 cm⁻¹; HRMS (ESI): calcd for $C_{33}H_{20}BF_2N_3O_2S_2$ [M+Na]⁺ 626.0950, found 626.0952.

2.7.4.31 Synthesis of 2-(4-(6-(4-(diphenylamino) phenyl)-2,2-difluoro-2H-1,3,2-dioxaborinin-4-yl) benzylidene) malononitrile (2.3-BF₂):

Red solid (0.024 g, yield = 44%), MP: 257-259°C; R_f = 0.13 in 1:3 EtOAc/hexanes; ¹H NMR (500 MHz, CDCl₃): δ 8.15 (d, J = 8.5 Hz, 2H), 7.99-7.95 (m, 4H), 7.79 (s, 1H), 7.38-7.36 (m, 4H), 7.23 (s, 1H), 7.19 (d, J = 8.0 Hz, 5H), 7.00 (s, 1H), 6.93 (d, J = 9.0 Hz, 2H); ¹¹B NMR (160 MHz,

CDCl₃): δ 1.20; ¹⁹F NMR (470 MHz, CDCl₃): δ -140.6; IR (neat): υ 2921, 2858, 2224, 1720,

1489, 1338, 1251, 1131, 1094, 926, 802, 756, 696 cm⁻¹; HRMS (ESI): calcd for $C_{31}H_{20}BF_2N_3O_2$ [M+H]⁺ 516.1689, found 516.1687.

2.7.4.32 Synthesis of 2-(4-(6-(4-(bis(4-(hexyloxy) phenyl) amino) phenyl)-2,2-difluoro-2H-1,3,2- dioxaborinin-4-yl) benzylidene) malononitrile (2.4-BF₂):

Violet solid (0.020 g, yield = 62%), MP: 257-258°C; $R_f = 0.5$ in 1:3 EtOAc/hexanes; ¹H NMR (500 MHz, CDCl₃): δ 8.15 (d, J = 6.0 Hz, 2H), 7.97 (d, J = 29.5 Hz, 4H), 7.81 (s, 1H), 7.14 (d, J = 5.0 Hz, 4H), 6.98-6.81 (m, 7H), 3.96 (s, 4H), 1.79 (s, 3H), 1.47 (s, 3H), 1.35 (s, 8H), 1.25 (s, 2H), 0.91 (s, 6H); B^{11} NMR

(160 MHz, CDCl₃): δ 1.19; F¹⁹ NMR (470 MHz, CDCl₃): δ -140.9; IR (neat): υ 2915, 2853, 2224, 1722, 1546, 1345, 1124, 1195, 1030 cm⁻¹; HRMS (ESI): calcd for C₄₃H₄₄BF₂N₃O₄ [M+H]⁺ 716.3466, Found 716.3465.

2.7.4.33 Synthesis of 2-(4-(2,2-difluoro-6-(9-hexyl-9H-carbazol-3-yl)-2H-1,3,2 -dioxaborinin-4-yl) benzylidene) malononitrile (2.5-BF₂):

Yellow solid (0.03 g, yield = 54%), MP: 257-259°C; $R_f = 0.5$ in 1:3 EtOAc/hexanes; ¹H NMR (400 MHz, CDCl₃): δ 8.97 (s, 1H), 8.26 (d, J = 8.0 Hz, 1H), 8.20-8.16 (m, 1H), 8.03 (d,

J = 7.6 Hz, 2H), 7.80 (s, 1H), 7.69-7.64 (s, 3H), 7.58-7.53 (m, 2H), 7.39 (d, J = 7.2 Hz, 1H), 7.32 (s, 1H), 4.35 (t, J = 6.8 Hz, 2H), 2.35 (t, J = 7.6 Hz, 1H), 2.03 (q, J = 6.8 Hz, 2H), 1.93-1.89 (m, 3H), 1.67 (s, 2H), 1.62-1.60 (m, 3H); B¹¹ NMR (128 MHz, CDCl₃): δ 1.34; F¹⁹ NMR (370 MHz, CDCl₃): δ -140.3;

IR (neat): υ 2915, 2853, 2213, 1732, 1574, 1551, 1469, 1247, 1185, 1086, 937, 751 cm⁻¹; HRMS (ESI): calcd for $C_{31}H_{26}BF_{2}N_{3}O_{2}$ [M+H]⁺ 522.2159, Found 522.2164.

2.7.4.34 Synthesis of 1-(4-(diphenyl amino) phenyl) butane-1,3-dione (2.67):⁴⁰

Ethyl acetate (0.4 ml, 3.91 mmol) was added to the stirred solution of NaH (0.18 g, 4.35

mmol) and 1-(4-(diphenyl amino) phenyl) ethan-1-one **2.18a** (0.25g, 0.87 mmol) in dry toluene (5 mL) at room temperature under N_2 atmosphere. The solution was allowed to stir at refluxed condition for 21 h. The reaction mixture was allowed to cool to room temperature

then neutralized with dil. HCl and extracted with EtOAc (2×20 mL). The organic phase was combined and dried over anhydrous sodium sulphate. The product was purified by column chromatography using 20% of EtOAc/hexane mixture. Yellow viscos (0.23 g, yield = 80%,); $R_f = 0.77$ in 1:5 EtOAc/hexanes; ¹H NMR (400 MHz, CDCl₃): δ 16.39 (s, 1H), 7.73 (d, J = 8.8Hz, 2H), 7.33-7.29 (m, 4H), 7.17-7.13 (m, 6H), 7.01 (d, J = 8.8 Hz, 2H), 6.09 (s, 1H), 2.16 (s, 3H); ¹³C NMR (100 MHz, CDCl₃): δ 191.6, 183.7, 151.7, 146.6, 129.6, 128.5, 125.8, 124.5, 120.3, 95.7, 25.4; IR (neat): v 3058, 3031, 1582, 1490, 1180, 833, 702, 518 cm¹; HRMS (ESI): calcd for $C_{22}H_{19}NO_2$ [M+Na]⁺ 352.1308, Found 352.1306.

2.7.4.35 Synthesis of 4-(2,2-difluoro-6-methyl-2H-1, dioxaborinin-4-yl)-N, N-diphenyl aniline (2.67-BF₂):

To a stirred solution of Corresponding 1,3-diketone substrate 2.67 (0.06 g, 0.18 mmol) in dry dichloromethane (3 mL), BF₃.OEt₂ (0.027 ml, 0.22 mmol) was added dropwise to the reaction mixture at room temperature and maintained for another 0.5 h. The reaction colour was changed instantly, while added boron tri fluoro diethyl etherate. The reaction was quenched

0.2N NaOH (10 mL) with water and extracted dichloromethane (2×10

mL) solution. The crude product was further purified with column chromatography technique. Red solid (0.067 g, yield = 97%), MP: 209-210°C; $R_f = 0.26$ in 1:5 EtOAc/hexanes; ¹H NMR $(500 \text{ MHz}, \text{CDCl}_3)$: δ 7.87 (d, J = 9.0 Hz, 2H), 7.37 (t, <math>J = 8.0 Hz, 4H), 7.24-7.18 (m, 6H), 6.93 (d, J = 9.0 Hz, 2H), 6.40 (s, 1H), 2.31 (s, 3H); ¹³C NMR (125 MHz, CDCl₃): δ 188.2, 180.9, 154.5, 145.3, 131.3, 130.0, 126.7, 126.1, 121.4, 118.3, 96.0, 24.3; B¹¹ NMR (160 MHz, CDCl₃): δ 0.91 (s, 1B); F^{19} NMR (470 MHz, CDCl₃): δ -140.1 (s, 2F); IR (neat): υ 3039, 2919, 1550, 1342, 774, 667, 517 cm⁻¹; HRMS (ESI): calcd for C₂₂H₁₈BF₂NO₂ [M+Na]⁺ 400.1291, Found 400.1291.

2.8 Reference

- 1. (a) Shirota, Y.; Kageyama, H. Chem. Rev. 2007, 107, 953. (b) Wenli, S.; RongCui, J.; Yan, Y.; XiaoMei, L.; WenBo, H.; QuLi, F.; Wei, H. Chin Sci Bull. 2013, 58, 2570. (c) Chowdhury, A.; Mukherjee, P. S. J. Org. Chem. 2015, 80, 4064. (d) Ghosh, K.; Saha, I.; Masanta, G.; Wang, E. B.; Parish, C. A. Tetrahedron Lett. 2010, 51, 343.
- 2. (a) Venkateswararao, A.; Thomas, K. R. J.; Lee, C.-P.; Li, C.-T.; Ho, K.-C. ACS Appl. Mater. Interfaces 2014, 6, 2528. (b) Ledwon, P. Org. Electron. 2019, 75, 105422. (c)

- Kala, K.; Manoj, N. *RSC Adv.* **2016**, *6*, 22615. (d) Yin, J.; Maa, Y.; Li, G.; Peng, M.; Lin, W. *Coord. Chem. Rev.* **2020**, *412*, 213257.
- (a) Patel, J. Z.; Parkkari, T.; Laitinen, T.; Kaczor, A. A.; Saario, S. M.; Savinainen, J. R.; Navia-Paldanius, D.; Cipriano, M.; Leppanen, J.; Koshevoy, I. O.; Poso, A.; Fowler, C. J.; Laitinen, J. T.; Nevalainen, T. J. Med. Chem. 2013, 56, 8484. (b) Ghosh, K.; Saha, I. J Incl Phenom. Macrocycl Chem. 2011, 70, 97. (c) Manuela, M.; Raposo, M.; Mauricio, A.; Fonseca, C.; Kirsch, G. Tetrahedron 2004, 60, 4071.
- (a) Chen, H.; Huang, H.; Huang, X.; Clifford, J. N.; Forneli, A.; Palomares, E.; Zheng, X.; Zheng, L.; Wang, X.; Shen, P.; Zhao, B.; Tan, S. *J. Phys. Chem. C.* 2010, 114, 3280.
 (b) Yadav, J. S.; Reddy, B. V. S.; Basak, A. K.; Visali, B.; Narsaiah, A. V.; Nagaiah, K. *Eur. J. Org. Chem.* 2004, 546. (c) Cai, L.; Moehl, T.; Moon, S.-J.; Decoppet, J.-D.; Humphry-Baker, R.; Xue, Z.; Bin, L.; Zakeeruddin, S. M.; Gratzel, M. *Org. Lett.* 2014, 16, 106. (d) Chen, J.; Ko, S.; Liu, L.; Sheng, Y.; Han, H.; Li, X. *New J. Chem.* 2015, 39, 3736.
- (a) D'Aleo, A.; Gachet, D.; Heresanu, V.; Giorgi, M.; Fages, F. *Chem. Eur. J.* 2012, 18, 12764.
 (b) Liu, X.; Xu, D.; Lu, R.; Li, B.; Qian, C.; Xue, P.; Zhang, X.; Zhou, H. *Chem. Eur. J.* 2011, 17, 1660.
 (c) Hu, Z.-J.; Tian, X.-H.; Zhao, X.-H.; Wang, P.; Zhang, Q.; Sun, P.-P.; Wu, J.-Y.; Yanga, J.-X.; Tian, Y.-P. *Chem. Commun.* 2011, 47, 12467.
- Dhar, A.: Kumar, N. S.; Asif, M.; Vekariya, R. L. New J. Chem. 2018, 42, 12024-12031.
- Frisch, M. J.; Trucks, G. W.; Schlegel, H. B.; Scuseria, G. E.; Robb, M. A.; Cheeseman, J. R.; Scalmani, G.; Barone, V.; Mennucci, B.; Petersson, G. A.; Nakatsuji, H.; Caricato, M.; Li, X.; Hratchian, H. P.; Izmaylov, A. F.; Bloino, J.; Zheng, G.; Sonnenberg, J. L.; Hada, M.; Ehara, M.; Toyota, K.; Fukuda, R.; Hasegawa, J.; Ishida, M.; Nakajima, T.; Honda, Y.; Kitao, O.; Nakai, H.; Vreven, T.; Montgomery, Jr. J. A.; Peralta, J. E.; Ogliaro, F.; Bearpark, M.; Heyd, J. J.; Brothers, E.; Kudin, K. N.; Staroverov, V. N.; Kobayashi, R.; Normand, J.; Raghavachari, K.; Rendell, A.; Burant, J. C.; Iyengar, S. S.; Tomasi, J.; Cossi, M.; Rega, N.; Millam, J. M.; Klene, M.; Knox, J. E.; Cross, J. B.; Bakken, V.; Adamo, C.; Jaramillo, J.; Gomperts, R.; Stratmann, R. E.; Yazyev, O.; Austin, A. J.; Cammi, R.; Pomelli, C.; Ochterski, J. W.; Martin, R. L.; Morokuma, K.; Zakrzewski, V. G.; Voth, G. A.; Salvador, P.; Dannenberg, J. J.; Dapprich, S.; Daniels, A. D.; Farkas, O.; Foresman, J. B.; Ortiz, J. V.; Cioslowski, J.; Fox, D. J. Gaussian 09, Revision A.02, Gaussian, Inc. Wallingford CT, 2009.

- 8. (a) Gratzel, M. Nature **2001**, 414, 338. (b) Li, B.; Wang, L.; Kang, B.; Wang, P.; Qiu, Y. Sol. Energy Mater. Sol. Cells **2006**, 90, 549.
- (a) Blakers, A. W.; Wang, A.; Milne, A. M.; Zhao, J.; Green, M. A. *Appl. Phys. Lett.* 1989, 55, 1363. (b) Hoppe, H.; Sariciftci, N. S. *J. Mater. Res.* 2004, 19, 1924. (c) Gunes,
 S.; Neugebauer, H.; Sariciftci, N. S. *Chem. Rev.* 2007, 107, 1324.
- (a) O'Regan, B.; Gratzel, M. Nature 1991, 353, 738. (b) Nazeeruddin, M. K.; Angelis, F. D.; Fantacci, S.; Selloni, A.; Viscardi, G.; Liska, P.; Ito, S.; Takeru, B.; Gratzel, M. J. Am. Chem. Soc. 2005, 127, 16835. (c) Wang, Z.-S.; Yamaguchi, T.; Sugihara, H.; Arakawa, H. Langmuir 2005, 21, 4272. (d) Gao, F.; Wang, Y.; Shi, D.; Zhang, J.; Wang, M.; Jing, X.; Humphry-Baker, R.; Wang, P.; Zakeeruddin, S. M.; Gratzel, M. J. Am. Chem. Soc. 2008, 130, 10720. (e) Mathew, S.; Yella, A.; Gao, P.; Humphry-Baker, R.; Curchod, B. F. E.; Ashari-Astani, N.; Tavernelli, I.; Rothlisberger, U.; Nazeeruddin, M. K.; Gratzel, M. Nat. Chem. 2014, 6, 242. (f) Hagfeldt, A.; Boschloo, G.; Sun, L.; Kloo, L.; Pettersson, H. Chem. Rev. 2010, 110, 6595.
- 11. Mishra, A.; Fischer, M. K. R.; Bauerle, P. Angew. Chem. Int. Ed. 2009, 48, 2474.
- 12. (a) Gong, J.; Liang, J.; Sumathy, K. *Renew. Sustain. Energy Rev.* **2012**, 16, 5848. (b) Gong, J.; Sumathy, K.; Qiao, Q.; Zhou, Z. *Renew. Sustain. Energy Rev.* **2017**, 68, 234.
- (a) Liang, M.; Xu, W.; Cai, F.; Chen, P.; Peng, B.; Chen, J.; Li, Z. J. Phys. Chem. C 2007, 111, 4465. (b) Li, G.; Jiang, K.-J.; Li, Y.-F.; Li, S.-L.; Yang, L.-M. J. Phys. Chem. C 2008, 112, 11591. (c) Li, R.; Lv, X.; Shi, D.; Zhou, D.; Cheng, Y.; Zhang, G.; Wang, P. J. Phys. Chem. C 2009, 113, 7469. (d) Lin, J. T.; Chen, P.-C.; Yen, Y.-S.; Hsu, Y.-C.; Chou, H.-H.; Yeh, M.-C. P. Org. Lett. 2009, 11, 97. (e) Wu, Y.; Zhu, W. Chem. Soc. Rev. 2013, 42, 2039.
- 14. (a) Lavis, L. D.; Raines, R. T. ACS Chem. Biol. 2008, 3, 142. (b) Lavis, L. D.; Raines, R. T. ACS Chem. Biol. 2014, 9, 855. (c) Li, K.; Qin, W.; Ding, D.; Tomczak, N.; Geng, J.; Liu, R.; Liu, J.; Zhang, X.; Liu, H.; Liu, B.; Tang, B. Z. Sci. Rep. 2013, 3, 1150.
- (a) Araneda, J. F.; Piers, W. E.; Heyne, B.; Parvez, M.; McDonald, R. *Angew. Chem. Int. Ed.* **2011**, *50*, 12214. (b) Shcherbakova, D. M.; Hink, M. A.; Joosen, L.; Gadella, T. W. J.; Verkhusha, V. V. *J. Am. Chem. Soc.* **2012**, *134*, 7913. (c) Zhang, J.; Chen, R.; Zhu, Z.; Adachi, C.; Zhang, X.; Lee, C.-S. *ACS Appl. Mater. Interfaces* **2015**, *7*, 26266.
- 16. a) Lin, W.; Yuan, L.; Cao, Z.; Feng, Y.; Song, J. Angew. Chem. Int. Ed. 2010, 49, 375.
 (b) Singh, V. K.; Prasad, R.; Koch, B.; Hasan, S. H.; Dubey, M. New J. Chem. 2017, 41, 5114. (c) Leong, C.; Lee, S. C.; Ock, J.; Li, X.; See, P.; Park, S. J.; Ginhoux, F.; Yun, S.-W.; Chang, Y.-T. Chem. Commun. 2014, 50, 1089. (d) Pal, K.; Sharma, V.;

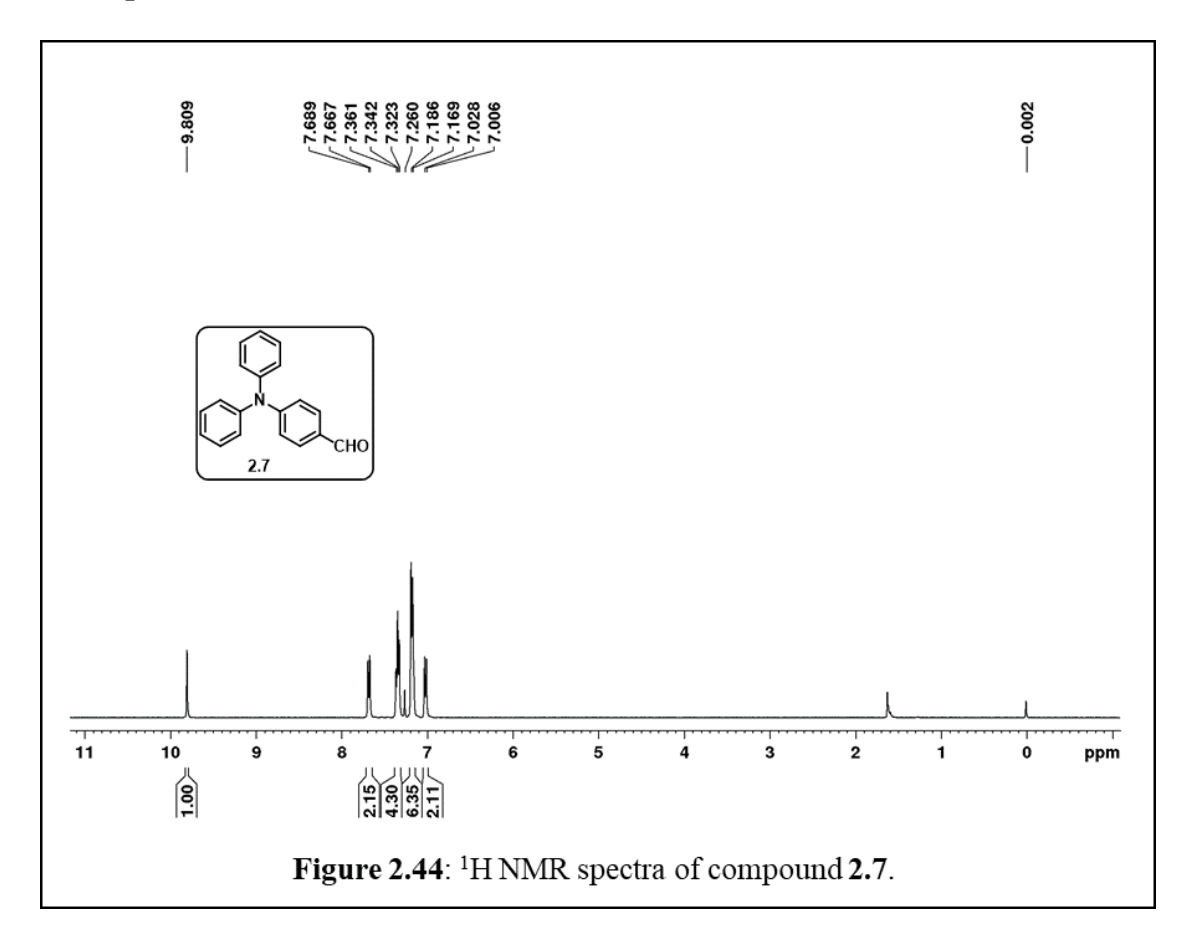
- Sahoo, D.; Kapuria, N.; Koner, A. L. *Chem. Commun.* **2018**, *54*, 523. (e) Karton-Lifshin, N.; Albertazzi, L.; Bendikov, M.; Baran, P. S.; Shabat, D. *J. Am. Chem. Soc.* **2012**, *134*, 20412. (f) Signore, G.; Nifosi, R.; Albertazzi, L.; Storti, B.; Bizzarri, R. *J. Am. Chem. Soc.* **2010**, *132*, 1276. (g) Zhang, L.; Su, F.; Kong, X.; Lee, F.; Sher, S.; Day, K.; Tian, Y.; Meldrum, D. R.; *ChemBioChem*, **2016**, *17*, 1719. (h) Zhang, K.; Wu, W.; Li, Y.; Sun, M.; Yu, H.; Wong, M. S. *RSC Adv.* **2016**, *6*, 115298.
- (a) Dumat, B.; Bordeau, G.; Aranda, A. I.; Mahuteau-Betzer, F.; Harfouch, Y. E.; Metge, G. Y. E.; Charra, F.; Fiorini-Debuisschert, C.; Teulade-Fichou, M.-P. Org. Biomol. Chem. 2012, 10, 6054. (b) Dumat, B.; Bordeau, G.; Faurel-Paul, E.; Mahuteau-Betzer, F.; Saettel, N.; Metge, G.; Fiorini-Debuisschert, C.; Charra, F.; Teulade-Fichou, M.-P. J. Am. Chem. Soc. 2013, 135, 12697. (c) Liu, Y.; Kong, M.; Zhang, Q.; Zhang, Z.; Zhou, H.; Zhang, S.; Li, S.; Wu, J.; Tian, Y. J. Mater. Chem. B, 2014, 2, 5430. (d) Kong, L.; Tian, Y.-p.; Chen, Q.-y.; Zhang, Q.; Wang, H.; Tan, D.-q.; Xue, Z.-m.; Wu, J.-y.; Zhou, H.-p.; Yang, J.-x. J. Mater. Chem. C 2015, 3, 570. (e) Li, Q.; Qian, Y. New J. Chem. 2016, 40, 7095. (f) Chennoufi, R.; Bougherara, H.; Gagey-Eilstein, N.; Dumat, B.; Henry, E.; Subra, F.; Bury-Moné, S.; Mahuteau-Betzer, F.; Tauc, P.; Teulade-Fichou, M.-P.; Deprez, E. Sci. Rep. 2016, 6, 21458.
- 18. a) Gavin, R. H.; Cytoskeleton Methods and Protocols, 2nd ed.; Brooklyn, New York, 2009; b) Jordan, M. A.; Wilson, L. Nat. Rev. Cancer 2004, 4, 253. c) Lukinavicius, G.; Mitronova, G. Y.; Schnorrenberg, S.; Butkevich, A. N.; Barthel, H.; Belov, V. N.; Hell, S. W. Chem. Sci. 2018, 9, 3324.
- a) Jordan, A.; Hadfield, J. A.; Lawrence, N. J.; McGown, A. T. *Med. Res. Rev.* 1998, 18, 259. b) Williams, Jr. R. C.; Shah, C.; Sackett, D. *Anal. Biochem.* 1999, 275, 264. c) Downing, K. H. *Annu. Rev. Cell Dev. Biol.* 2000, 16, 89. d) Shaner, N. C.; Campbell, R. E.; Steinbach, P. A.; Giepmans, B. N. G.; Palmer, A. E.; Tsien, R. Y. *Nat. Biotechnol.* 2004, 22, 1567. e) Mohan, L.; Raghav, D.; Ashraf, S. M.; Sebastian, J.; Rathinasamy, K. *Biomed. Pharmacol. J.* 2018, 105, 506.
- 20. (a) Zhang, H.; Wang, C.; Jiang, T.; Guo, H.; Wang, G.; Cai, X.; Yang, L.; Zhang, Y.; Yu, H.; Wang, H.; Jiang, K. *Anal. Chem.* **2015**, *87*, 5216.
- 21. Suzuki, Y.; Sawada, J.-I.; Hibner, P.; Ishii, H.; Matsuno, K.; Sato, M.; Witulski, B.; Asai, A. *Dyes Pigm.* **2017**, *145*, 233-238.
- 22. Lukinavicius, G.; Reymond, L.; D'Este, E.; Masharina, A.; Göttfert, F.; Ta, H.; Güther, A.; Fournier, M.; Rizzo, S.; Waldmann, H.; Blaukopf, C.; Sommer, C.;

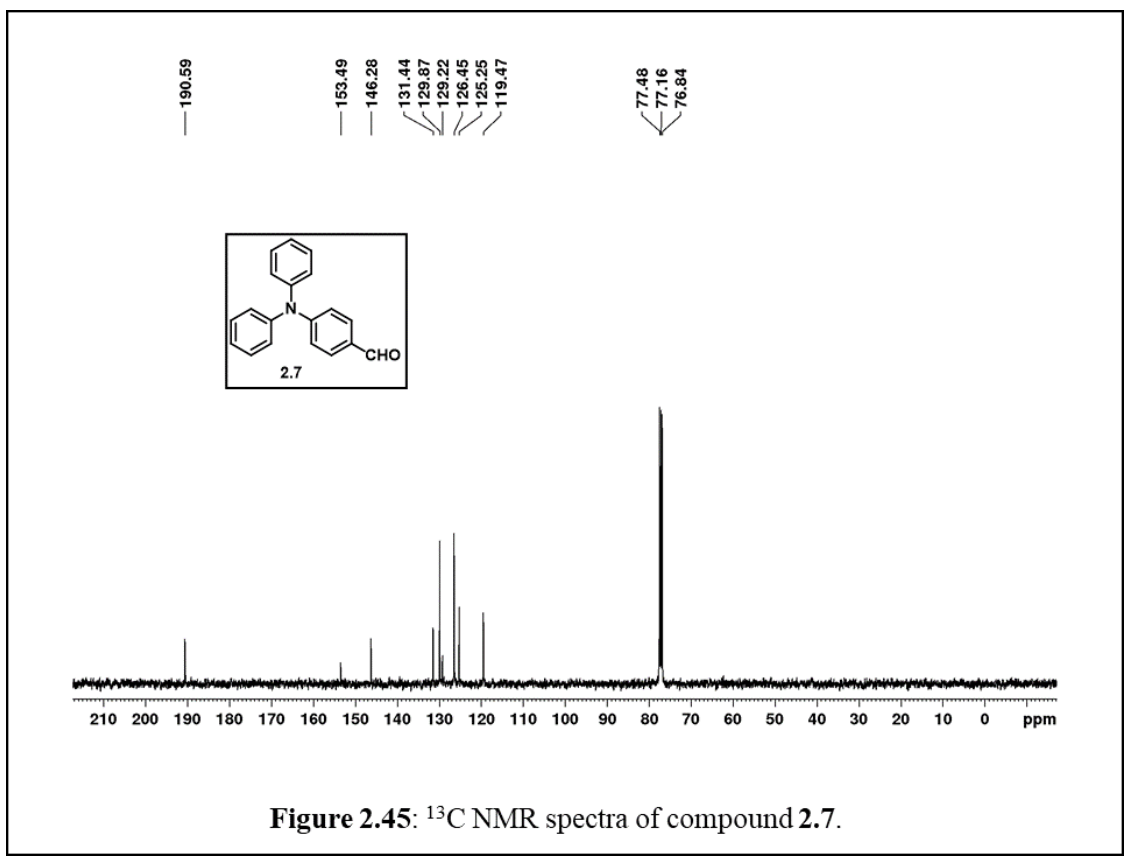
- Gerlich, D. W.; Arndt, H.-D.; Hell, S. W.; Johnsson, K. Nat. Methods, **2014**, 11, 731-733.
- 23. Mosmann, T. J Immunol Methods 1983, 65, 55.
- 24. Tron, G. C.; Pirali, T.; Sorba, G.; Pagliai, F.; Busacca, S.; Genazzani, A. A. *J. Med. Chem.* **2006**, *49*, 3033-3044.
- 25. (a) Dzombak, D. A.; Ghosh, R. S.; Wong-Chong, G. M. Cyanide in Water and Soil: Chemistry, Risk and Management, CRC Press, 2005, 41-54. (b) Young, C.; Tidwell, L.; Anderson, C. Cyanide: Social Industrial and Economic Aspects, The Minerals, Metals, and Materials Society, Warrendale, 2001.
- 26. Burnworth, M.; Rowan, S. J.; Weder, C. Chem. Eur. J. 2007, 13, 7828-7836.
- 27. (a) Way, J. L. *Pharmacologic Aspests of Cyanide and its Antagonism*, (Eds.: B. Vennesland, E. F. Comm, J. Knownles, J. Westly, F. Wissing), Academic Press, London, **1981**, pp. 29-49 (b) Kulig, K. W. *Cyanide Toxicity*, U.S. Department of Health and Human Services, Atlanta, GA, **1991**.
- 28. Guidelines for Drinking-Water Quality, World Health Organization, 4th Edn, 2017.
- 29. Suzuki, T.; Hioki, A.; Kurahashi, M. Anal. Chim. Acta 2003, 476, 159-165.
- 30. (a) Riojas, A. A. C.; Wong, A.; Planes, G. A.; Sotomayor, M. D. P. T.; Rosa-Toro, A. L.; Baena-Moncada, A. M. Sens. Actuators B 2019, 287, 544-550. (b) Ding, G.; Zhou, H.; Xu, J.; Lu, X. Chem. Commun. 2014, 50, 655-657.
- (a) Al-Saidi, H. M.; Al-Harbi, S. A.; Aljuhani, E. H.; El-Shahawi, M. S. *Talanta* 2016, 159, 137-142.
 (b) Cacace, D.; Ashbaugh, H.; Kouri, N.; Bledsoe, S.; Lancaster, S.; Chalk, S. *Anal. Chim. Acta* 2007, 589, 137-141.
 (c) Deepa, B.; Balasubramanian, N.; Nagaraja, K. S. *Anal. Lett.* 2003, 36, 2865-2874.
 (d) Scoggins, M. W. *Anal. Chem.* 1972, 44, 1294-1296.
- 32. (a) Kage, S.; Nagata, T.; Kudo, K.; *J. Chromatogr. B: Biomed. Appl.* 1996, 675, 27-32;
 (b) Youso, S. L.; Rockwood, G. A.; Lee, J. P.; Logue, B. A. *Anal. Chim. Acta* 2010, 677, 24-28. (c) Desharnais, B.; Huppe, G.; Lamarche, M.; Mireault, P.; Skinner, C. D. *Forensic Sci. Int.* 2012, 222, 346-351. (d) Jackson, R.; Logue, B. A. *Anal. Chim. Acta* 2017, 960, 18-39. (e) Christison, T. T.; Rohrer, J. S. *J. Chromatogr. A* 2007, 1155, 31-39.
- 33. (a) Wang, F.; Wang, L.; Chen, X.; Yoon, J. *Chem. Soc. Rev.* **2014**, *43*, 4312-4324. (b) Xu, Z.; Chen, X.; Kim, H. N.; Yoon, J. Y. *Chem. Soc. Rev.* **2010**, *39*, 127-137. (c) Wu, X.; Xu, B.; Tong, H.; Wang, L. *Macromolecules* **2011**, *44*, 4241-4248. (d) Hou, L.; Li,

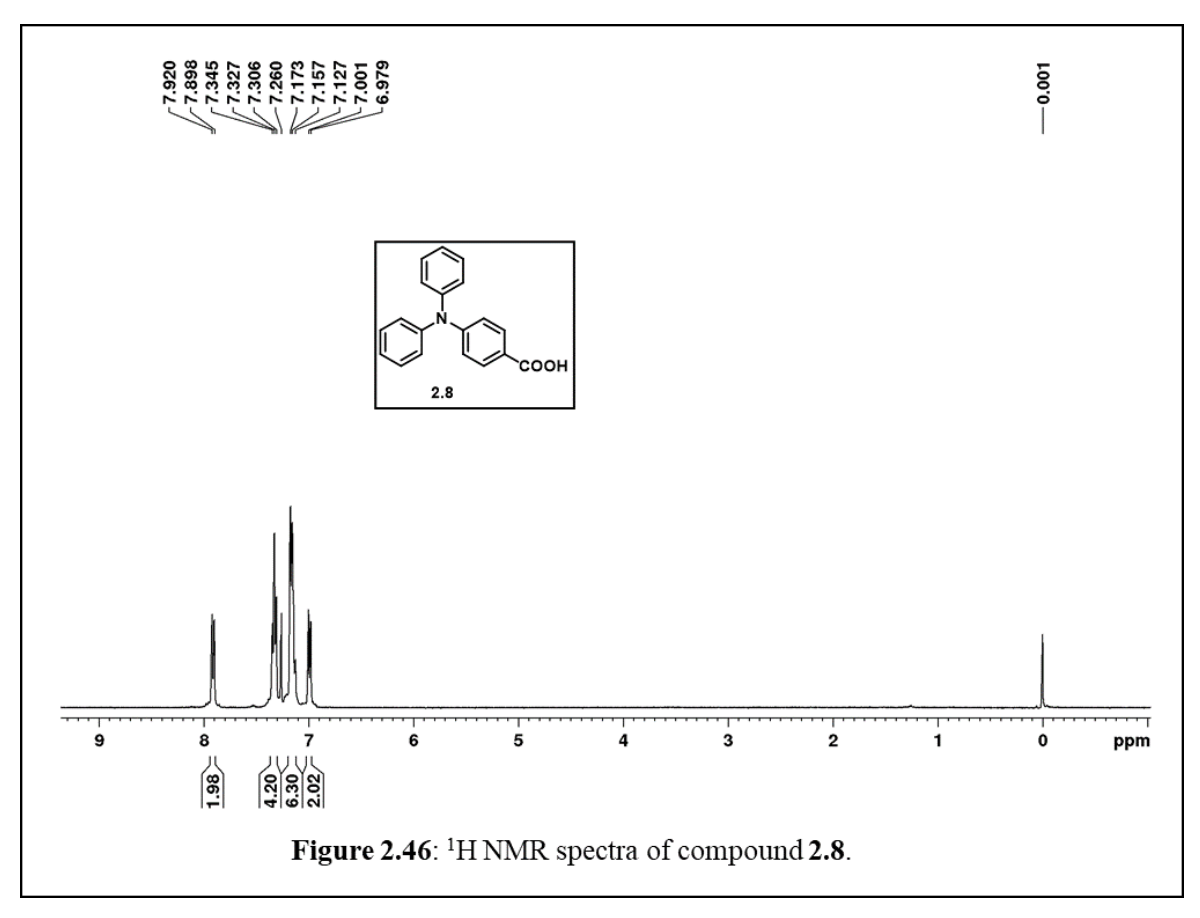
- F.; Guo, J.; Zhang, X.; Kong, X.; Cui, X. T.; Dong, C.; Wang, Y.; Shuang, S. *J. Mater. Chem. B* **2019**, *7*, 4620-4629.
- 34. (a) Gholamzadeh, P.; Ziarani, G. M.; Lashgari, N.; Badiei, A.; Shayesteh, A.; Jafari, M. *J. Fluoresc* 2016, 26, 1857-1864. (b) Shaily, A. Kumar, N. Ahmed, *Ind. Eng. Chem. Res.* 2017, 56, 6358-6368. (c) Dalapati, R.; Nandi, S.; Reinsch, H.; Bhunia, B. K.; Mandal, B. B.; Stock, N.; Biswas, S. *Crys. Eng. Comm.* 2018, 20, 4194-4201. (d) Dasgupta, J.; Ma, P. K. *Anal. Chim. Acta*, 2010, 673, 117-125.
- 35. (a) Lin, Q.; Lu, T. T.; Zhu, X.; Wei, T. B.; Li, H.; Zhang, Y. M. Chem. Sci. 2016, 7, 5341-5346. (b) Sun, S.-S.; Lees, A. J. J. Am. Chem. Soc. 2000, 122, 8956-8967. (c) Miyaji, H.; Sessler, J. L. Angew. Chem. Int. Ed. 2001, 113, 154-157. (d) Yao, L.; Zhou, J.; Liu, J.; Feng, W.; Li, F. Adv. Funct. Mater. 2012, 22, 2667-2672. (e) Shi, B. B.; Zhang, P.; Wei, T. B.; Yao, H.; Lin, Q.; Zhang, Y. M. Chem. Commun. 2013, 49, 7812-7814. (f) Cao, W.; Zheng, X.; Fang, D.; Jin, L. Dalton Trans. 2014, 43, 7298-7303. (g) Isar, P.; Rao, M. R.; Ravikanth, M. Eur. J. Org. Chem. 2018, 24, 3095-3104. (h) Liu, T.; Liu, X.; Valencia, M. A.; Sui, B.; Zhang, Y.; Belfield, K. D. Eur. J. Org. Chem. 2017, 27, 3957-3964.
- 36. (a) Garcia, F.; Garcia, J. M.; Garcia-Acosta, B.; Martinez-Manez, R.; Sancenon, F.; Soto, J. Chem. Commun. 2005, 22, 2790-2792. (b) Sun, M.; Wang, S.; Yang, Q.; Fei, X.; Li, Y.; Li, Y. RSC Adv. 2014, 4, 8295-8299. (c) Li, J.; Gao, J.; Xiong, W.; Li, P.; Zhang, H.; Zhao, Y.; Zhang, Q. Chem. Asian. J. 2014, 9, 121-125. (d) Wang, P.; Yao, Y.; Xue, M. Chem. Commun. 2014, 50, 5064-5067. (e) Zhang, Y.; Li, D.; Li, Y.; Yu, J. Chem. Sci. 2014, 5, 2710-2716. (f) Bera, M. K.; Chakraborty, C.; Singh, P. K.; Sahu, C.; Sen, K.; Maji, S.; Das, A. K.; Malik, S. J. Mater. Chem. B, **2014**, 2, 4733-4739. (g) Yue, Y.; Huo, F.; Yin, C.; Chao, J.; Zhang, Y. Sens. Actuators B 2015, 212, 451–456. (h) Huo, F.; Kang, J.; Yin, C.; Chao, J.; Zhang, Y. Sens. Actuators B 2015, 215, 93-98. (i) Xiong, K.; Huo, F.; Yin, C.; Yang, Y.; Chao, J.; Zhang, Y.; Xu, M. Sens. Actuators B 2015, 220, 822-828. (j) Liu, T.; Huo, F.; Li, J.; Cheng, F.; Yin, C. Sens. Actuators B **2017**, 239, 526-535. (k) Yina, C.; Huo, F.; Xu, M.; Barnes, C. L.; Glass, T. E. Sens. Actuators B 2017, 252, 592-599. (1) Zou, Q.; Tao, F.; Wu, H.; Yu, W. W.; Li, T.; Cui, Y. Dyes Pigm. 2019, 164, 165-173. (m) Lakshmi, P. R.; Manivannan, R.; Jayasudha, P.; Elango, K. P. Anal. Methods, 2018, 10, 2368-2375. (n) Jayasudha, P.; Manivannan, R.; Ciattini, S.; Chelazzi, L.; Elango, K. P. Sens. Actuators B, 2017, 242, 736-745. (o) Jeong, E.; Yoon, S.; Lee, H. S.; Kumar, A.; Chae, P. S. Dyes Pigm. 2019, 162, 348-357. (p) Li, Q.; Wang, Z.; Song, W.; Ma, H.; Dong, J.; Quan, Y.; Ye, X.; Huang, Z.

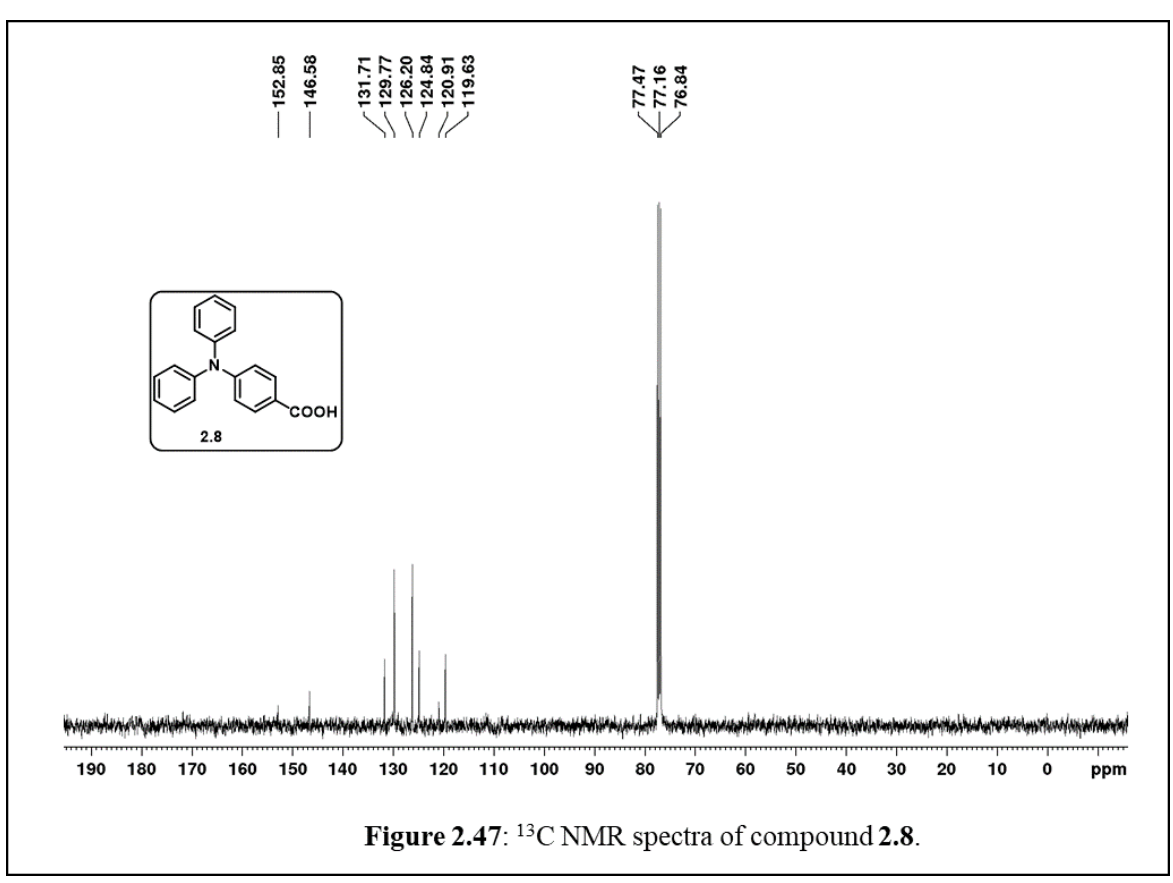
- Dyes Pigm. **2019**, 161, 389-395. (q) Pati, P. B.; Zade, S. S. Eur. J. Org. Chem. **2012**, 33, 6555-6561. (r) Li, Z.; Dai, Y.; Lu, Z.; Pei, Y.; Song, Y.; Zhang, L.; Guo, H. Eur. J. Org. Chem. **2019**, 22, 3614-3621. (s) Kwon, N.; Baek, G.; Swamy, K. M. K.; Lee, M.; Xu, Q.; Kim, Y.; Kim, S.; Yoon, J. Dyes Pigm. **2019**, 171, 107679-107687.
- 37. (a) Miyaji, H.; Sessler, J. L. *Angew. Chem. Int. Ed.* **2001**, *40*, 154. (b) Xu, Z.; Chen, X.; Kim, H.N.; Yoon, J. *Chem. Soc. Rev.* **2010**, *39*, 127.
- 38. a) Yang, X.; Chen, X.; Lu, X.; Yan, C.; Xu, Y.; Hang, X.; Qu, J.; Liu, R. *J. Mater. Chem. C* **2016**, *4*, 383. (b) Thanayupong, E.; Suttisintong, K.; Sukwattanasinitt, M.; Niamnont, N. *New J. Chem.* **2017**, *41*, 4058. (c) Wang, S.; Xu, H.; Yang, Q.; Song, Y.; Li, Y. *RSC Adv.* **2015**, *5*, 47990. (d) Zhang, Q.; Zhang, J.; Zuo, H.; Wang, C.; Shen, Y. *Tetrahedron*, **2016**, *72*, 1244.
- 39. (a) Guliyev, R.; Ozturk, S.; Sahin, E.; Akkaya, E. U. *Org. Lett.* 2012, *14*, 1528. (b) Huh, J. O.; Do, Y.; Lee, M. H. *Organometallics* 2008, *27*, 1022. (c) Wang, L.; Li, L.; Cao, D. *Sens. Actuators B* 2017, *241*, 1224. (d) Piyanuch, P.; Sirirak, J.; Kamkaew, A.; Weeranantanapan, O.; Promarak, V.; Burgess, K.; Wanichacheva, N. *ChemPlusChem* 2019, *84*, 252.
- 40. Liu, M.; Zhai, L.; Sun, J.; Xue, P.; Gong, P.; Zhang, Z.; Sun, J.; Lu, R. *Dyes Pigm*. **2016**, *128*, 271.
- (a) Saha, S.; Ghosh, A.; Mahato, P.; Mishra, S.; Mishra, S. K.; Suresh, E.; Das, S.; Das, A. Org. Lett. 2010, 12, 3406.
 (b) Kumari, N.; Jha, S.; Bhattacharya, S. J. Org. Chem. 2011, 76, 8215-8222.
 (c) Housecroft, C. E.; Sharpe, A. G. In Inorganic Chemistry, 3rd ed.; Pearson Education, Ltd.: Harlow, 2008, 537.
- 42. (a) Guliyev, R.; Ozturk, S.; Sahin, E.; Akkaya, E. U. *Org. Lett.* 2012, *14*, 1528-1531.
 (b) Yu, Y.; Shu, T.; Fu, C.; Yu, B.; Zhang, D.; Luo, H.; Chen, J.; Dong, C. *J. Lumin.* 2017, *186*, 212–218. (c) Wang, L.; Li, L.; Cao, D. *Sens. Actuators B* 2017, *241*, 1224–1234. (d) Sarveswari, S.; Beneto, A. J.; Siva, A. *Sens. Actuators B* 2017, *245*, 428-434.

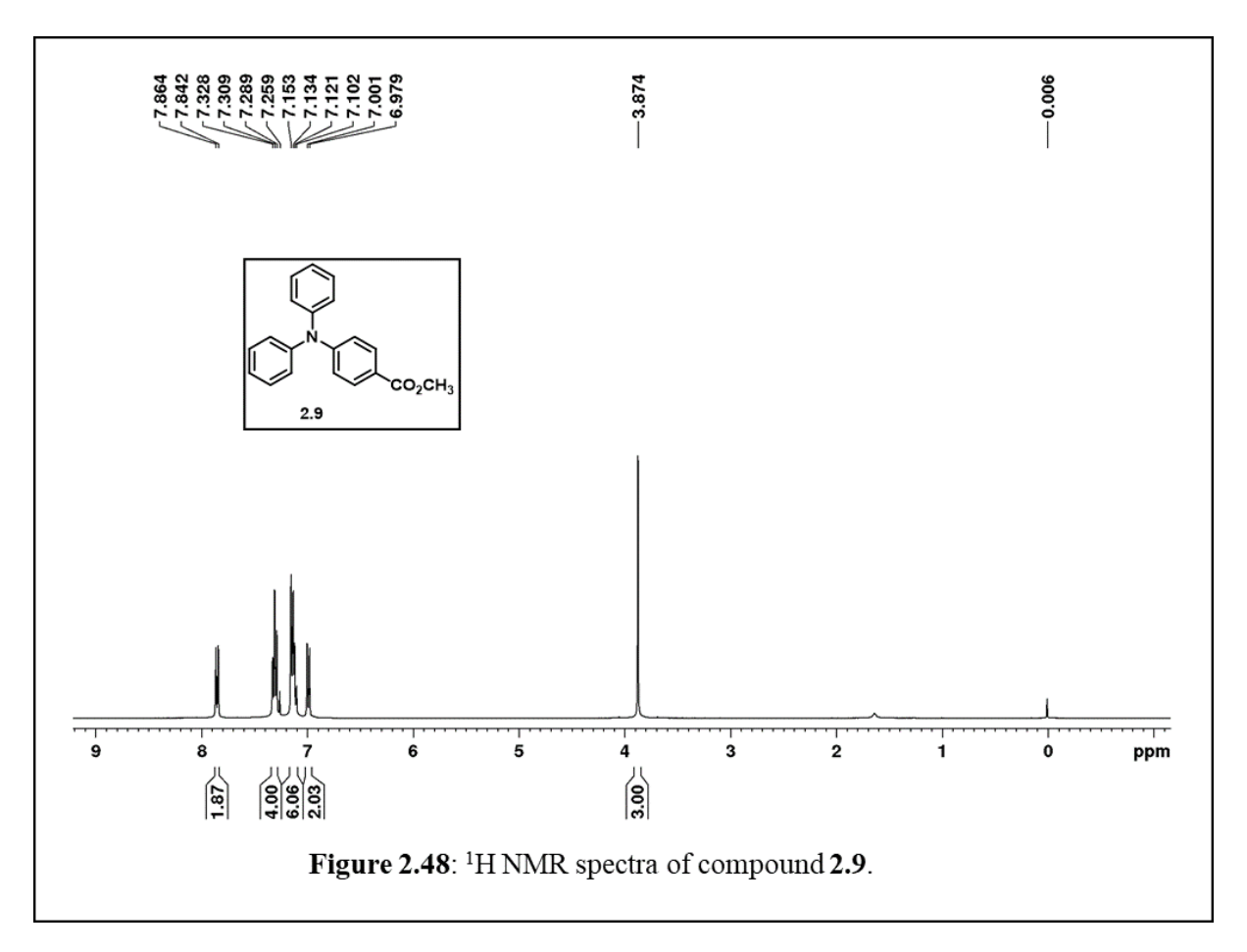
2.9 Representative ¹H, ¹³C, ¹¹B, ¹⁹F NMR

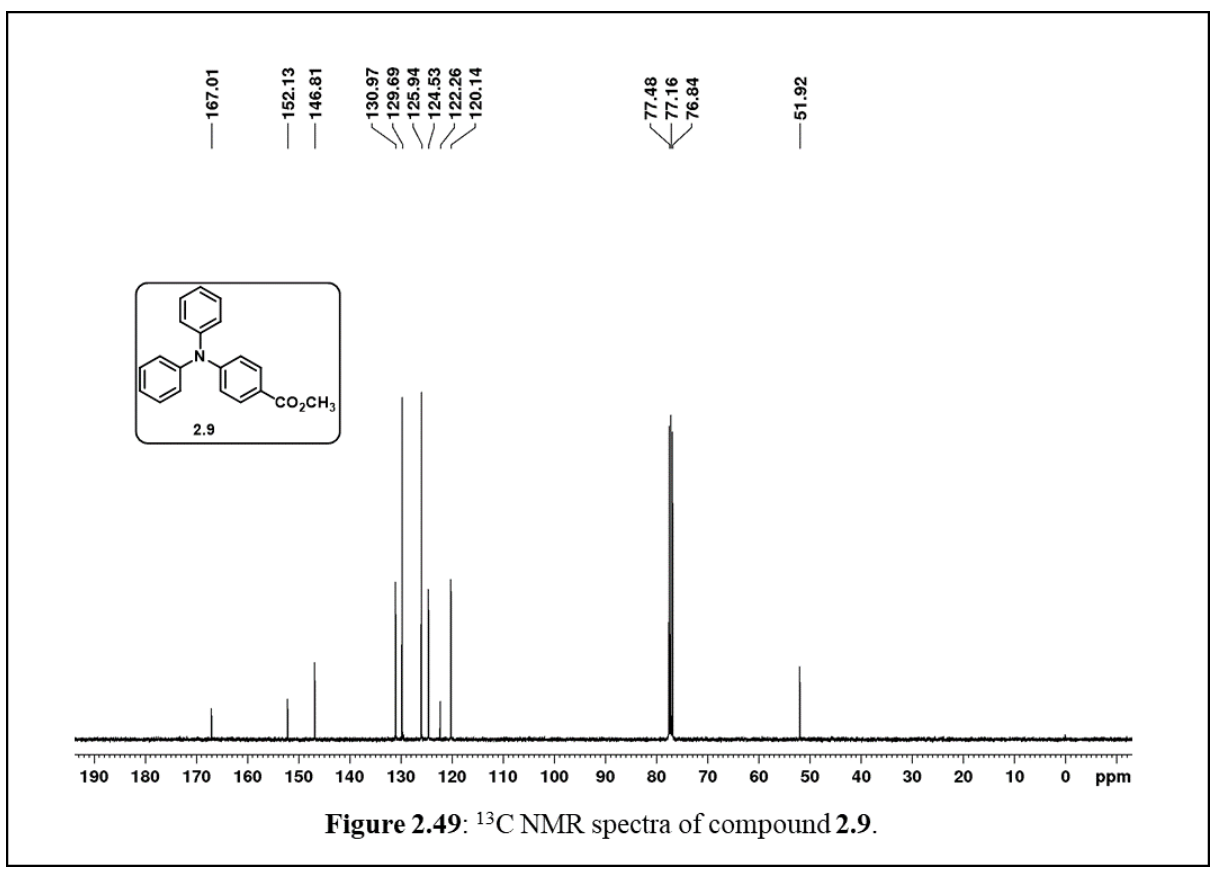


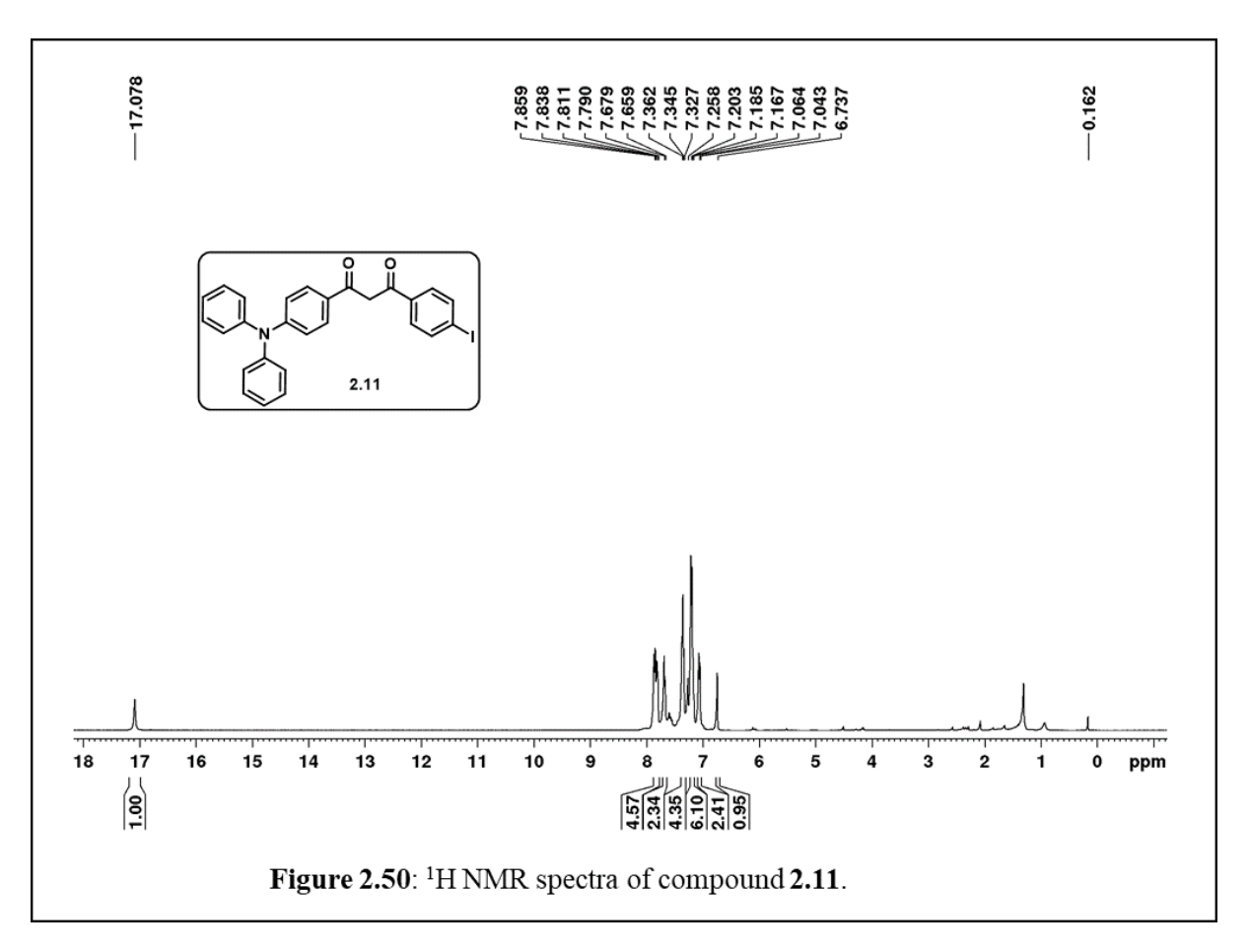


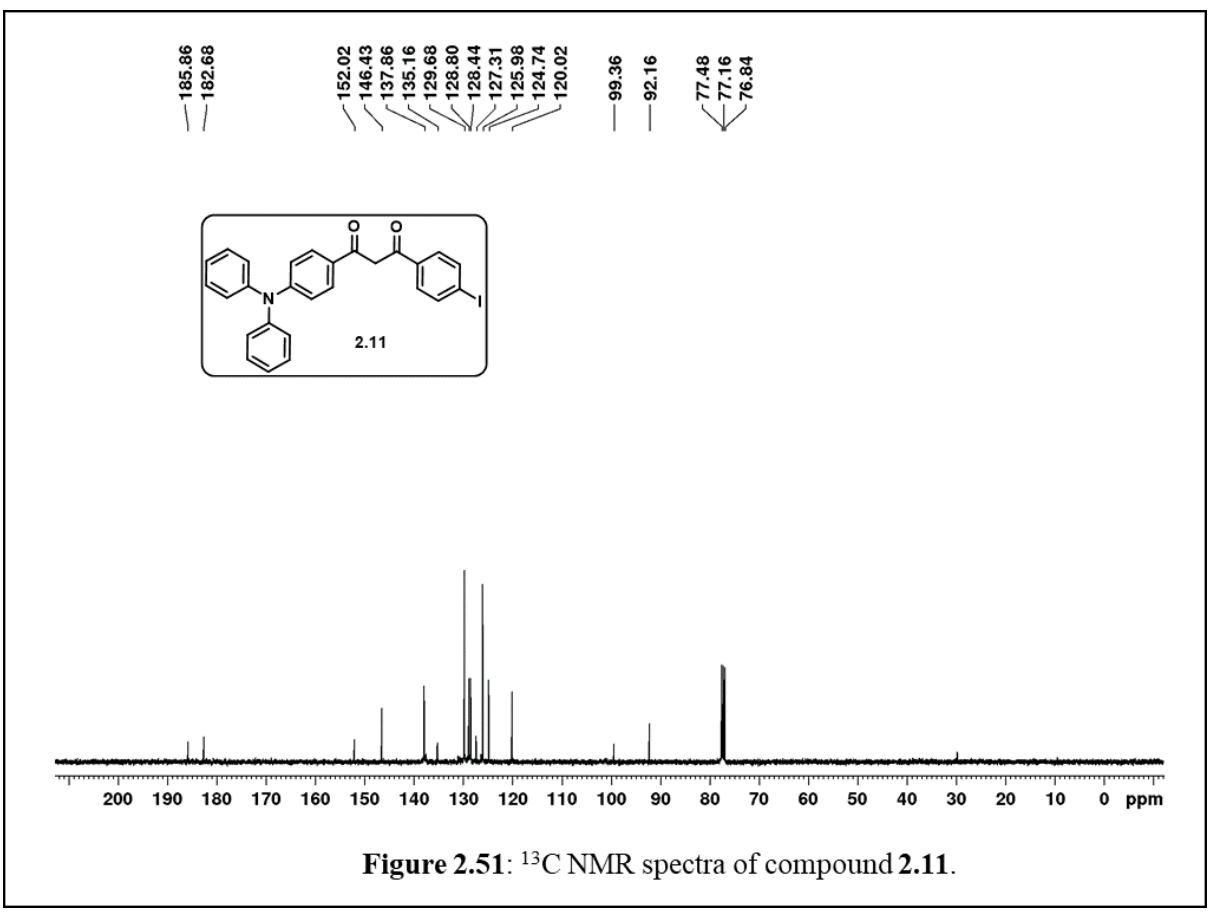


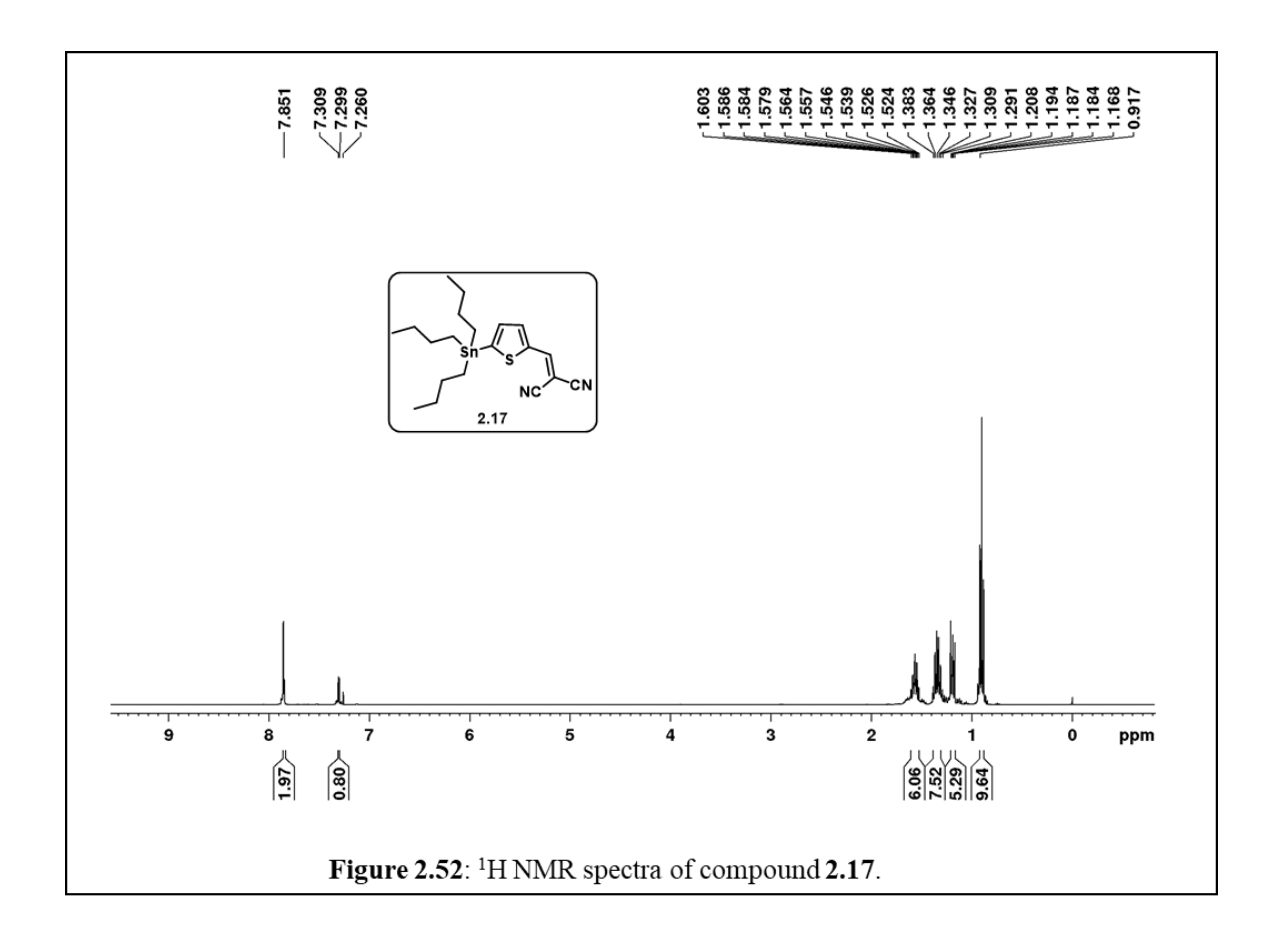


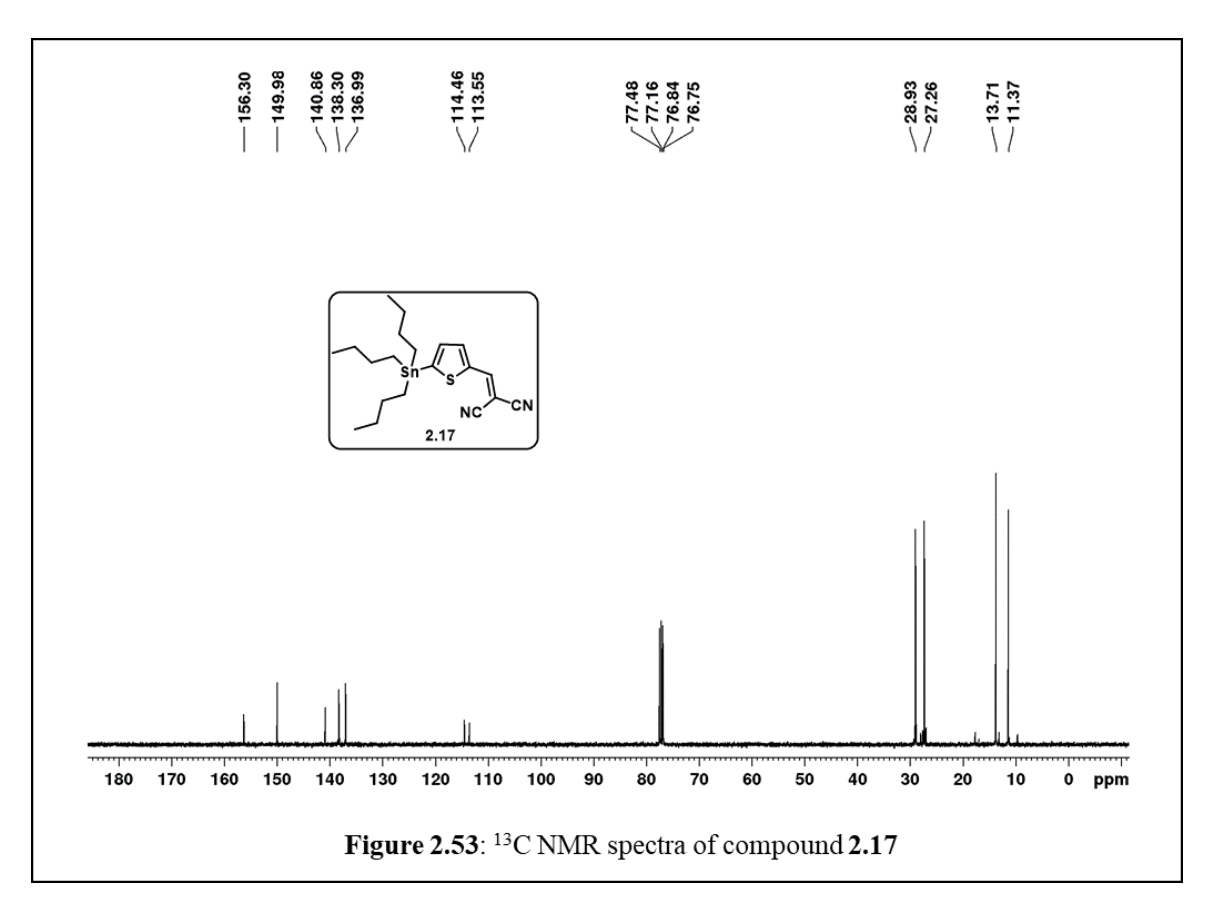


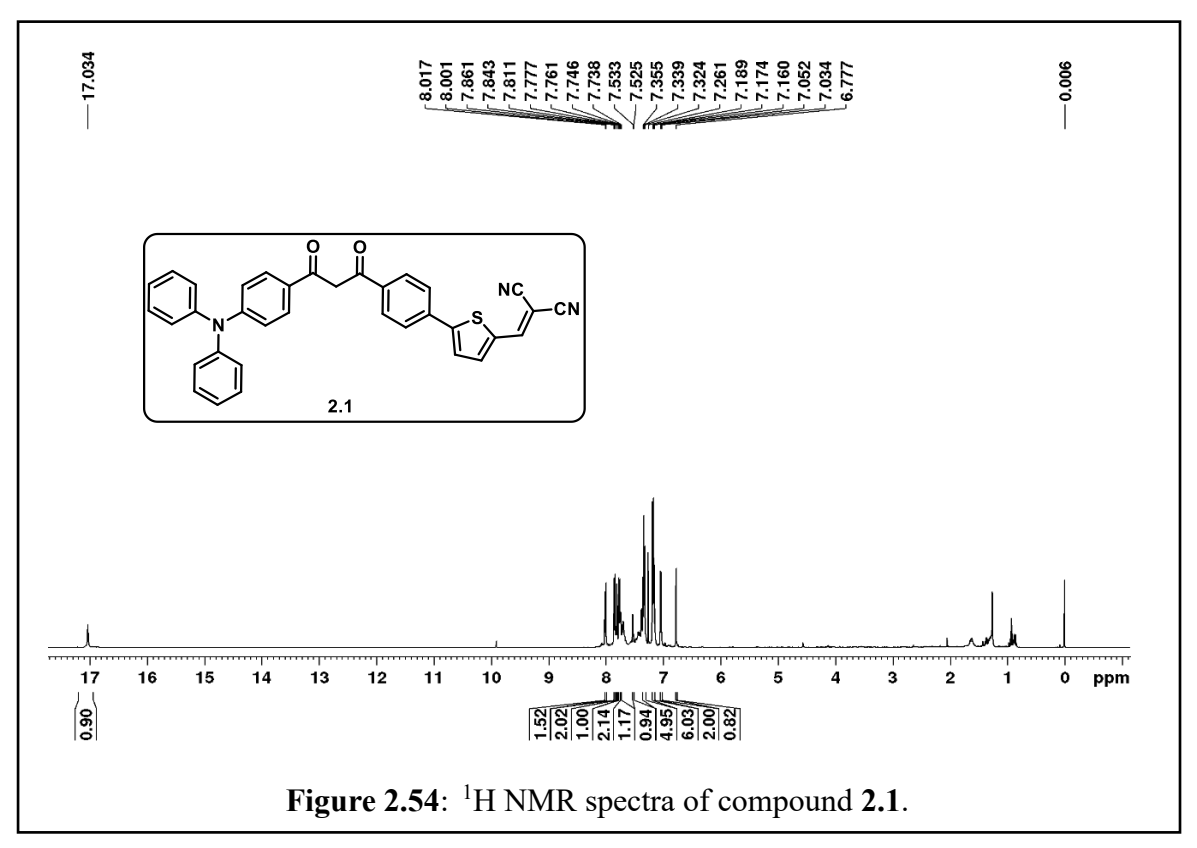


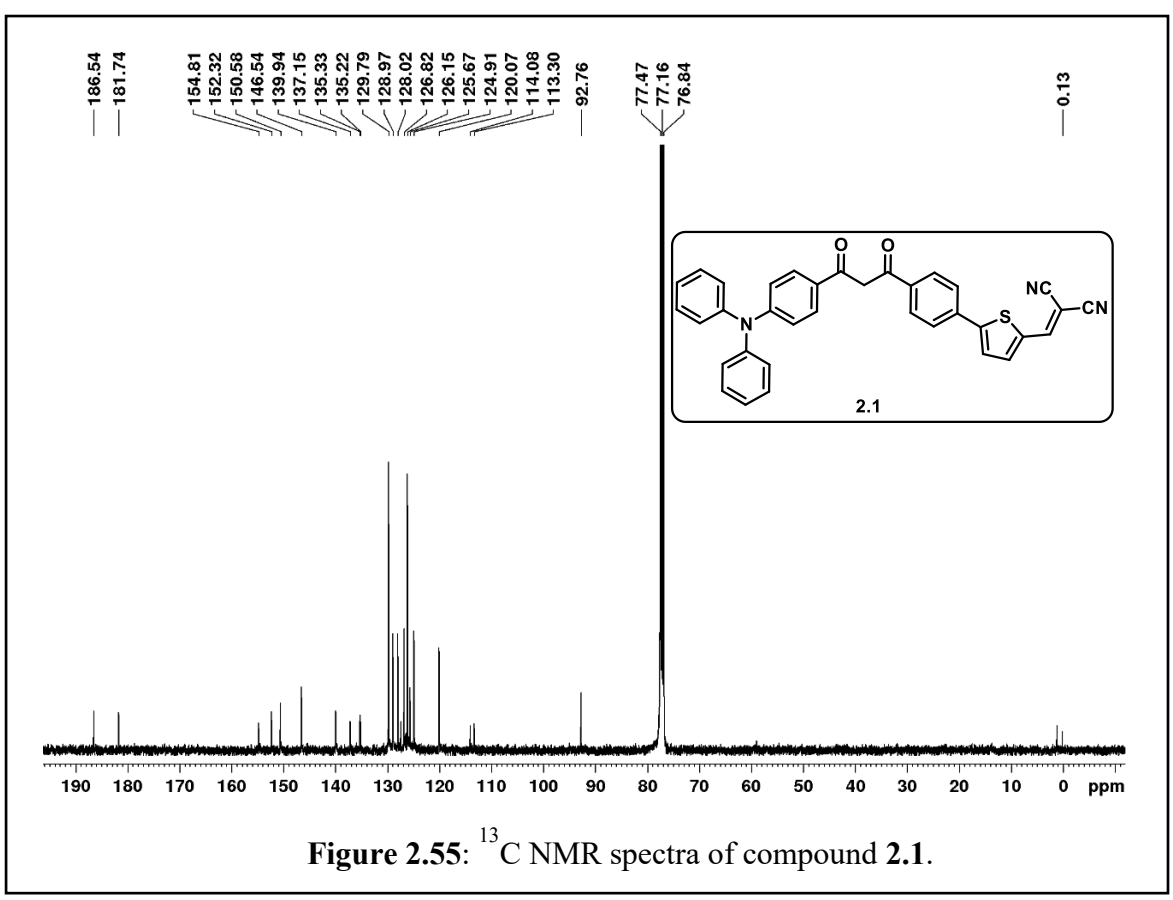


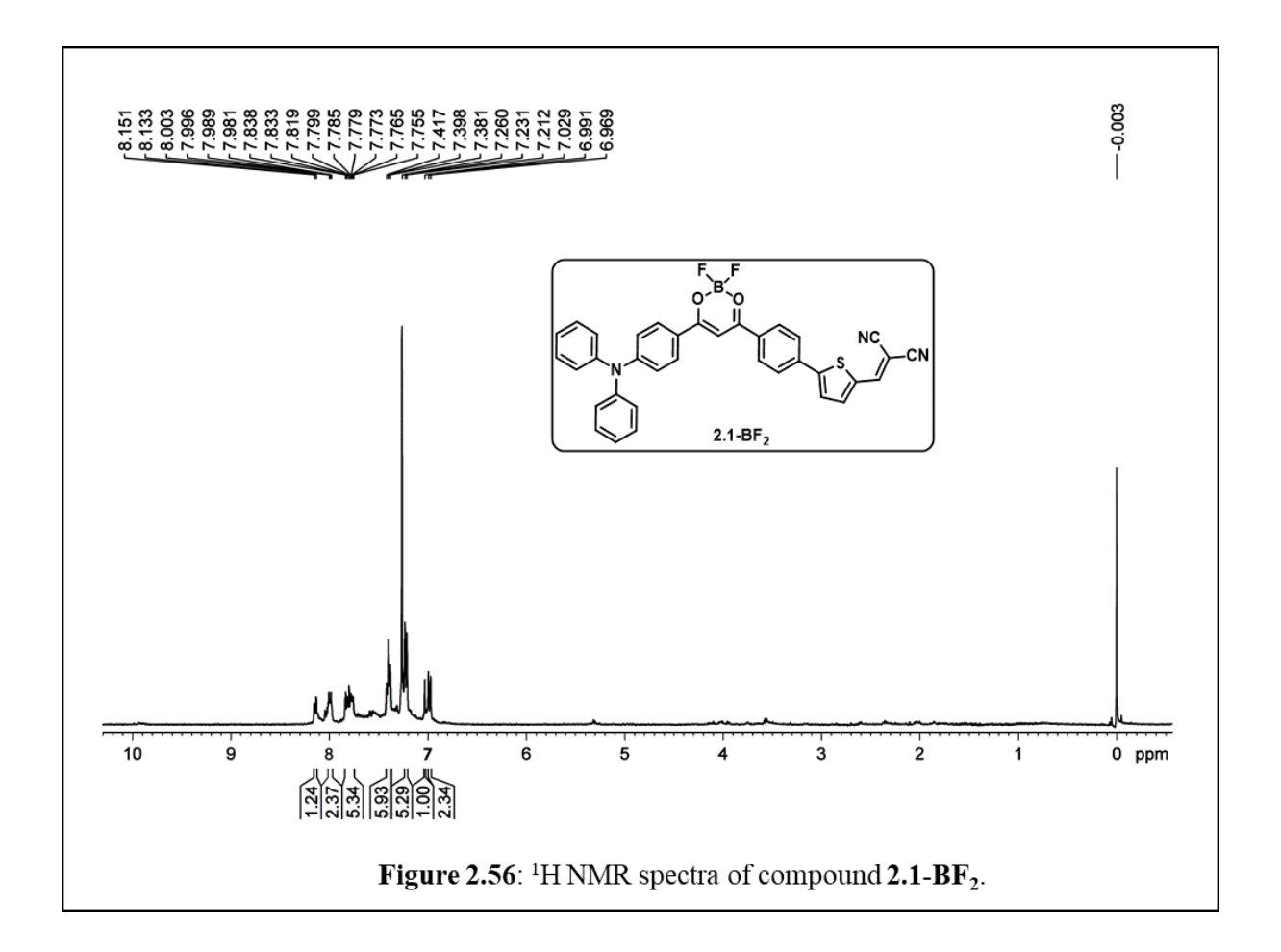


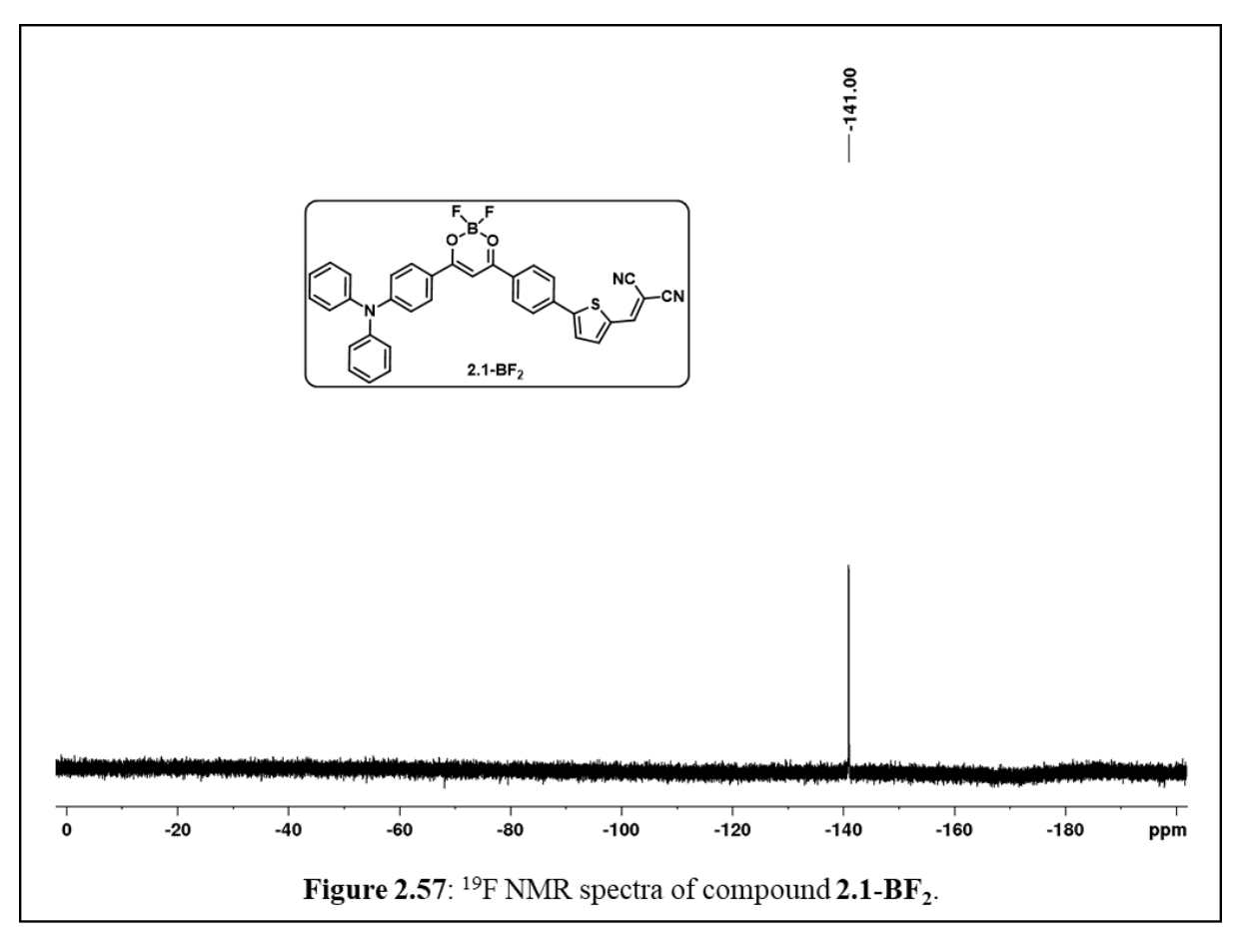


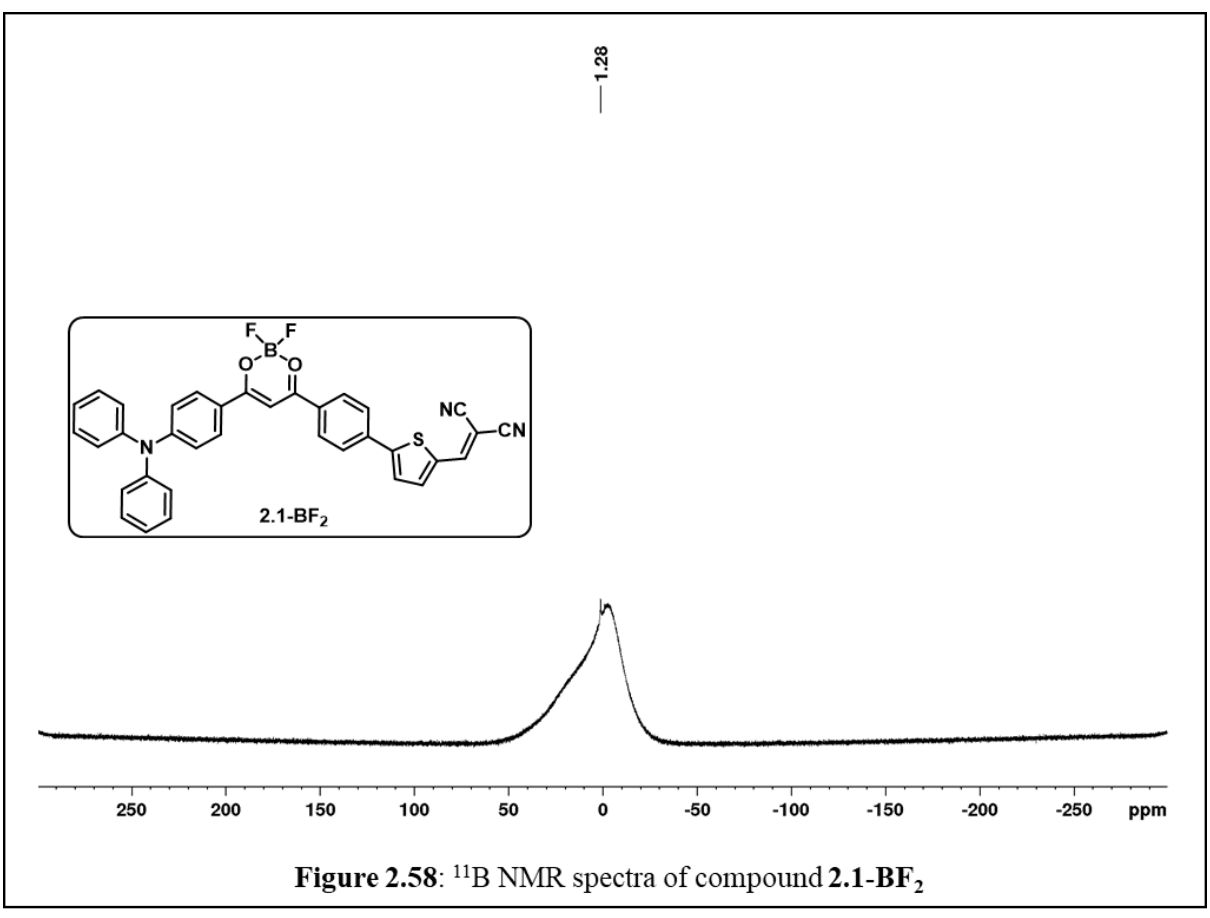


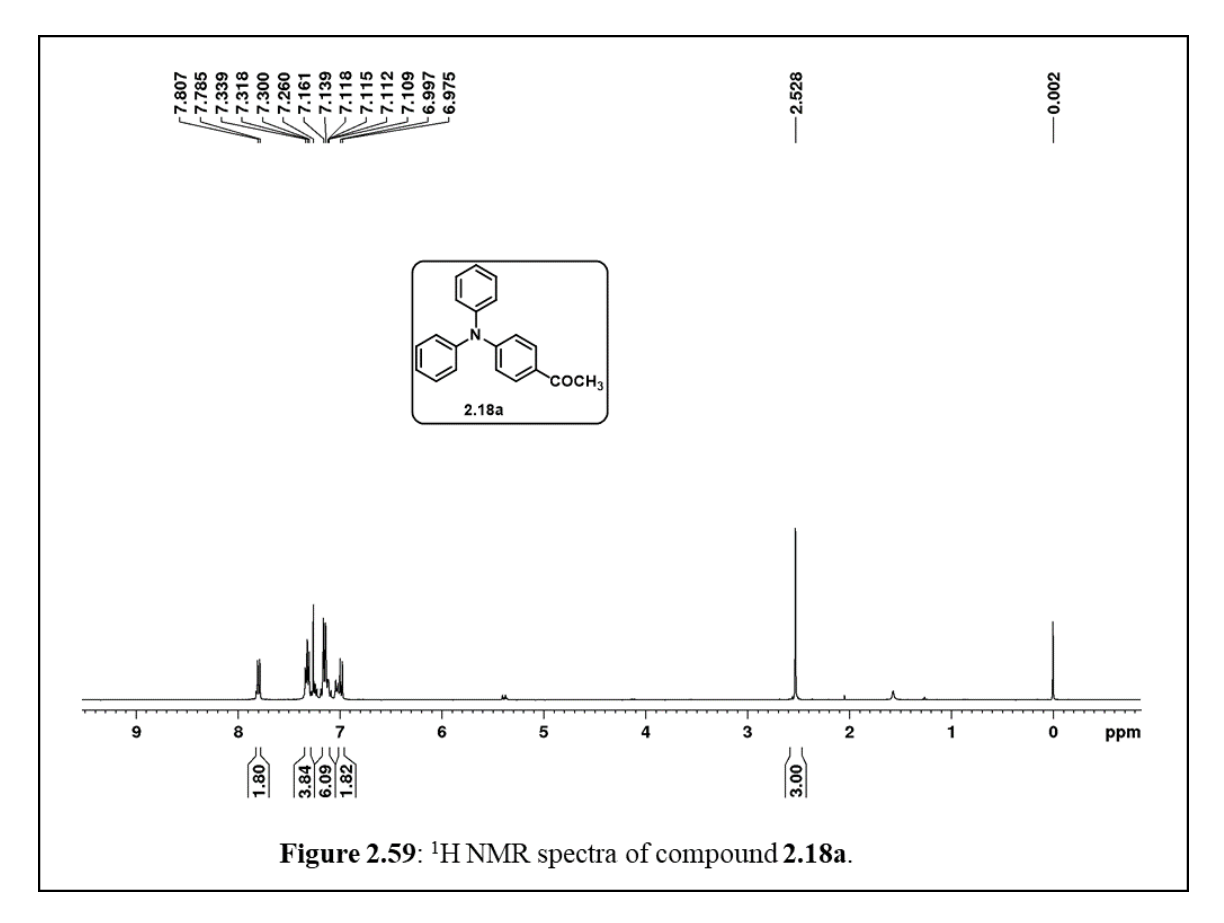


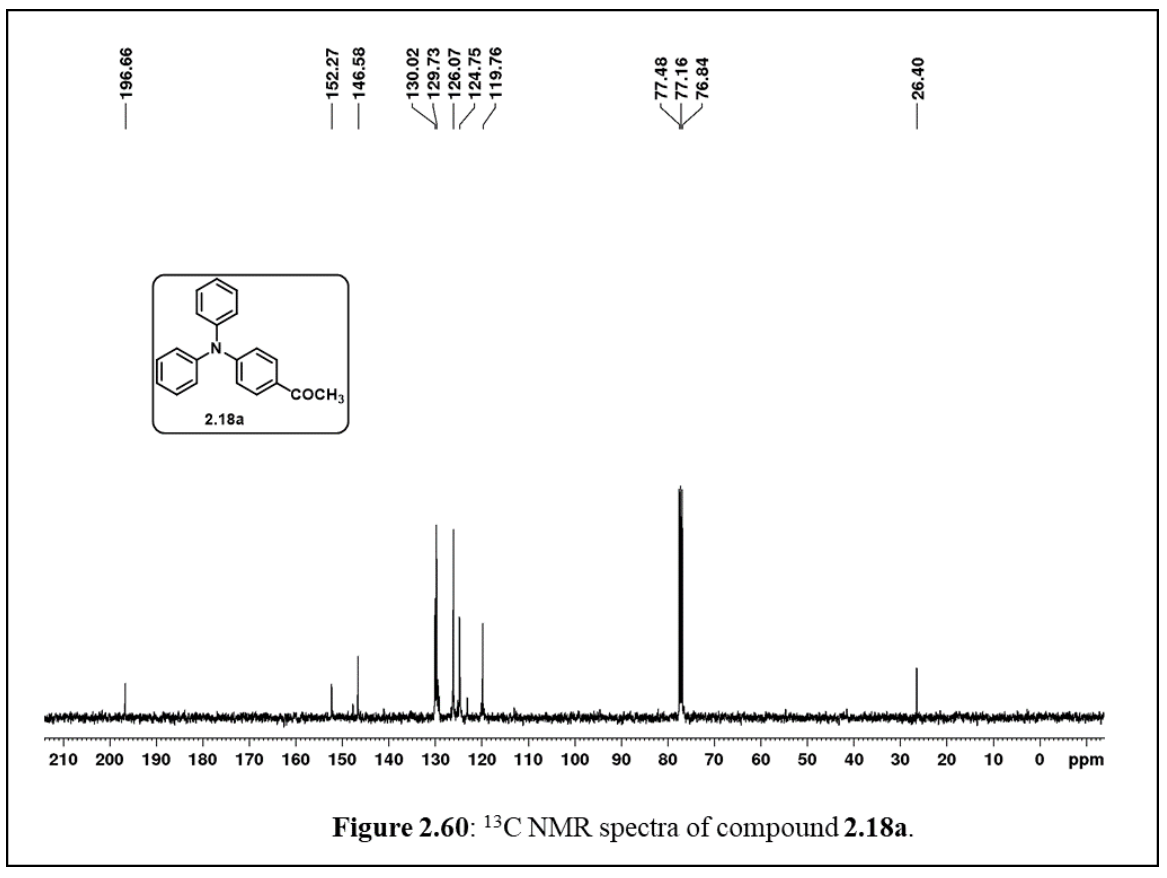


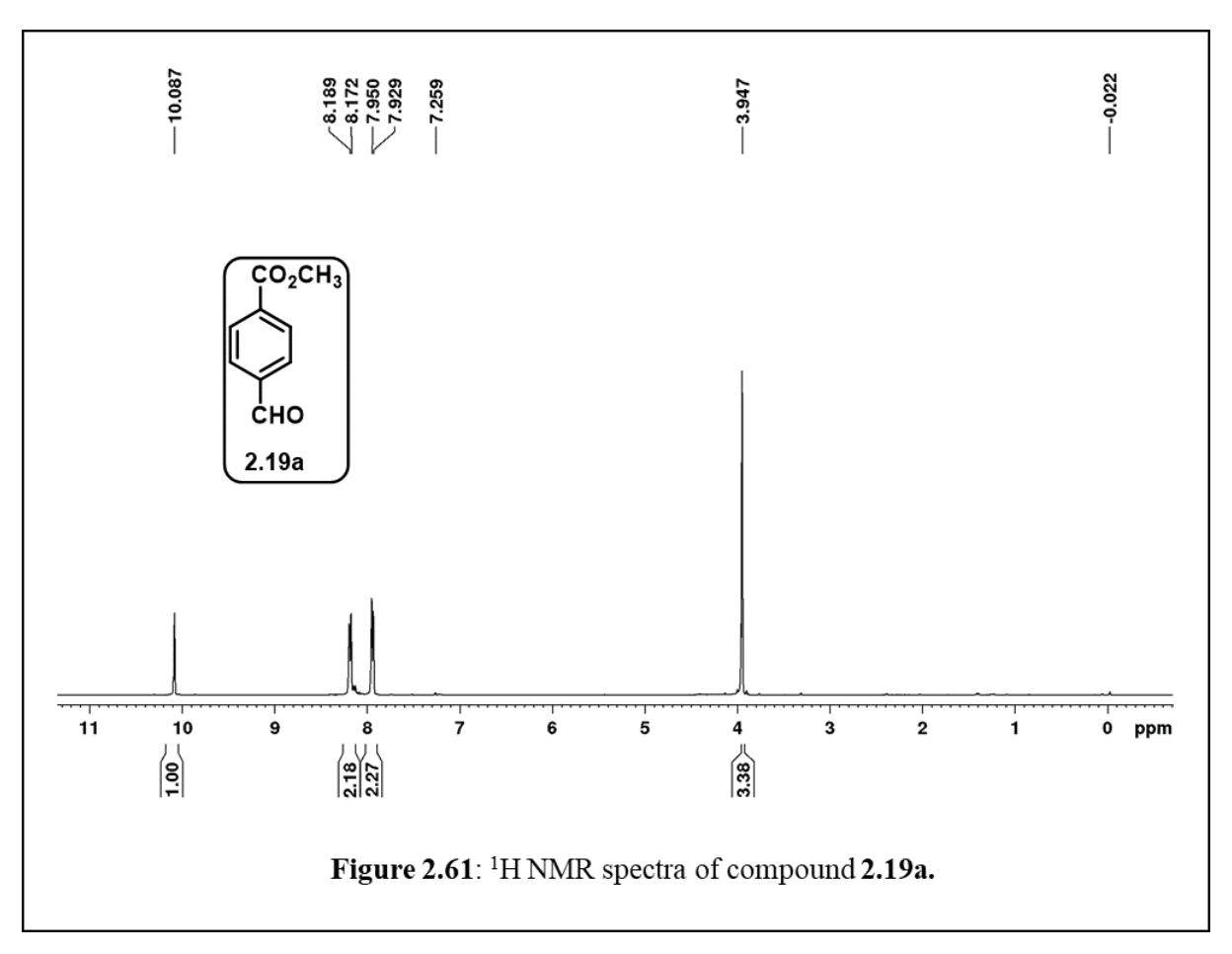


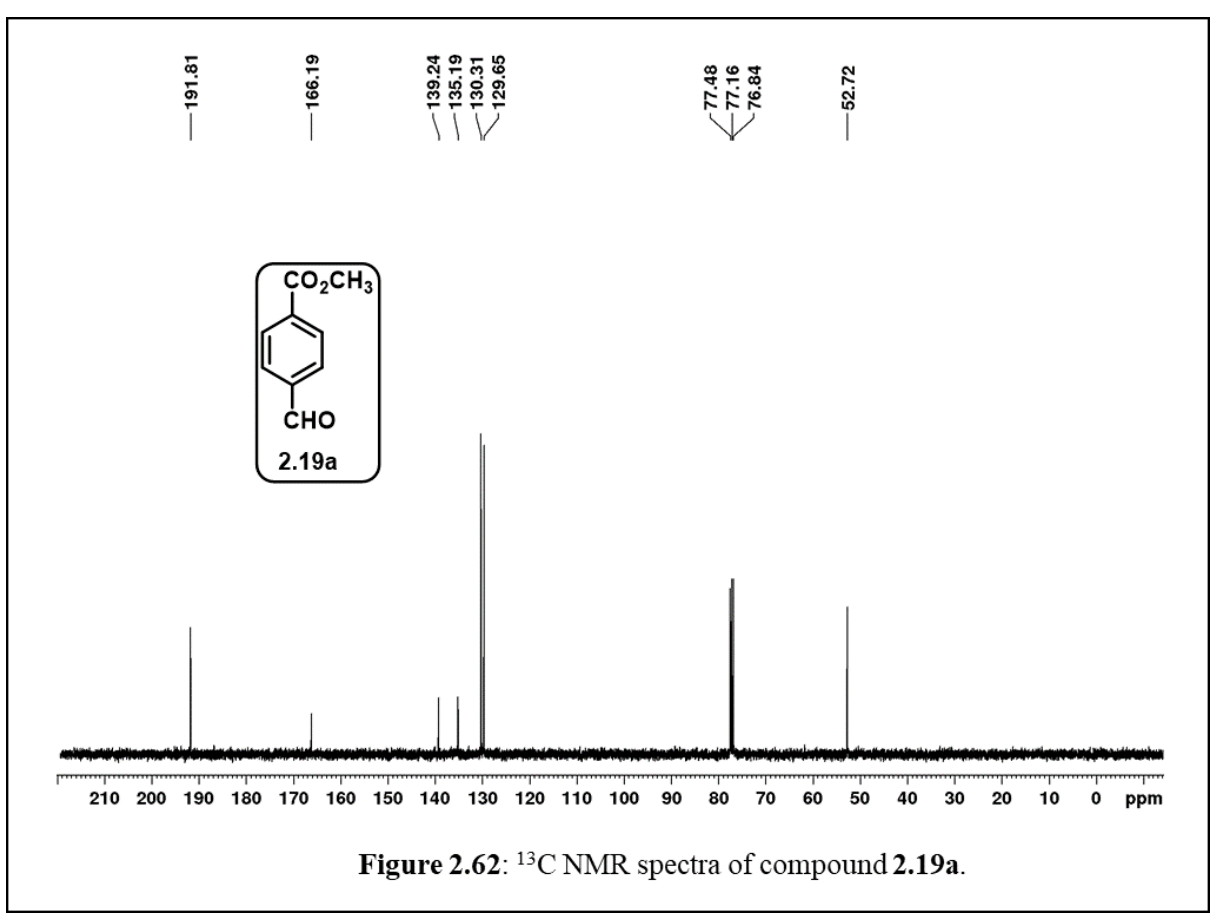


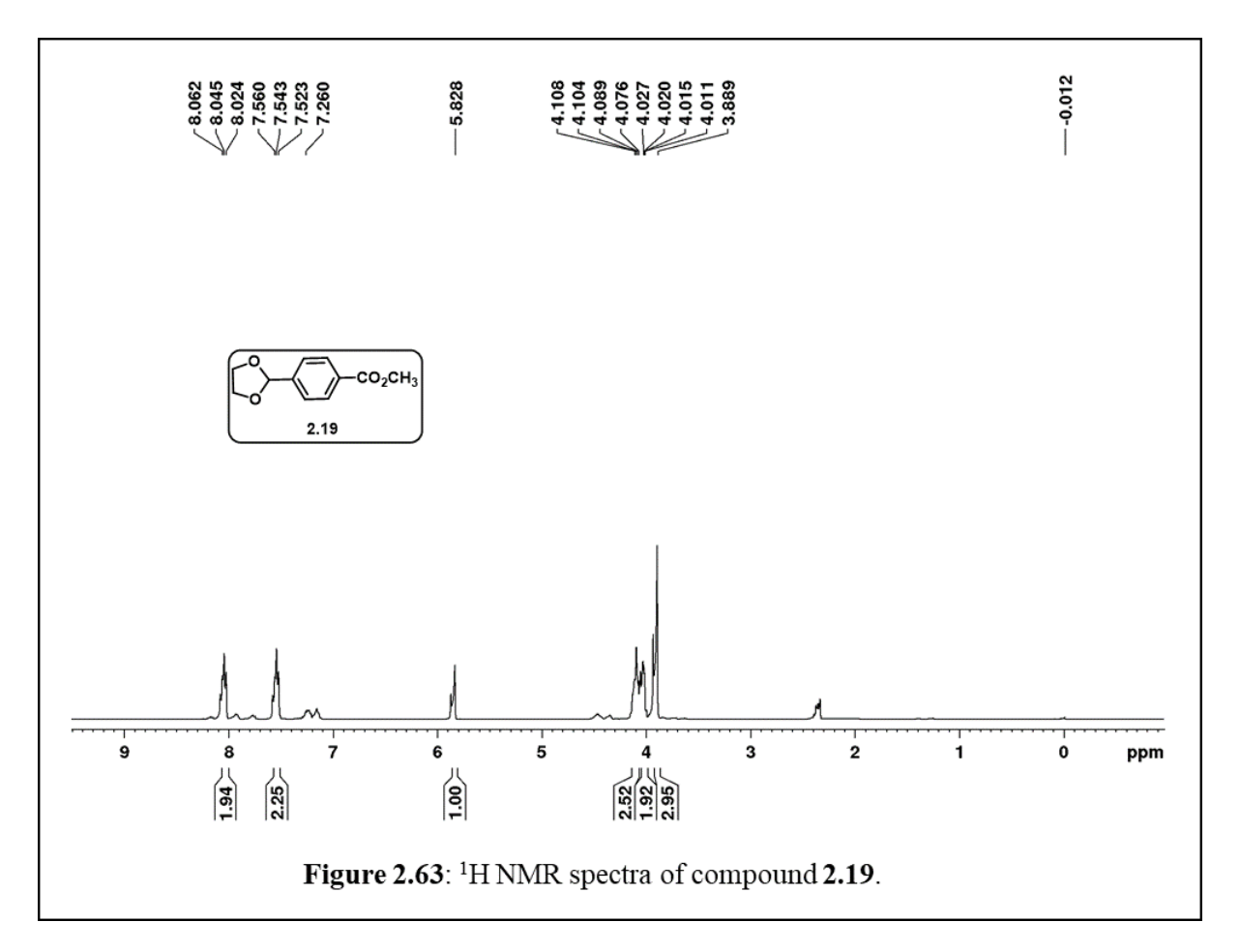


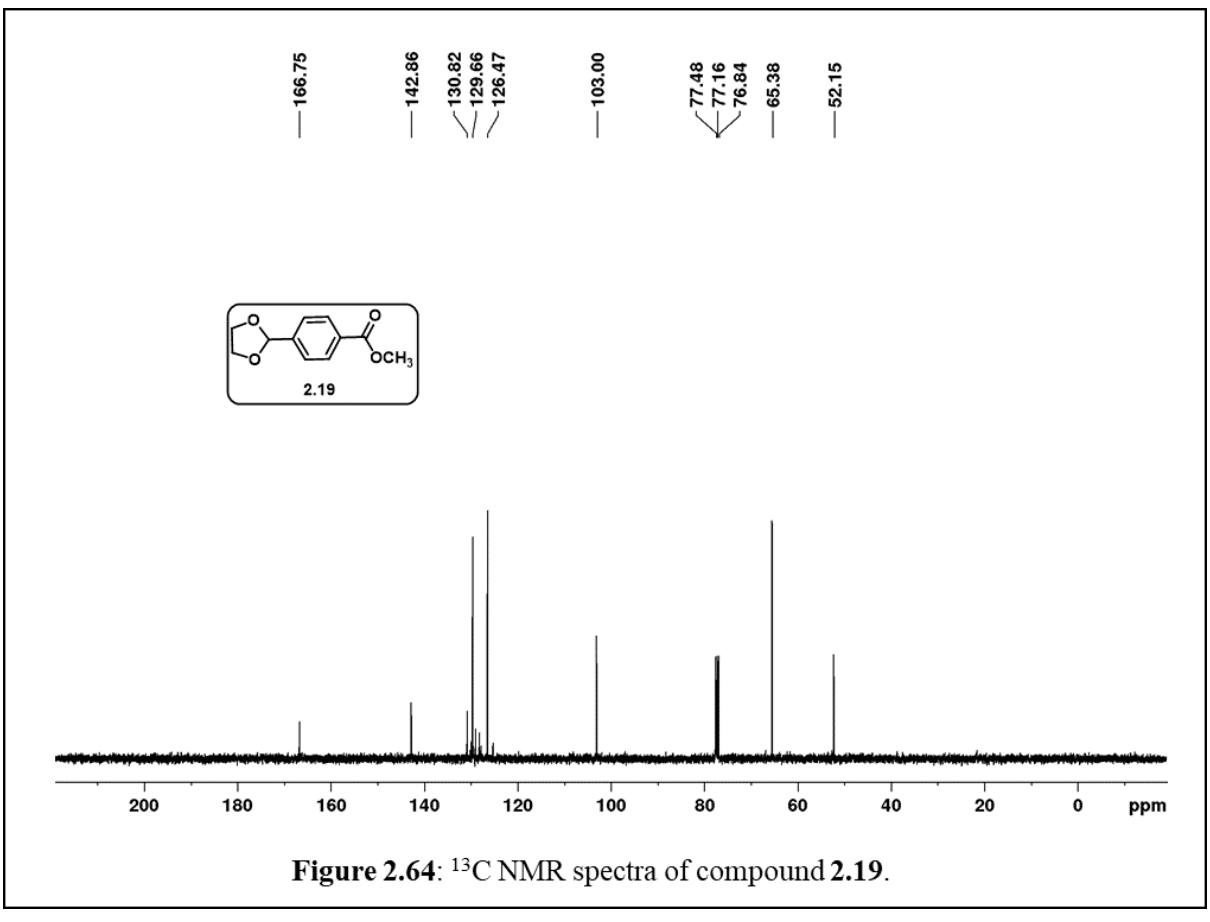


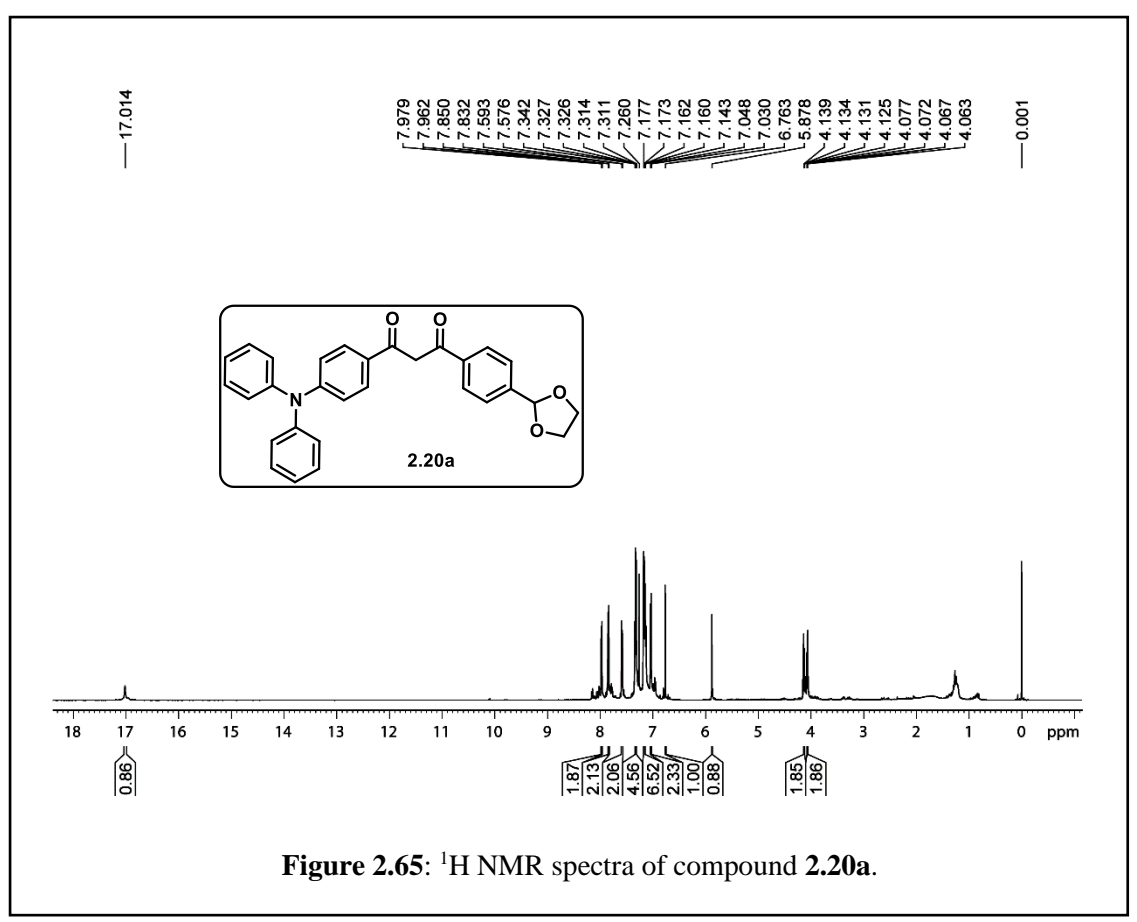


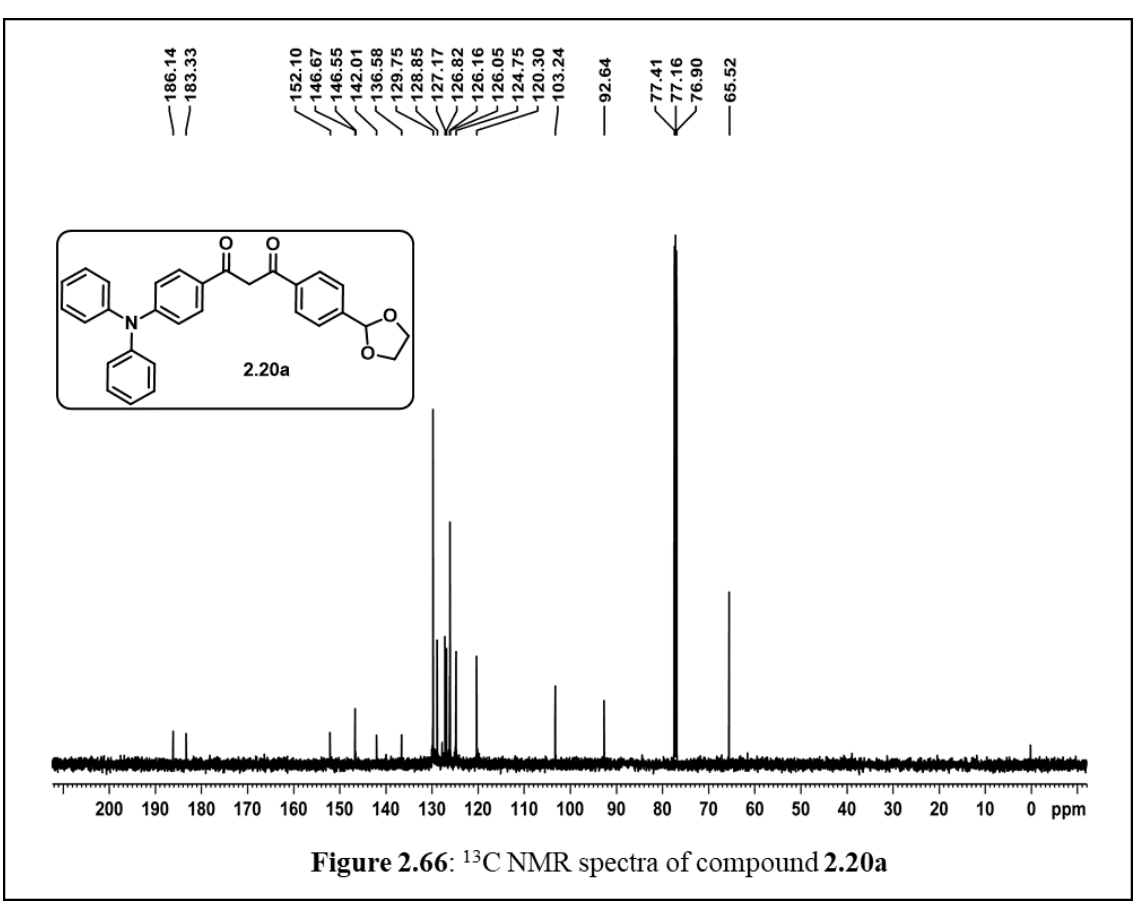


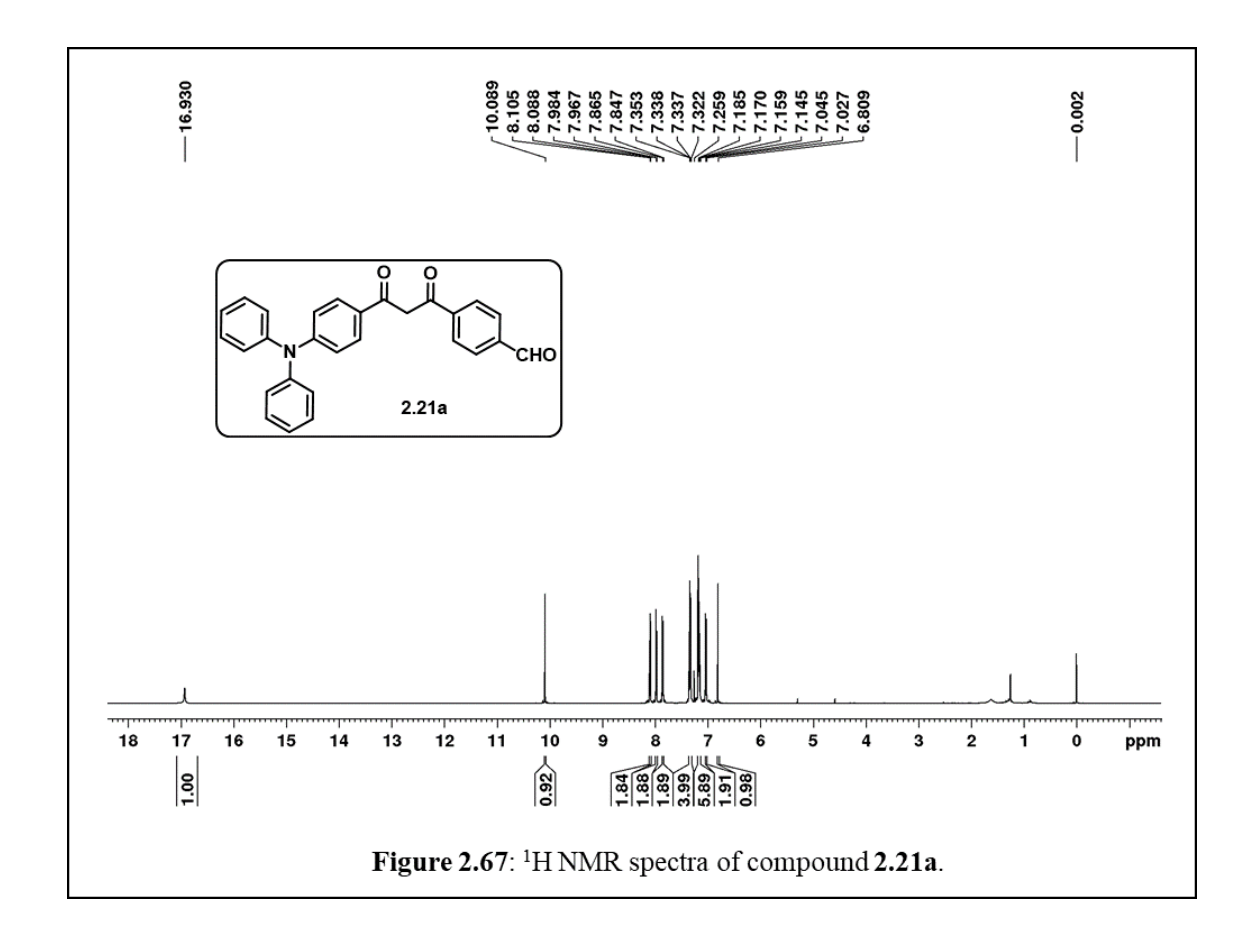


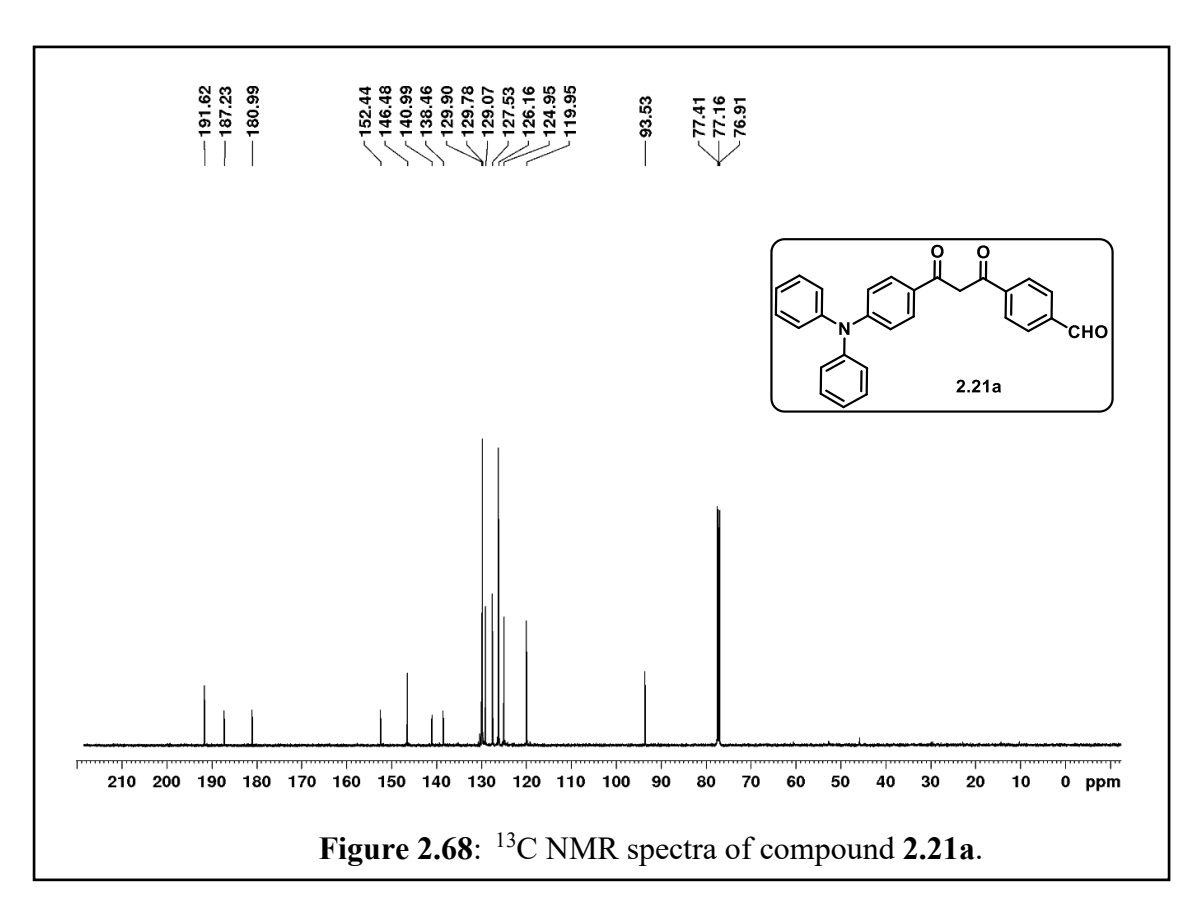


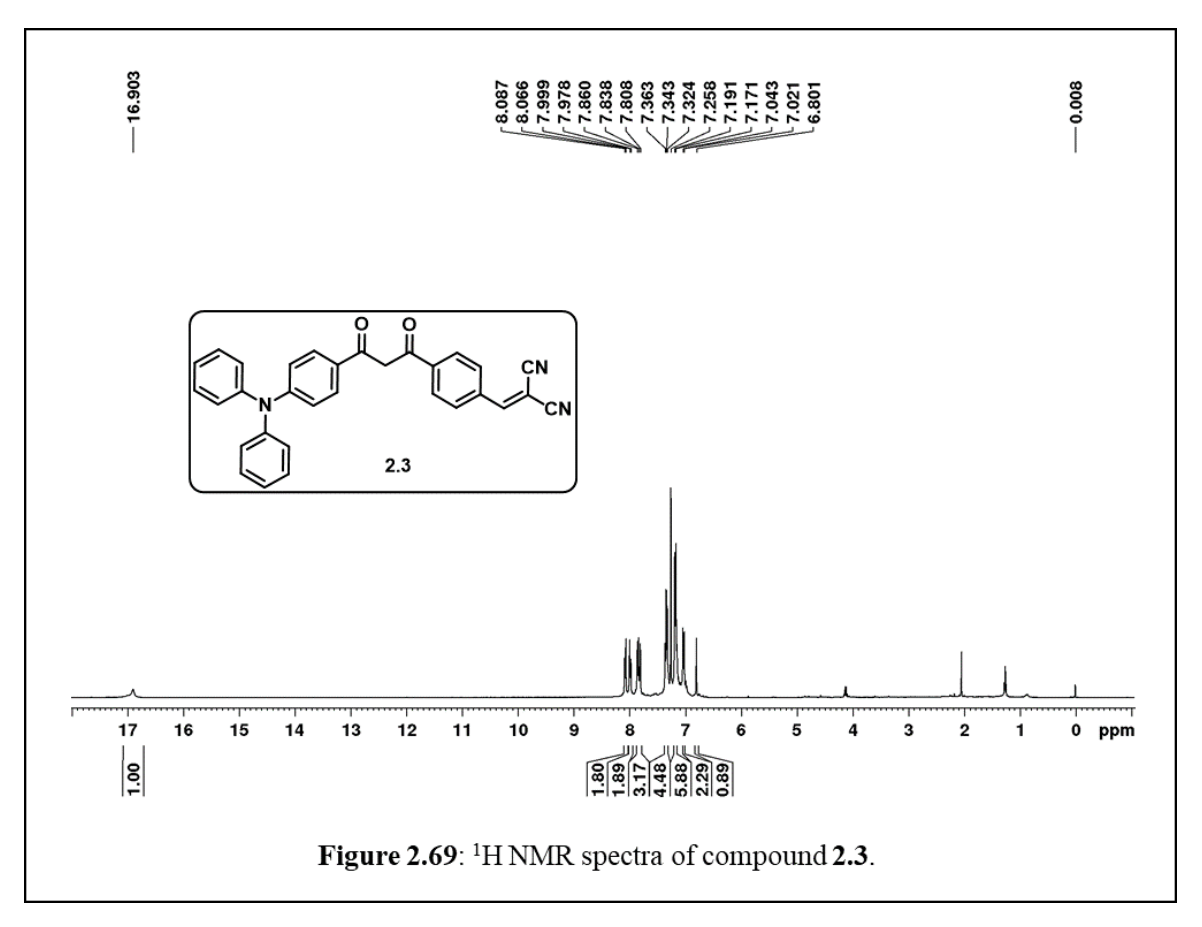


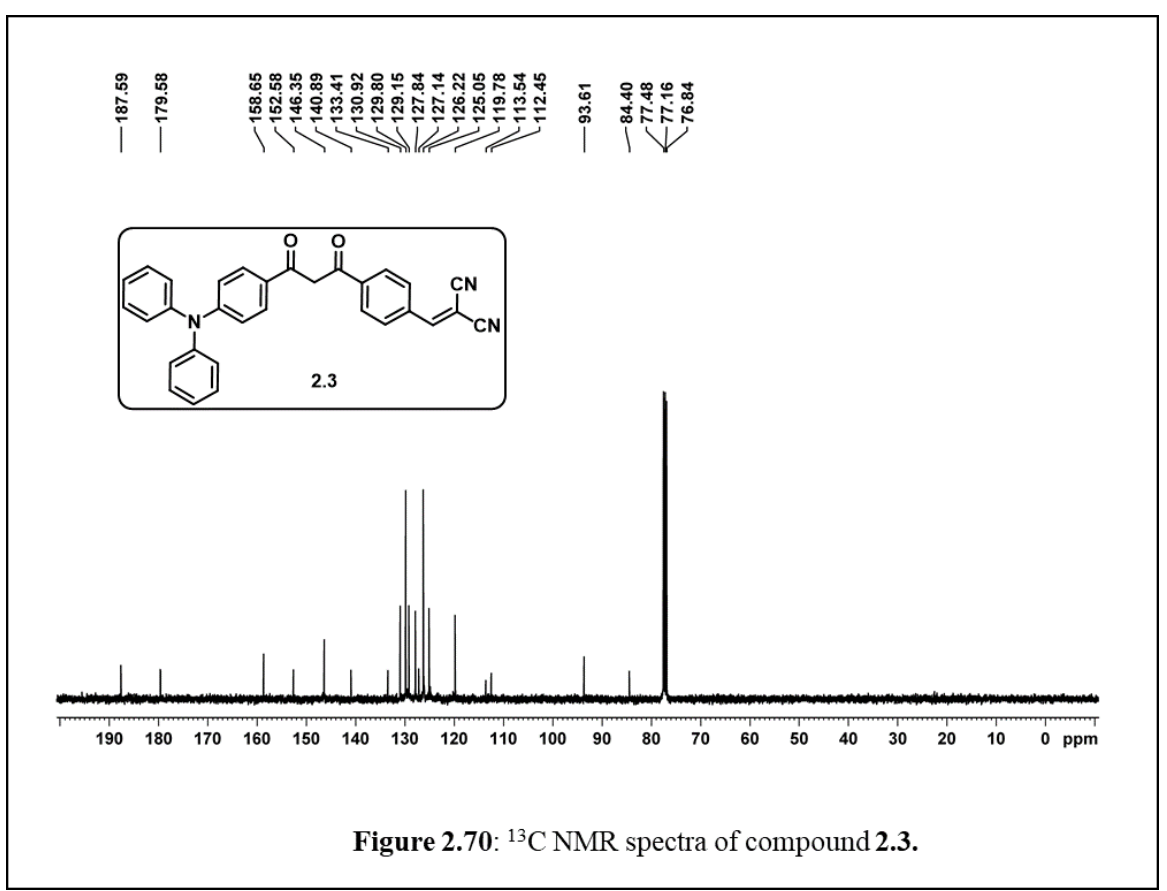


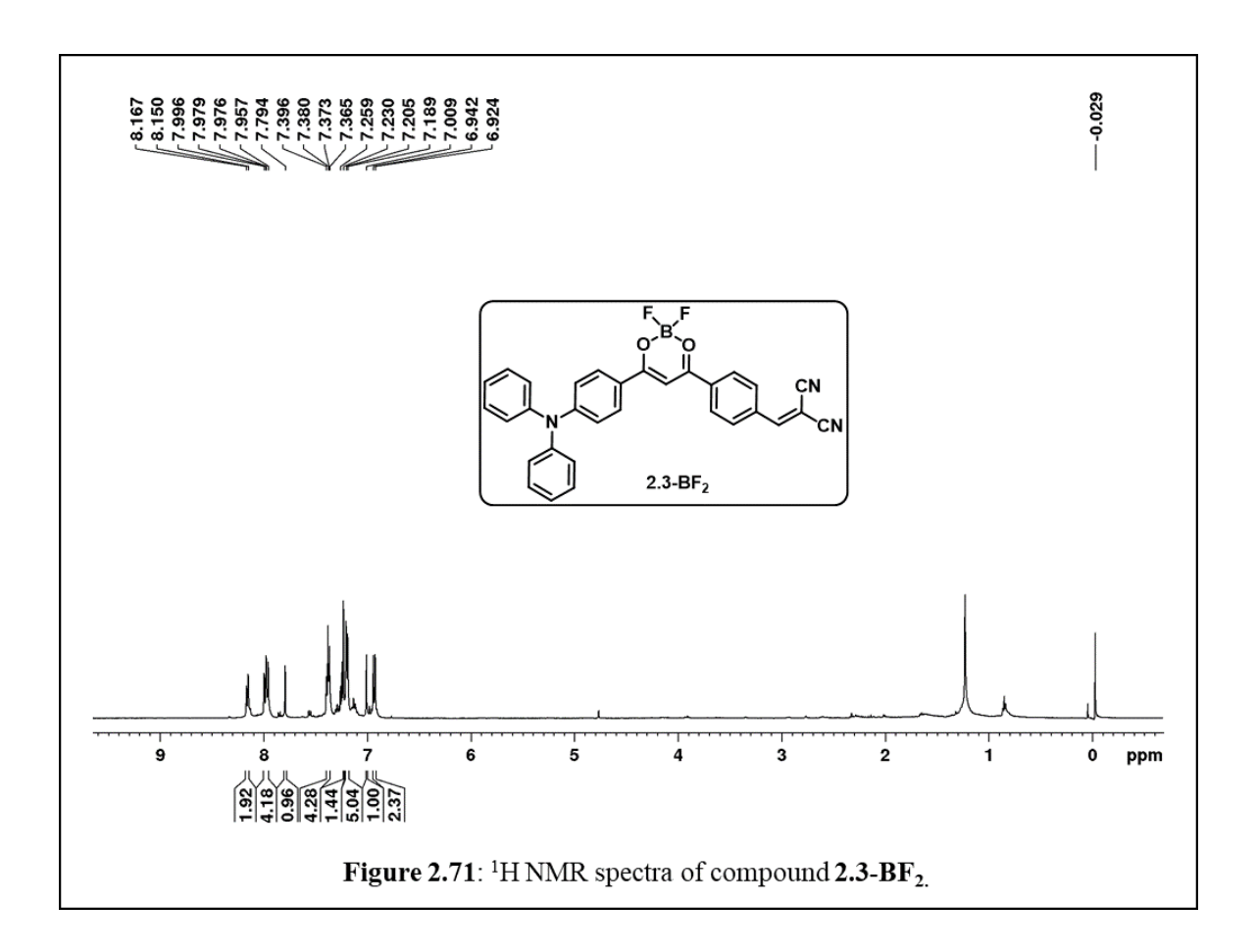


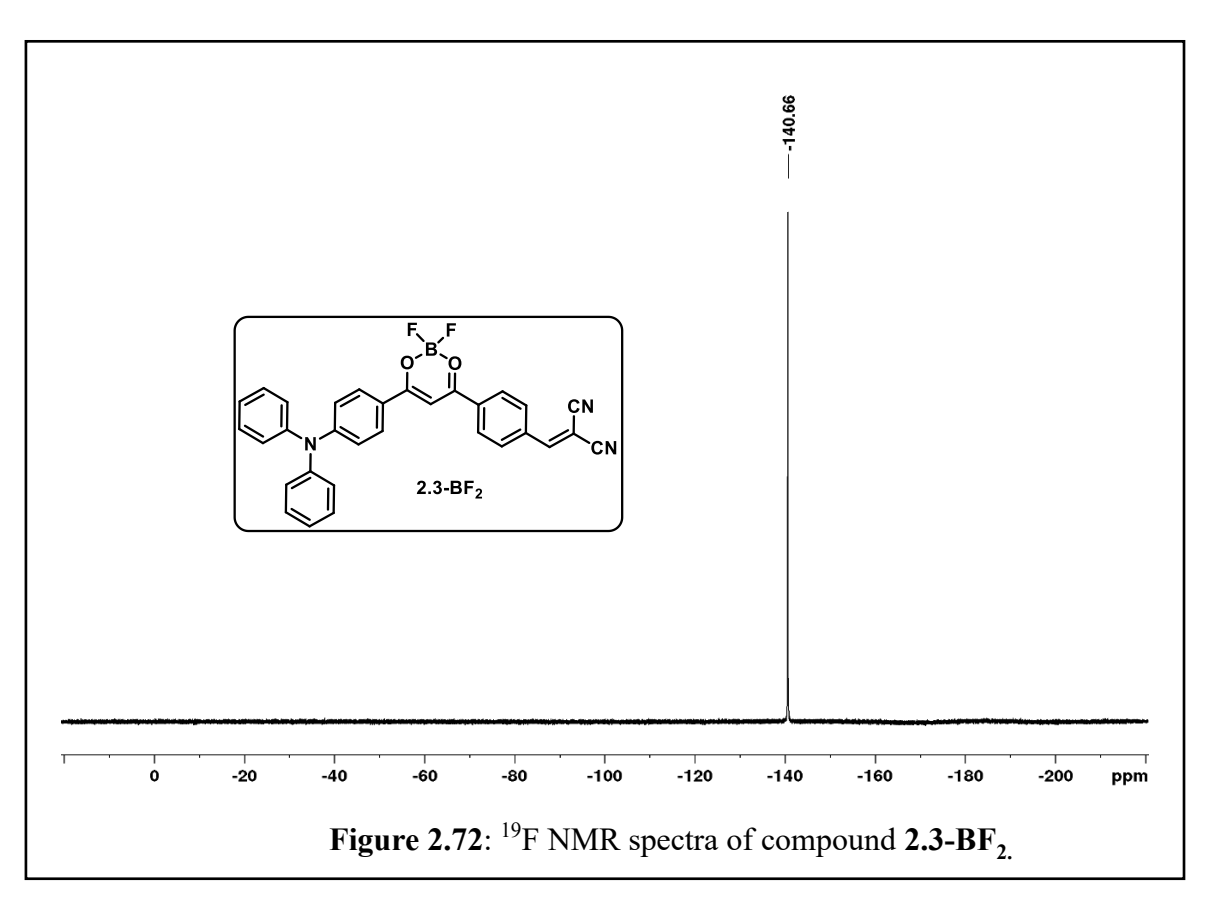


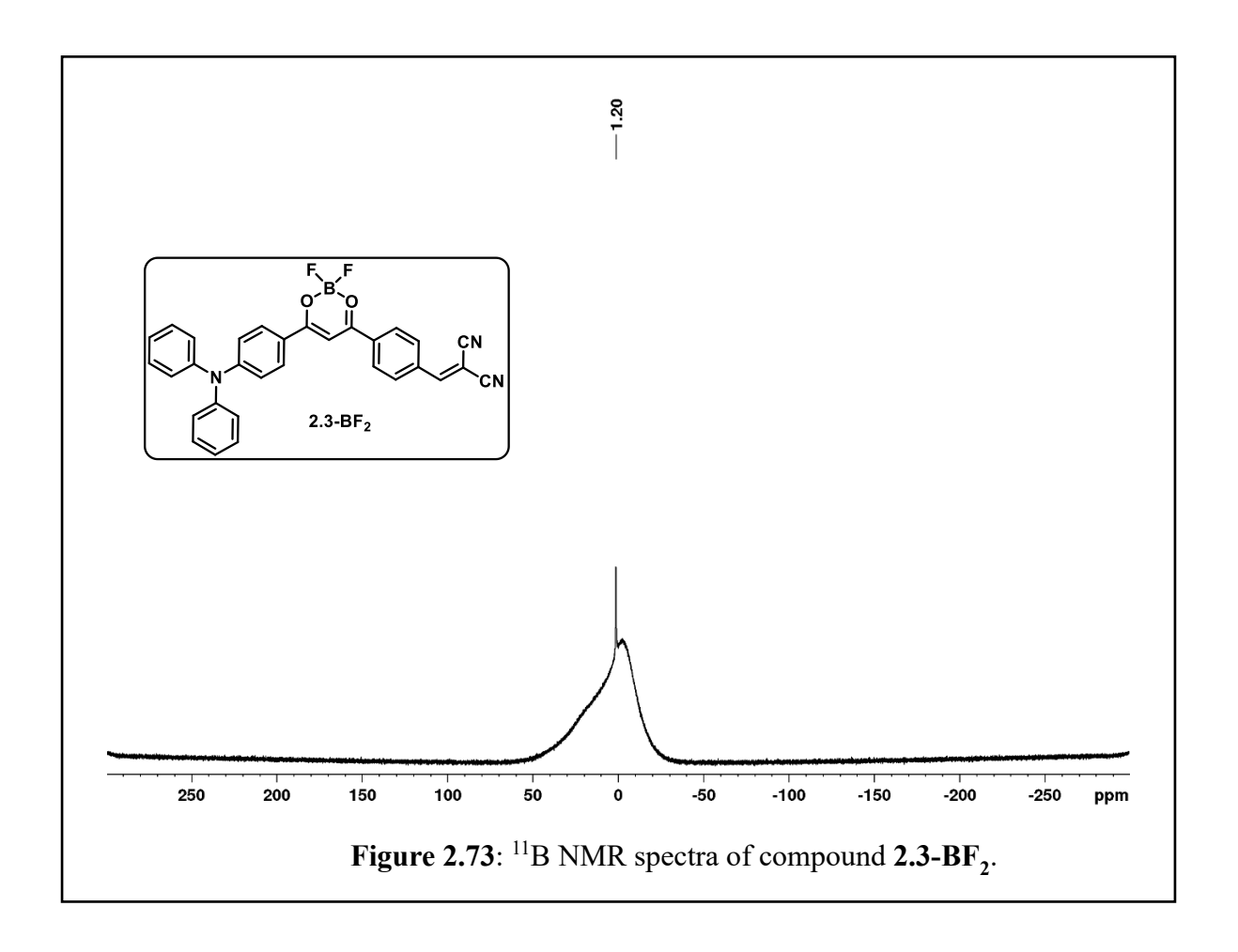


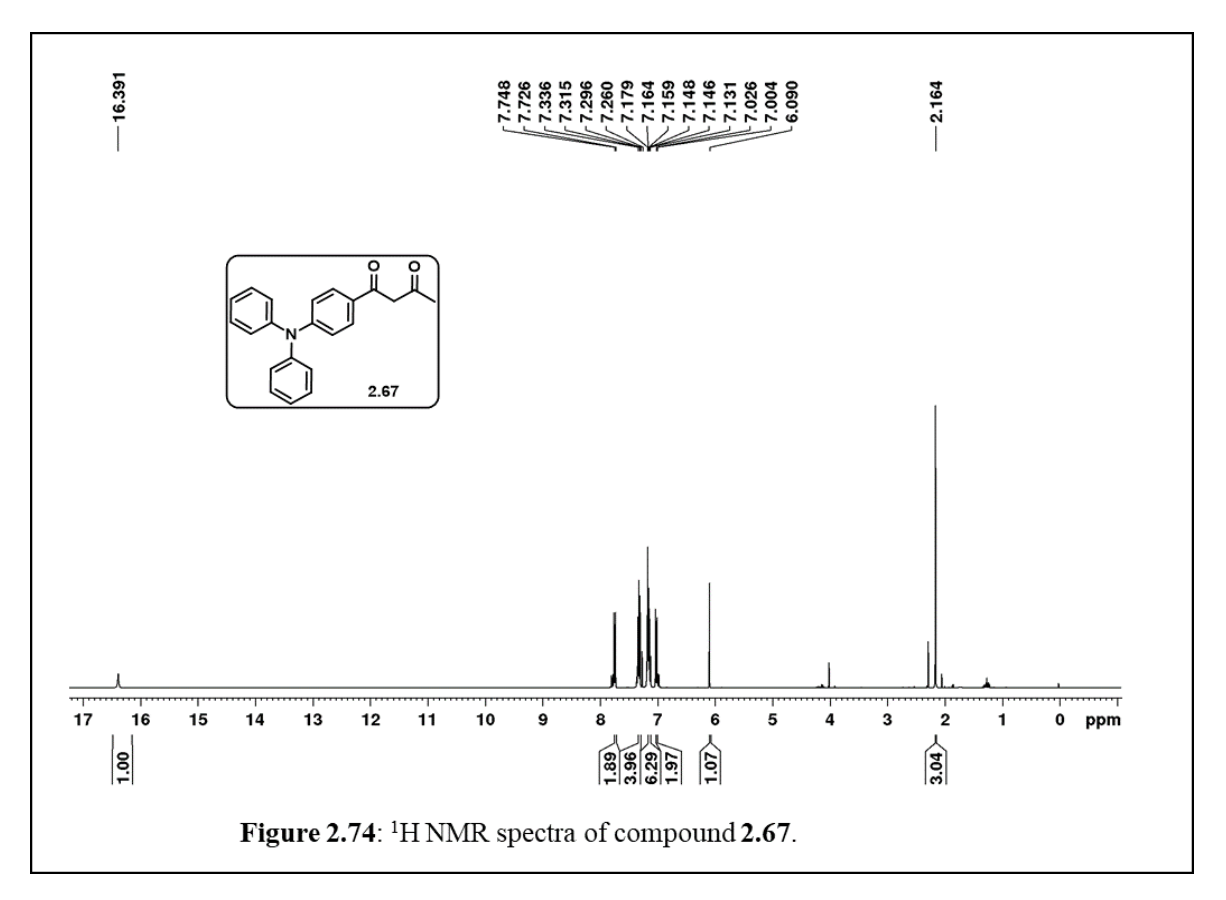


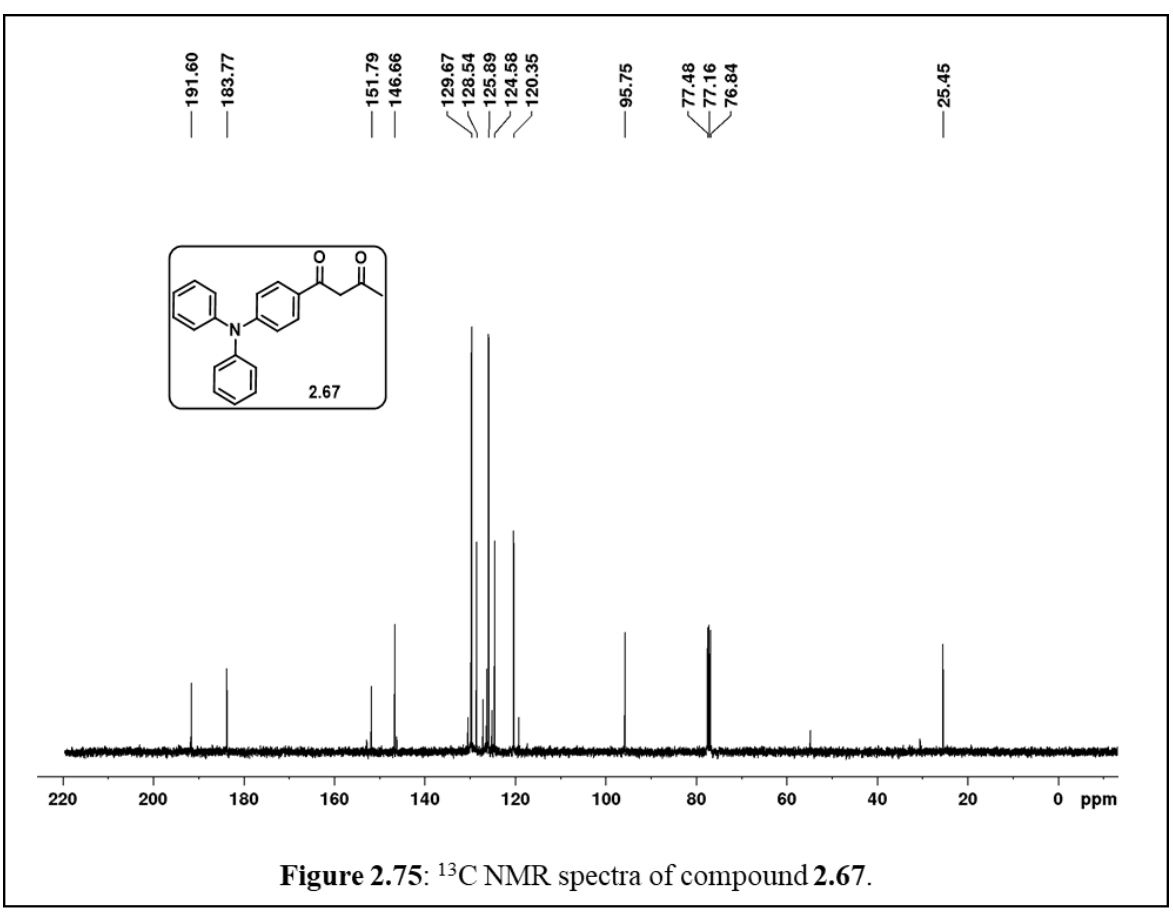


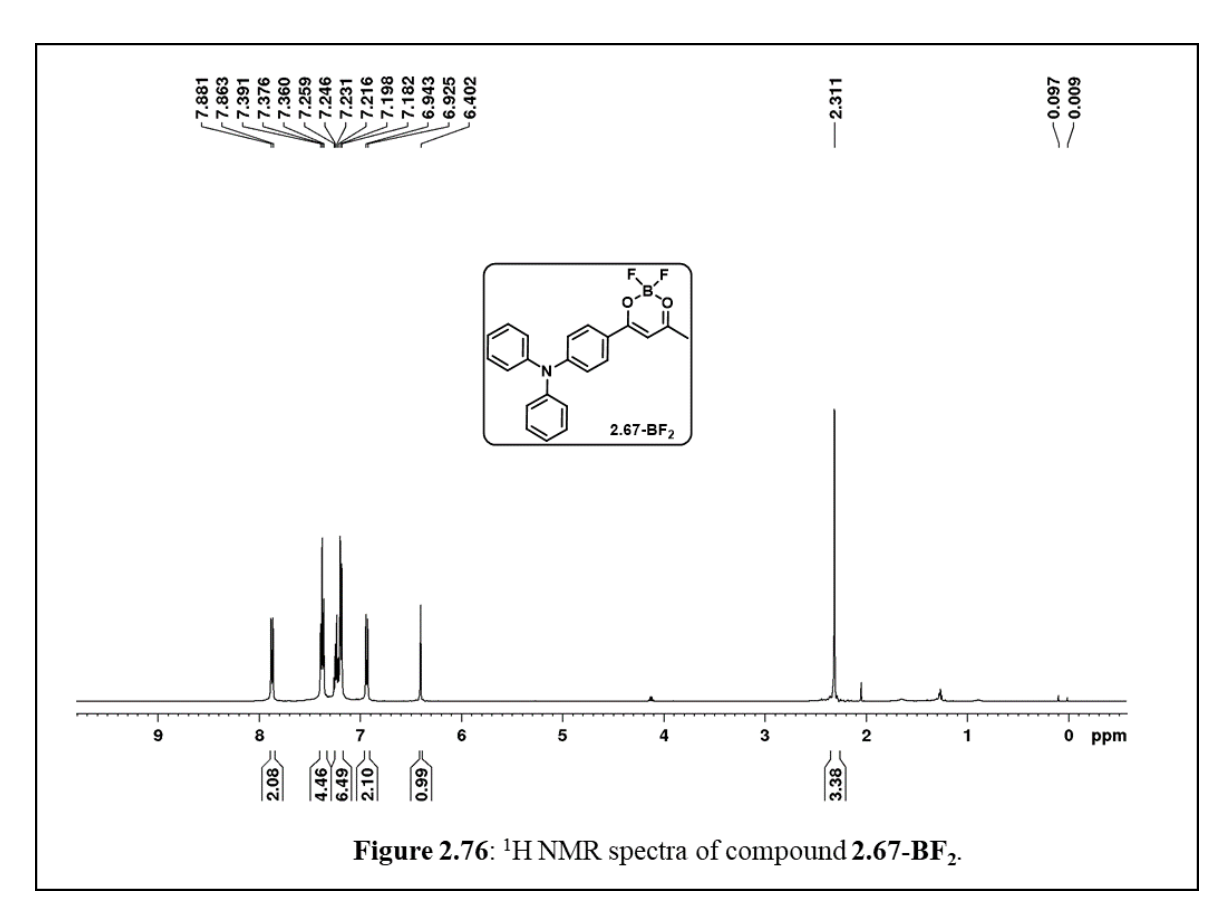


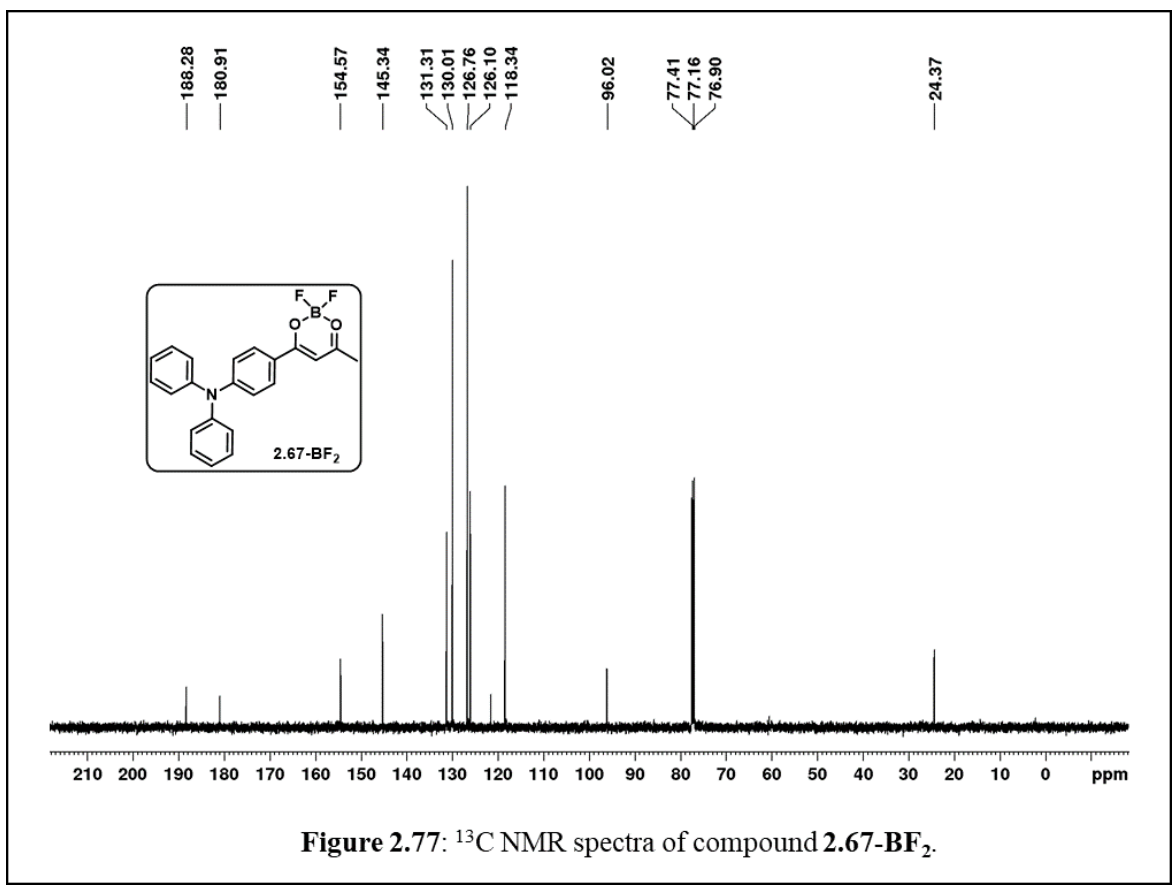


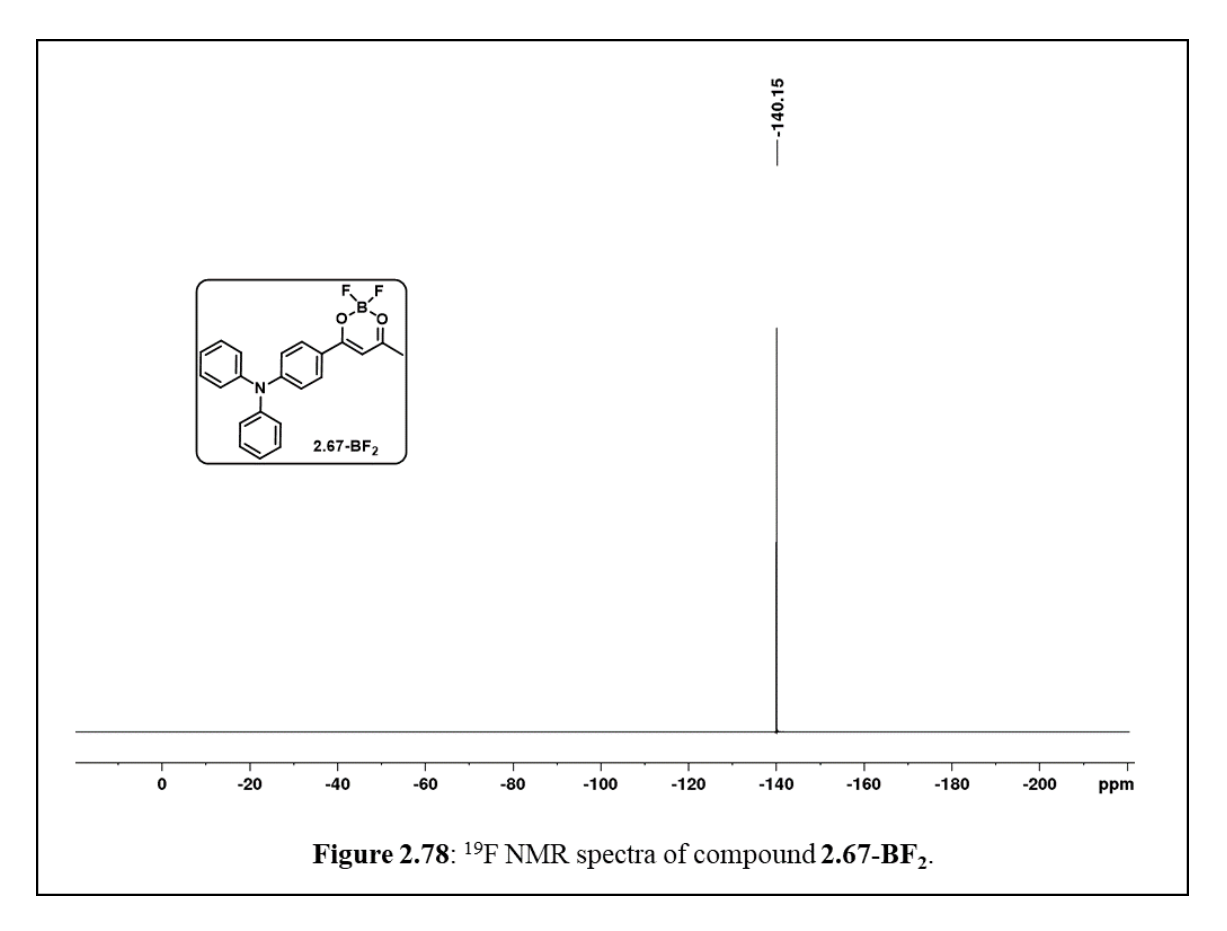


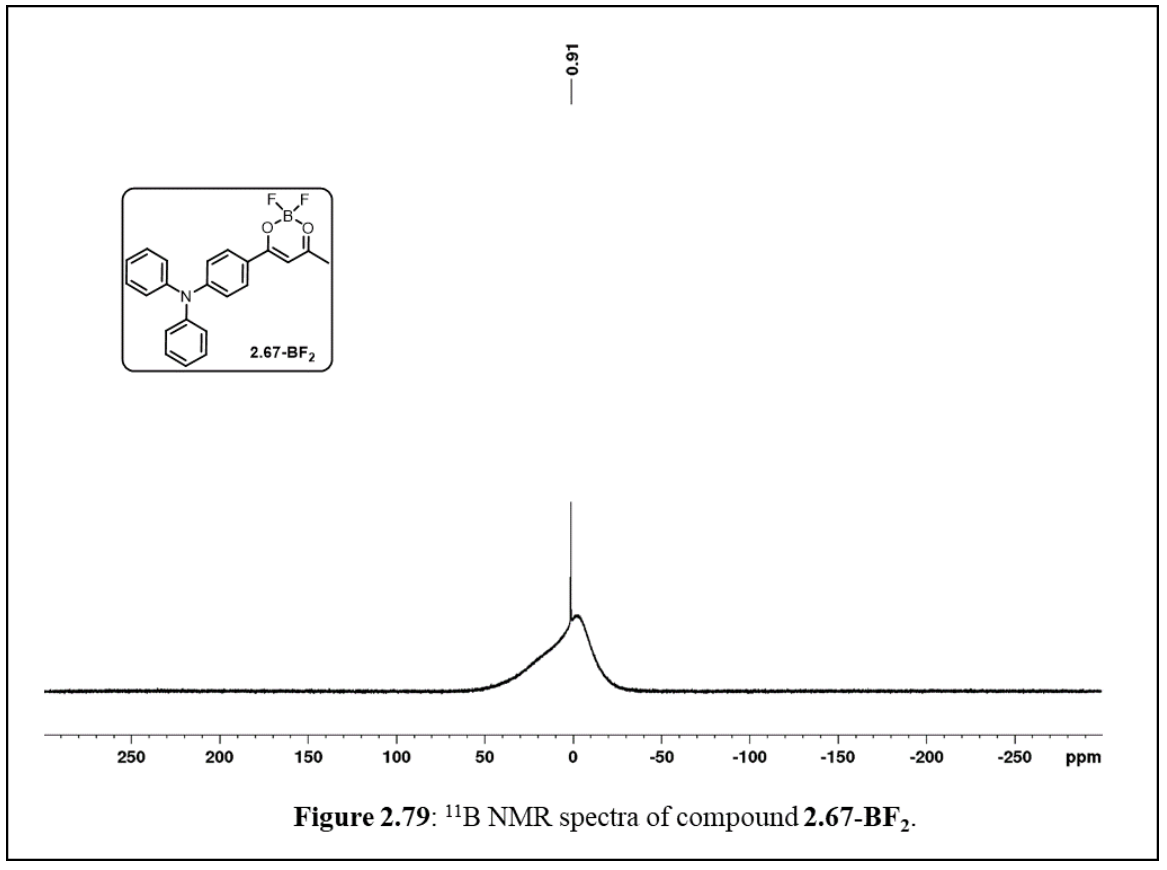












Bis-Donor Incorporated Donor- Acceptor Systems and Their Applications in Bio-Imaging and DSSC

3.1 Introduction

Donor-acceptor systems having more than one donor group expands the potential of the donor-acceptor systems for different applications. In this regard, compounds containing bisdonors have gained interest and find better applications than the corresponding mono donor containing derivatives. First of all, they make the systems to absorb and emit at higher wavelength region, which is good for many applications, especially imaging as many of the biomolecules absorb in lower wavelength region. Some of the multi-donor containing donor-acceptor systems are presented in Figure 3.1. They are mainly applied in imaging, DSSC, OLED, etc.

$$H_3C \qquad CH_3 \qquad COOH$$

$$\eta = 6.8\%$$

$$3.4$$

$$Arakawa and co workers$$

$$Nazeeruddin and co-workers$$

$$\eta = 3.30\%$$

$$3.6$$

$$Park and co-workers$$

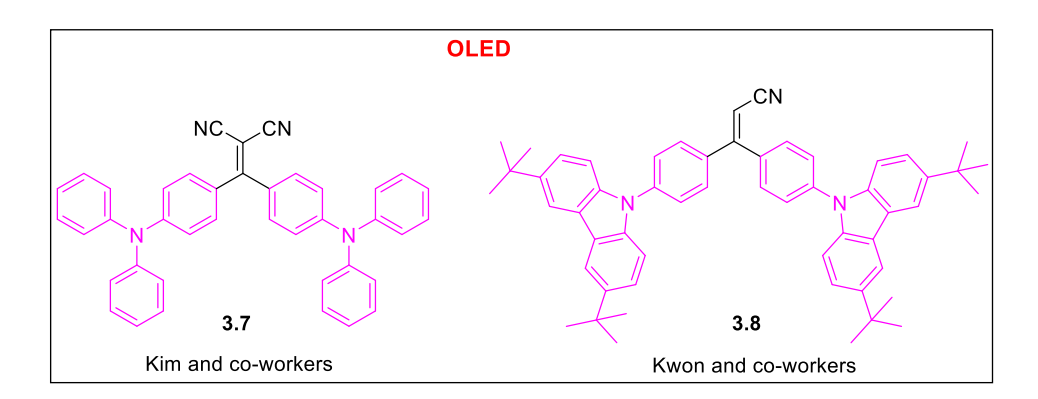


Figure 3.1. Representative donor-acceptor systems having more than one donor units.

Lee and co-workers^{1a} have reported carbazole based donor-acceptor systems based on **3.1** for live-cell imaging applications. These organic dyes have been tested for their cytotoxicity and used for the bio-imaging of A549 and HeLa cancer cell lines. Zhou *et al.*^{1b} have designed triazine containing triphenylamine derivatives **3.2** having one, two, and three branches with two-photon absorption charateristics for the bio-imaging of HeLa and HCF-7 cancer cells. Qian and co-workers^{1c} have developed donor-acceptor based on triphenylamine connected to two

alkyl-substituted carbazoles and BODIPY unit **3.3**. These dyes exhibited AIEE properties and were applied for live-cell imaging of MCF-7 cancer cell lines.

In 2003, Arakawa and co-workers^{2a} reported diene or triene linked bis-donor acceptors showing applications in dye-sensitized solar cells. The dye **3.4** generated a maximum power conversion efficiency of 6.8%. Nazeeruddin and co-workers^{2b} have reported methoxy substituted triphenylamine containing bis-donor acceptor system **3.5** for dye-sensitized solar cell applications. This particular dye produced a PCE of 7.03%. Park and co-workers ^{2c} reported a D-A system based on quinoxaline acceptor linked bistriphenylamine unit **3.6** and attained a maximum power conversion efficiency of 3.30%.

Kim and co-workers^{3a} reported triphenylamine derivatives having malononitrile acceptor **3.7** for thermally activated delayed fluorescent emitter which find application in the field of organic light-emitting diodes (OLEDs). Also, Kwon and co-workers^{3b} have developed a set of donor-acceptor systems for organic light-emitting diodes (OLEDs) applications. Acceptors such as malanonitrile and acrylonitrile in combination with phenoxazine, dimethylacridine, and tert-butylcarbazole donors were tested. One of the compounds, **3.8** is shown in Figure 3.1.

From the experience that we gained during the microtubules imaging application using 1,3-dicarbonyl-bridged donor-acceptor systems, we thought that the aryl rings attached to the 1,3-dicarbonyl moiety is responsible for the selective binding with microtubules. Similar rigid structural feature is present in combretastatin which binds to colchicin binding site of microtubule. Combretastatin is a cis-stilbene derivative having the aryl groups oriented in the same direction. In this regard, we designed a couple of donor-acceptor systems having the aryl groups rigidly oriented in the same direction (Figure 3.2). Another reason is that these compounds are relatively simpler and easier to make in high yields.

Figure 3.2. Design of bis-donor containing D-A systems

3.2 Synthesis of the Bis-Donor Containing Donor-Acceptor Systems

The designed bis-donor containing donor-acceptor systems 3.11 and 3.12 were synthesized following the Scheme 3.1. The synthesis starts with the addition of corresponding lithiated aryl compound 3.13 and 3.14 on p-(diphenylamino)benzaldehyde 3.15 and pcarbazoloylbenzaldehyde 3.16 ^{4,5} to make the respective diarylmethanols 3.17 and 3.18. The secondary alcohols were found to be unstable at room temperature. However, they were stable for a few days at below -5 °C. We tried to synthesize some more derivatives having hexyloxy groups incorporated into the triphenylamine moiety. Unfortunately, it has been found to be highly unstable under the lithiation reaction conditions. These diarylmethanols were oxidized to the corresponding ketone derivatives 3.19 and 3.20 using IBX. Initially, the oxidation reaction was attempted with MnO₂. Unfortunately, it resulted in poor yield of the desired product even when 20 equivalents of MnO₂ was used. The diaryl ketones **3.19** and **3.20** were treated with TiCl₄ and Et₃N separately to make the α,β -unsaturated aldehydes 3.21 and 3.22 respectively. 6a This reaction progress through the formation of an iminium ion followed by metalation which eventually results in the α,β -unsaturated aldehyde. These compounds upon Knoevenagel reaction with cyanoacetic acid separately in the presence of piperidine resulted in the desired probes 3.11 and 3.12.6b, 6c While the compound 3.11 is red the compound 3.12 is yellowish red in color.

Scheme 3.1. Synthetic route of bis-donor based donor-acceptor systems.

The final compounds were characterized by various spectroscopic analysis. The molecular structure of compound **3.11** was confirmed by single crystal X-ray diffraction analysis (Figure 3.3). Single crystals of **3.11** were grown in toluene solvent at room temperature. The X-ray diffraction of **3.11** shows a monoclinic primitive lattice with a space group P 21/n and unit cell dimensions of a = 14.3812(16) Å, b = 16.947(2) Å, c = 27.654(4) Å, α = 90, β = 103.394(6), and γ = 90. The X-ray structure revealed that the phenyl rings attached to the diene are non-planer. Each unit cell of **3.11** contains 8 molecules, as seen in Figure 3.3. Further, each molecule is involved in intermolecular hydrogen bonding with another molecule just like in a carboxylic acid dimer.

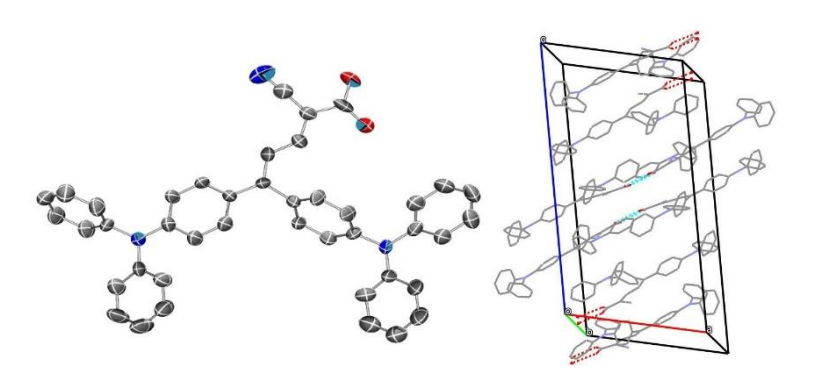


Figure 3.3. ORTEP structure of **3.11** (50% probability for thermal ellipsoids; hydrogen atoms are omitted for clarity) and its crystal packing.

3.3 Optical Properties

The absorption spectra of novel dual donor organic dyes **3.11** and **3.12** were recorded using their solutions in dichloromethane. The results are shown in Figure. 3.4 and the corresponding photophysical properties are summarized in Table 1. Two types of bands were observed in the UV-Vis absorption spectra. The band at the 280-350 nm is assigned to $\pi \rightarrow \pi^*$ transition of carbazole and triphenylamine moiety. The broad band from 370 to 560 nm with strong intensity was assigned as the intramolecular charge transfer (ICT) from the donor moiety to the acceptor moiety. Comparatively, lesser absorption maximum value for the carbazole containing compound **3.12** than that of triphenylamine containing compound **3.11** may be attributed to the rigidity of the system that disfavoured effective conjugation.⁷ Both the compounds have high molar extinction coefficient (Table 1).

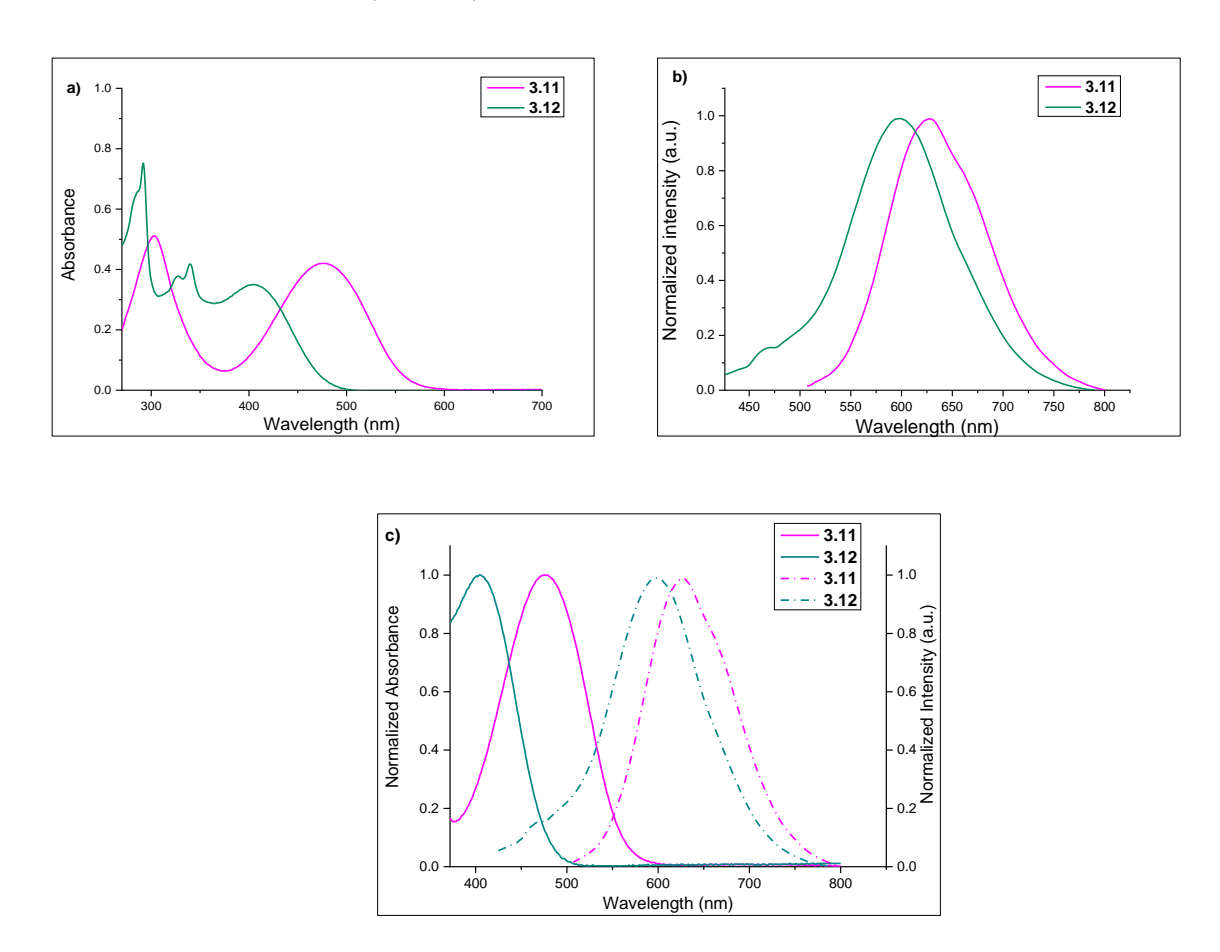


Figure 3.4. a) Absorption spectra of compounds **3.11** and **3.12**; b) Emission spectra of compounds **3.11** and **3.12**; c) Comparison of Stokes shifts for dyes **3.11** and **3.12**, solid lines for UV-Visible and dashdot lines for emission spectra. The UV-Vis and emission were recorded by using 1×10^{-5} M solutions in dichloromethane.

Table 1. Photophysical properties of dyes **3.11** and **3.12**.

Dyes	λ _{max} (nm)	λ_{em} (nm)	Stokes Shift (nm)	ε (M ⁻¹ cm ⁻¹)	$\mathbf{\phi_f}^{(a)}$	$\tau_{\rm f}({\rm ns})$
3.11	476	627	151	42,060	0.21	2.12 ns
3.12	405	598	193	35,180	0.35	3.13 ns

⁽a) Fluorescein in 0.1M NaOH was used as the reference $[\Phi f = 0.95 \pm 0.03]$

The emission spectra of the bis-donor based donor-acceptor systems were recorded by exciting at their respective absorption maxima using their solutions in dichloromethane, and the results are summarized in Table 1 and Figure. 3.4b. Emission of both the dyes **3.11** and **3.12** appeared as a single band at 627 nm and 598 nm, respectively. The triphenylamine derivative **3.11** exhibited a comparatively red-shifted band than that of the N-phenylcarbazole containing derivative **3.12**. Both the dyes displayed significant Stokes shift; 151 nm for **3.11** and 193 nm for **3.12**, respectively (Figure 3.4c, Table 1). The lifetime of the dyes **3.11** and **3.12** have also been investigated, and both were found to exhibit single exponential decay. The dye-containing N-phenylcarbazole group **3.12** showed a higher lifetime value of 3.13 ns, while compound **3.11** showed 2.12 ns (Table 1). The quantum efficiency of fluorescence of these dyes **3.11** and **3.12** are 0.21 and 0.35, respectively.

3.4 Cyclic Voltammetric Studies

The electrochemical oxidation and reduction potential of dyes **3.11** and **3.12** were determined by cyclovoltammetry using solutions of the compounds in acetonitrile solvent at room temperature at a 100mV s⁻¹ scan rate. While Bu₄NClO₄ was used as a supporting electrolyte, Ag/Ag⁺ and Pt were used as a reference electrode and working as well as the counter electrodes respectively. Both the dyes exhibited the oxidation and reduction potential in an electrochemical experiment and the redox potential for the dyes **3.11** and **3.12** are shown in Figure 3.5. The electrochemical parameters of dyes **3.11** and **3.12** are displayed in Table 2. The oxidation potential was observed from the donor moiety (triphenylamine and N-phenyl carbazole), whereas the reduction potential from the acceptor moiety (cyanoacrylic acid). The dye **3.11** exhibited an oxidation potential of 0.79 V and a reduction potential of 0.64 V with a difference of 0.15 V. Dye **3.12** showed oxidation and reduction potentials at a little higher value than that of dye **3.11**. The oxidation and reduction potentials of dye **3.12** are 1.0 V and 0.92 V

respectively and the difference being 0.08 V. The HOMO values were calculated from the oxidation potential of both the dyes and the LUMO values were obtained from the Tauc plot in UV-Visible spectra. A comparison of the experimental and the theoretical values are displayed in Table 2.

Table 2. Cyclic Voltammetry

Dye	\mathbf{E}° onset $(\mathbf{V})^{\mathrm{a}}$	HOMO (eV) ^b	LUMO (eV) ^c	HOMO (eV) ^d	LUMO (eV) ^d
3.11	0.60	-5.4	-3.1	-5.28	-2.53
3.12	0.85	-5.66	-2.95	-5.66	-2.93

^a Obtained from cyclic voltammetry, ${}^{b}HOMO(eV) = -(Eox- E(Ag/Ag+) + 4.8) eV$, ${}^{c}E_{LUMO} = Eg-HOMO$, ${}^{d}DFT$ calculation by Gaussian 09 software.

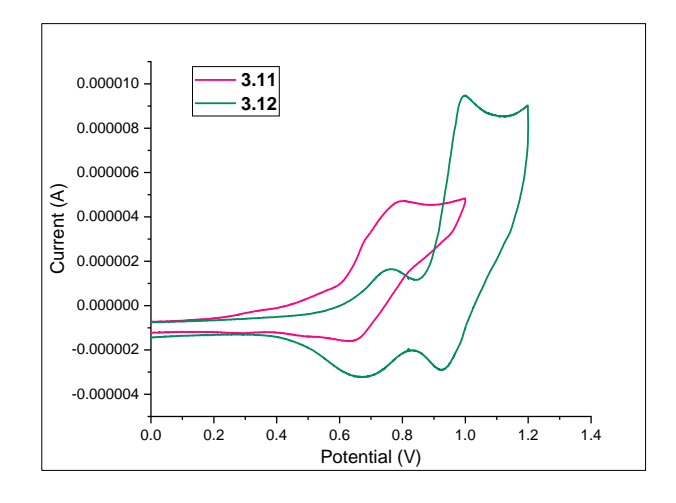


Figure 3.5. Cyclic Voltammogram of donor-acceptor systems **3.11** and **3.12** in 0.10 M Bu₄NClO₄/ CH₃CN, Scan Rate 100 mV s⁻¹ and reference electrode Ag/Ag⁺, working electrode Pt.

3.5 DFT Studies

Density Functional Theory (DFT) calculations were performed to optimize the geometry and to study the HOMO and LUMO energy levels of these dyes **3.11** and **3.22** by Gaussian 09 package using B3LYP/6-31G basic sets.⁸

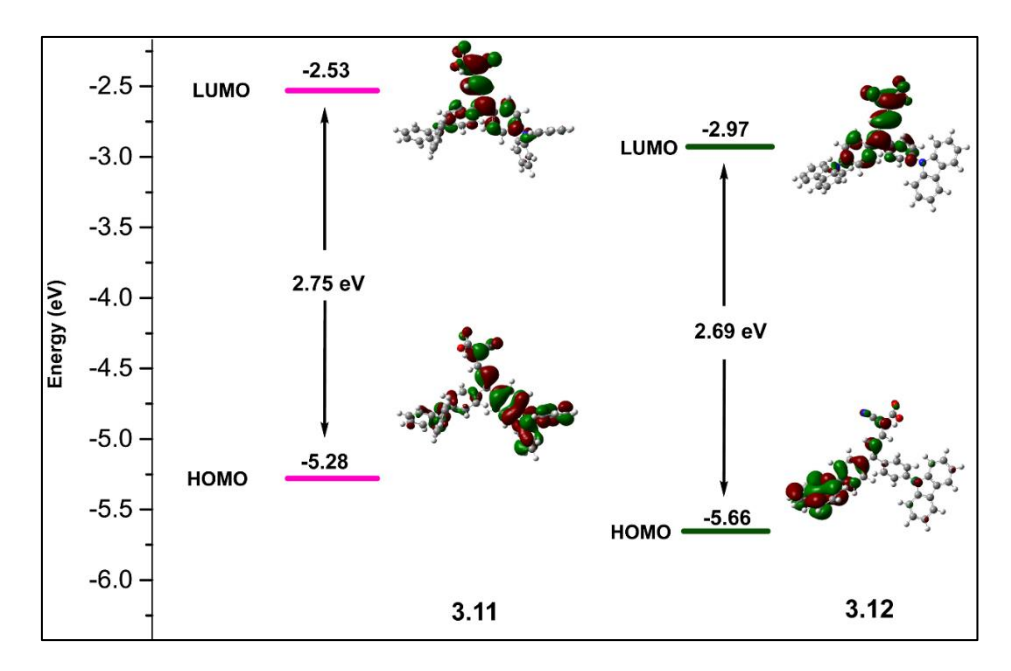


Figure 3.6. Molecular orbital energy diagram of the HOMO and LUMO of 3.11 and 3.12.

The optimized ground state structure of the dyes **3.11** and **3.12** showed similar structural coordinates as that of the crystal structure of the dye **3.11**. The time-dependent DFT (TD-DFT) calculation of **3.11** and **3.12** showed a HOMO-LUMO energy gap of 2.75 eV and 2.69 eV, respectively. The π orbitals of the highest occupied molecular orbital (HOMO) of **3.11** are mainly localized on one of the donor units along with extended double bonds connected to the acceptor unit (cyanoacetic acid). Similarly, in the case of dye **3.12**, the HOMO orbitals are localized only on a single N-phenyl carbazole unit. On the other hand, lowest unoccupied molecular orbital (LUMO), π^* orbitals are localized on the cyano acrylic acid and extended upto the phenyl rings connected extended double bonds in both the dyes. Moreover, both the dyes have pronounced charge distribution between HOMO and LUMO. The strong transition with a low energy gap may be due to the intramolecular charge transfer from donor moiety to acceptor moiety.

3.6 Application in Bio-Imaging

Fluorescence imaging of cells plays a significant role in the field of biological sciences to study the functions and dynamics of biomolecules inside the cell. In the previuos chapter (chapter 2), the 1,3-dicarbonyl bridged donor-acceptor compounds showed excellent and specific imaging of microtubules. Since both the 1,3-dicrabonyl and their corresponding BF₂ complexes showed similar properties, it was believed that only the aryl groups attached to the carbonyl groups are responsible for imaging. In this respect, it was anticipated that the

compounds **3.11** and **3.12** which posses the aryl group orienting in the same direction might also show selective imaging properties.

3.6.1 Effect of Donor-Acceptor Compounds on Cell Viability and Cell Migration

The fluorescent dyes with large Stokes shifts have been of great importance in the field of bio-imaging. The dye **3.11** and **3.12** have exhibited a Stokes shift of 151 nm and 193 nm, respectively. The cell viability of these compounds were evaluated on human cervical cancer cell line (HeLa), human breast cancer (MCF7), and normal human embryonic kidney (HEK293T) cells using the MTT assay method.⁹ Normal HEK293T was also taken to evaluate whether the compounds have different effect on a normal cell. The IC₅₀ values of these dyes for 24 h on different cell lines were calculated and are presented in Table 3.

Table 3. *In vitro* cytotoxic evaluation of bis-donor based donor-acceptor derivatives against HeLa, MCF7, HEK293T cell lines.

S.No	Dye	Ic ₅₀ ±SD (μg/ml) on HeLa	Ic ₅₀ ±SD (μg/ml) on MCF7	Ic ₅₀ ±SD (μg/ml) on HEK293T
1	3.11	13.51±1.22	67.01±5.76	NA
2	3.12	NA	NA	NA

Exponentially growing cells were treated with different concentrations of donor-acceptor derivatives for 24 h, and the cell growth inhibition was analysed through MTT assay.

The results indicate that the dye **3.11** showed significant cytotoxic/antiproliferative activity on HeLa and MCF cell lines in a dose-dependent manner with an IC₅₀ value of 13.51±1.22 and 67.01±5.76 respectively, for 24 h. Interestingly, the dye **3.11** showed less cytotoxic/antiproliferative activity on human normal embryonic kidney cells (HEK293T). These outcome indicate that the dye **3.11** may be used as an antiproliferative agent. Furthermore, the dye **3.12** displays less cytotoxic/antiproliferative activity on all the three different cell lines, human cervical cancer cell line (HeLa), human breast cancer (MCF7) and human normal embryonic kidney cells (HEK293). The MTT data are plotted in Figure 3.7.

To examine the effect of dyes **3.11** and **3.12** on the migration of cells, a wound-healing assay was performed. Figure 3.8 displays the results of these experiments. As seen in the figure incubation of cells with the dye **3.12** at a concentration of 20 μ g/mL had no significant effect

 $^{{}^{\}S}IC_{50}$ is defined as the concentration, which results in a 50% decrease in cell number as compared with that of the control cultures in the absence of a test compound and has been calculated using the respective regression analysis. The values represent the mean \pm SE of three individual observations.

on cell migration in comparison to that of the untreated control cells at 24 h. In contrast, compound 3.11, at $20\mu g/mL$ concentration, showed a significant effect on cell migration. These experimental data indicate that 3.12 did not interfere with the proliferation and migration of the cells, which is a highly beneficial property to develop fluorescent probes. Based on the cell viability and migration assays we used $10\mu g/mL$ concentration for colocalization studies.

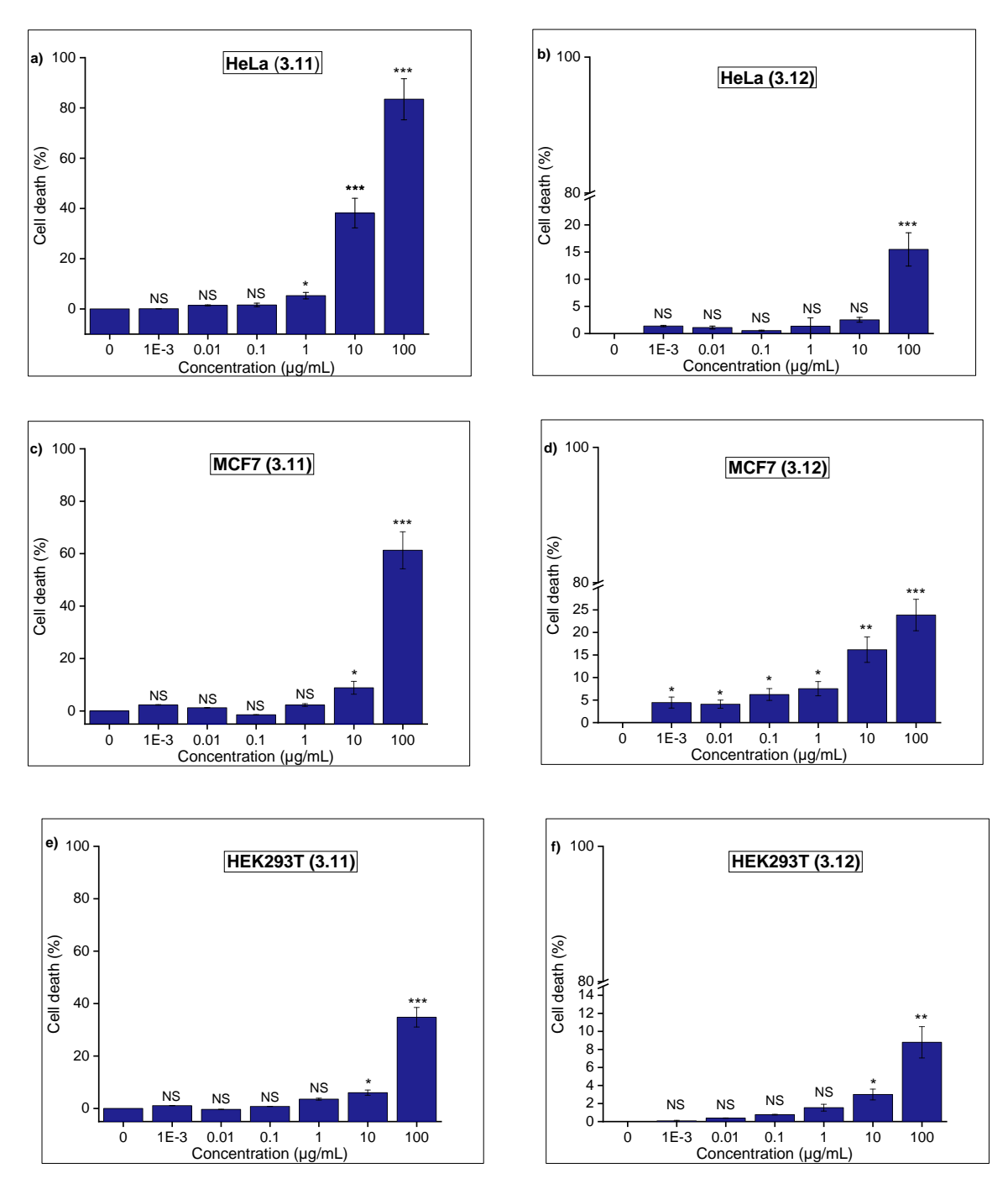


Figure 3.7. Effect of bis-donor based donor-acceptor dyes **3.11** and **3.12** on % of cell death of HeLa cancer cells, MCF7 cancer cells, and HEK293T normal cells.

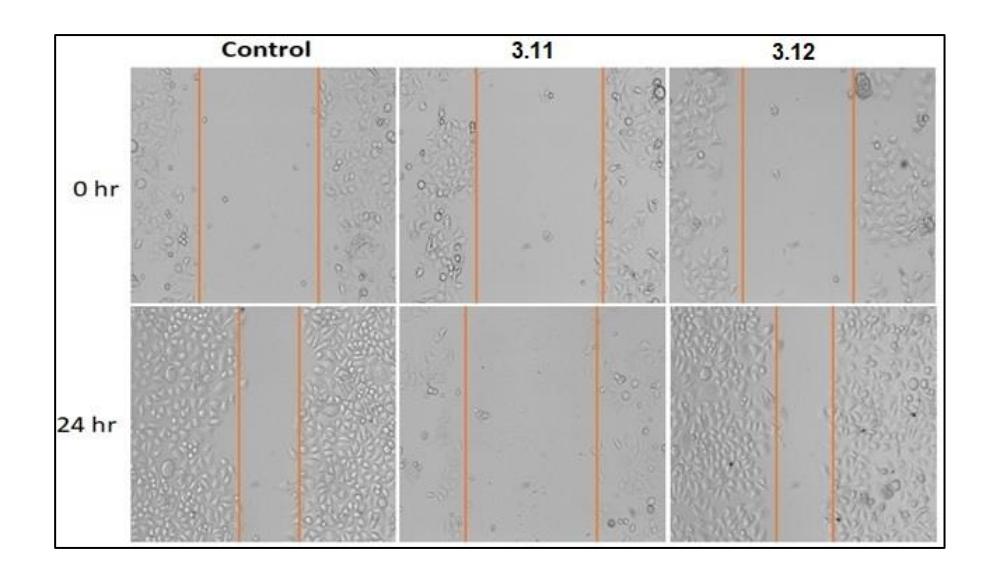


Figure 3.8. Effect of bis-donor based donor-acceptor dyes on the migration of HeLa cancer cells. After mechanical wounding, confluent HeLa cells were treated with dye **3.11**, **3.12**, and DMSO control. Representative photomicrographs of the wounded cell monolayer at 0 hr and 24 h have been shown; the scale bar is $100 \mu m$.

We have studied the photostability of the dyes **3.11** and **3.12** by irradiating their solution in dichloromethane separately in a fluorescent spectrophotometer and recorded their fluorescence spectra at every 5 minutes interval. This was done for a period of 1 h. The intensity of fluorescence is taken as a function of stability and the values are plotted in Figure 3.9. The dyes were found to have good photostability as their fluorescence intensity were above 94% for a period of 60 min.

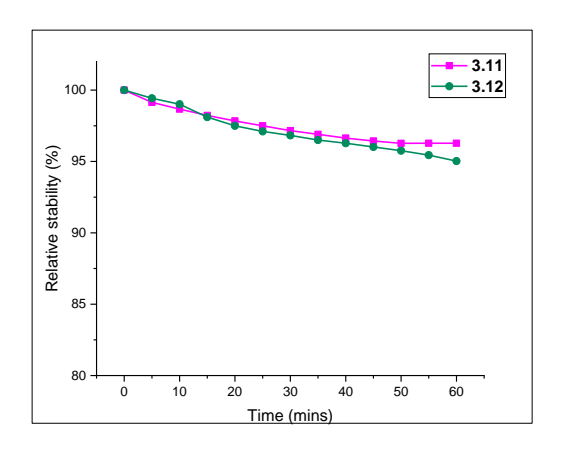


Figure 3.9. Photostability of dye 3.11 and 3.12.

3.6.2 Colocalization of Donor-Acceptor Compounds in HeLa Cells:

Preliminary fluorescence microscopy observations displayed that 3.11 and 3.12 were permeable into the cell, accumulated in the cytoplasm and remarkably emitted green fluorescence. As experienced with the prvious set of compounds (Chapter 2), these compounds also seemed like binding to microtubules. To evaluate this, we performed co-localization experiments for tubulin binding in microtubules of living cancer cells using Alexa Fluor 546 red and the dyes 3.11 / 3.12 in the same cell. The dyes 3.11 and 3.12 were visualized by green fluorescence, which was evenly distributed in the cytoplasm and surrounded the nuclei (Figure 3.10a). The images obtained due to Alexa Fluor 546 red staining were also similar (Figure 3.10c). Merged images indicated a clean overlap of these two images (green and red) producing a similar yellow image (Figure 3.10d). The result clearly suggests that dyes **3.11** and **3.12** are cell-permeable and bind to microtubules in living cells. It has to be noted that the image obtained using compound 3.11 is not that clear as that of compound 3.12. Perhaps, the cytotoxic effect of compound 3.11 might be responsible for this. Furthermore, we have tested the dye **3.12** for the imaging of HeLa cancer cell line without adding any antibodies. This experiment revealed that our dye **3.12** has directly stained the β-tubulin in HeLa cancer cells (Figure 3.11) giving a bright green image of the microtubules directly and specifically.

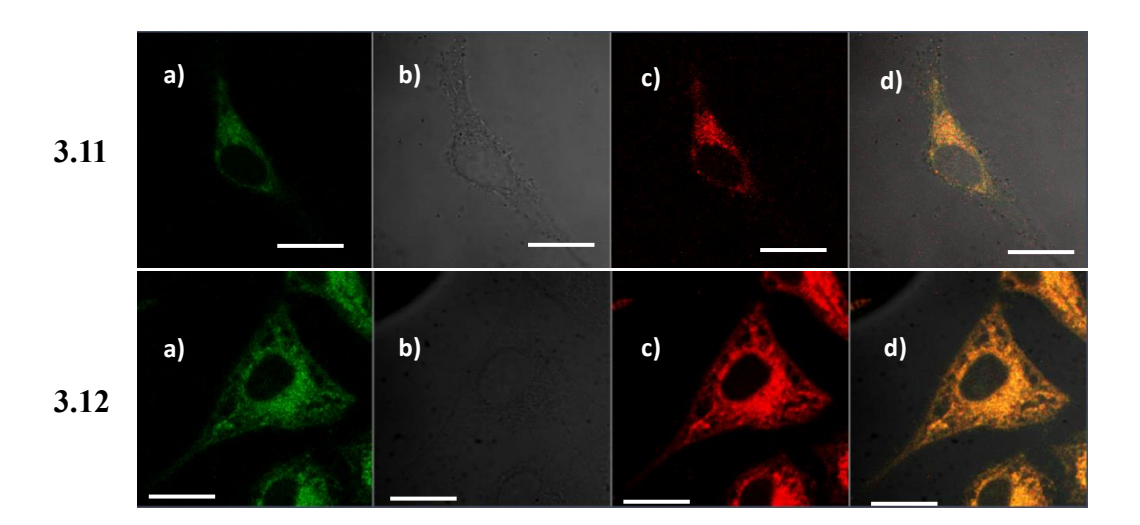


Figure 3.10. Confocal images of HeLa cancer cells co-stained with β -tubulin and dyes. a) Organic dyes **3.11** and **3.12** (Green channel: excited at 488-500 nm and emission at 550 nm); b) Bright field; c) β -tubulin (red channel: excited at 543-550 nm and emission at 700 nm); d) Merging all the images. Scale bar is 10 μm.

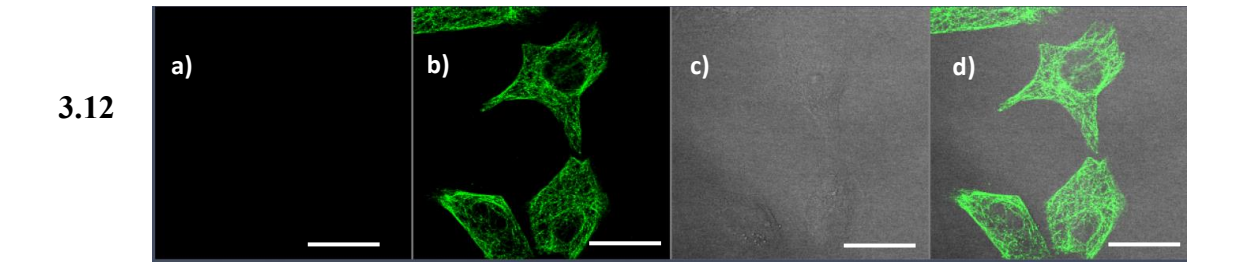


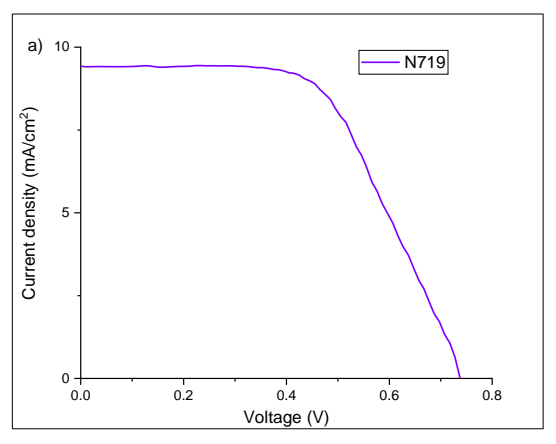
Figure 3.11. Confocal images of HeLa cancer cells without antibodies of β -tubulin. a) Without antibodies of β -tubulin; b) **3.12** (Green channel: excited at 488-500 nm and emission at 550 nm); c) Bright field; d) Overlapping all the above images

3.7 Application of the Dyes 3.11 and 3.12 in DSSC

Dye sensitized solar cells were fabricated uging the dyes **3.11** and **3.12** following the protocol described in the chapter 2. All the dyes were adsorbed well on to the mesoporous TiO_2 nanocrystals. The thickness of mesoporous TiO_2 was optimized to 10μ m and the nanocrystalline layer to 2μ m. The thickness of layers was maintained same for all the devices. The photovoltaic performances of the dyes **3.11** and **3.12** (D(D)- π -A) were determined under a simulated AM 1.5G irradiation (100 mWcm⁻²) with iodide/iodine electrolyte (0.6 M 1,2-dimethyl-3-propylimidazolium iodide, 0.1 M LiI, 0.05 M I₂, and 0.5 M 4-tert-butyl pyridine in acetonitrile). The photovoltaic parameters such as fill factor (FF), short circuit photocurrent (J_{sc}), open circuit voltage (V_{oc}), and the power conversion efficiency (PCE) have been summarized in Table 4, and the photocurrent density-voltage (J-V) plot is given in Figure 3.12.

Table 4. Parameters of dye-sensitized solar cell performance in compound **3.11**, **3.12** with reference **N719**.

Dye	$J_{\rm sc}({ m mA/cm}^2)$	V _{oc} (V)	FF	η (%)
3.11	1.6	0.55	70	0.64
3.12	1.74	0.57	69	0.68
N719	9.40	0.740	58.5	4.01



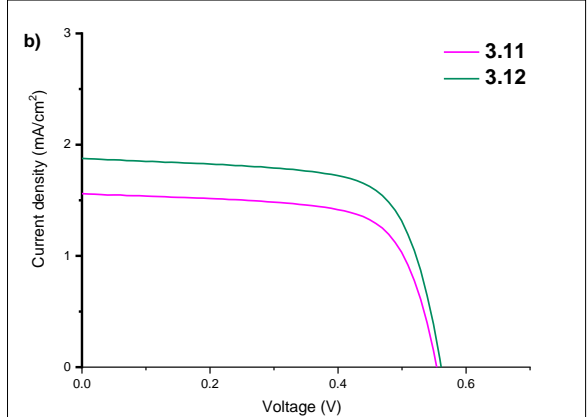


Figure 3.12. Photocurrent density- voltage (J-V) curves for the donor-acceptor $(D(D)-\pi-A)$ based dyesensitized solar TiO_2 electrodes. a) Reference **N719** dye; b) Dye **3.11** and **3.12.**

The photocurrent-voltage (*J-V*) curves revealed that the **N719** reference cell exhibited a power conversion efficiency of 4.01% with an open-circuit voltage of 0.740 V and a short circuit current density of 9.40 mA/cm² and the maximum power conversion efficiency attained using dyes **3.11** and **3.12** being 0.64% and 0.68%, respectively. This result indicates that the bis-donor based donor-acceptor systems of based on triphenylamine **3.11** and N-phenyl carbazole **3.12** (D(D)- π -A) showed response in DSSC. The fill factor for **3.11** and **3.12** are higher than that of the reference **N719** dye.

3.8 Conclusion

In summary, a couple of bis-donor (triphenylamine, N-phenyl carbazole) based donor-acceptor were synthesized successfully in high overall yields. Photophysical, electrochemical and DFT studies were carried out on these compounds. These high Stokes shifts bearing compounds showed promising application in live-cell imaging of microtubules. These compounds showed good selectivity towards binding to β-tubulin as revealed by the colocalization studies. While the carbazole based compound is non-toxic to both the cancer and normal cells studied, the triphenylamine containing compound showed different cytotoxicity effects to normal and cancer cells. Interestingly, this triphenylamine containing compound is more cytotoxic towards cancer cells compared to the normal cell. This unique character may advantageously be used to develop anti-proliferative agents. Studies in this direction would be of greater impact in the cancer research. The compounds showed some activity in DSSC. However, the efficiencies are not impressive. Optimization of the device fabrication may help to improve the efficiency.

3.9 Experimental Section

3.9.1 General Information.

For general information, see: chapter 2, section 2.7.1. For device fabrication, see: chapter 2, section 2.7.2. For biological experiments such as imaging, cytotoxicity measurements, and wound healing assay, see: chapter 2, section 2.7.3.

3.9.2 Cell Lines and Cell Culture:

The cell lines HeLa (<u>human cervical cancer</u>), MCF7 (human breast cancer), and HEK293K (normal human embryonic kidney) cell lines have obtained from the National Centre for Cellular Sciences (NCCS), Pune, India. Cells were cultured in DMEM media, supplemented with 10% heat-inactivated foetal bovine serum (FBS), 1 mM NaHCO₃, 2 mM glutamine, 100 units/ml penicillin, and 100 μ g/ml streptomycin. The cells were maintained in culture at 37° C in an atmosphere of 5% CO₂.

3.9.3 Experimental Procedure and Analytical data

3.9.3.1 Synthesis of 4-bromo-N, N-diphenyl aniline (3.13):^{4b}

The compound **3.13** was prepared from the literature procedure. ^{4b} To a stirred solution of 4-bromo aniline (2 g, 11.62 mmol), iodobenzene (3.2 mL, 29.06 mmol), CuI

(0.44 g, 2.32 mmol), 1,10-phenanthroline (0.42 g, 2.32 mmol) in toluene (60 mL) was added to t-BuOK (6.5 g, 58.13 mmol) and refluxed for 12 h. The reaction progress was monitored by TLC. After completion reaction, the reaction mixture was filtered through Whatman filter paper. The filtrate was

reduced under vacuum. The residue was purified by column chromatography using 1:5 EtOAc/hexanes at $R_f = 0.8$. brown solid (2.76 g, yield = 73%); ¹H NMR (400 MHz, CDCl₃): δ 7.29 (d, J = 8.8 Hz, 2H), 7.23 (t, J = 7.6 Hz, 4H), 7.06-6.99 (m, 6H), 6.92 (d, J = 8.0 Hz, 2H); ¹³C NMR (100 MHz, CDCl₃): δ 147.4, 147.1, 132.2, 129.4, 125.2, 124.5, 123.3, 114.8.

3.9.3.2 Synthesis of 9-(4-bromophenyl)-9H-carbazole (3.14):5b

The mixture of carbazole (2 g, 11.96 mmol), dibromo benzene (5.66 g, 24 mmol), trans

1,2-cyclohexane (0.14 g, 1.2 mmol), CuI (0.28 g, 1.2 mmol), K₃PO₄ (3.8 g, 17.94 mmol) in toluene (15 mL) were refluxed for 20 h. The mixture was washed with aqueous NH₄HCO₃ solution (100 mL) and extract with chloroform (2×30mL). The organic layer was combined dried with NaSO₄.

The crude was purified by column chromatography using 1:20 EtOAc/hexanes at $R_f = 0.62$. Pale yellow solid (2.4 g, yield = 62%); ¹H NMR (500 MHz, CDCl₃): δ 8.25 (d, J = 8.0 Hz, 2H), 7.78 (d, J = 8.5 Hz, 2H), 7.53-7.45 (m, 6H),7.42-7.39 (m, 2H); ¹³C NMR (125 MHz, CDCl₃): δ 140.6, 136.8, 133.1, 128.6, 126.1, 123.5, 120.8, 120.4, 120.3, 109.6.

3.9.3.3 Synthesis of 4-(diphenyl amino) benzaldehyde (3.15):^{4a}

 $POCl_3$ (1.3 mL, 8.15 mmol) was added dropwise to a solution of triphenylamine (1 g, 4.0 mmol) in dry DMF (10 mL) at 0°C and allowed to stir 50-55 °C for 14 h. The reaction progress

was monitored by TLC using 20% EtOAc/hexanes mixture as a mobile phase. After completion of the reaction, the reaction mixture was poured into ice-cold water and extracted with EtOAc (2×50 mL). The organic layer was washed with H₂O (50 mL) and brine solution (10 mL). The organic layer was dried over NaSO₄, filtered, concentrated using under vacuum. The

product was purified by column chromatography using 1:5 EtOAc/hexanes at R_f = 0.80. Pale yellow solid (0.8 g, yield = 72%); MP: 149-150°C; ¹H NMR (400 MHz, CDCl₃): δ 9.80 (s, 1H), 7.67 (d, J = 8.8 Hz, 2H), 7.34 (t, J = 7.6 Hz, 4H), 7.17 (d, J = 6.8 Hz, 6H), 7.01 (d, J = 8.8 Hz, 2H); ¹³C NMR (100 MHz, CDCl₃): δ 190.5, 153.4, 146.2, 131.4, 129.8, 129.2, 126.4, 125.2, 119.4.

3.9.3.4 Synthesis of 4-(9H-carbazol-9-yl) benzaldehyde (3.16):^{5a}

To a stirred solution of carbazole (1 g, 5.98 mmol), K_2CO_3 (2.5 g, 17.94 mmol) in DMF (20 mL), 4-fluoro benzaldehyde was added and maintained 150°C for 12 h. The reaction mixture poured into ice water.

The resulting precipitate was collected by filtration and washed with water, methanol, ethanol, and n-hexane consecutively. The filtrate was dried under vacuum. Pale yellow solid (1.5 g, yield = 92%); 1 H NMR (500 MHz, CDCl₃): δ 10.07 (s, 1H), 8.18 (d, J = 5.5 Hz, 2H), 8.08 (d, J = 7.0 Hz, 2H), 7.74 (d, J = 6.5 Hz, 2H), 7.51 (s, 2H), 7.46 (s, 2H), 7.37 (s, 2H); 13 C NMR

(125 MHz, CDCl₃): δ 190.9, 143.2, 140.0, 134.5, 131.3, 126.6, 126.3, 123.9, 120.8, 120.5, 109.7.

3.9.3.5 Synthesis of bis (4-(diphenyl amino) phenyl) methanol (3.17):

To a stirred solution of compound **3.13** (0.47 g, 1.47 mmol) in dry THF (15 mL), 1.6 M n-BuLi in hexane (2 mL, 2.44 mmol) was added at -78 °C and allow to stir for 1 h. Then,

compound **3.15** (0.3 g, 1.22 mmol) was added to the reaction mixture and maintained -78 $^{\circ}$ C for 2 h followed by room temperature for 12 h. The reaction progress was monitored by TLC. The reaction mixture neutralized with saturated NH₄Cl (2×15 mL) solution and extracted with EtOAc (2×15 mL). The

product was purified by column chromatography using 1:5 EtOAc/hexanes at R_f = 0.46. Pale brown viscos (0.4 g, yield = 53%); ¹H NMR (500 MHz, CDCl₃): δ 7.24-7.22 (m, 10H), 7.10 (d, J = 8.0 Hz, 8H), 7.04-6.99 (m, 10H), 5.37 (s, 1H); ¹³C NMR (125 MHz, CDCl₃): δ 147.9, 147.1, 136.3, 129.3, 129.2, 128.5, 127.6, 124.5, 124.4, 123.8, 123.4, 122.9, 79.7; IR (neat): υ 2090, 1641, 1579, 1473, 1268, 1006, 763, 682 cm⁻¹; HRMS (ESI): calcd for $C_{37}H_{30}N_{2}O$ [M+H]⁺ 519.2431, Found 519.2430.

3.9.3.6 Synthesis of bis(4-(9H-carbazol-9-yl) phenyl) methanol (3.18):

To a stirred solution of compound 3.14 (1 g, 3.10 mmol) in dry THF (20 mL), 1.6 M n-

BuLi in hexane (3.9 mL, 6.20 mmol) was added at -78 °C and allow to stir for 1 h. Then, compound **3.16** (0.84 g, 3.10 mmol) was added to the reaction mixture and maintained -78 °C for 2 h followed by room temperature for 12 h. The reaction progress was monitored by TLC. The reaction mixture neutralized with

saturated NH₄Cl (2×20 mL) solution and extracted with EtOAc (2×20 mL). The product was purified by column chromatography using 1:5 EtOAc/hexanes at R_f = 0.55. Pale brown solid (0.87 g, yield = 55%); MP: 112-113°C; ¹H NMR (400 MHz, CDCl₃): δ 8.30 (t, J = 11.0 Hz, 4H), 7.74-7.66 (m, 7H), 7.58-7.53 (m, 9H), 7.45-7.44 (m, 4H), 6.00 (s, 1H); ¹³C NMR (100 MHz, CDCl₃): δ 142.5, 140.79, 140.74, 137.1, 128.0, 127.0, 126.0, 123.4, 120.4, 120.1, 109.8, 75.5; IR (neat): υ 1919, 1738, 1596, 1477, 1227, 1014, 772, 660 cm⁻¹; HRMS (ESI): calcd for $C_{37}H_{26}N_2O$ [M+H]⁺ 515.2118, Found 515.2122.

3.9.3.7 Synthesis of bis (4-(diphenyl amino) phenyl) methanone (3.19):

IBX (0.49 g, 1.73 mmol) was added to the stirred solution of compound 3.17 (0.6 g, 1.15

mmol) in acetonitrile (8): (1) DMSO (15 mL) at open air condition and allow to stir room temperature for 3 h. The reaction was monitored by TLC. The reaction mixture was filtered through filter paper and the filtrate was extracted with CHCl₃ (2×15 mL).

The product was purified by column chromatography using 1:5 EtOAc/hexanes at $R_f = 0.58$. Pale yellow solid (0.37 g, yield = 62%); MP: 149-151°C; ¹H NMR (400 MHz, CDCl₃): δ 7.69 (d, J = 8.8 Hz, 4H), 7.31 (t, J = 8.0 Hz, 8H), 7.17 (d, J = 7.6 Hz, 8H), 7.12 (t, J = 7.6 Hz, 4H) 7.02 (d, J = 8.4 Hz, 4H); ¹³C NMR (100 MHz, CDCl₃): δ 194.0, 151.5, 146.8, 132.1, 131.7, 130.6, 129.6, 128.2, 126.1, 125.9, 124.4, 120.0; IR (neat): υ 3029, 1738, 1581, 1308, 1169, 966, 749, 693 cm⁻¹; HRMS (ESI): calcd for $C_{37}H_{28}N_2O$ [M+H]⁺ 517.2274, Found 517.2276.

3.9.3.8 Synthesis of bis(4-(9H-carbazol-9-yl) phenyl) methanone (3.20):

IBX (0.32 g, 1.16 mmol) was added to a stirred solution of compound 3.18 (0.4 g, 0.77

mmol) in acetonitrile (8): (1) DMSO (12 mL) at open air condition and allow to stir room temperature for 3 h. The reaction was monitored by TLC. The reaction mixture was filtered through filter paper and the filtrate was extracted with

CHCl₃ (2×15 mL). The product was purified by column chromatography using 1:5 EtOAc/hexanes at $R_f = 0.67$. Pale yellow solid (0.25 g, yield = 67%); MP: 140-142°C; ¹H NMR (500 MHz, CDCl₃): δ 8.19-8.17 (m, 8H), 7.81 (d, J = 8.5 Hz, 4H), 7.57 (d, J = 8.0 Hz, 4H), 7.47 (td, J = 7.0, 1.0 Hz, 4H), 7.35 (t, J = 8.0 Hz, 4H); ¹³C NMR (125 MHz, CDCl₃): δ 194.6, 142.0, 140.4, 135.9, 132.0, 126.5, 126.3, 124.0, 120.8, 120.6, 109.9; IR (neat): υ 3048, 1651, 1596, 1306, 1163, 930, 735, 688 cm⁻¹; HRMS (ESI): calcd for $C_{37}H_{24}N_2O$ [M+H]⁺ 513.1961, Found 513.1962.

3.9.3.9 Synthesis of 3,3-bis (4-(diphenyl amino) phenyl) acrylaldehyde (3.21):^{6a}

To a stirred solution of compound 3.19 (0.2 g, 0.38 mmol) in dry DCM (15 mL), TiCl₄

(0.42 mL, 3.87 mmol) was added and allow stir 0°C for 0.5 h. Et₃N (0.54 mL, 3.87 mmol) was added to the reaction mixture at 0°C and maintained room temperature for 3 h. The crude was poured into the water (20 mL) and extract with DCM (2×20mL).

The organic layer was collected and dried over NaSO₄ and solvent was removed by under reduced pressure. The product was purified by column chromatography using 1:5 EtOAc/hexanes at $R_f = 0.67$. Pale yellow solid (0.18 g, yield = 85%); MP: 107-108°C; ¹H NMR (500 MHz, CDCl₃): δ 9.54 (d, J = 8.0 Hz, 1H), 7.30-7.26 (m, 8H), 7.24 (d, J = 4.0 Hz, 2H), 7.16-7.12 (m, 10H) 7.10-7.04 (m, 6H), 6.98 (d, J = 9.0 Hz, 2H), 6.48 (d, J = 8.0 Hz, 1H); ¹³C NMR (125 MHz, CDCl₃): δ 193.7, 162.1, 150.3, 149.2, 147.2, 146.9, 132.1, 130.7, 130.1, 129.8, 129.64, 129.61, 128.3, 125.6, 125.3, 124.9, 124.3, 123.9, 121.4, 121.0; IR (neat): υ 3033, 2830, 1655, 1581, 1449, 1315, 1073, 921, 750 cm⁻¹; HRMS (ESI): calcd for $C_{39}H_{30}N_{2}O$ [M+H]⁺ 543.2431, Found 543.2433.

3.9.3.10 Synthesis of 3,3-bis(4-(9H-carbazol-9-yl) phenyl) acrylaldehyde (3.22):

To a stirred solution of compound **3.20** (0.2 g, 0.39 mmol) in dry DCM (15 mL), TiCl₄ (0.43 mL, 3.9 mmol) was added and allow stir 0°C for 0.5 h. Et₃N (0.54 mL, 3.9 mmol) was

added to the reaction mixture at 0°C and maintained room temperature for 3 h. The crude was poured into the water (20 mL) and extract with DCM (2×20mL). The organic layer was collected and dried over NaSO₄ and solvent was removed by under reduced pressure. The product was purified by column

chromatography using 1:5 EtOAc/hexanes at R_f = 0.80. Pale yellow solid (0.19 g, yield = 90%); MP: 246-248°C; ¹H NMR (400 MHz, CDCl₃): δ 9.78 (d, J = 9.5 Hz, 1H), 8.19 (d, J = 9.0 Hz, 4H), 7.77 (d, J = 10.5 Hz, 2H), 7.71 (s, 3H), 7.67 (d, J = 10.0 Hz, 2H), 7.59-7.54 (m, 4H), 7.51-7.45 (m, 5H), 7.35 (q, J = 9.0 Hz, 4H), 6.81 (d, J = 10.0 Hz, 1H); ¹³C NMR (100 MHz, CDCl₃): δ 193.0, 160.1, 140.5, 140.4, 140.2, 139.3, 138.0, 135.2, 132.4, 130.3, 128.0, 126.9, 126.8, 126.2, 123.87, 123.84, 120.6, 109.89, 109.83; IR (neat): υ 3054, 1666, 1594, 1332, 1225, 1016, 915, 779, 695 cm⁻¹; HRMS (ESI): calcd for $C_{39}H_{26}N_{2}O$ [M+Na]⁺ 561.1937, Found 561.1941.

3.9.3.11 Synthesis of (Z)-2-cyano-5,5-bis (4-(diphenyl amino) phenyl) penta-2,4-dienoic acid (3.11):

Piperidine (2 drops) were added to the stirred solution of compound 3.21 (0.16 g, 0.29

mmol), cyano acetic acid (0.05 g, 0.58 mmol) in dry CH₃CN, the mixture was heated at reflux for 3 h. Then, the solvent was dried over under reduced pressure. The crude was acidified with 1N HCl (5 mL) followed by extract with CHCl₃ (2×10mL), organic layer was dried over with NaSO₄. The solvent was concentrated with under vacuum. The product was purified by

column chromatography using 1:10 MeOH/EtOAc at $R_f = 0.56$. Red solid (0.13 g, yield = 72%); MP: 260-262°C; ¹H NMR (500 MHz, CDCl₃/ CD₃OD (2:1)): δ 7.84 (d, J = 12.5 Hz, 1H), 7.23-7.16 (m, 10H), 7.08-7.06 (m, 8H),7.03-6.99 (m, 6H), 6.96 (t, J = 4.0 Hz, 2H), 6.947-6.940 (m, 1H), 6.90 (d, J = 9.0 Hz, 2H); ¹³C NMR (125 MHz, CDCl₃/ CD₃OD (2:1)): δ 167.9, 156.6, 151.0, 149.5, 148.7, 147.0, 146.8, 133.5, 131.7, 130.9, 130.1, 129.4, 125.3, 125.2, 123.9, 123.7, 121.2, 120.4, 117.7; IR (neat): υ 3033, 2930, 2211, 1584, 1314, 1143, 920, 828, 750 cm⁻¹; HRMS (ESI): calcd for $C_{42}H_{31}N_3O_2$ [M+H]⁺ 610.2489, Found 610.2491.

3.9.3.12 Synthesis of (E)-5,5-bis(4-(9H-carbazol-9-yl) phenyl)-2-cyanopenta-2,4-dienoic acid (3.12):

Piperidine (2 drops) were added to the stirred solution of compound 3.22 (0.10 g, 0.18

mmol), cyano acetic acid (0.03 g, 0.37 mmol) in dry CH₃CN, the mixture was heated at reflux for 3 h. Then, the solvent was dried over under reduced pressure. The crude was acidified with 1N HCl (5 mL) followed by extract with CHCl₃ (2×10mL), organic layer was dried over with NaSO₄. The solvent was concentrated with under vacuum. The product was

purified by column chromatography using 1:10 MeOH/EtOAc at R_f = 0.22. Red solid (0.1 g, yield = 89%); MP: 289-291°C; ¹H NMR 500 MHz, CDCl₃/CD₃OD (2:1)): δ 8.06 (t, J = 7.5 Hz, 4H), 7.67-7.59 (m, 5H), 7.49-7.44 (m, 5H), 7.38-7.34 (m, 7H), 7.23 (d, J = 5.0 Hz, 5H); ¹³C NMR (125 MHz, CDCl₃/CD₃OD (2:1)): δ 164.1, 157.1, 152.3, 140.4, 140.3, 139.9, 139.2, 138.5, 136.1, 132.2, 130.6, 126.87, 126.81, 126.1, 123.7, 123.0, 120.4, 109.7; IR (neat): υ 2921, 2850, 2216, 1598, 1333, 1149, 914, 841, 722 cm⁻¹; HRMS (ESI): calcd for C₄₂H₂₇N₃O₂ [M+H]⁺ 628.1995, Found 628.1993.

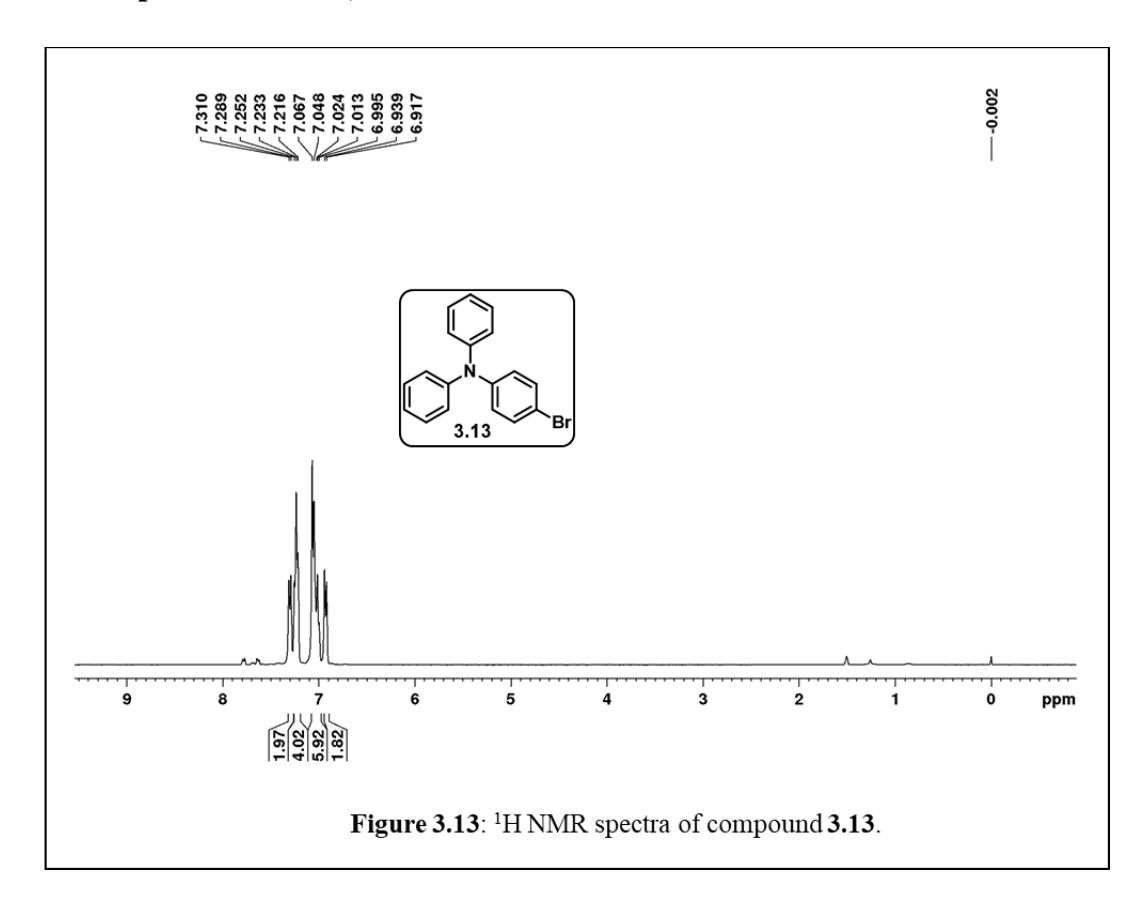
3.10 References

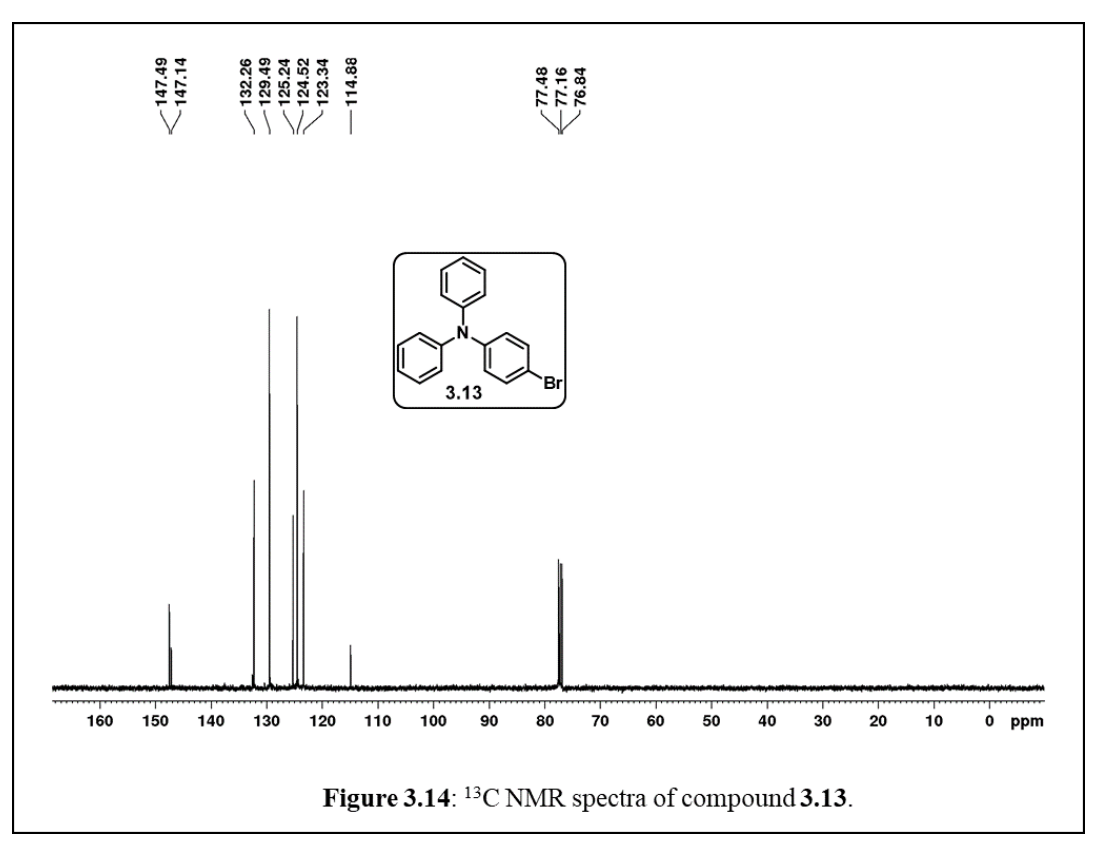
- (a) Zhang, J.; Chen, W.; Kalytchuk, S.; Li, K. F.; Chen, R.; Adachi, C.; Chen, Z.; Rogach, A. L.; Zhu, G.; Yu, P. K. N.; Zhang, W.; Cheah, K. W.; Zhang, X.; Lee, C.-S. ACS Appl. Mater. Interfaces 2016, 8, 11355. (b) Zhou, H.; Zheng, Z.; Xu, G.; Yu, Z.; Yang, X.; Cheng, L.; Tian, X.; Kong, L.; Wu, J.; Tian, Y. Dyes Pigm. 2012, 94, 570. (c) Li, Q.; Qian, Y. New J. Chem. 2016, 40, 7095.
- 2. (a) Hara, K.; Sato, T.; Katoh, R.; Furube, A.; Yoshihara, T.; Murai, M.; Kurashige, M.; Ito, S.; Suga, S.; Arakawa, H. *Adv. Funct. Mater.* **2005**, *15*, 246. (b) Hagberg, D. P.; Yum, J.-H.; Lee, H. J.; Angelis, F. D.; Marinado, T.; Karlsson, K. M.; Humphry-Baker, R.; Sun, L.; Hagfeldt, A.; Grätzel, M.; Nazeeruddin, Md. K. *J. Am. Chem. Soc.* **2008**, *130*, 6259. (c) Chang, D. W.; Lee, H. J.; Kim, J. H.; Park, S. Y.; Park, S.-M.; Dai, L.; Baek, J.-B. *Org. Lett.* **2011**, *13*, 3880.
- 3. (a) Sohn, S.; Koh, B. H.; Baek, J. Y.; Byun, H. C.; Lee, J. H.; Shin, D.-S.; Ahn, H.; Lee, H.-K.; Hwang, J.; Jung, S.; Kim, Y.-H. *Dyes pigm.* **2017**, *140*, 14-21. (b) Im, J. B.; Lampande, R.; Kim, G. H.; Lee, J. Y.; Kwon, J. H. *J. Phys. Chem. C* **2017**, *121*, 1305 1314.
- (a) Patel, J. Z.; Parkkari, T.; Laitinen, T.; Kaczor, A. A.; Saario, S. M.; Savinainen, J. R.; Navia-Paldanius, D.; Cipriano, M.; Leppanen, J.; Koshevoy, I. O.; Poso, A.; Fowler, C. J.; Laitinen, J. T.; Nevalainen, T. *J. Med. Chem.* 2013, 56, 8484. (b) Shi, L.; He, C.; Zhu, D.; He, Q.; Li, Y.; Chen, Y.; Sun, Y.; Fu, Y.; Wen, D.; Cao, H.; Cheng, J. *J. Mater. Chem.* 2012, 22, 11629.
- (a) Hwang, A.-R.; Han, W.-S.; Wee, K.-R.; Kim, H. Y.; Cho, D. W.; Min, B. K.; Nam, S. W.; Pac, C.; Kang, S. O. *Phys. Chem. C* 2012, *116*, 1973. (b) Wang, C.; Li, X.; Pan, Y.; Zhang, S.; Yao, L.; Bai, Q.; Li, W.; Lu, P.; Yang, B.; Su, S.; Ma, Y. *ACS Appl. Mater. Interfaces* 2016, 8, 3041.
- (a) Bharathi, P.; Periasamy, M. Org. Lett. 1999, 1, 857. (b) Zhao, X.; Liu, J.; Wang, H.; Zou, Y.; Li, S.; Zhang, S.; Zhou, H.; Wu, J.; Tian, Y. Dalton Trans. 2015, 44, 701. (c) Jung, I.; Lee, J. K.; Song, K. H.; Song, K.; Kang, S. O.; Ko, J. J. Org. Chem. 2007, 72, 3652.
- 7. Yadav, S. B.; Kothavale, S.; Sekar, N. J. Photochem. Photobiol. A 2019, 382, 111937.
- 8. Frisch, M. J.; Trucks, G. W.; Schlegel, H. B.; Scuseria, G. E.; Robb, M. A.; Cheeseman, J. R.; Scalmani, G.; Barone, V.; Mennucci, B.; Petersson, G. A.; Nakatsuji, H.; Caricato, M.; Li, X.; Hratchian, H. P.; Izmaylov, A. F.; Bloino, J.; Zheng, G.; Sonnenberg, J. L.;

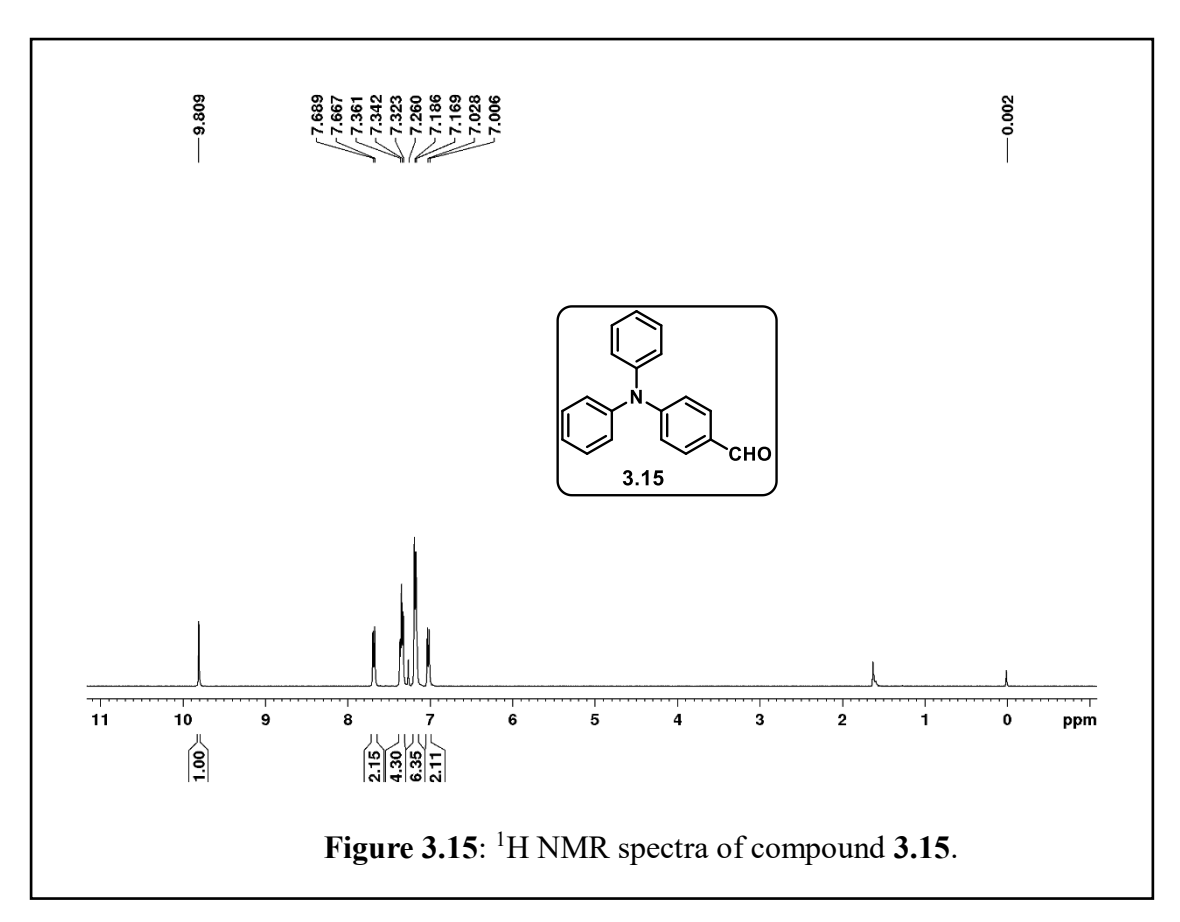
Hada, M.; Ehara, M.; Toyota, K.; Fukuda, R.; Hasegawa, J.; Ishida, M.; Nakajima, T.; Honda, Y.; Kitao, O.; Nakai, H.; Vreven, T.; Montgomery, Jr. J. A.; Peralta, J. E.; Ogliaro, F.; Bearpark, M.; Heyd, J. J.; Brothers, E.; Kudin, K. N.; Staroverov, V. N.; Kobayashi, R.; Normand, J.; Raghavachari, K.; Rendell, A.; Burant, J. C.; Iyengar, S. S.; Tomasi, J.; Cossi, M.; Rega, N.; Millam, J. M.; Klene, M.; Knox, J. E.; Cross, J. B.; Bakken, V.; Adamo, C.; Jaramillo, J.; Gomperts, R.; Stratmann, R. E.; Yazyev, O.; Austin, A. J.; Cammi, R.; Pomelli, C.; Ochterski, J. W.; Martin, R. L.; Morokuma, K.; Zakrzewski, V. G.; Voth, G. A.; Salvador, P.; Dannenberg, J. J.; Dapprich, S.; Daniels, A. D.; Farkas, O.; Foresman, J. B.; Ortiz, J. V.; Cioslowski, J.; Fox, D. J. *Gaussian 09, Revision A.02*, Gaussian, Inc. Wallingford, CT, **2009**.

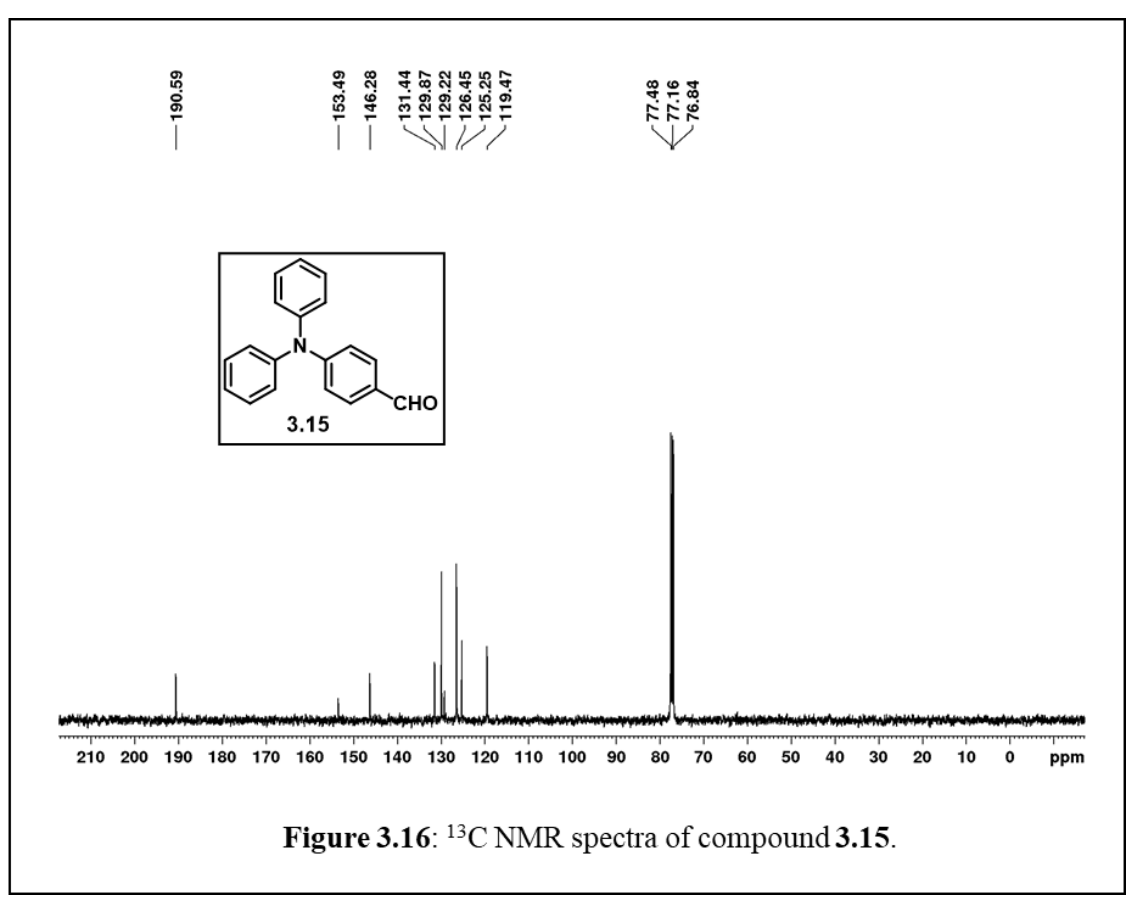
9. Mosmann, T. J Immunol Methods 1983, 65, 55.

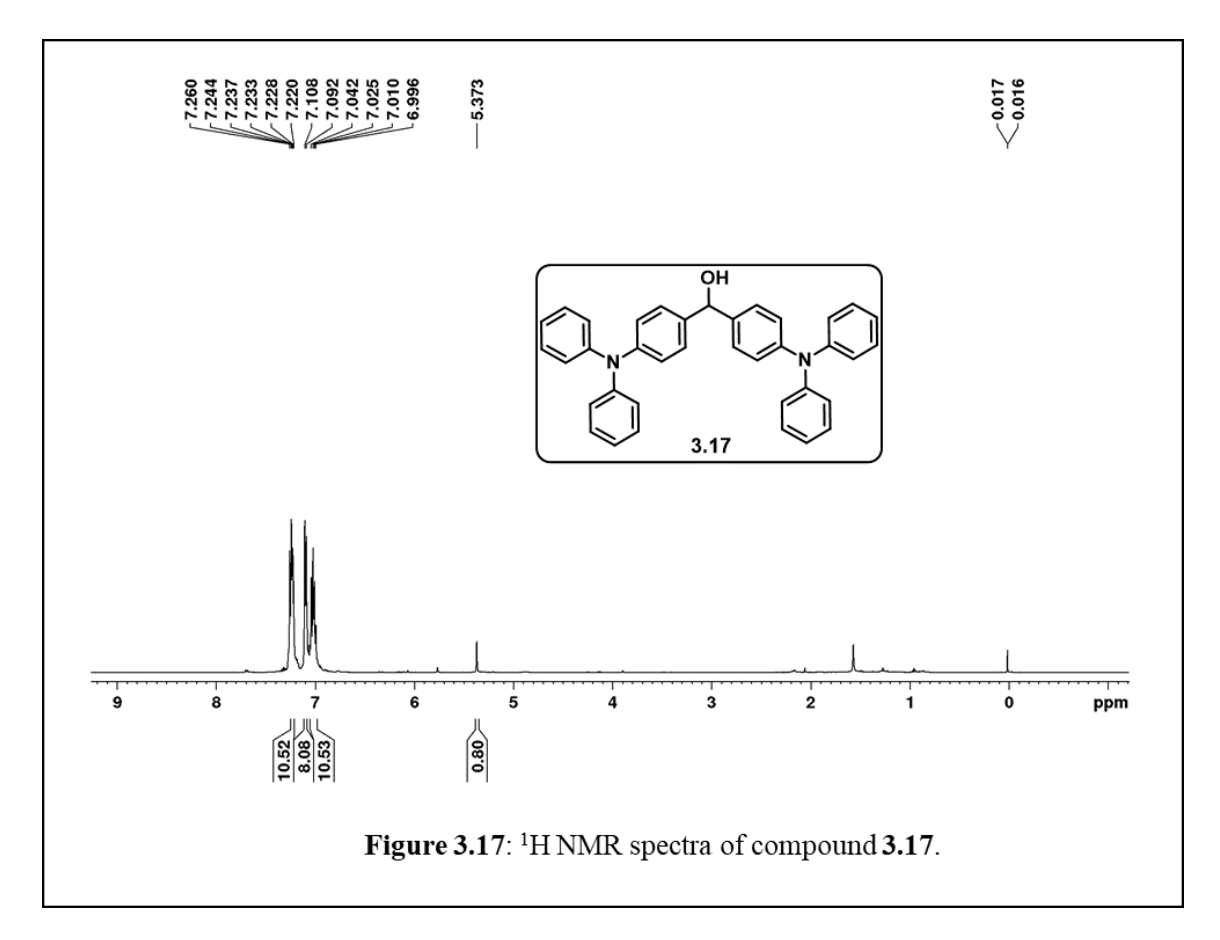
3.11 Representative ¹H, ¹³C NMR

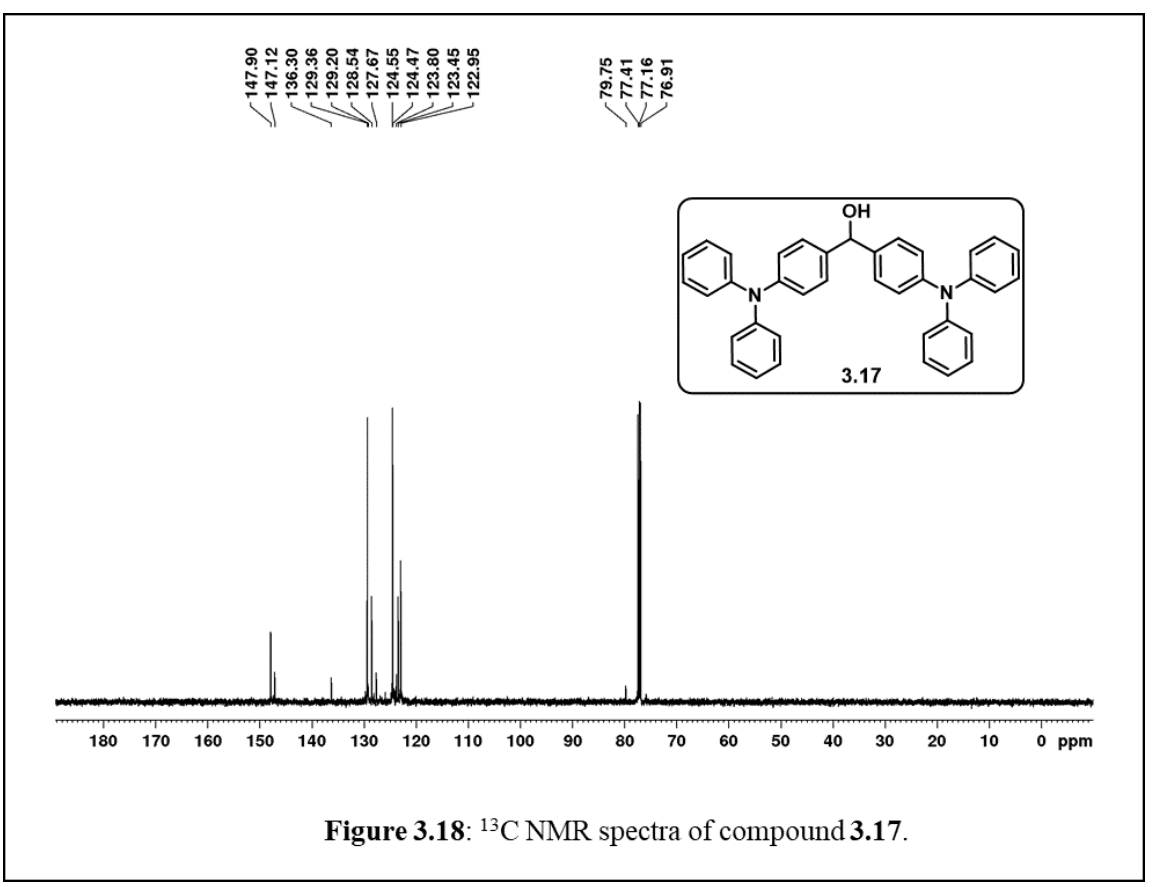


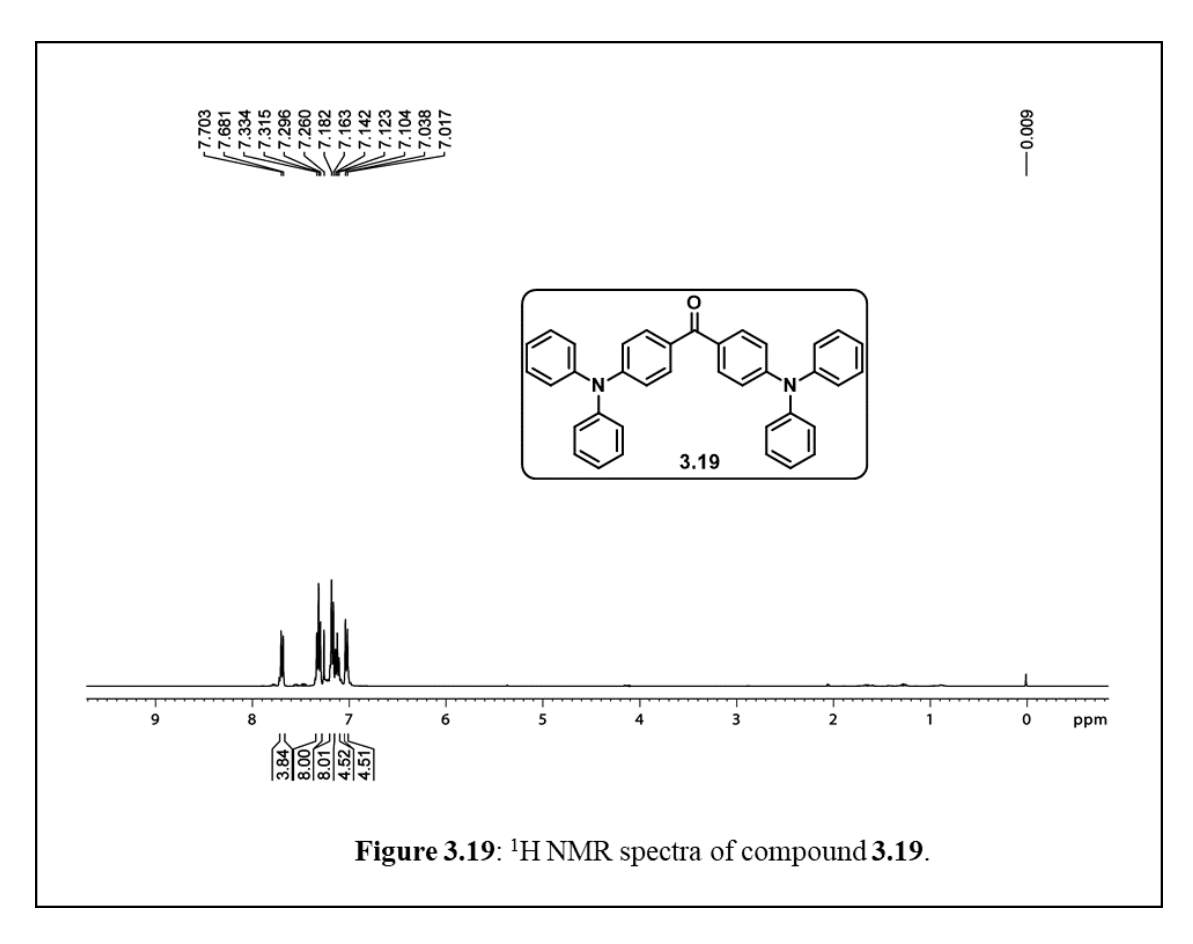


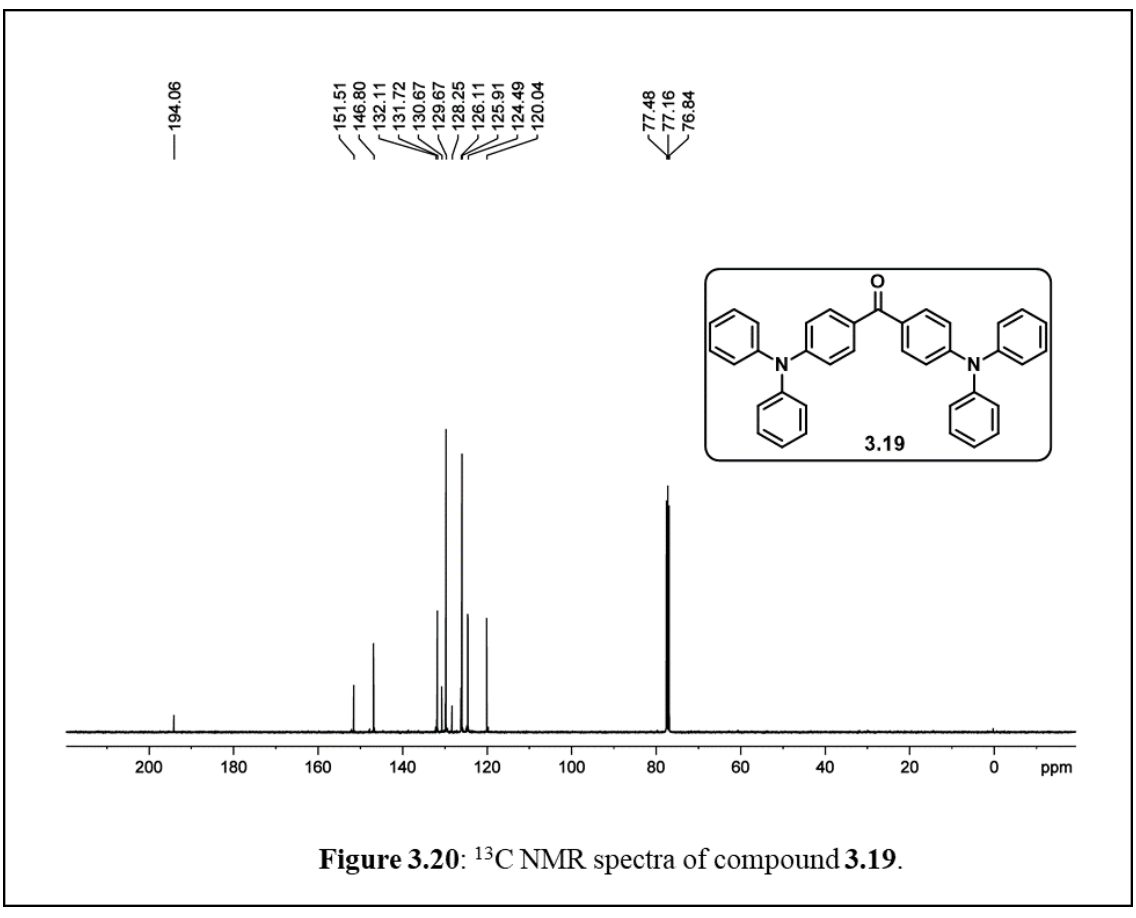


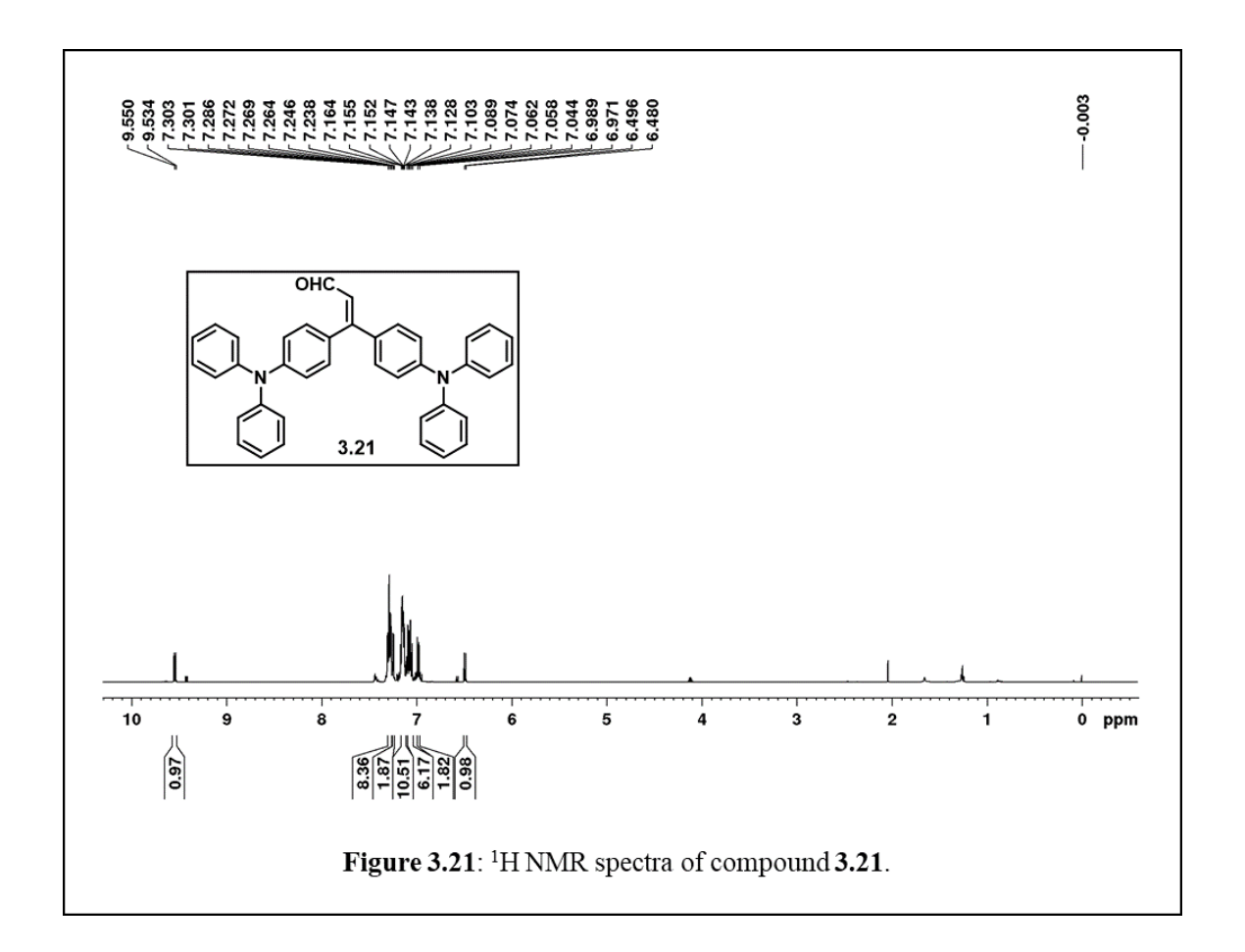


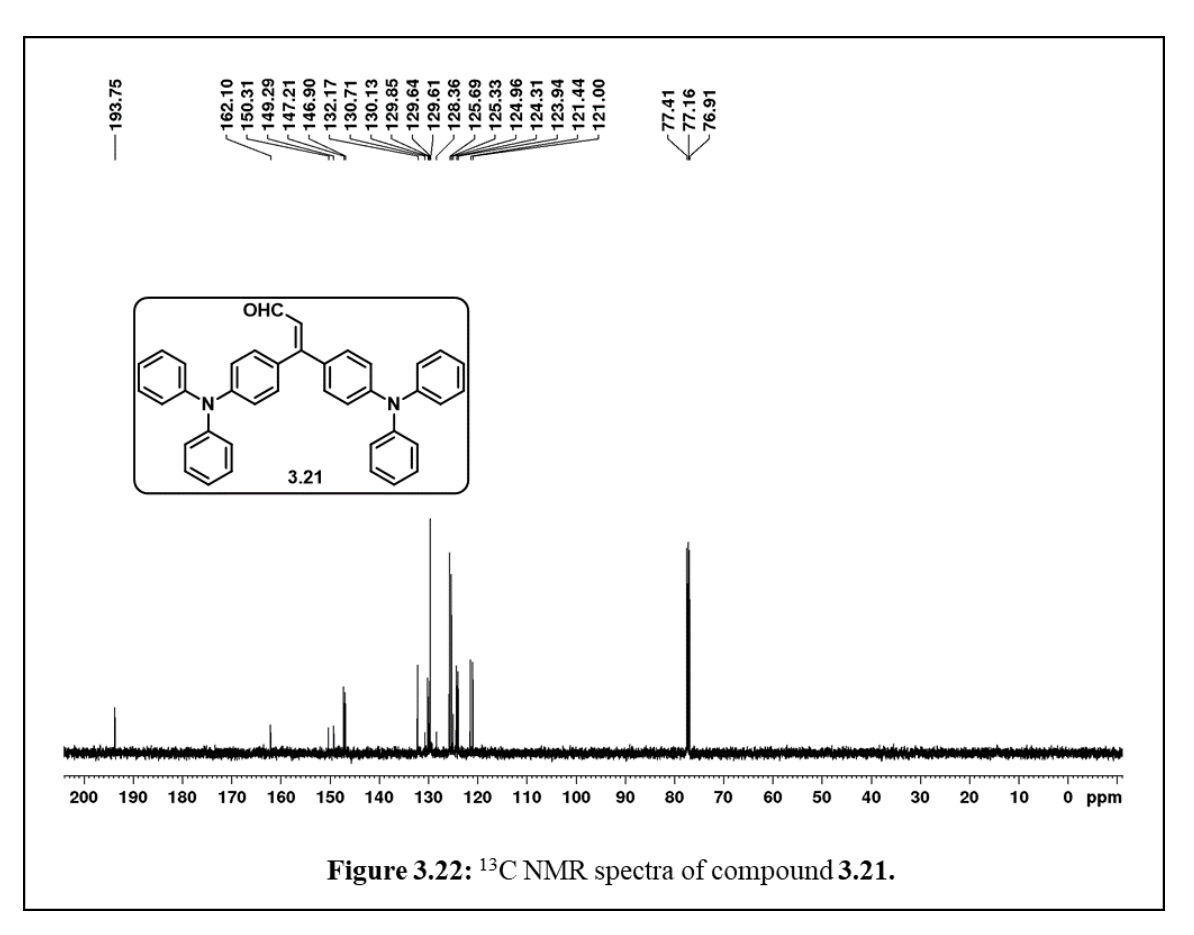


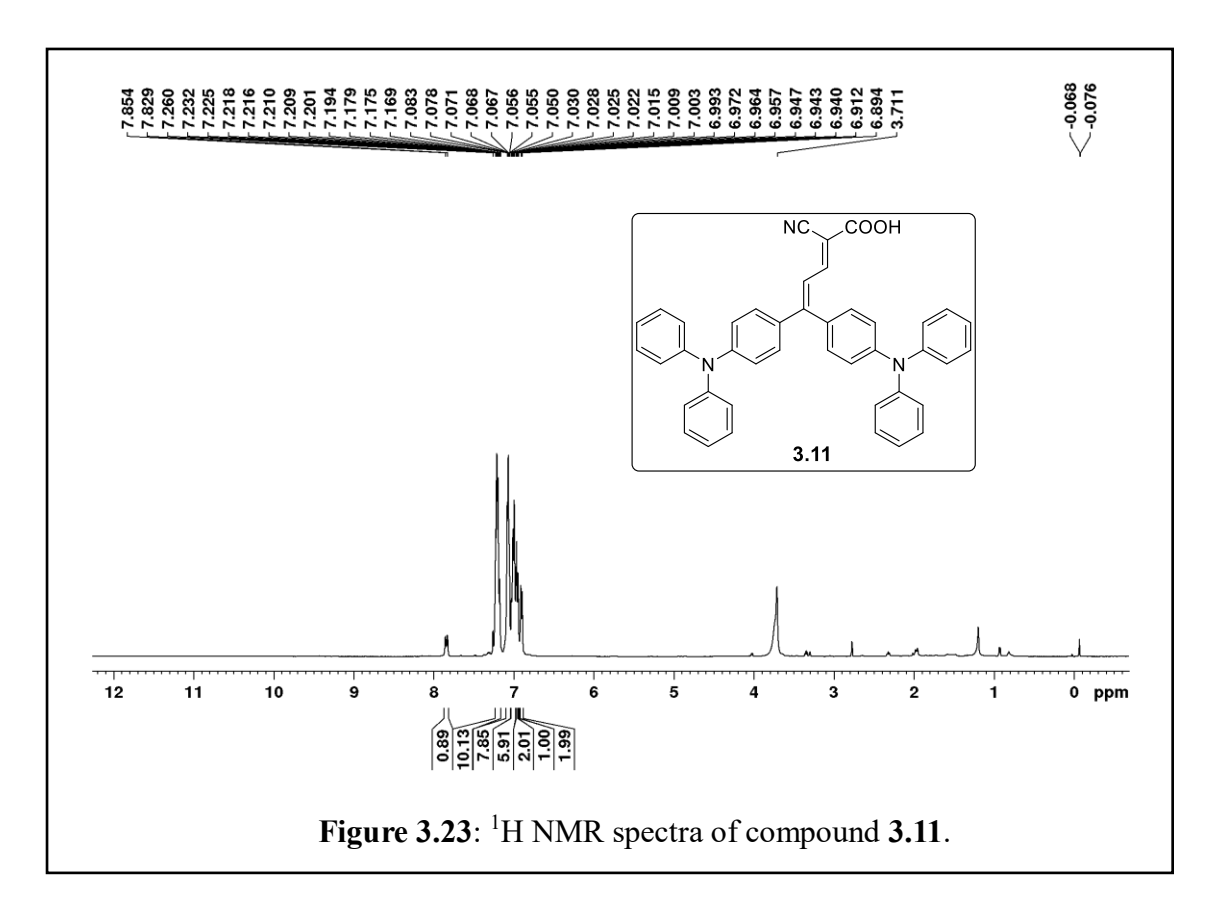


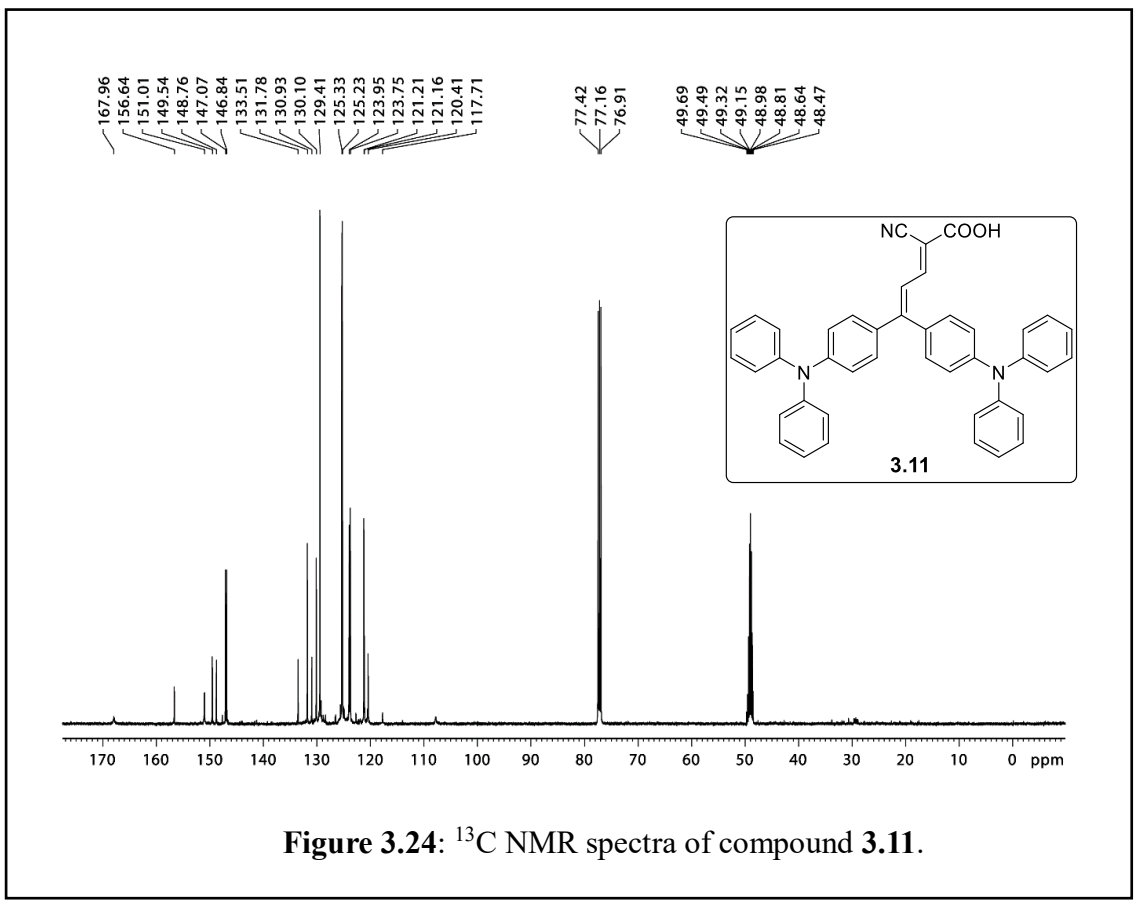












Bis-Acceptor Based Donor-Acceptor Systems and Their Application in DSSC

4.1 Introduction

In the previous chapter donor-acceptor systems containing bis-donor groups have been discussed. Compounds containing multiple acceptor units at different places have also been evaluated by different research groups. Keeping more acceptor moieties enhances the intramolecular charge transfer (ICT) from the donor moiety thereby reduce the HOMO-LUMO energy gap. Generally, compounds containing multiple cyano groups have been of greater interest in this regard. In 2007, Leriche *et al.* a reported donor-acceptor systems containing dicyano and tricyanovinylene groups linked to triphenylamine through a thiophene bridge **4.1** and **4.2** to study the structure-electronic properties. It was found that the tricyano derivatives exhibited absorption maximum 70 nm higher than that of the dicyanovinylene derivatives.

In 2010, Lee and co-workers^{2b} synthesized and studied the photophysical properties of molecular systems containing triphenylamine and multicyano groups for solar cell applications. They have investigated the optoelectronic properties of the synthesized organic dyes **4.3-4.6**. By increasing the number of cyano groups, the intramolecular charge transfer of new molecules can be tuned to get broad absorption bands in the near-infrared region.

Figure 4.1. Molecular structure of multi-cyano derivatives.

Sun and co-workers^{3a} designed a set of new donor-acceptor systems **4.7** and **4.8** having different number of electron-withdrawing groups for the application in dye-sensitized solar cells. They have concluded that increasing the number of cyano group in the donor-acceptor system had a significant influence in the photophysical, electrochemical, and photovoltaic properties. Boschloo and co-workers^{3b} reported a triphenylamine derivative armed on each phenyl ring with dicyanovinylene through thiophene ring **4.9**. The power conversion efficiency of the bulk heterojunction device made from this dye with poly (3,4-ethylene dioxythiophene): poly(styrene sulfonate) (PEDOT:PSS) was found to be 0.3%. He and co-workers^{4a} have synthesized a similar system by using two units of *n*-hexylthiophene in the π -bridge. These dyes improved the power conversion efficiency and the compound **4.10** was found to have 3.0% by using the solution-processed bulk-heterojunction organic solar cells (OSCs) method.

Lee and co-workers

Figure 4.2. Selected molecular structures of acceptor enriched donor-acceptors for solar cell applications.

Blanchard and co-workers^{4b} have reported the system in which triphenylamine is connected to tetracyano butadiene on each phenyl ring through varying numbers of thiophene bridge for application in organic solar cell. The dye **4.11** showed a maximum PCE of 1.0% with C_{60} acceptor, using the bilayer heterojunction method for device preparation.

4.1.1 Effect of Acceptor Geometry in DSSC

Many donor-acceptor systems developed so far utilizes cyanoacetic acid to constitute the acceptor moiety. The acid is used for attaching it to the TiO_2 surface. There is a chance for these systems to exist in E- and Z-isomers. This is pronounced when the olefin is tetrasubstituted. The effect of the E- and Z- configurations on the PCE of such donor-acceptor systems has not been studied so far. However, it has been studied with compounds having a CF_3 group in the place of CN. In 2013, Fang and co-workers⁵ reported E- and Z- isomers of trifluoromethyl acrylic acid derivatives and studied their efficiencies in dye-sensitized solar cell. Here, a phenothiazine group is attached with vinylene trifluoromethyl acrylic acid through a thiophene unit. Phenothiazine and thiophene units acts as donor and π -spacer, respectively. Whereas, the trifluoromethyl acrylic acid group acts as a strong acceptor/withdrawing unit where the carboxylic acid would anchor to titanium dioxide nanocrystals in the devices made using them. In this newly designed donor-acceptor dyes **4.14a** and **4.14b**, the Z-isomer has achieved a power conversion efficiency of 4.05%, which is much higher than the corresponding E-isomer. The E- isomers showed a PCE of 1.35%.

COOH
$$D_1(E)$$

$$D_2(Z)$$

$$\eta = 1.35\%$$

$$\eta = 4.05\%$$

$$4.14a$$

$$Fang and co-workers$$

Figure 4.3. Chemical structure of dyes containing *E*- and *Z*- isomers

From this literature study, we noticed that only a few reports are available for the acceptor enriched donor-acceptor systems for the application in organic solar cells as well as dyesensitized solar cells. Also, only one report exists that reports the differential behaviour of *E*-and *Z*- isomers at the acceptor moiety for dye-sensitized solar cells (DSSCs). In this line, we

have synthesized *E*- and *Z*- isomers of acceptor enriched donor-acceptor systems that have triphenylamine and N-phenyl carbazole donors for dye-sensitized solar cell application.

4.2 Synthesis of the Acceptor Enriched Donor-Acceptor Systems

A set of four acceptor enriched donor-acceptor compounds as shown in Figure 4.4 have been synthesized successfully having triphenylamine or N-phenylcarbazole as donor and cyanoacrylic acid and dicyano vinylene acceptors. The synthetic route for their synthesis is depicted in Scheme 4.1. The synthesis of intermediate compounds **4.22** and **4.23** involves; aryl lithium addition followed by oxidation. The compound **4.20** and **4.21** were prepared by the reaction of lithiated ethylene glycol protected p-bromobenzaldehyde **4.19**⁶ separately with a p-substituted aromatic aldehyde **4.17** and **4.18**.^{7,8}

Figure 4.4. Synthesized acceptor enriched organic dyes.

The secondary alcohols **4.20** and **4.21**, thus obtained, were oxidized in the presence of IBX to afford the corresponding ketone derivatives **4.22** and **4.23**. These compounds were deprotected with PTSA.H₂O in acetone at room temperature to afford compounds **4.24** and **4.25**, respectively. These two compounds were subjected to Knoevenagel condensation reaction separately with malononitrile in the presence of PPh₃ under neat conditions at 80 °C to obtain compounds **4.26** and **4.27** respectively. In these reactions, the Knoevenagel reaction occurred at the aldehyde function. The compounds **4.26** and **4.27** were subjected to one more Knoevenagel type reaction at the ketone site by reacting them with ethyl cyanoacetate in the presence of TiCl₄ and 4-methylmorpholine to obtain **4.28** and **4.29** respectively. These compounds were difficult to separate and along with ethyl cyanoacetate based impurity. Hydrolysis of **4.28** and **4.29** with LiOH afforded the target compounds **4.15a**, **4.15b**, **4.16a**,

and **4.16b**. While the E and Z isomers of compounds **4.28** and **4.29** were inseparable mixture, the E and Z isomers of the final acid derivatives (**4.15a** and **4.15b**; **4.16a** and **4.16b**) were separable to certain extend by column chromatography. In both the cases, the E isomer was the major product. We tried to make a few more derivatives containing aliphatic chain incorporated on the triphenylamine unit. Unfortunately, we could not get those derivatives due to the lack of stability of the product alcohol derivative under lithiation conditions.

Scheme 4.1. Synthetic route for the preparation of organic dyes 4.15a, 4.15b, 4.16a, and 4.16b.

The assignment of E and Z isomers was based on the 1H NMR spectroscopy. There are four doublets integrating for 2 protons each corresponding to the protons present in the two para disubstituted aryl rings. The two doublets appearing at the downfield region (7.85-8.00 and 7.35-7.50 ppm) are assigned to the protons of the aryl ring having dicyanovinylene group. This ring has two electron withdrawing groups at the para positions and so the aryl ring is

electron deficient. On the other hand, the protons present in the aryl ring attached to the electron donating diphenylamine group are expected to appear at comparatively upfield region. In this, the protons ortho to the amino group will have more electron density and thus the doublet appearing at 6.85-6.95 ppm is assigned to them. Whereas, the protons on the aryl ring meta to the amino group will appear at the comparatively downfield region due to the electron pulling nature of the cyano and carboxylic acid groups. So, the protons H_a and H_b are assigned to the doublets appearing at 7.1-7.2 ppm. In these two isomers, the cyano group is expected to have pronounced deshielding anisotropic effect as the carboxylic acid will have spatial constraints. So, the H_b in the *E*-isomer will be deshielded by the cyano group. Hence the more polar compound is assigned *E*-configuration (4.15b) and the less polar compound is assigned *Z*-configuration (4.15a) (Figure 4.5).

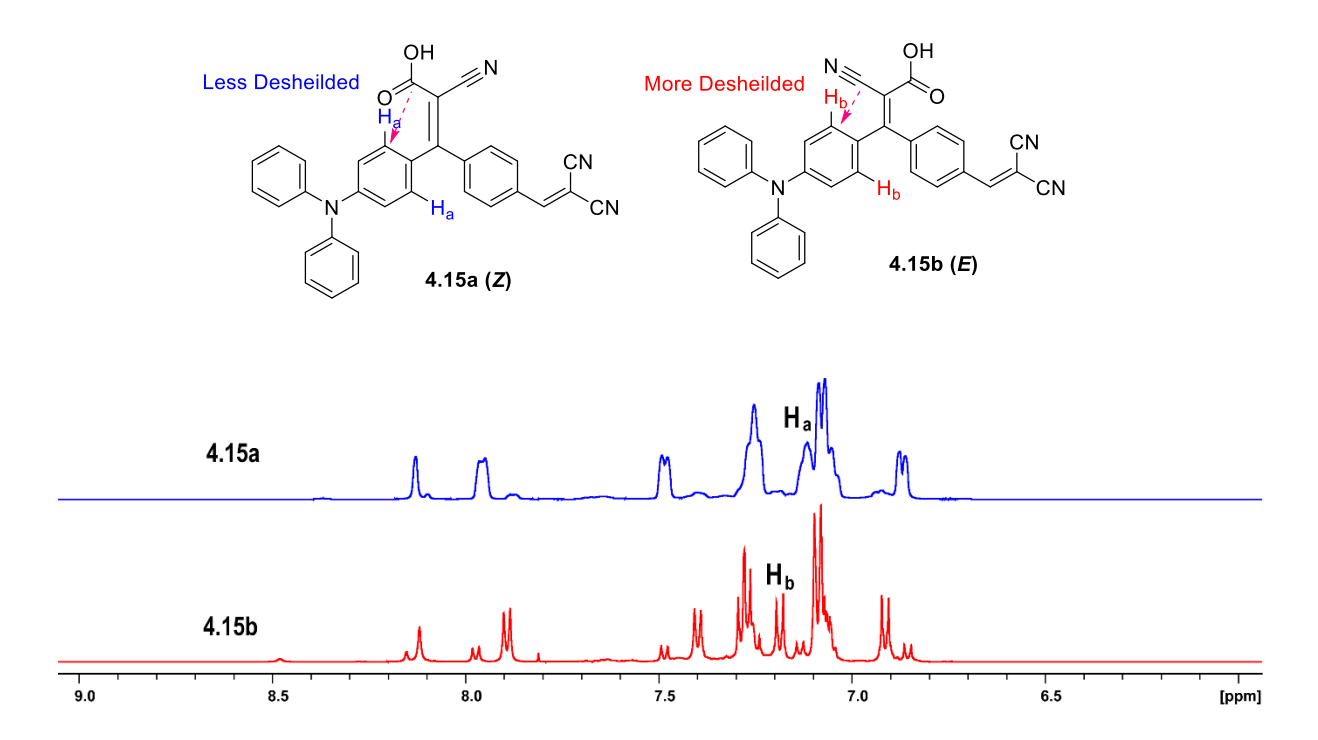


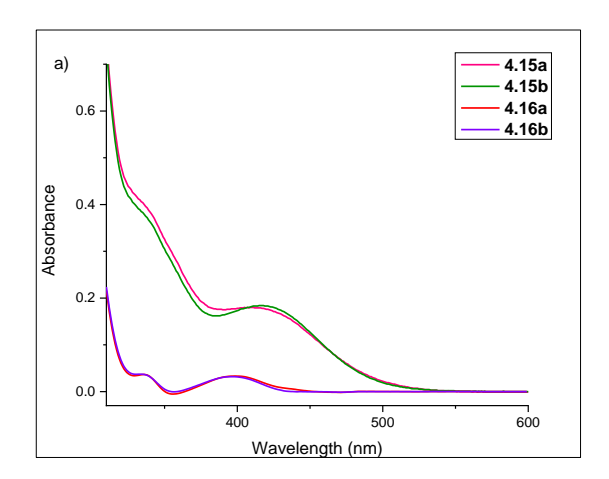
Figure 4.5. Comparison of ${}^{1}H$ NMR spectra in E and Z isomers.

4.3 Optical Properties

The absorption spectra of the acceptor-enriched triphenylamine and N-phenyl carbazole based donor-acceptor organic dyes in THF solvent were recorded and the results are shown in Figure 4.6a. Their elaborate photophysical properties are presented in Table 1. As seen in the table the absorption maximum for both the E and Z isomers in each case (4.15a and 4.15b; 4.16a and 4.16b) were very close. The solubility of these compounds were found to be weak

Chapter 4

in non-polar solvents compared to that in polar solvents. Two bands were observed in UV-Vis spectra having a strong absorption band appearing at 355-480 nm and a weak band at 320-350 nm. The strong absorption band of the donor-acceptors were assigned to the intramolecular charge transfer between the donor unit to the acceptor moiety of dicyanovinylene in the terminal. The shorter wavelength shoulder bands (340 nm for **4.15a**, 339 nm for **4.15b**, 338 nm for **4.16a** and 338 nm for **4.16b**) were attributed to the weak intramolecular charge transfer involving the donor moiety to the cyanoacrylic acid moiety.



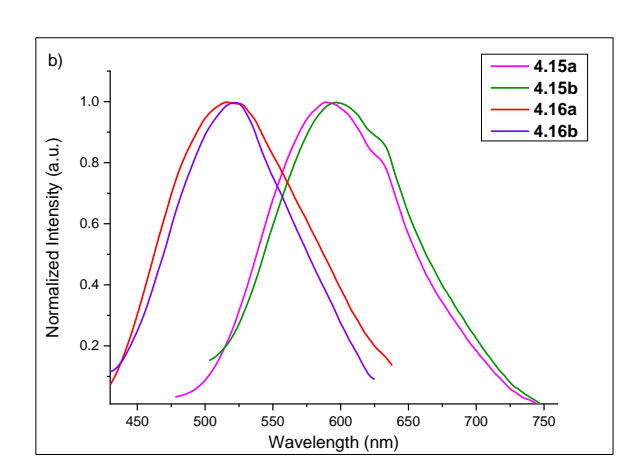


Figure 4.6. a) Absorption spectra of compounds **4.15a**, **4.15b**, **4.16a**, and **4.16b**; b) Normalized emission spectra of compounds **4.15a**, **4.15b**, **4.16a**, and **4.16b**. The UV-Vis and emission were recorded by using 1×10^{-5} M concentration in the THF solvent.

The emission spectra of the donor-acceptor organic dyes were recorded in the THF solvent by exciting at their corresponding longer wavelength absorption maximum, and the results are shown in Figure 4.6b. The triphenylamine derivatives **4.15a** and **4.15b** were excited at 421 nm and 423 nm, respectively, and their corresponding emission bands were obtained at 590 nm and 598 nm. The N-phenyl carbazole derivatives **4.16a** and **4.16b** exhibited their emission band at 517 nm and 521 nm, respectively. All four compounds displayed a single broadband of emission peak. In contrast to the absorption maximum, the emission maximum of the *E*- and *Z*-isomers in both the cases were different. The Stokes shifts of the *E* isomers were slightly higher than that of the *Z* isomers in both the cases. Fluorescence lifetime measurements were also carried out. All the compounds exhibited single exponential decay in THF. The lifetime of new organic dyes **4.15a**, **4.15b**, **4.16a**, and **4.16b** are 2.6 ns, 2.84 ns, 2.55 ns, and 2.84 ns, respectively. The quantum yield of all the derivatives was in the range of 0.05 to 0.1. When we compare the emission of the *E*- and *Z*-isomers in both the cases, the emission occurred at a

slightly higher wavelength for the *E*-isomer. The same trend is followed by other parameters such as Stokes shift, fluorescence quantum yield, and lifetime.

Table 1. Photophysical properties of dyes 4.15a-4.16b series in THF.

Dye	λ _{max} (nm)	λ em (nm)	Stokes Shift (nm)	$\mathbf{\phi_f}^{(a)}$	$\tau_{\rm f}({\rm ns})$
4.15a (Z)	421	590	169	0.05	2.6 ns
4.15b (<i>E</i>)	423	598	175	0.1	2.84 ns
4.16a (Z)	400	517	137	0.06	2.55 ns
4.16b (<i>E</i>)	400	521	141	0.08	2.84 ns

⁽a) Fluorescein in 0.1M NaOH was used as the reference $[\Phi f = 0.95 \pm 0.03]$

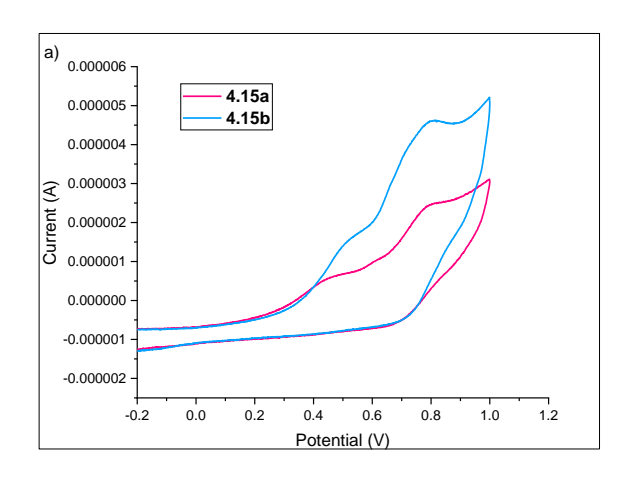
4.4 Cyclic Voltammetry

The redox behavior of dyes **4.15a**, **4.15b**, **4.16a**, and **4.16b** were evaluated individually using cyclovoltammetry in DMF solvent at room temperature at a scan rate of 100mV s^{-1} with Bu₄NClO₄ as a supporting electrolyte. Here, Ag/Ag⁺ acts as a reference electrode, a Pt disc acts as a working electrode, and a Pt wire is used as a counter electrode. The cyclic voltammogram of dyes **4.15a**, **4.15b**, and **4.16a**, **4.16b** are shown in Figure 4.7a, and 4.7b and the electrochemical parameters are summarized in table 2. All the compounds exhibited excellent oxidation and reduction curve. The *E* and *Z* isomers exhibited the same curve pattern in the cyclic voltammetry. Isomers **4.15a** and **4.15b** showed an oxidation potential of 0.79 V. On the other hand, the dyes **4.16a** and **4.16b** were found to have an oxidation potential of 0.64 V and 0. 70 V, respectively. The HOMO energy values of all the dyes have been calculated from the oxidation potential from cyclic voltammetry, and the LUMO energy values were obtained from their UV spectra by using the Tauc Plot.

Table 2. Cyclic Voltammetry of dye 4.15a – 4.16b

Dye	E° onset	НОМО	LUMO	НОМО	LUMO
	$(\mathbf{V})^{a}$	$(eV)^b$	$(eV)^c$	$(eV)^d$	$(eV)^d$
4.15a (Z)	0.67	-5.47	-2.85	-5.81	-3.38
4.15b (E)	0.60	-5.4	-2.8	-5.65	-3.44
4.16a (Z)	0.50	-5.3	-2.4	-5.93	-3.55
4.16b (<i>E</i>)	0.55	-5.35	-2.4	-5.83	-3.61

^a Obtained from cyclic voltammetry, ^bHOMO(eV) =-(Eox- E(Ag/Ag+) + 4.8) eV, ${}^{c}E_{LUMO} = E_{g}$ -HOMO, ^d DFT calculation by Gaussian 09 software.



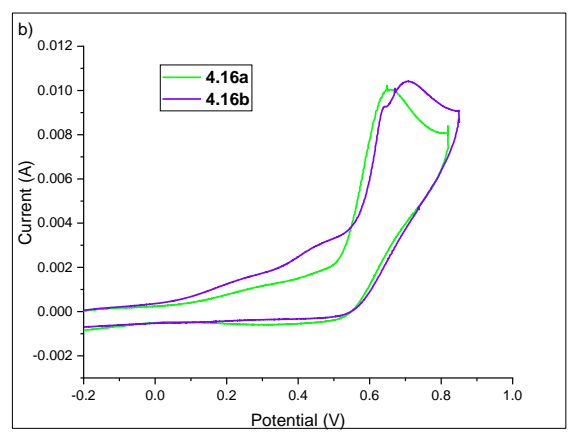


Figure 4.7. a) Cyclic voltammogram of the donor-acceptor systems **4.15a** and **4.15b**. b) Cyclic voltammogram of donor-acceptors **4.16a** and **4.16b**.

4.5 DFT studies

Time-dependent density functional theory (TD-DFT) calculation was performed to establish the electronic structure and to study the energy levels of these dyes (**4.15a**, **4.15b**, **4.16a**, and **4.16b**) by Gaussian 09 package using B3LYP/6-31G basic sets. The energies of each compound were calculated by TD-DFT calculation using B3LYP/6-31G basic sets, and the generated frontier molecular orbitals structures are shown in Figure 4.8. The HOMO (H) are localized on the donor unit triphenylamine in the dyes **4.15a** and **4.15b** and N-phenyl carbazole unit in the dyes **4.16a** and **4.16b** in addition to cyanoacrylic acid. On the other hand,

the LUMO (L) are mainly located on the dicyanovinylene and the phenyl ring connected to it in all the cases. Some amount of LUMO is also present on the cyano acrylic acid moiety.

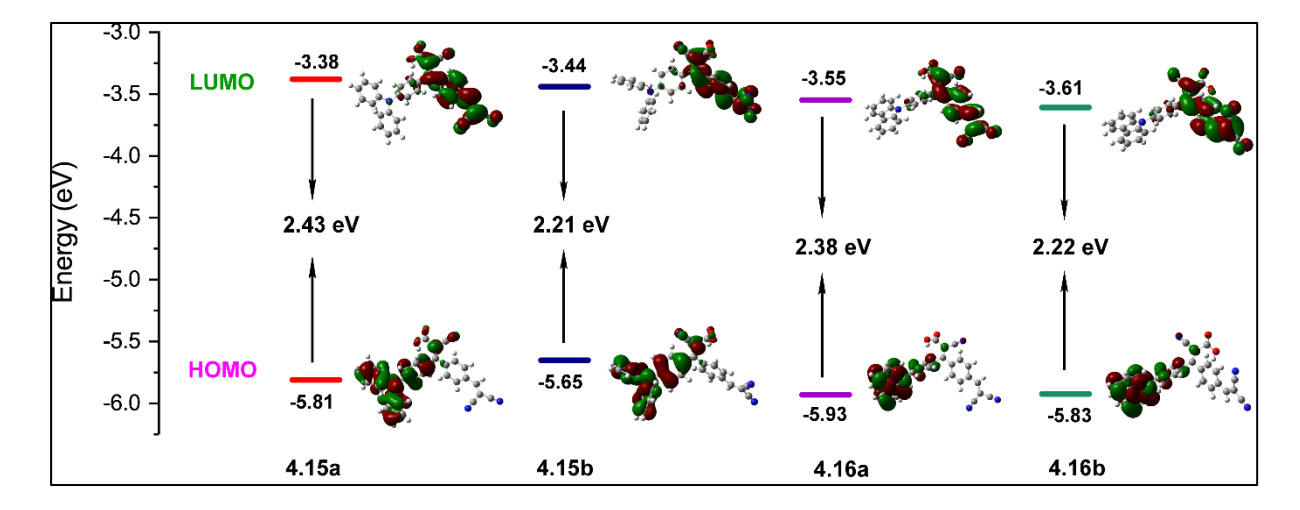


Figure 4.8. Molecular orbital energy diagram of the HOMO-LUMO of 4.15a, 4.15b, 4.16a, and 4.16b dyes.

The energy gap of dyes **4.15a**, **4.15b**, **4.16a** and **4.16b** were calculated as 2.43 eV, 2.21 eV, 2.38 eV, and 2.22 eV respectively. All the dyes have small HOMO-LUMO band gaps, and thus facile excitation from HOMO to LUMO is viable. Careful analysis of the results indicates that Z isomers show a marginally higher bandgap than that of the E isomers in both the derivatives.

4.6 Application in Dye-Sensitized Solar Cell.

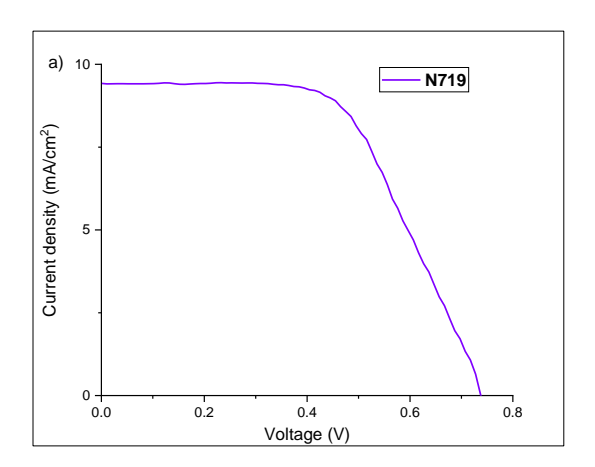
Following the literature survey, we have fabricated devices using **4.15a** and **4.15b** dyes and studied their efficiencies in dye-sensitized solar cells (DSSCs). Due to limited accessibility to the experiments, the other two compounds **4.16a** and **4.16b**, were not tested. Both the dyes were adsorbed well to the mesoporous TiO_2 nanocrystals, and the photovoltaic parameters such as fill factor (FF), short circuit photocurrent (J_{sc}), open circuit (V_{oc}) and the power conversion efficiency (PCE) are detailed in Table 3. The photocurrent density (J-V) curve is displayed in Figure 4.9.

The photovoltaic current parameters of dye-sensitized solar cell have been determined using a simulated AM 1.5G irradiation (100mWcm^{-2}) with iodine electrolyte (0.6 M 1,2-dimethyl-3-n-propylimidazolium iodide, 0.1 M LiI, 0.05 M I₂, and 0.5 M 4-tert-butylpyridine in acetonitrile). The thickness of mesoporous TiO_2 has been kept as $10 \mu \text{m}$ and the nanocrystalline layer to $2 \mu \text{m}$. The thickness of the layers was maintained the same in all the devices.

Table 3. DSSC parameters of dyes 4.15a, 4.15b, and reference N719.

Dye	$J_{\rm sc}$ (mA/cm ²)	V _{oc} (V)	FF	η (%)
4.15a (Z)	0.24	0.554	61.8	0.1
4.15b (E)	0.47	0.623	77.5	0.22
N719	9.40	0.740	58.5	4.01

The **N719** reference devices exhibited a power conversion efficiency of 4.01% with an open-circuit voltage of 0.740 V and a short circuit current density of 9.40 mA/cm². The device made out of the dye **4.15b** exhibited a better performance when compared with that made using the *Z*-isomer **4.15a**.



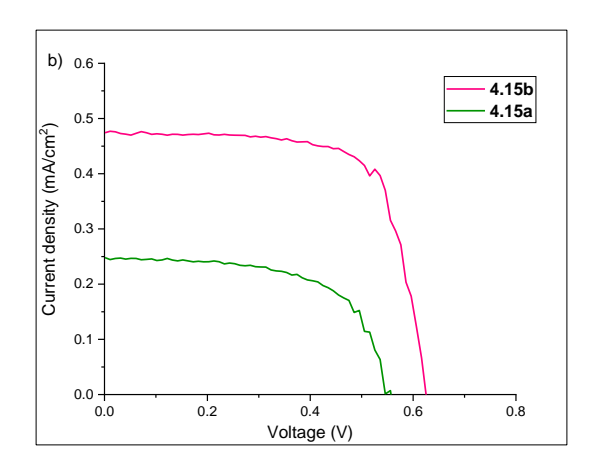


Figure 4.9. Photocurrent density-voltage (J-V) curves for the donor-acceptor based dye-sensitized solar TiO_2 electrodes. a) Reference **N719** dye; b) Dye **4.15a** and **4.15b**.

The device made using the E-isomer **4.15b** exhibited a power conversion efficiency of 0.22% with an open-circuit voltage of 0.62 V with a short circuit current density of 0.47 mA/cm² and the one made with the Z-isomer **4.15a** has performed with a power conversion efficiency of 0.1% with an open circuit voltage 0.55 V, short circuit voltage 0.24 mA/cm². The devices with **4.15a** and **4.15b** exhibited a better fill factor when compared with the reference devices **N719**.

4.7 Conclusion

A set of acceptors enriched organic dyes **4.15a**, **4.15b**, **4.16a**, and **4.16b** have been synthesized successfully, and their photophysical properties were evaluated. While the absorption characteristics of both *Z*- and *E*-isomers were almost similar, the emission properties were slightly different for the isomers. The *E*-isomer possessed slightly higher emission maximum, Stokes shift, fluorescence quantum yield, and lifetime. These dyes exhibit oxidation-reduction potential with low bandgap. The dyes **4.15a** and **4.15b** were tested for their application in dye-sensitized solar cells (DSSC). Both the dyes responded to the (*J-V*) experiments. The dyes **4.15a** and **4.15b** generated a power conversation efficiency of 0.1% and 0.22%, respectively.

4.8 Experimental Section

4.8.1 General Information.

General information, see: chapter 2, section 2.7.1. For device fabrication, see: chapter 2, section 2.7.2.

4.8.2 Experimental Procedure and Analytical Data

4.8.2.1 Synthesis of 4-(diphenyl amino) benzaldehyde (4.17):⁷

 $POCl_3$ (1.3 mL, 8.15 mmol) was added dropwise to the solution of triphenylamine (1 g, 4.0 mmol) in dry DMF (10 mL) at 0°C and allowed to stir 50-55 °C for 14 h. The reaction progress

was monitor by TLC using 20% EtOAc/ Hexane mixture as a mobile phase. After completion of the reaction, the reaction mixture was poured into ice-cold water and extracted with EtOAc ($2 \times 50 \text{mL}$). The organic layer was washed with H₂O (50 mL) and brine solution (10 mL). The organic layer

was dried over NaSO₄, filtered, concentrated using under vacuum. The product was purified by column chromatography using 1:5 EtOAc/hexanes at R_f = 0.80. Pale yellow solid (0.8 g, yield = 72%); MP: 149-150°C; ¹H NMR (400 MHz, CDCl₃): δ 9.80 (s, 1H), 7.67 (d, J = 8.8 Hz, 2H), 7.34 (t, J = 7.6 Hz, 4H), 7.17 (d, J = 6.8 Hz, 6H), 7.01 (d, J = 8.8 Hz, 2H); ¹³C NMR (100 MHz, CDCl₃): δ 190.5, 153.4, 146.2, 131.4, 129.8, 129.2, 126.4, 126.2, 119.4.

4.8.2.2 Synthesis of 4-(9H-carbazol-9-yl) benzaldehyde (4.18):8

To a stirred solution of carbazole (1 g, 5.98 mmol), K₂CO₃ (2.5 g, 17.94 mmol) in DMF (20 mL), 4-fluoro benzaldehyde (0.742 g, 5.98 mmol) was added and maintained 150°C for 12 h. The reaction mixture poured into ice water.

The resulting precipitate was collected by filtration and washed with water, methanol, ethanol, and n-hexane consecutively. The filtrate was dried under vacuum. Pale yellow solid (1.5 g, yield = 92%); ¹H NMR (500 MHz, CDCl₃): δ 10.07

under vacuum. Pale yellow solid (1.5 g, yield = 92%); 1 H NMR (500 MHz, CDCl₃): δ 10.07 (s, 1H), 8.18 (d, J = 6.5 Hz, 2H), 8.08 (d, J = 6.5 Hz, 2H), 7.74 (d, J = 7.0 Hz, 2H), 7.51 (s, 2H), 7.46 (s, 2H), 7.37 (s, 2H); 13 C NMR (125 MHz, CDCl₃): δ 190.9, 143.2, 140.0, 134.5, 131.3, 126.6, 126.3, 123.9, 120.8, 120.5, 109.7.

4.8.2.3 Synthesis of 2-(4-bromophenyl)-1,3-dioxolane (4.19):⁶

4-bromo benzaldehyde (1.5 g, 8.10 mmol), ethylene glycol (0.9 mL, 16.21 mmol), and PTSA.H₂O (0.3 g, 1.62 mmol) were taken in toluene (40 mL) and allowed to stir vigorously for 16 h under reflux condition using a Dean-Stark setup. The reaction mixture was then poured into 10% aqueous NaOH (100 mL)

solution and extracted with EtOAc (2 × 30 mL) and washed with water. The organic layer was

solution and extracted with EtOAc (2 × 30 mL) and washed with water. The organic layer was combined and dried over anhydrous sodium sulfate. The organic phase was concentrated under vacuum. The crude was directly used for next step without further purification. Brown liquid (1.5 g, yield = 80%); 1:5 EtOAc/hexanes at R_f = 0.56. ¹H NMR (400 MHz, CDCl₃): δ 7.51 (d, J = 8.4 Hz, 2H), 7.35 (d, J = 8.4 Hz, 2H), 5.75 (s, 1H), 4.08-4.06 (m, 2H), 4.01-3.99 (m, 2H); ¹³C NMR (100 MHz, CDCl₃): δ 137.0, 131.5, 128.2, 123.2, 103.0, 65.3.

4.8.2.4 Synthesis of (4-(1,3-dioxolan-2-yl) phenyl) (4-(diphenyl amino) phenyl) methanol (4.20):

To a stirred solution of compound **4.19** (1.26 g, 5.48 mmol) in dry THF (20 mL), 1.6 M n-BuLi in hexane (4.6 mL, 7.31 mmol) was added at -78 °C and allow to stir for 1 h. Then,

compound **4.17** (1 g, 3.65 mmol) was added to the reaction mixture and maintained -78 °C for 2 h followed by room temperature for 12 h. The reaction progress was monitored by TLC. The reaction mixture neutralized with saturated NH₄Cl

(2×20 mL) solution and extracted with EtOAc (2×20 mL). The product was purified by column chromatography using 1:5 EtOAc/hexanes at R_f = 0.16. Pale yellow viscos (0.8 g, yield = 52%); ¹H NMR (400 MHz, CDCl₃): δ 7.44 (d, J = 8.0 Hz, 4H), 7.22 (q, J = 7.6 Hz, 6H), 7.06 (d, J =

7.6 Hz, 4H), 7.02-6.98 (m, 4H), 5.79 (d, J = 2.4 Hz, 2H), 4.13-4.11 (m, 2H), 4.04-4.01 (m, 2H); ¹³C NMR (100 MHz, CDCl₃): δ 147.7, 147.4, 145.1, 137.8, 137.1, 129.3, 127.6, 126.7, 126.5, 124.3, 123.8, 122.9, 103.6, 75.8, 65.4; IR (neat): υ 3391, 2870, 1697, 1486, 1313, 1076, 752, 694 cm⁻¹; HRMS (ESI): calcd for $C_{28}H_{25}NO_3$ [M+H]⁺ 424.1907, Found 424.1907.

4.8.2.5 Synthesis of (4-(1,3-dioxolan-2-yl) phenyl) (4-(9H-carbazol-9-yl) phenyl) methanol (4.21):

To a stirred solution of compound 4.19 (1.3 g, 5.52 mmol) in dry THF (20 mL), 1.6 M n-

BuLi in hexane (4.6 mL, 7.37 mmol) was added at -78 °C and allow to stir for 1 h. Then, compound **4.18** (1 g, 3.68 mmol) was added to the reaction mixture and maintained -78 °C for 2 h followed by room temperature for 12 h. The reaction progress

was monitored by TLC. The reaction mixture neutralized with saturated NH₄Cl (2×20 mL) solution and extracted with EtOAc (2×20 mL). The product was purified by column chromatography using 1:5 EtOAc/hexanes at $R_f = 0.22$. Pale yellow viscos (0.76 g, yield = 49%); ¹H NMR (500 MHz, CDCl₃): δ 8.18 (d, J = 8.0 Hz, 2H), 7.58 (d, J = 8.0 Hz, 2H), 7.55-7.49 (m, 6H), 7.42 (d, J = 4.0 Hz, 4H), 7.35-7.31 (m, 2H), 5.90 (s, 1H), 5.83 (s, 1H), 4.13-4.12 (m, 2H), 4.04-4.03 (m, 2H), 2.98 (br s, 1H); ¹³C NMR (125 MHz, CDCl₃): δ 144.8, 142.9, 140.8, 137.4, 136.9, 128.0, 127.0, 126.8, 126.6, 125.9, 123.4, 120.3, 120.0, 109.8, 103.5, 75.6, 65.3; IR (neat): v 3415, 2881, 1597, 1449, 1334, 1015, 722, 663 cm⁻¹; HRMS (ESI): calcd for $C_{28}H_{23}NO_3$ [M+H]⁺ 422.1751, Found 422.1747.

4.8.2.6 Synthesis of (4-(1,3-dioxolan-2-yl) phenyl) (4-(diphenyl amino) phenyl) methanone (4.22):

IBX (0.81 g, 2.89 mmol) was added to the stirred solution of compound **4.20** (1 g, 1.92 mmol) in acetonitrile (8): (1) DMSO (15 mL) at open air condition and allow to stir room

temperature for 3 h. The reaction was monitored by TLC. The reaction mixture was filtered through—filter paper and the filtrate was extracted with CH_2Cl_2 (2×20 mL). The product was purified by column chromatography using 1:5 EtOAc/hexanes at $R_f = 0.56$. Yellow solid (0.7 g, yield = 86%); MP: 139-140°C;

¹H NMR (400 MHz, CDCl₃): δ 7.78 (d, J = 7.6 Hz, 2H), 7.69 (d, J = 8.8 Hz, 2H), 7.58 (d, J = 8.0 Hz, 2H), 7.32 (t, J = 7.6 Hz, 4H), 7.19-7.12 (m, 6H), 7.00(d, J = 8.4 Hz, 2H), 5.88 (s, 1H), 4.15-4.12 (m, 2H), 4.07-4.06 (m, 2H); ¹³C NMR (100 MHz, CDCl₃): δ 194.8, 152.1, 146.5,

141.5, 139.2, 132.0, 129.8, 129.7, 126.3, 126.1, 124.7, 119.5, 103.2, 65.4; IR (neat): υ 2874, 2221, 1642, 1578, 1485, 1311, 1276, 751, 695 cm⁻¹; HRMS (ESI): calcd for $C_{28}H_{23}NO_3$ [M+H]⁺ 422.1751, Found 422.1750.

4.8.2.7 Synthesis of (4-(1,3-dioxolan-2-yl) phenyl) (4-(9H-carbazol-9-yl) phenyl) methanone (4.23):

IBX (0.79 g, 2.84 mmol) was added to the stirred solution of compound **4.21** (0.8 g, 1.89 mmol) in acetonitrile (8): (1) DMSO (10 mL) at open air condition and allow to stir room

temperature for 3 h. The reaction was monitored by TLC. The reaction mixture was filtered through filter paper and the filtrate was extracted with CH_2Cl_2 (2×15 mL). The product was purified by column chromatography using 1:5 EtOAc/hexanes

at $R_f = 0.54$. Pale yellow solid (0.58 g, yield = 73%); MP: 155-157°C; ¹H NMR (500 MHz, CDCl₃): δ 8.16 (d, J = 8.0 Hz, 2H), 8.07 (d, J = 8.0 Hz, 2H), 7.94 (d, J = 7.5 Hz, 2H), 7.72 (d, J = 8.0 Hz, 2H), 7.68 (d, J = 8.0 Hz, 2H), 7.54 (d, J = 8.5 Hz, 2H), 7.46 (t, J = 8.0 Hz, 2H), 7.34 (t, J = 7.5 Hz, 2H), 5.92 (s, 1H), 4.17-4.15 (m, 2H), 4.09-4.06 (m, 2H); ¹³C NMR (125 MHz, CDCl₃): δ 195.1, 142.4, 141.7, 140.2, 138.0, 135.8, 131.8, 130.0, 126.5, 126.2, 123.8, 120.6, 120.4, 109.8, 102.9, 65.4; IR (neat): υ 3052, 2884, 1654, 1595, 1478, 1226, 1168, 750, 696 cm⁻¹; HRMS (ESI): calcd for $C_{28}H_{21}NO_3$ [M+H]⁺ 420.1594, Found 420.1594.

4.8.2.8 Synthesis of 4-(4-(diphenyl amino) benzoyl) benzaldehyde (4.24):

To a stirred solution of substituted compound **4.22** (0.3 g, 0.71 mmol) in acetone (5 mL), PTSA.H₂O (0.03 g, 0.14 mmol) was added to it and stirred room temperature for 4 h under

nitrogen atmosphere condition. The reaction progress was monitored by TLC using 20% EtOAc/Hexanes mixture. The reaction mixture was neutralized with NaHCO₃ (15 mL) and extracted with EtOAc (2×15 mL). The solvent was reduced under vacuum. The product was purified by column chromatography

using 1:5 EtOAc/hexanes at $R_f = 0.51$. Yellow viscos (0.8 g, yield = 92%); ¹H NMR (400 MHz, CDCl₃): δ 10.09 (s, 1H), 7.96 (d, J = 8.0 Hz, 2H), 7.87 (d, J = 8.0 Hz, 2H), 7.68 (d, J = 7.6 Hz, 2H), 7.33 (t, J = 8.0 Hz, 4H), 7.19-7.13 (m, 6H), 6.99 (d, J = 8.8 Hz, 2H); ¹³C NMR (100 MHz, CDCl₃): δ 194.0, 191.7, 152.5, 146.2, 143.8, 138.0, 132.1, 129.9, 129.7, 129.4, 128.4, 126.2, 125.0, 119.1; IR (neat): υ 3056, 2844, 1703, 1554, 1313, 1144, 755, 698 cm⁻¹; HRMS (ESI): calcd for $C_{26}H_{19}NO_2$ [M+H]⁺ 378.1489, Found 378.1487.

4.8.2.9 Synthesis of 4-(4-(9H-carbazol-9-yl) benzoyl) benzaldehyde (4.25):

To a stirred solution of substituted compound 4.23 (0.42 g, 1.0 mmol) in acetone (5 mL), PTSA.H₂O (0.03 g, 0.2 mmol) was added to it and stirred room temperature for 4 h under

nitrogen atmosphere condition. The reaction progress was monitored by TLC using 20% EtOAc/Hexanes mixture. The reaction mixture was neutralized with NaHCO₃ (15 mL) and extracted with EtOAc (2×15 mL). The product was purified by

column chromatography using 1:5 EtOAc/hexanes at R_f = 0.70. Pale yellow solid (0.35 g, yield = 93%); MP: 144-146°C; ¹H NMR (500 MHz, CDCl₃): δ 10.1 (s, 1H), 8.15 (d, J = 7.5 Hz, 2H), 8.07 (d, J = 8.5 Hz, 2H), 8.04-8.01 (m, 4H), 7.76 (d, J = 8.5 Hz, 2H), 7.54 (d, J = 8.5 Hz, 2H), 7.45 (t, J = 8.5 Hz, 2H), 7.33 (t, J = 8.0 Hz, 2H); ¹³C NMR (125 MHz, CDCl₃): δ 194.7, 191.6, 142.47, 142.43, 140.2, 138.7, 135.0, 132.0, 130.3, 129.7, 126.4, 126.3, 124.0, 120.8, 120.6, 109.8; IR (neat): ν 3053, 2929, 1699, 1594, 1447, 1334, 1202, 719, 679 cm⁻¹; HRMS (ESI): calcd for $C_{26}H_{17}NO_2$ [M+H]⁺ 376.1332, Found 376.1332.

4.8.2.10 Synthesis of 2-(4-(4-(diphenyl amino) benzoyl) benzylidene) malononitrile (4.26):⁹

Malononitrile (0.05 g, 0.73 mmol), compound **4.24** (0.23 g, 0.60 mmol), and PPh₃ (0.03 g, 0.12 mmol) were stirred at 80°C for 4 h. The reaction was monitor by TLC using 20%

EtOAc/Hexane mobile phase. The reaction was diluted with water (10 mL) and extracted with EtOAc (2×15 mL). The organic layer was dried over anhydrous sodium sulphate and dried over under vacuum. The product was purified by column

chromatography using 1:3 EtOAc/hexanes at $R_f = 0.56$. Red solid (0.19 g, yield = 73%); MP: 208-210°C; ¹H NMR (400 MHz, CDCl₃): δ 7.99 (d, J = 8.4 Hz, 2H), 7.87 (d, J = 8.0 Hz, 3H), 7.67 (d, J = 8.8 Hz, 2H), 7.35 (t, J = 8.0 Hz, 4H), 7.20-7.15 (m, 6H), 7.00 (d, J = 8.8 Hz, 2H); ¹³C NMR (100 MHz, CDCl₃): δ 193.2, 158.8, 152.7, 146.1, 143.7, 133.0, 132.1, 130.4, 130.3, 129.8, 128.0, 126.3, 125.2, 119.0, 113.4, 112.3, 84.5; IR (neat): υ 3036, 2226, 1649, 1580, 1311, 1216, 751, 691 cm⁻¹; HRMS (ESI): calcd for $C_{29}H_{19}N_{3}O$ [M+H]⁺ 426.1601, Found 426.1601.

4.8.2.11 Synthesis of 2-(4-(4-(9H-carbazol-9-yl) benzylidene) malononitrile **(4.27)**:

Malononitrile (0.11 g, 1.73 mmol), compound **4.25** (0.65 g, 1.73 mmol), and PPh₃ (0.09 g, 0.34 mmol) were stirred at 80°C for 4 h. The reaction was monitor by TLC using 20% EtOAc/Hexane mobile phase. The reaction was diluted with water (20 mL) and extracted with

EtOAc (2×15 mL). The organic layer was dried over anhydrous

sodium sulphate and dried over under vacuum. The product was purified by column chromatography using 1:5 EtOAc/hexanes at $R_f = 0.40$. Red solid (0.61 g, yield = 84%); MP: 212-214°C; ¹H NMR (500 MHz, CDCl₃): δ 8.15 (d, J = 7.5 Hz, 2H), 8.06 (t, J = 8.5 Hz, 4H), 8.01 (d, J = 8.0 Hz, 2H), 7.85 (s, 1H), 7.77 (d, J = 8.0 Hz, 2H), 7.54 (d, J = 8.5 Hz, 2H), 7.45 (t, J = 8.0 Hz, 2H), 7.34 (d, J = 7.5 Hz, 2H); ¹³C NMR (125 MHz, CDCl₃): δ 193.9, 158.5, 142.6, 142.1, 140.2, 134.7, 133.9, 132.0, 130.7, 130.6, 126.5, 126.4, 124.0, 120.9, 120.6, 113.3, 112.2, 109.8, 85.4; IR (neat): υ 3005, 2221, 1662, 1591, 1478, 1304, 1219, 749, 614 cm⁻¹; HRMS (ESI): calcd for C₂₉H₁₇N₃O [M+Na]⁺ 446.1264, Found 446.1263.

4.8.2.12 Synthesis of ethyl 2-cyano-3-(4-(2,2-dicyanovinyl) phenyl)-3-(4-(diphenylamine) **phenyl)** acrylate (4.28):¹⁰

The mixture of compound 4.26 (0.36 g, 0.84 mmol), ethyl cyano acetate (0.9 mL, 8.46 mmol), 4-methyl morpholine (0.93 mL, 8.46 mmol) in dry CH₂Cl₂ (10 mL) were allow to stir

at 0°C for 10 min. TiCl₄ (0.92 mL, 8.46 mmol) was added to it and the reaction allow to stir room temperature for 30 min. The reaction progress was monitored by TLC. The reaction mixture poured into the water (20 mL), washed with ammonium chloride solution (30 mL) and extracted with dichloromethane (2×15 mL).

The product was purified by column chromatography using 1:3 EtOAc/hexanes at $R_f = 0.54$. Red viscos (0.37 g, yield = 84%); **Major isomer**; ¹H NMR (500 MHz, CDCl₃): δ 8.25 (br s, 1H), 8.06-8.00 (m, 2H), 7.56 (d, J = 9.5 Hz, 1H), 7.33-7.30 (m, 5H), 7.27 (br s, 1H), 7.18-7.11(m, 6H), 6.96 (d, J = 10.5 Hz, 1H), 6.93-6.90 (m, 2H), 4.39 (q, J = 7.5 Hz, 2H), 1.40 (t, J = 7.5Hz. 3H); ¹³C NMR (125 MHz, CDCl₃): δ 167.3, 162.7, 162.2, 153.7, 151.6, 146.3, 144.1, 132.2, 131.8, 130.6, 130.1, 129.7, 128.3, 126.4, 125.2, 118.8, 117.6, 115.2, 104.2, 100.8, 62.9, 13.9; **Minor isomer**; ¹H NMR (500 MHz, CDCl₃): δ 8.26 (br s, 1H), 8.06-8.00 (m, 2H), 7.56 (d, J =9.5 Hz, 1H), 7.33-7.30 (m, 5H), 7.27 (br s, 1H), 7.18-7.11 (m, 6H), 6.96 (d, J = 10.5 Hz, 1H), 6.93-6.90 (m, 2H), 4.40 (q, J = 7.0 Hz, 2H), 1.40 (t, J = 6.5 Hz, 3H); ¹³C NMR (125 MHz, CDCl₃): δ 166.7, 162.7, 162.0, 153.4, 150.9, 145.9, 143.4, 132.5, 131.4, 130.9, 129.7, 128.9, 126.1, 124.8, 119.2, 117.1, 115.1, 104.8, 102.4, 63.0, 13.9; IR (neat): υ 3042, 2981, 2213, 1720, 1558, 1317, 1176, 834 cm⁻¹; HRMS (ESI): calcd for $C_{34}H_{24}N_4O_2$ [M+Na]⁺ 543.1791, Found 543.1794.

4.8.2.13 Synthesis of ethyl 3-(4-(9H-carbazol-9-yl) phenyl)-2-cyano-3-(4-(2,2-dicyanovinyl) phenyl) acrylate (4.29):

Ethyl cyano acetate (1.2 mL, 11.80 mmol), compound **4.27** (0.5 g, 1.18 mmol), 4-methyl morpholine (1.3 mL, 11.80 mmol) in dry CH₂Cl₂ (20 mL) the mixture was allowed to stir at

0°C for 10 min. TiCl₄ (1.3 mL, 11.80 mmol) was added to it and the reaction allow to stir room temperature for 30 min. The reaction progress was monitored by TLC. The reaction mixture poured into the water (30 mL), washed with ammonium chloride solution (40 mL) and extracted with dichloromethane

(2×20 mL). The product was purified by column chromatography using 1:3 EtOAc/hexanes at R_f = 0.6. Red viscos (0.52 g, yield = 86%); **Major isomer;** 1 H NMR (500 MHz, CDCl₃): δ 8.29 (s, 1H), 8.14 (t, J = 7.5 Hz, 4H), 7.67-7.63 (m, 4H), 7.53-7.49 (m, 2H), 7.45-7.39 (m, 4H), 7.32 (t, J = 7.0 Hz, 2H), 4.41 (q, J = 7.0 Hz, 2H), 1.42 (t, J = 7.5 Hz, 3H); 13 C NMR (125 MHz, CDCl₃): δ 166.3, 162.0, 153.4, 143.0, 141.2, 140.2, 135.6, 133.9, 131.9, 130.9, 129.9, 126.5, 126.3, 123.9, 120.8, 120.5, 116.4, 115.2, 109.9, 106.0, 105.2, 63.0, 13.9; **Minor isomer;** 1 H NMR (500 MHz, CDCl₃): δ 8.27 (s, 1H), 8.06 (d, J = 8.5 Hz, 4H), 7.67-7.63 (m, 4H), 7.53-7.49 (m, 2H), 7.45-7.39 (m, 4H), 7.32 (t, J = 7.0 Hz, 2H), 4.41 (q, J = 7.0 Hz, 2H), 1.42 (t, J = 7.5 Hz, 3H); 13 C NMR (125 MHz, CDCl₃): δ 165.8, 161.9, 153.0, 142.3, 140.1, 136.2, 133.0, 131.9, 131.0, 130.8, 129.9, 126.4, 126.2, 123.8, 120.6, 120.5, 116.2, 115.0, 109.7, 105.4, 104.7, 63.0, 13.8; IR (neat): υ 3030, 2983, 2221, 1723, 1597, 1478, 1334, 1207, 756, 612 cm $^{-1}$; HRMS (ESI): calcd for C_{34} H₂₂N₄O₂ [M+H] $^+$ 519.1816, Found 519.1813.

4.8.2.14 Synthesis of (Z)-2-cyano-3-(4-(2,2-dicyanovinyl) phenyl)-3-(4-(diphenyl amino) phenyl) acrylic acid (4.15a):¹⁰

To a stirred solution of ester derivative of compound **4.28** (0.28 g, 0.53 mmol) in CH₃CN (10 mL), LiOH (excess, 0.45 g, 10.75 mmol) dissolved in water (10 mL) was treated to it and

allowed to stir room temperature for 4 h. The acetonitrile solvent was removed under reduced pressure. The crude was extracted with EtOAc (3×15 mL) and acidified with 10% HCl water solution. The product was purified by column chromatography using 1:3 MeOH/EtOAc at $R_f = 0.41$. **Z- isomer**; Red solid (0.035)

g, yield = 14%); MP: 237-239°C; ¹H NMR (500 MHz, CDCl₃ (1): (3) CD₃OD): δ 8.12 (s, 1H), 7.95 (d, J = 7.0 Hz, 2H), 7.48 (d, J = 7.0 Hz, 2H), 7.25 (t, J = 7.0 Hz, 4H), 7.11 (br s, 2H), 7.08-7.05 (m, 6H), 6.86 (d, J = 7.0 Hz, 2H); ¹³C NMR (125 MHz, CDCl₃ (1): (3) CD₃OD): δ 167.5, 166.2, 156.4, 149.0, 146.4, 142.4, 133.3, 130.4, 129.9, 129.3, 128.8, 124.8, 123.4, 119.7, 118.3, 117.2, 116.3, 110.4, 109.9; IR (neat): υ 3005, 2206, 1584, 1486, 1326, 1275, 752, 695 cm⁻¹; HRMS (ESI): calcd for C₃₂H₂₀N₄O₂ [M+H]⁺ 493.1659, Found 493.1649.

4.8.2.15 Synthesis of (E) -2-cyano-3-(4-(2,2-dicyanovinyl) phenyl)-3-(4-(diphenyl amino) phenyl) acrylic acid (4.15b):

The product was purified by column chromatography using 1:3 MeOH/EtOAc at $R_f = 0.12$.

Cis and trans isomers were separated. *E*- **isomer**; Red solid (0.08 g, yield = 30%); MP: 251-253°C; 1 H NMR (500 MHz, CDCl₃ (1): (3) CD₃OD): δ 8.11 (s, 1H), 7.89 (d, J = 8.0 Hz, 2H), 7.39 (d, J = 8.5 Hz, 2H), 7.29-7.26 (m, 4H), 7.18 (d, J = 9.0 Hz, 2H), 7.09-7.06 (m, 6H), 6.91 (d, J = 9.0 Hz, 2H); 13 C NMR (125 MHz,

CDCl₃ (1): (3) CD₃OD): δ 167.5, 166.2, 157.1, 149.1, 146.2,146.1, 142.1, 132.7, 130.2, 129.4, 128.6, 124.6, 124.5, 123.3, 123.2, 119.5, 118.2, 116.9, 109.9; IR (neat): υ 2924, 2201, 1712, 1462, 1320, 1262, 750, 690 cm⁻¹; HRMS (ESI): calcd for $C_{32}H_{20}N_4O_2$ [M+H]⁺ 493.1659, Found 493.1665.

4.8.2.16 Synthesis of (Z)-3-(4-(9H-carbazol-9-yl) phenyl)-2-cyano-3-(4-(2,2-dicyanovinyl) phenyl) acrylic acid (4.16a):

To a stirred solution of ester derivative of compound **4.29** (0.2 g, 0.38 mmol) in CH₃CN (10 mL), LiOH (excess, 0.32 g, 7.71 mmol) dissolved in water (10 mL) was treated to it and

allowed to stir room temperature for 4 h. The acetonitrile solvent was removed under reduced pressure. The crude was extracted with EtOAc (3×15 mL) and acidified with 10% HCl water solution. The product was purified by column chromatography using 1:5 MeOH/EtOAc at $R_f = 0.36$. Cis and trans isomers were

separated. **Z- isomer**; Red solid (0.04 g, yield = 20%); MP: 227-229°C; ¹H NMR (500 MHz, DMSO-d₆): δ 8.37 (s, 1H), 8.23 (t, J = 7.5 Hz, 3H), 8.08-8.04 (m, 2H), 7.98 (d, J = 7.9 Hz, 1H), 7.87 (d, J = 8.4 Hz, 1H), 7.65 (d, J = 8.6 Hz, 1H), 7.49-7.46 (m, 2H), 7.44 (d, J = 5.0 Hz, 3H), 7.31-7.28 (m, 3H); ¹³C NMR (125 MHz, DMSO-d₆): δ 163.8, 162.7, 147.2, 146.0, 140.9, 139.8, 139.5, 135.0, 131.8, 131.1, 130.1, 129.3, 129.1, 126.5, 126.3, 125.2, 123.2, 122.9, 120.7, 120.3, 109.9, 109.7; IR (neat): υ 2919, 2207, 1596, 1448, 1315, 1226, 1103, 749 cm⁻¹; HRMS (ESI): calcd for C₃₂H₁₈N₄O₂ [M+Na]⁺ 491.1503, Found 491.1499.

4.8.2.17 Synthesis of (E)-3-(4-(9H-carbazol-9-yl) phenyl)-2-cyano-3-(4-(2,2-dicyanovinyl) phenyl) acrylic acid (4.16b):

The product was purified by column chromatography using 1:5 MeOH/EtOAc at $R_f = 0.23$.

E- isomer; Red solid (0.083 g, yield = 44%); MP: 238-241°C; ¹H NMR (500 MHz, DMSO-d₆): δ 8.35 (s, 1H), 8.26 (t, J = 8.5 Hz, 3H), 8.08-8.05 (m, 2H),

7.95 (d, J = 8.5 Hz, 1H), 7.86 (d, J = 8.5 Hz, 1H), 7.68 (d, J = 8.5 Hz, 1H), 7.56 (d, J = 7.0 Hz, 2H), 7.45 (d, J = 4.0 Hz, 3H), 7.33 (t, J = 8.0 Hz, 3H); ¹³C NMR (125 MHz, DMSO-d₆): δ

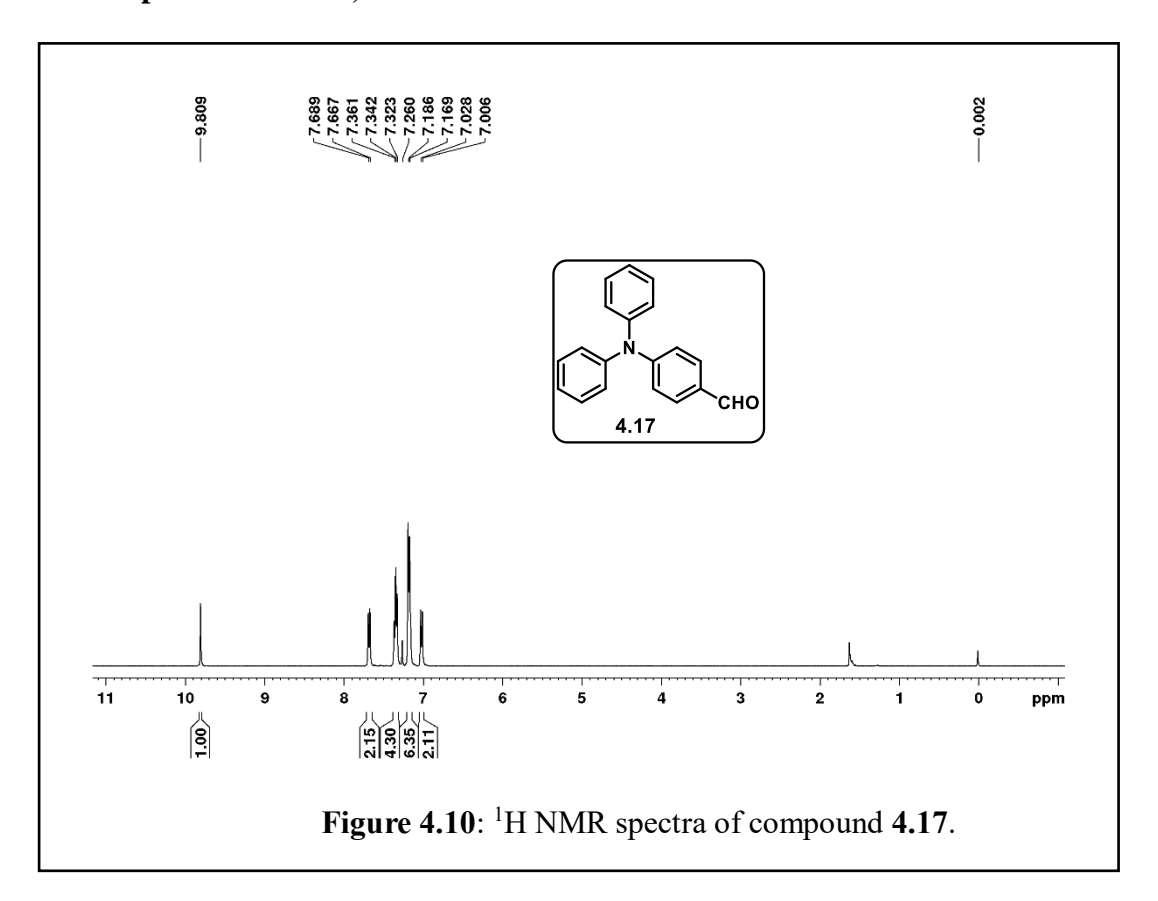
165.1, 163.5, 159.9, 149.9, 146.6, 142.2, 141.6, 139.8, 139.7, 135.3, 133.3, 131.0, 130.0, 129.9, 129.6, 126.4, 126.3, 125.2, 124.2, 122.9, 120.5, 120.3, 109.7; IR (neat): υ 2922, 2206, 1597, 1449, 1358, 1226, 1102, 749 cm⁻¹; HRMS (ESI): calcd for $C_{32}H_{18}N_4O_2$ [M+Na]⁺ 491.1503, Found 491.1505.

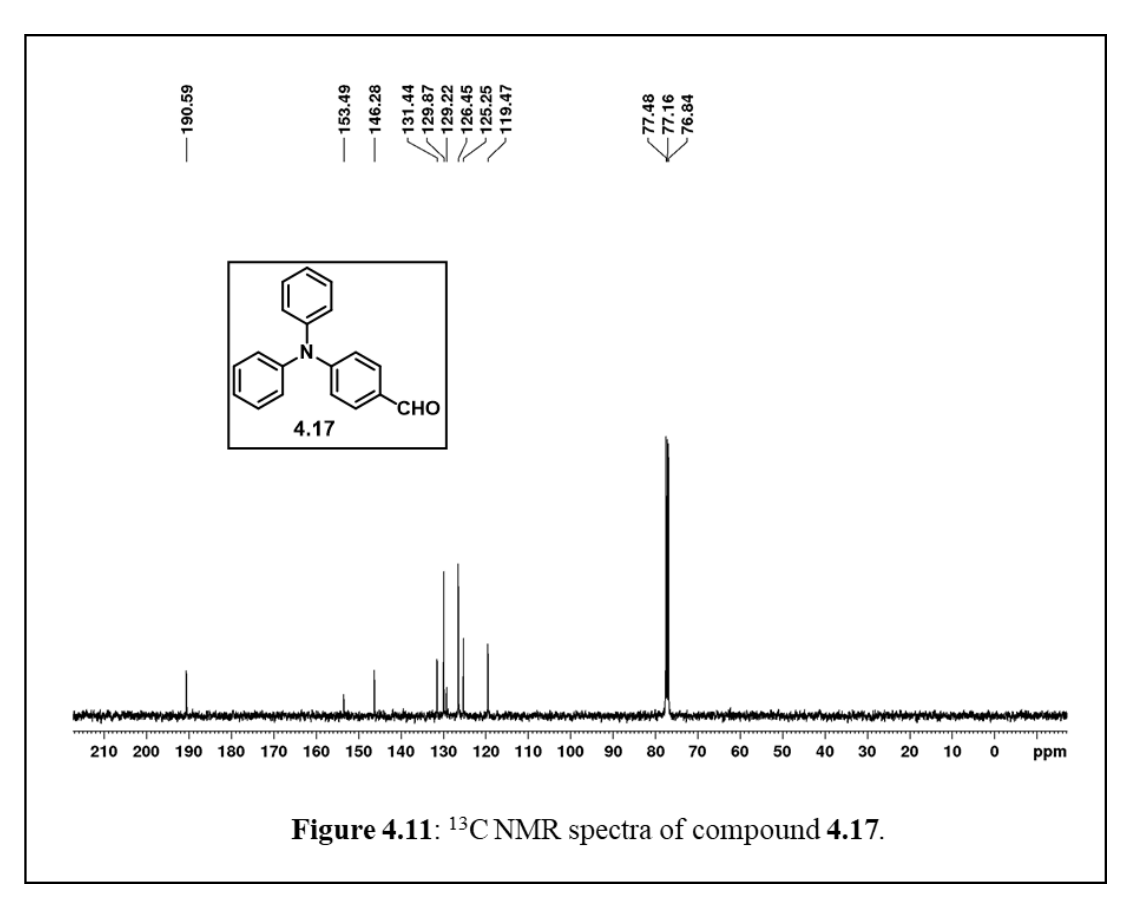
4.9 References

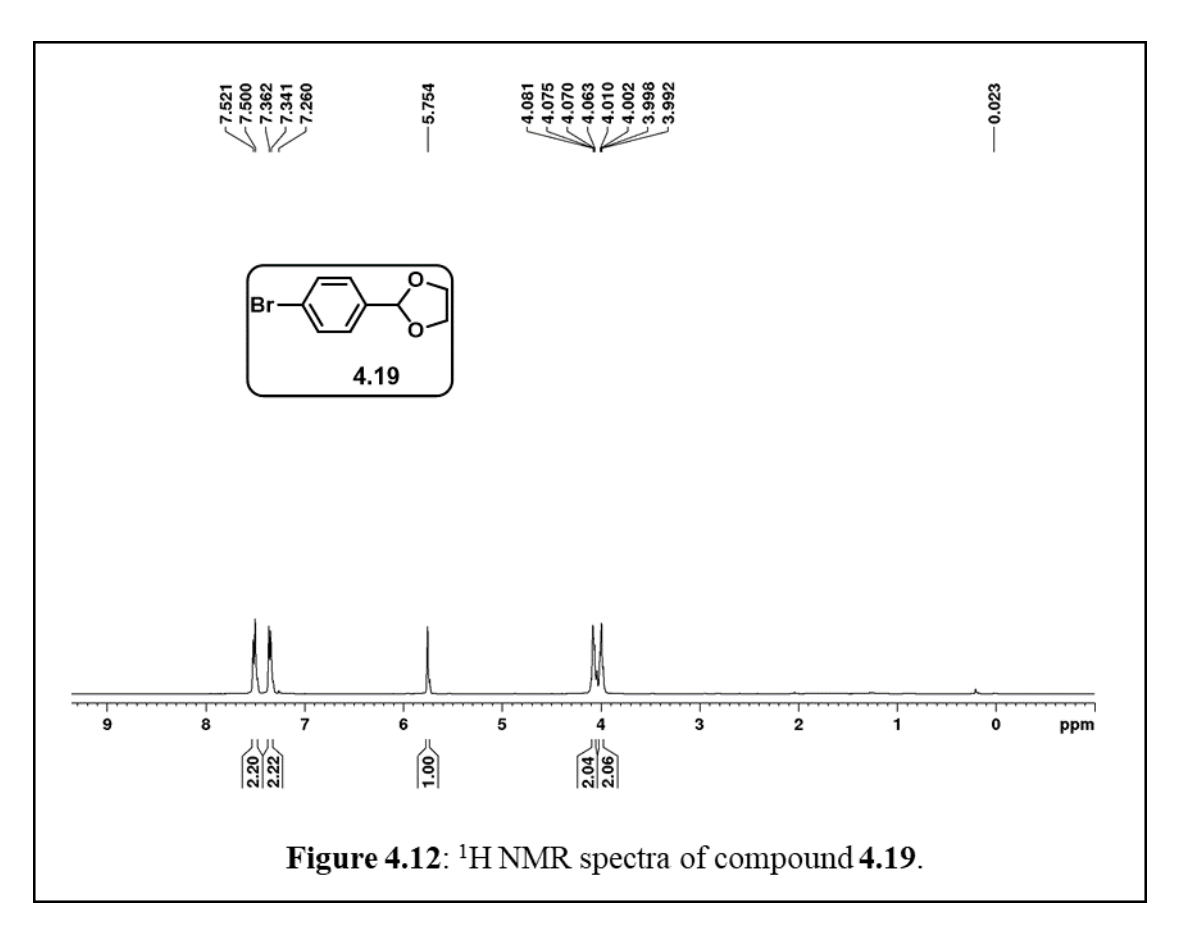
- 1. Kato, S.; Diederich, F. Chem. Commun. 2010, 46, 1994.
- (a) Leriche, P.; Frere, P.; Cravino, A.; Aleveque, O.; Roncali, J. J. Org. Chem. 2007,
 72, 8332. (b) Tang, X.; Liu, W.; Wu, J.; Lee, C.-S.; You, J.; Wang, P. J. Org. Chem.
 2010, 75, 7273.
- 3. (a) Qin, P.; Wiberg, J.; Gibson, E. A.; Linder, M.; Li, L.; Brinck, T.; Hagfeldt, A.; Albinsson, B.; Sun, L. *J. Phys. Chem. C* **2010**, *114*, 4738. (b) Unger, E. L.; Ripaud, E.; Leriche, P.; Cravino, A.; Roncali, J.; Johansson, E. M. J.; Hagfeldt, A.; Boschloo, G. *J. Phys. Chem. C* **2010**, *114*, 11659.
- (a) Zhang, J.; Deng, D.; He, C.; He, Y.; Zhang, M.; Zhang, Z.-G.; Zhang, Z.; Li, Y. Chem. Mater. 2011, 23, 817. (b) Leliege, A.; Blanchard, P.; Rousseau, T.; Roncali, J. Org. Lett. 2011, 13, 3098.
- 5. Hong, J.; Lai, H.; Liu, Y.; Yuan, C.; Li, Y.; Liu, P.; Fang, Q. RSC Adv. 2013, 3, 1069.
- 6. Wang, B.; Li, P.; Yu, F.; Chen, J.; Qu, Z.; Han, K. Chem. Commun. 2013, 49, 5790.
- 7. (a) Patel, J. Z.; Parkkari, T.; Laitinen, T.; Kaczor, A. A.; Saario, S. M.; Savinainen, J. R.; Navia-Paldanius, D.; Cipriano, M.; Leppanen, J.; Koshevoy, I. O.; Poso, A.; Fowler, C. J.; Laitinen, J. T.; Nevalainen, T. *J. Med. Chem.* **2013**, *56*, 8484.
- 8. Hwang, A.-R.; Han, W.-S.; Wee, K.-R.; Kim, H. Y.; Cho, D. W.; Min, B. K.; Nam, S. W.; Pac, C.; Kang, S. O. *Phys. Chem. C* **2012**, *116*, 1973.
- 9. Yadav, J. S.; Reddy, B. V. S.; Basak, A. K.; Visali, B.; Narsaiah, A. V.; Nagaiah, K. Eur. J. Org. Chem. 2004, 546.
- 10. Wielopolski, M.; Marszalek, M.; Brunetti, F. G.; Joly, D.; Calbo, J.; Arago, J.; Moser, J.-E.; Humphry-Baker, R.; Zakeeruddin, S. M.; Delgado, J. L.; Gratzel, M.; Ortı, E.; Martın, N. *J. Mater. Chem. C*, **2016**, *4*, 3798.
- Frisch, M. J.; Trucks, G. W.; Schlegel, H. B.; Scuseria, G. E.; Robb, M. A.; Cheeseman, J. R.; Scalmani, G.; Barone, V.; Mennucci, B.; Petersson, G. A.; Nakatsuji, H.; Caricato, M.; Li, X.; Hratchian, H. P.; Izmaylov, A. F.; Bloino, J.; Zheng, G.; Sonnenberg, J. L.; Hada, M.; Ehara, M.; Toyota, K.; Fukuda, R.; Hasegawa, J.; Ishida, M.; Nakajima, T.; Honda, Y.; Kitao, O.; Nakai, H.; Vreven, T.; Montgomery, Jr. J. A.; Peralta, J. E.; Ogliaro, F.; Bearpark, M.; Heyd, J. J.; Brothers, E.; Kudin, K. N.; Staroverov, V. N.; Kobayashi, R.; Normand, J.; Raghavachari, K.; Rendell, A.; Burant, J. C.; Iyengar, S. S.; Tomasi, J.; Cossi, M.; Rega, N.; Millam, J. M.; Klene, M.; Knox, J. E.; Cross, J. B.; Bakken, V.; Adamo, C.; Jaramillo, J.; Gomperts, R.; Stratmann, R. E.; Yazyev, O.;

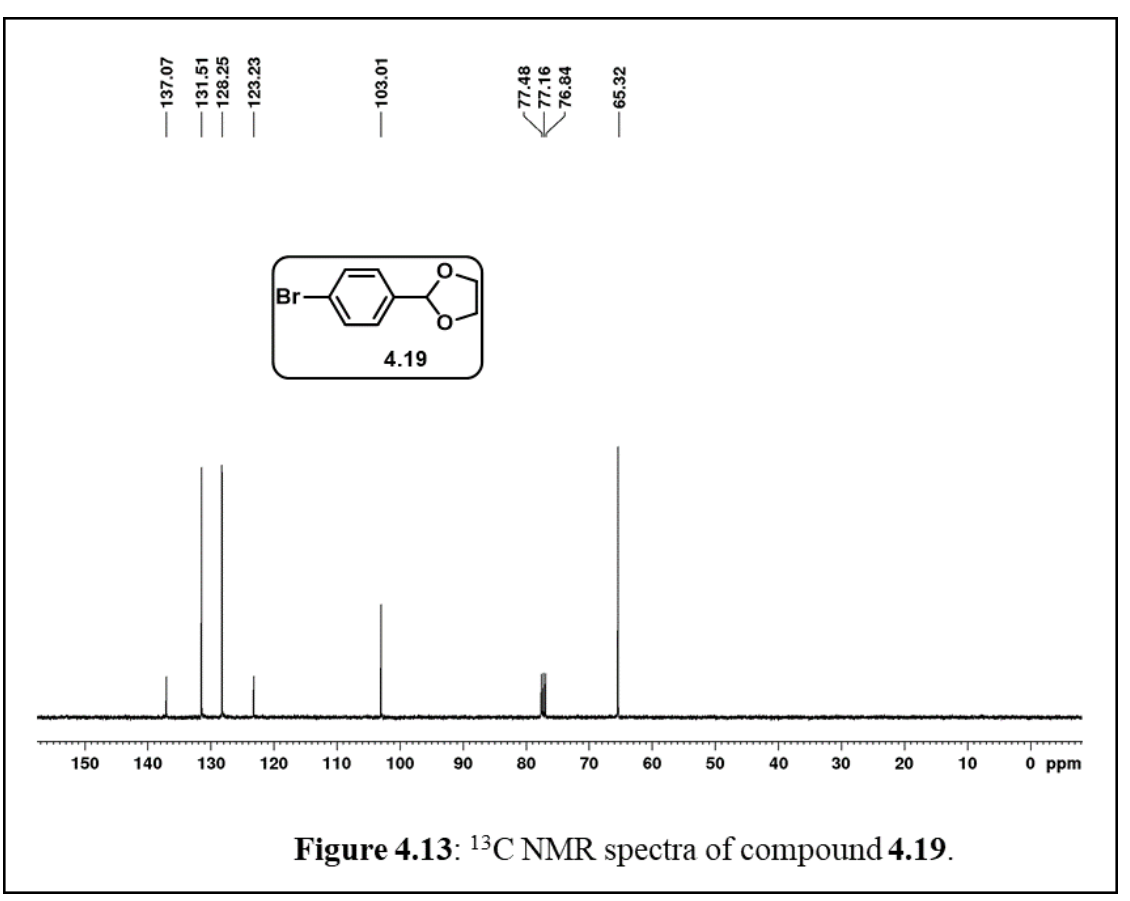
Austin, A. J.; Cammi, R.; Pomelli, C.; Ochterski, J. W.; Martin, R. L.; Morokuma, K.; Zakrzewski, V. G.; Voth, G. A.; Salvador, P.; Dannenberg, J. J.; Dapprich, S.; Daniels, A. D.; Farkas, O.; Foresman, J. B.; Ortiz, J. V.; Cioslowski, J.; Fox, D. J. *Gaussian 09, Revision A.02*, Gaussian, Inc. Wallingford, CT, **2009**.

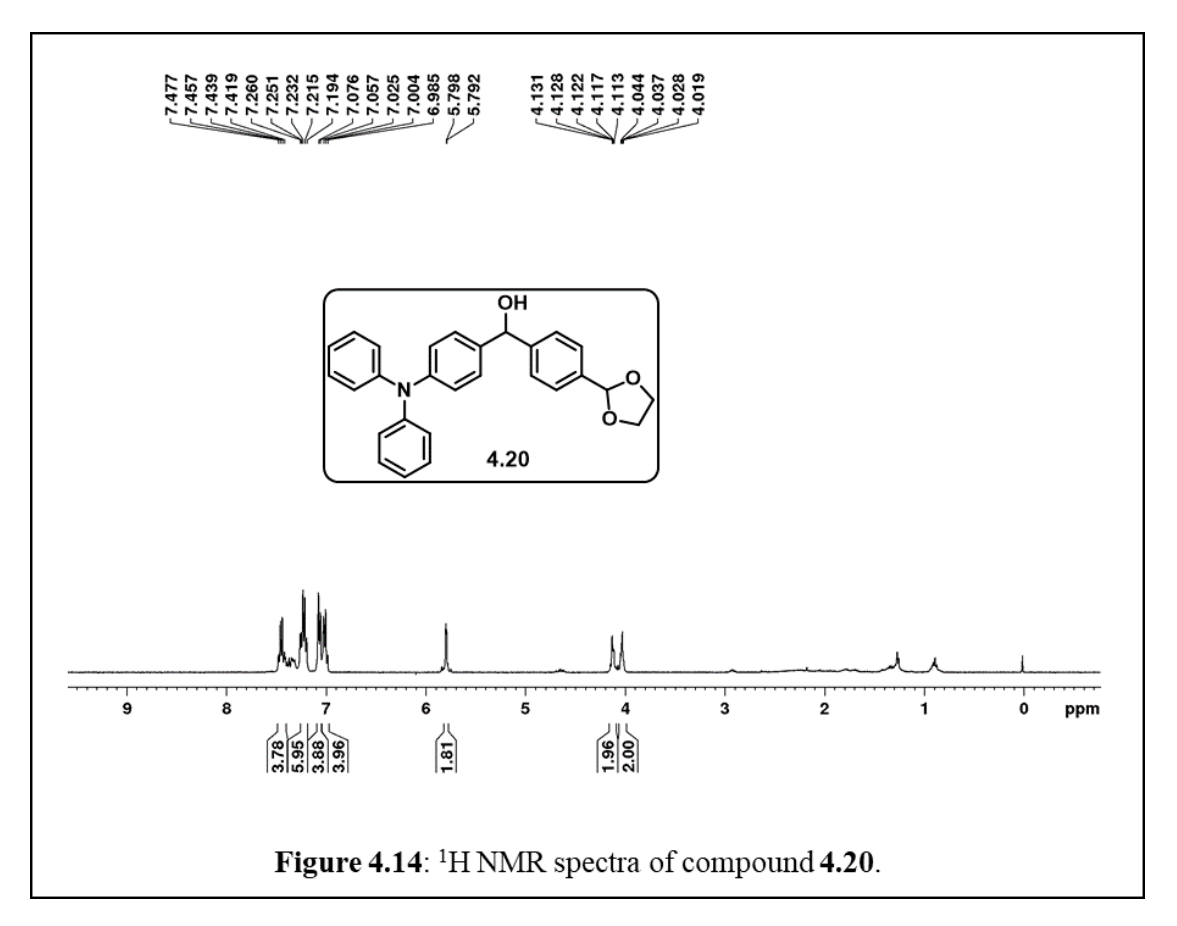
4.10 Representative ¹H, ¹³C NMR

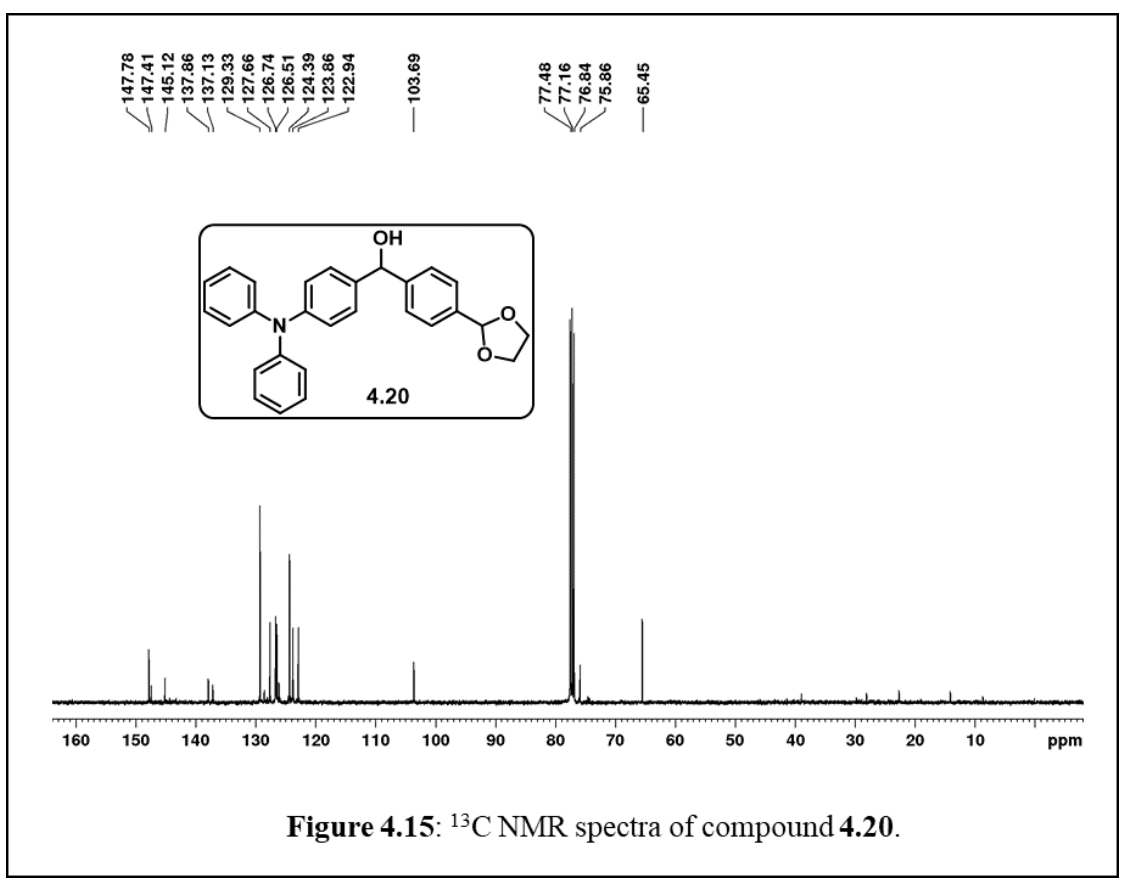


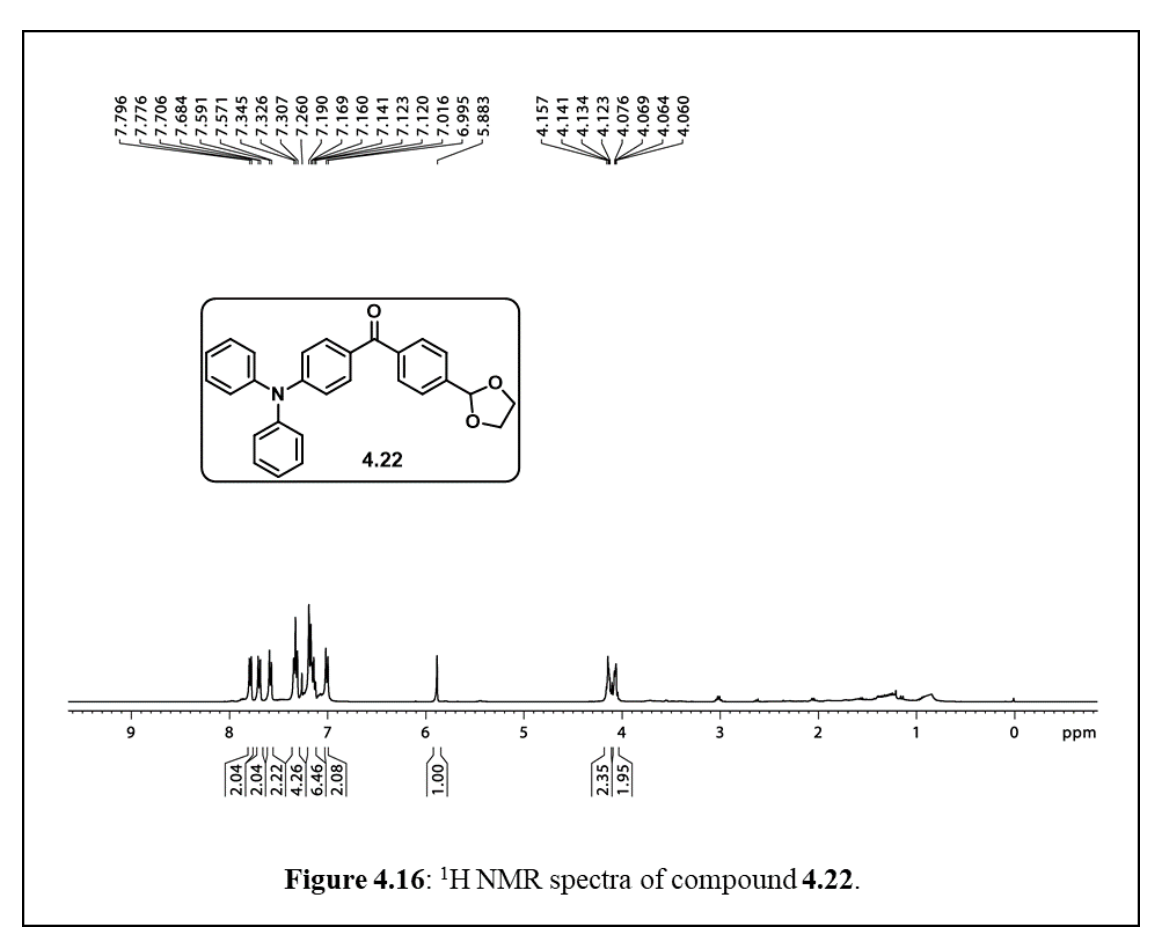


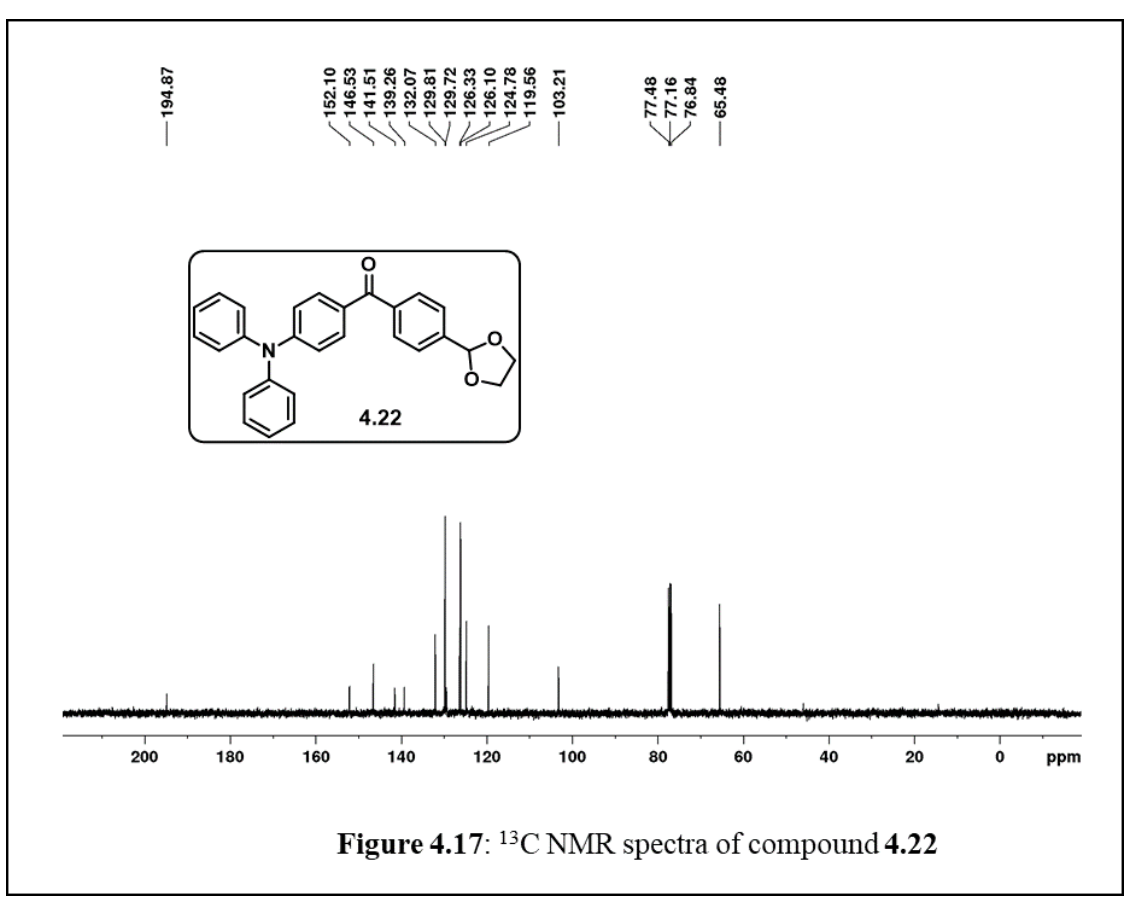


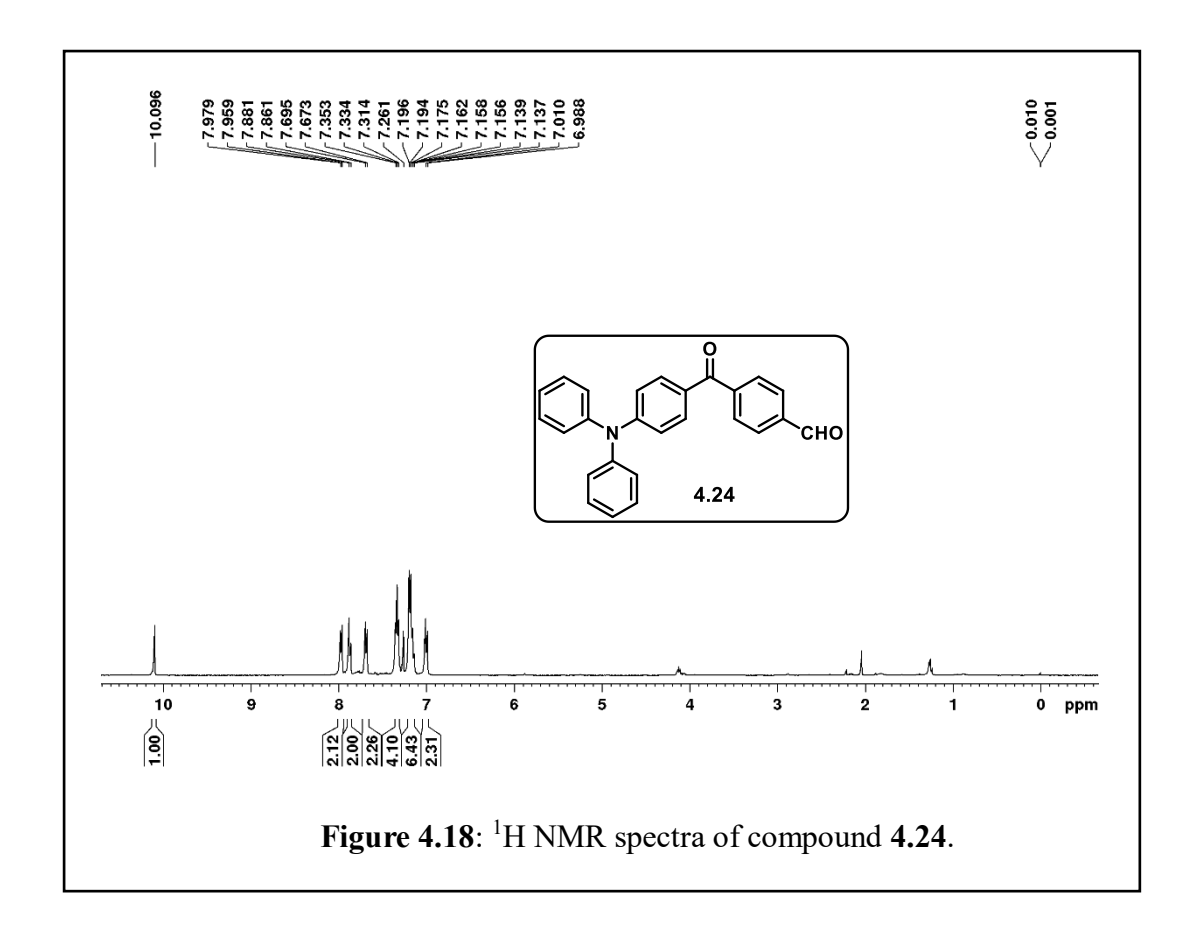


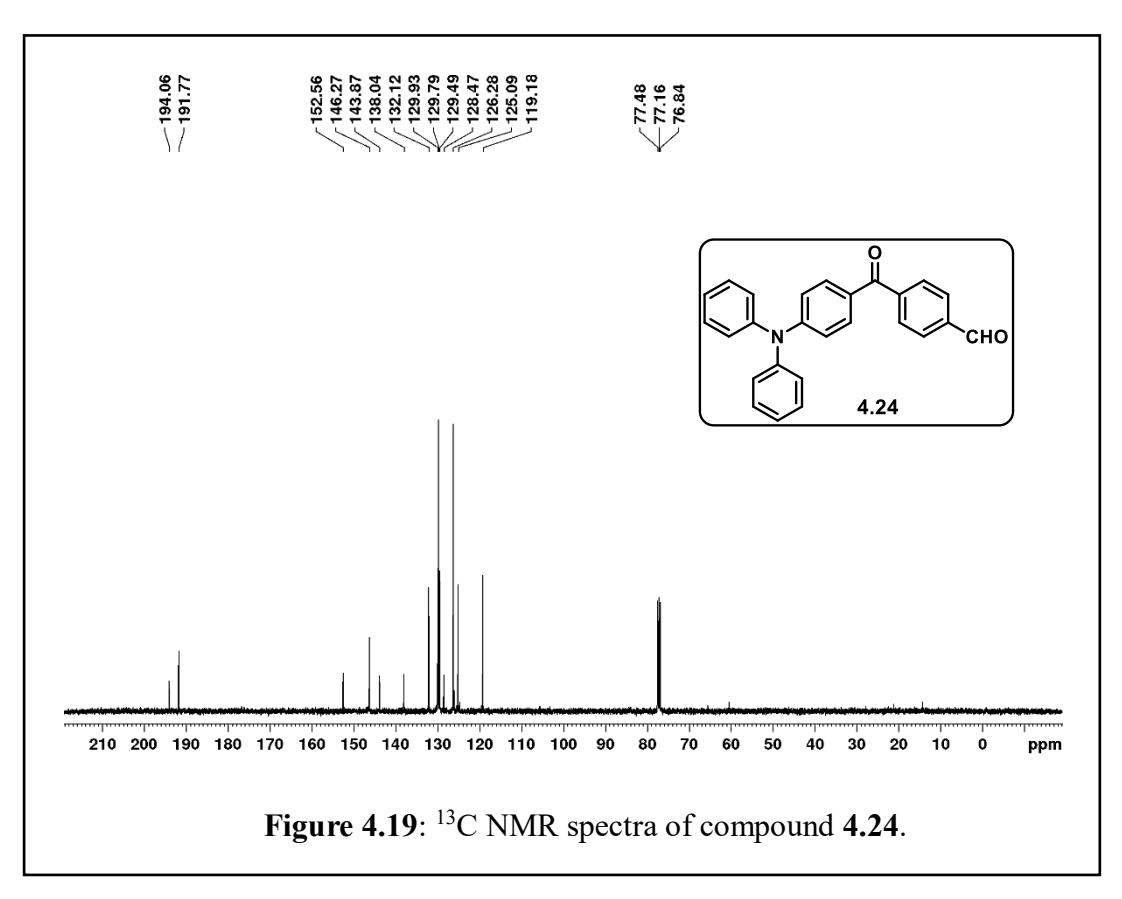


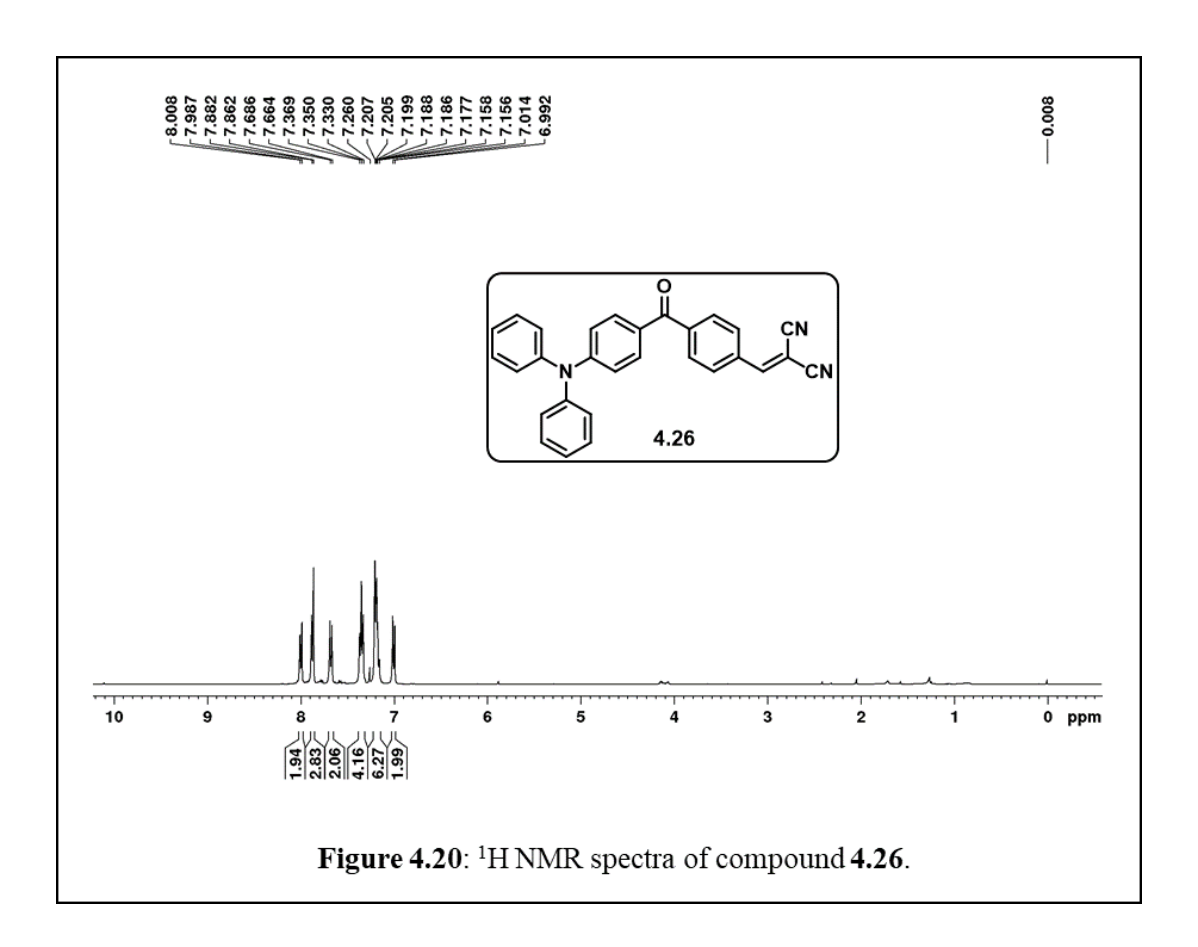


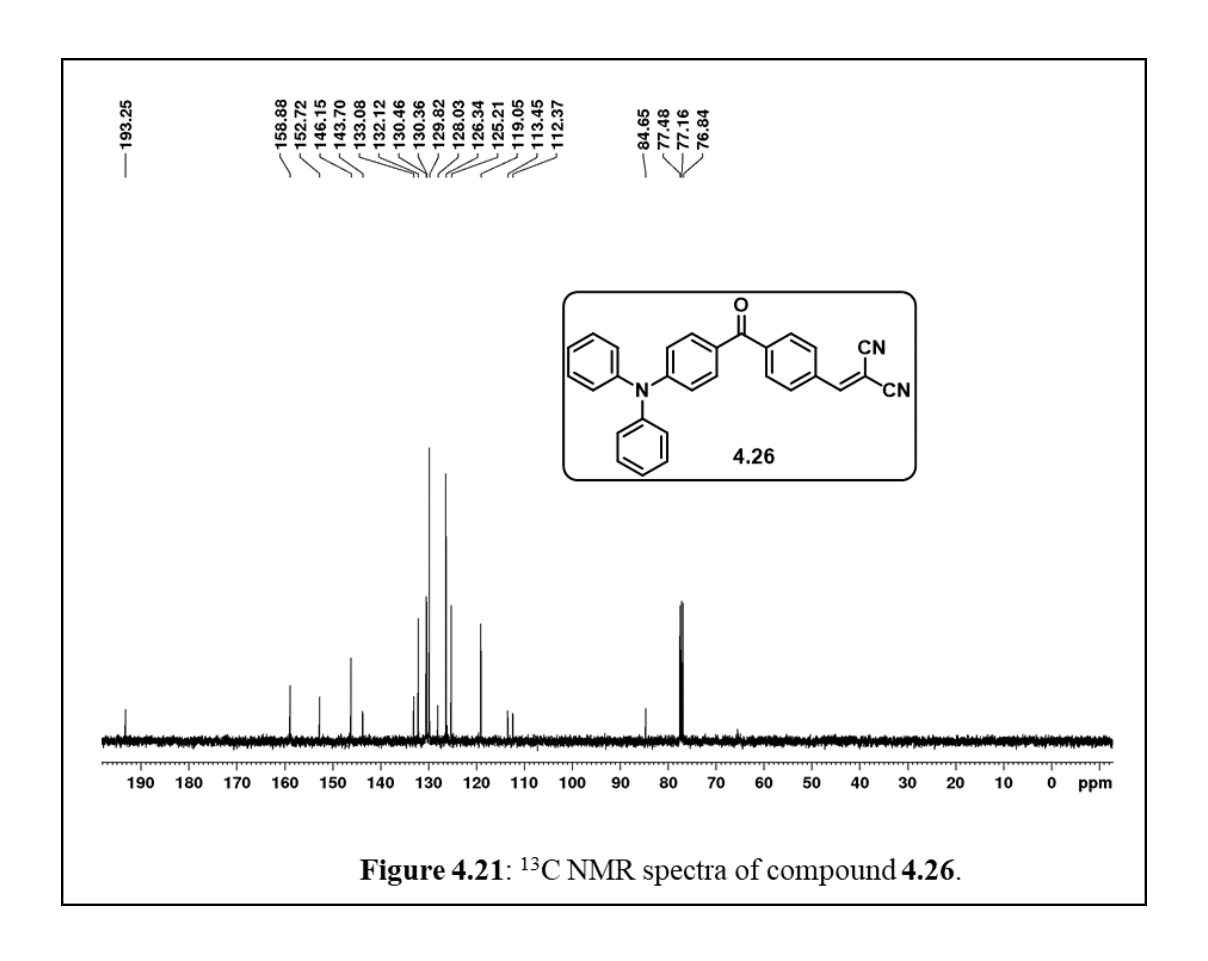


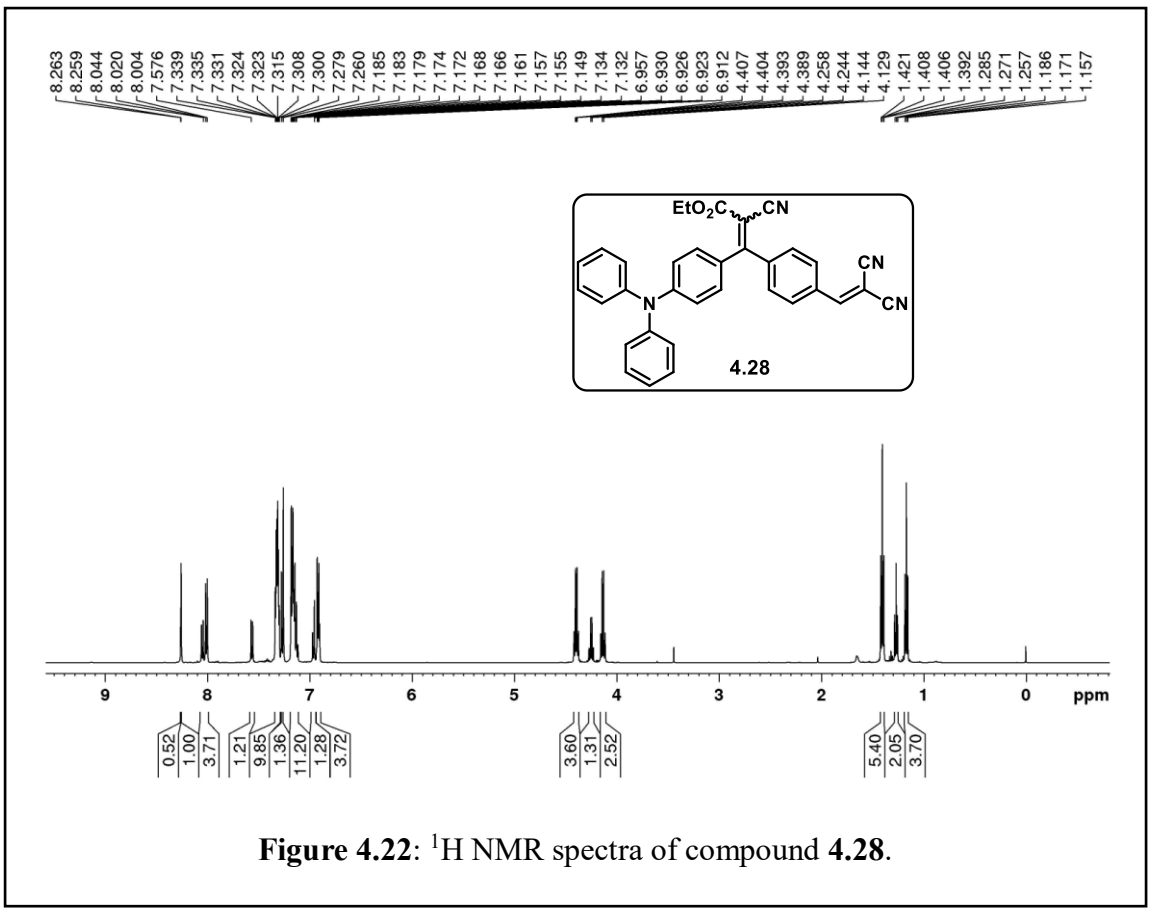


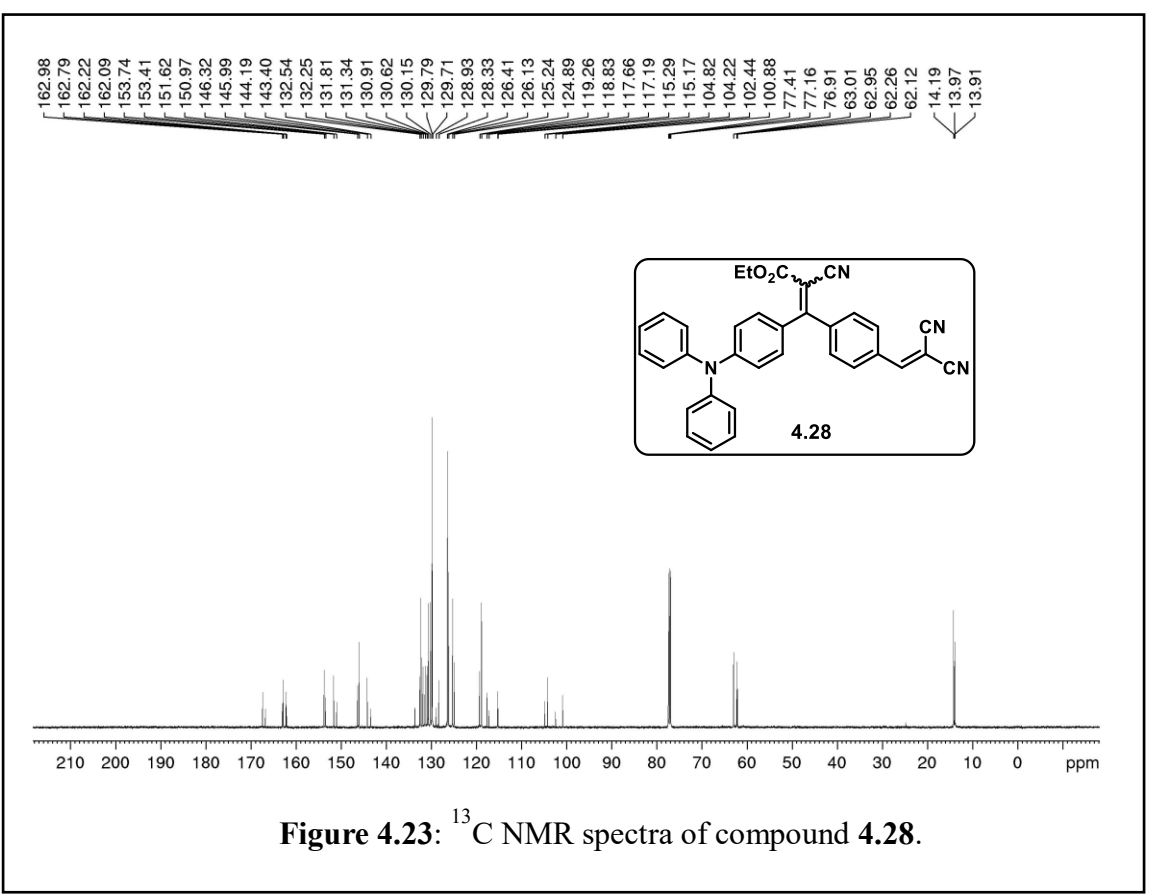


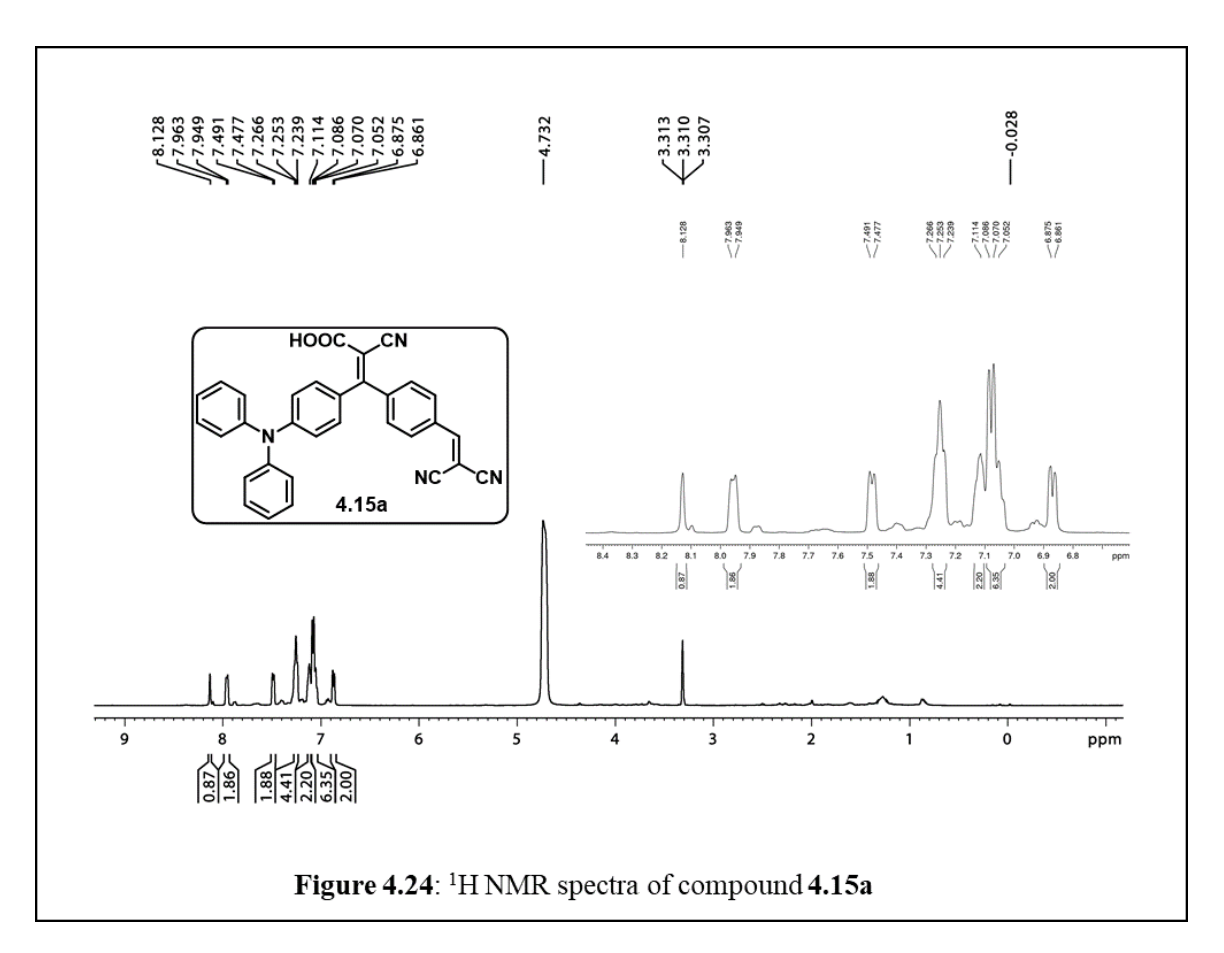


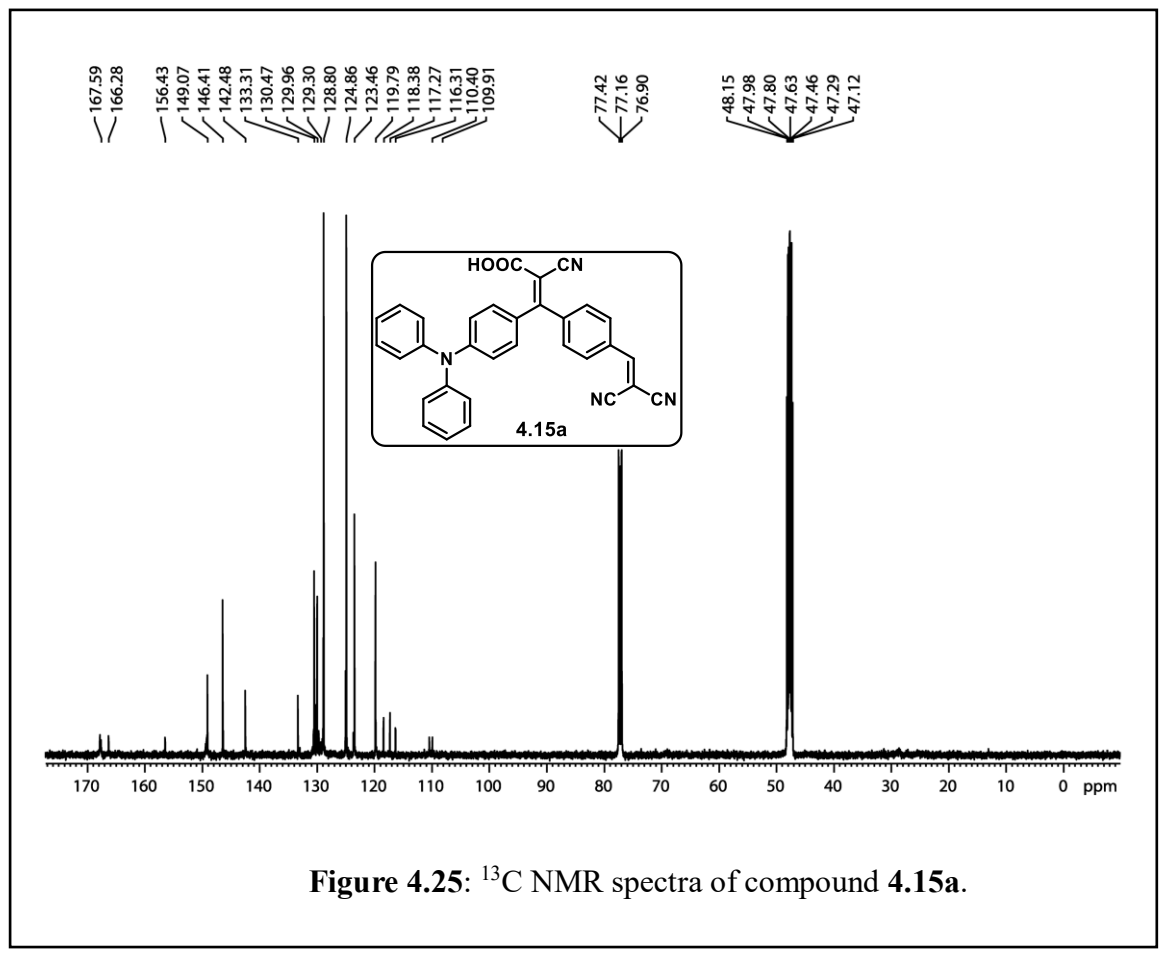


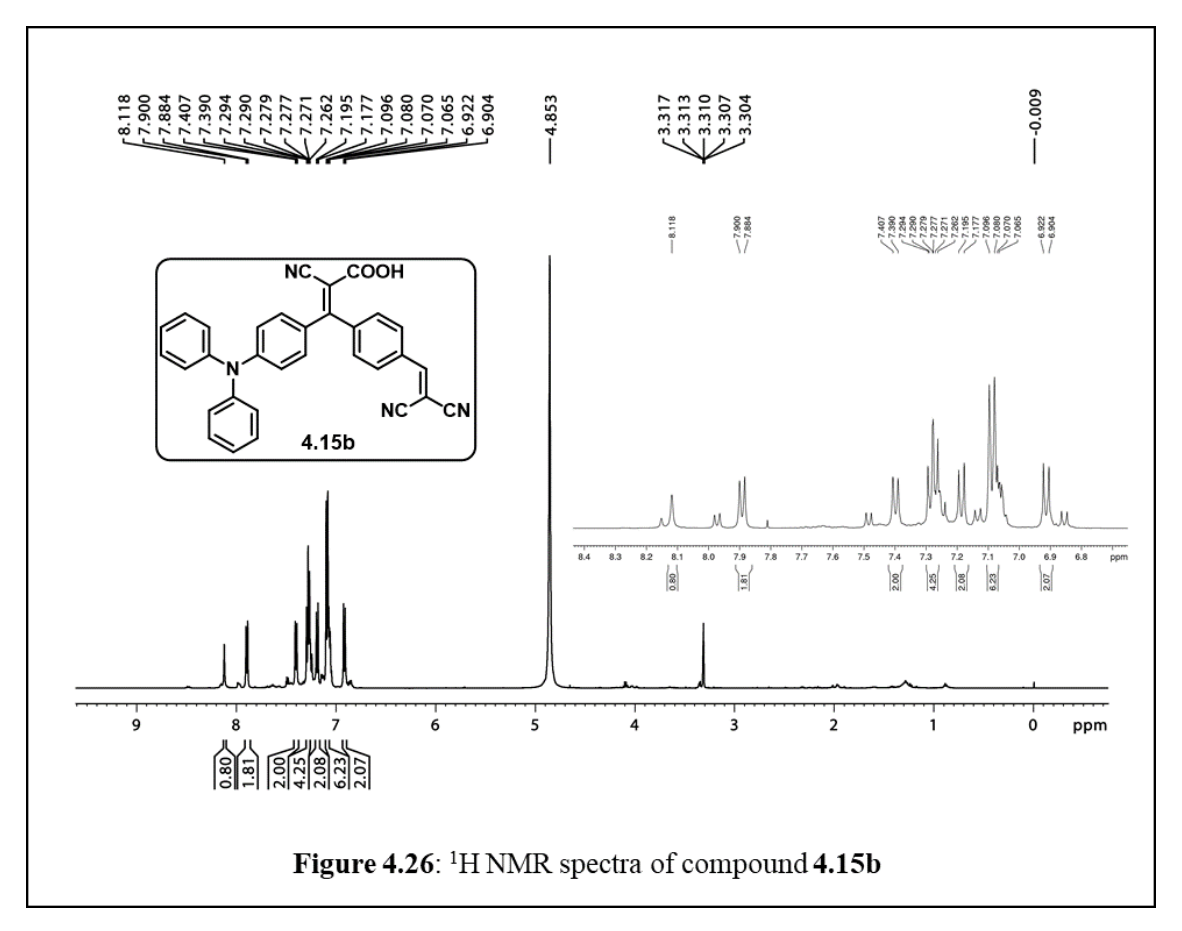












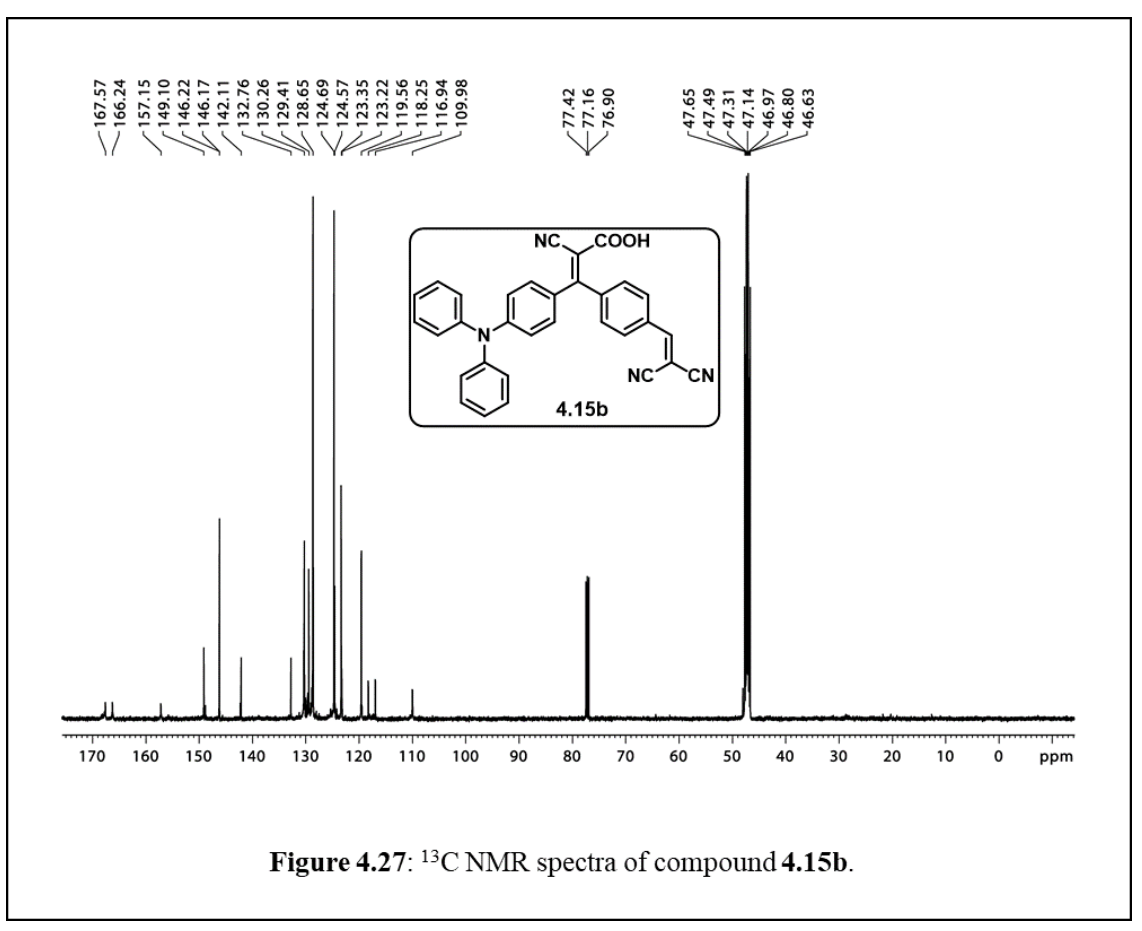


Table 1. Crystal data and structure refinement for 2.1

Identification code	2.1
Empirical formula	$C_{35}H_{23}N_3O_2S$
Formula weight	549.62
Temperature	296(2) K
Wavelength	0.71073 Å
Crystal system	Monoclinic
Space group	P 21/n
Unit cell dimensions	a = 7.969(2) Å α = 90° b=6.9630(17)Å β = 91.834(9) ° c = 49.787(12) Å γ = 90°
Volume	2761.0(12) Å ³
Z	4
Density (calculated)	1.322 Mg/m^3
Absorption coefficient	0.225 mm ⁻¹
F (000)	576
Crystal size	0.230 x 0.160 x 0.140 mm ³
Theta range for data collection	2.456 to 28.061°
Index ranges	-10<=h<=10, -9<=k<=9, -64<=l<=64
Reflections collected	77777
Independent reflections	6346 [R(int) = 0.3060]
Completeness to theta = 24.247°	99.6 %
Absorption correction	Semi-empirical from equivalents
Max. and min. transmission	0.979 and 0.965
Refinement method	Full-matrix least-squares on F ²
Data / restraints / parameters	6346 / 0 / 375
Goodness-of-fit on F ²	1.021
Final R indices [I>2sigma(I)]	R1 = 0.0793, $wR2 = 0.1532$
R indices (all data)	R1 = 0.1986, $wR2 = 0.1898$
Extinction coefficient	0.0075(11)
Largest diff. peak and hole	0.420 and -0.441 e.Å ⁻³
CCDC	1949082

Table 2. Crystal data and structure refinement for 2.2

Identification code	2.2
Empirical formula	$C_{33}H_{21}N_3O_2S_2$
Formula weight	555.65
Temperature	296(2) K
Wavelength	0.71073 Å
Crystal system	Triclinic
Space group	P -1
Unit cell dimensions	a = 7.444(3) Å α = 79.624(10) ° b = 9.125(3) Å β = 87.935(11) ° c = 22.465(8) Å γ =69.647(11)°
Volume	1406.7(8) Å ³
Z	2
Density (calculated)	$1.312 \mathrm{Mg/m^3}$
Absorption coefficient	0.225 mm ⁻¹
F(000)	576
Crystal size	$0.100 \times 0.080 \times 0.050 \text{ mm}^3$
Theta range for data collection	2.420 to 24.247°.
Index ranges	-8<=h<=8, -10<=k<=10, -25<=l<=25
Reflections collected	32522
Independent reflections	4513 [R(int) = 0.2271]
Completeness to theta = 24.247°	99.2 %
Absorption correction	Semi-empirical from equivalents
Max. and min. transmission	0.989 and 0.978
Refinement method	Full-matrix least-squares on F ²
Data / restraints / parameters	4513 / 0 / 365 1.081
Goodness-of-fit on F ²	
Final R indices [I>2sigma(I)]	R1 = 0.0863, $wR2 = 0.1677$
R indices (all data)	R1 = 0.1744, $wR2 = 0.2063$
Extinction coefficient	n/a
Largest diff. peak and hole	$0.405 \text{ and } -0.578 \text{ e.Å}^{-3}$
CCDC	1949083

Table 3. Crystal data and structure refinement for 2.3

Identification code	2.3
Empirical formula	$C_{31}H_{21}N_3O_2$
Formula weight	467.51
Temperature	296(2) K
Wavelength	0.71073 Å
Crystal system	Triclinic
Space group	P -1
Unit cell dimensions	a = 6.9369(7) Å α = 89.127(4) ° b = 8.8727(10) Å β = 83.386(4) ° c = 21.218(2) Å γ = 74.621(4) °.
Volume	1250.6(2) Å ³
Z	2
Density (calculated)	1.241 Mg/m^3
Absorption coefficient	0.079 mm ⁻¹
F (000)	488
Crystal size	$0.090 \times 0.070 \times 0.050 \text{ mm}^3$
Theta range for data collection	2.555 to 27.547°
Index ranges	-8<=h<=8-11<=k<=11, -27<=l<=27
Reflections collected	22268
Independent reflections	5454 [R(int) = 0.0675]
Completeness to theta = 24.247°	99.6 %
Absorption correction	Semi-empirical from equivalents
Max. and min. transmission	0.996 and 0.993
Refinement method	Full-matrix least-squares on F ²
Data / restraints / parameters	5454 / 0 / 329
Goodness-of-fit on F ²	1.020
Final R indices [I>2sigma(I)]	R1 = 0.0686, $wR2 = 0.1686$
R indices (all data)	R1 = 0.1343, $wR2 = 0.2002$
Extinction coefficient	n/a
Largest diff. peak and hole	0.464 and -0.559 e.Å- ³
CCDC	1949084

181

Table 4. Crystal data and structure refinement for 3.11

Identification code	3.11
Empirical formula	$C_{42}H_{31}N_3O_2$
Formula weight	609.70
Temperature	296(2) K
Wavelength	0.71073 Å
Crystal system	Monoclinic
Space group	P 21/n
Unit cell dimensions	$a = 14.3812(16) \text{ Å } \alpha = 90^{\circ}.$
	b = 16.947(2) Å β= 103.394(6) °
	$c = 27.654(4) \text{ Å } \gamma = 90^{\circ}.$
Volume	6556.5(14) Å ³
Z	8
Density (calculated)	1.235 Mg/m^3
Absorption coefficient	0.076 mm ⁻¹
F(000)	2560
Crystal size	0.100 x 0.080 x 0.060 mm ³
Theta range for data collection	2.199 to 20.905°.
Index ranges	-14<=h<=14, -16<=k<=16, -27<=l<=27
Reflections collected	77575
Independent reflections	6919 [R(int) = 0.4045]
Completeness to theta = 20.905°	99.7 %
Absorption correction	Semi-empirical from equivalents
Max. and min. transmission	0.995 and 0.992
Refinement method	Full-matrix least-squares on F ²
Data / restraints / parameters	6919 / 0 / 848
Goodness-of-fit on F ²	1.011
Final R indices [I>2sigma(I)]	R1 = 0.0818, $wR2 = 0.1475$
R indices (all data)	R1 = 0.2048, $wR2 = 0.1940$
Extinction coefficient	0.0010(2)
Largest diff. peak and hole	0.214 and -0.207 e.Å ⁻³
CCDC	2006744

List of Publications

- 1. Synthesis of Highly Functionalized Pyrrolidine Derivatives from Easily Accessible Diethyl (*E*)-4-Oxohex-2-enedioate. Ganesh Kumar Thota, **Duraiyarasu Tamilarasan**, and Rengarajan Balamurugan, *Eur. J. Org. Chem.* **2017**, 6417–6426.
- Reversible Addition of Cyanide to Triphenylamine Attached Difluoroboron β-Diketonate Facilitated Selective Colorimetric and Fluorimetric Detection of Cyanide Ion. Duraiyarasu Tamilarasan, Ramalingam Suhasini, Viruthachalam Thiagarajan and Rengarajan Balamurugan, *Eur. J. Org. Chem.* 2020, 993–1000.
- 3. Ligand/Antibody Free Imaging of Microtubules in Live Cells Using 1,3-Dicarbonyl Bridged Donor-Acceptor and Related Compounds. **Duraiyarasu Tamilarasan**, Loka Reddy Velatooru, Ramalingam Suhasini, Viruthachalam Thiagarajan, Bramanandam Manavathi, Rengarajan Balamurugan. *ACS Appl. Bio Mater.* **2020**, (*Under Revision*)
- 4. Dual Donor (D(D)-π-A) based Donor-Acceptor Systems with Enhanced Large Stokes Shifts for Live Cell Imaging Application. **Duraiyarasu Tamilarasan**,^a Loka Reddy Velatooru,^b Bramanandam Manavathi.^b Rengarajan Balamurugan,^a (*Manuscript to be submitted*)

Patent

 Diphenylamino-methylene malononitrile based compounds as fluorescence probes Rengarajan Balamurugan, **Duraiyarasu Tamilarasan**, Bramanandam Manavathi, Loka Reddy, WIPO Application No.PCT/IB2019/057180; *Indian Patent* 201841031942, **2018** (*Under Evaluation*).

Poster and Oral Presentations

- Presented Poster on "Synthesis of Triphenylamine Based Donor-Acceptor with β-Diketone Unit for Optical Applications" in the 12th Annual In-House Symposium Chemfest-2015 held at School of Chemistry, University of Hyderabad, Hyderabad.
- 2. Presented Poster on "1,3-Diketone Bridged Donor-Acceptor Systems for Optical Applications" in the 21st International conference on organic synthesis (ICOS 21) in Dec 11-16, 2016, held at IIT Bombay, Mumbai, India.
- 3. Presented Oral and Poster "Synthesis and Characterization of BF₂ Complexed Triphenylamine Linked 1,3-Diketone and its Application in Cyanide Ion Sensing" in the **15th Annual In-House Symposium Chemfest-2018** at School of Chemistry, University of Hyderabad, Hyderabad.

Workshop

 Attended International winter course on "Organic Solar Cells: Principles and Practices" on Nov.2-10, 2016, Organized by Laboratory of Molecular Photonics & Electronics (LAMP), Department of Physics, National Institute of Technology, Calicut, Kerala.

Triphenylamine and Carbazole Based Donor-Acceptor Systems for Dye-Sensitized Solar Cell, Bio-Imaging, and Sensor Applications

by Tamilarasan D

Submission date: 25-Jun-2020 10:45AM (UTC+0530)

Submission ID: 1349380347

File name: Thesis_Tamil.pdf (5.83M)

Word count: 18773

Character count: 95673

Triphenylamine and Carbazole Based Donor-Acceptor Systems for Dye-Sensitized Solar Cell, Bio-Imaging, and Sensor **Applications**

ORIGINALITY REPORT

SIMILARITY INDEX

6%

15%

6%

INTERNET SOURCES

PUBLICATIONS

STUDENT PAPERS

School of Chemistry University of Hyderabad Hyderabad-46, India.

PRIMARY SOURCES

Duraiyarasu Tamilarasan, Ramalingam Suhasini, Viruthachalam Thiagarajan, Rengarajan Balamurugan. "Reversible Addition of Cyanide to Triphenylamine Attached Difluoroboron β-Diketonate Facilitated Selective Colorimetric and Fluorimetric Detection of Cyanide Ion", European Journal of Organic Dr. R. Balamurugan **Professor** Chemistry, 2020

Publication

repository.hkbu.edu.hk

Internet Source

Submitted to University of Hong Kong Student Paper

s-space.snu.ac.kr

Internet Source

Anders Hagfeldt, Gerrit Boschloo, Licheng Sun, Lars Kloo, Henrik Pettersson. "Dye-Sensitized Solar Cells", Chemical Reviews, 2010

- "Electron Transfer in Chemistry", Wiley, 2001
- <1%
- Raoul R. Nigmatullin, Paolo Lino, Guido Maione.
 "New Digital Signal Processing Methods",
 Springer Science and Business Media LLC,
 2020

<1%

Publication

Won Sik Yoon, Dong Won Kim, Jun-Mo Park, Illhun Cho, Oh Kyu Kwon, Dong Ryeol Whang, Jin Hong Kim, Jung-Hwa Park, Soo Young Park. "A Novel Bis-Lactam Acceptor with Outstanding Molar Extinction Coefficient and Structural Planarity for Donor–Acceptor Type Conjugated Polymer", Macromolecules, 2016

<1%

Publication

9 worldwidescience.org

<1%

Shyamaprosad Goswami, Krishnendu Aich, Sangita Das, Bholanath Pakhira et al. " A Triphenyl Amine-Based Solvatofluorochromic Dye for the Selective and Ratiometric Sensing of OCI in Human Blood Cells ", Chemistry - An Asian Journal, 2015

<1%

Publication

12	Submitted to IIT Delhi Student Paper	<1%
13	Jiayu Wang, Kuan Liu, Lanchao Ma, Xiaowei Zhan. "Triarylamine: Versatile Platform for Organic, Dye-Sensitized, and Perovskite Solar Cells", Chemical Reviews, 2016 Publication	<1%
14	ir.nctu.edu.tw Internet Source	<1%
15	www.michappclub.com Internet Source	<1%
16	www.hohoteco.idv.tw Internet Source	<1%
17	Submitted to Associatie K.U.Leuven Student Paper	<1%
18	strathprints.strath.ac.uk Internet Source	<1%
19	tel.archives-ouvertes.fr Internet Source	<1%
20	doras.dcu.ie Internet Source	<1%
21	Ganesan, Paramaguru, Aravindkumar Chandiran, Peng Gao et al. "Molecular Engineering of 2-Quinolinone Based Anchoring	<1%

Groups for Dye-Sensitized Solar Cells", The Journal of Physical Chemistry C

Publication

22	Submitted to Queen Mary and Westfield College Student Paper	<1%
23	Submitted to University of Strathclyde Student Paper	<1%
24	researchrepository.wvu.edu Internet Source	<1%
25	Submitted to University of Bath Student Paper	<1%
26	Chuanjiang Qin, Wenqin Peng, Kun Zhang, Ashraful Islam, Liyuan Han. "A Novel Organic Sensitizer Combined with a Cobalt Complex Redox Shuttle for Dye-Sensitized Solar Cells", Organic Letters, 2012	<1%
27	Albinsson, Bo, Mattias P. Eng, Karin Pettersson, and Mikael U. Winters. "Electron and energy transfer in donorâ€"acceptor systems with conjugated molecular bridges", Physical Chemistry Chemical Physics, 2007. Publication	<1%
28	Submitted to Universiti Putra Malaysia Student Paper	<1%

29	Submitted to Universiteit van Amsterdam Student Paper	<1%
30	Submitted to Savitribai Phule Pune University Student Paper	<1%
31	www.hytest.fi Internet Source	<1%
32	dspace.lib.niigata-u.ac.jp Internet Source	<1%
33	ubm.opus.hbz-nrw.de Internet Source	<1%
34	www.medworm.com Internet Source	<1%
35	Hong, Jia, Hua Lai, Yanmei Liu, Chao Yuan, Yuxue Li, Ping Liu, and Qiang Fang. "New organic dyes containing E- or Z-trifluoromethyl acrylic acid as the electron acceptors for dyesensitized solar cell applications: an investigation of the effect of molecular configuration on the power conversion efficiency of the cells", RSC Advances, 2013.	<1%
36	pubs.acs.org Internet Source	<1%
37	www.mrs.org Internet Source	<1%

38	Kumar, Dhirendra, K. R. Justin Thomas, Chuan-Pei Lee, and Kuo-Chuan Ho. "Organic Dyes Containing Fluorene Decorated with Imidazole Units for Dye-Sensitized Solar Cells", The Journal of Organic Chemistry Publication	<1%
39	oparu.uni-ulm.de Internet Source	<1%
40	Zang, Xu-Feng, Zu-Sheng Huang, Han-Lun Wu, Zafar Iqbal, Lingyun Wang, Herbert Meier, and Derong Cao. "Molecular design of the diketopyrrolopyrrole-based dyes with varied donor units for efficient dye-sensitized solar cells", Journal of Power Sources, 2014. Publication	<1%
41	vibdoc.com Internet Source	<1%
42	link.springer.com Internet Source	<1%
43	documents.mx Internet Source	<1%
44	Amaresh Mishra, Markus K. R. Fischer, Peter Bäuerle. "Metal-Free Organic Dyes for Dye-Sensitized Solar Cells: From Structure: Property Relationships to Design Rules", Angewandte Chemie International Edition, 2009	<1%

45	Wangdong Zeng, Yiming Cao, Yu Bai, Yinghui Wang, Yushuai Shi, Min Zhang, Fangfang Wang, Chunyue Pan, Peng Wang. "Efficient Dye-Sensitized Solar Cells with an Organic Photosensitizer Featuring Orderly Conjugated Ethylenedioxythiophene and Dithienosilole Blocks", Chemistry of Materials, 2010 Publication	<1%
46	www.coursehero.com Internet Source	<1%
47	Michael Bendikov, Fred Wudl, Dmitrii F. Perepichka. "Tetrathiafulvalenes, Oligoacenenes, and Their Buckminsterfullerene Derivatives: The Brick and Mortar of Organic Electronics", Chemical Reviews, 2004 Publication	<1%
48	www.nserc-green.ulaval.ca Internet Source	<1%
49	Submitted to King Abdullah University of Science and Technology (KAUST) Student Paper	<1%
50	www.journal.csj.jp Internet Source	<1%
51	Zheng, J.S "Effect of carbon nanofiber microstructure on oxygen reduction activity of	<1%

supported palladium electrocatalyst", Electrochemistry Communications, 200705

Publication

52	Submitted to UT, Dallas Student Paper	<1%
53	Submitted to The University of Manchester Student Paper	<1%
54	Submitted to University of North Texas Student Paper	<1%
55	Submitted to Higher Education Commission Pakistan Student Paper	<1%
56	research.chalmers.se Internet Source	<1%

Exclude quotes On
Exclude bibliography On

Exclude matches

< 14 words